NASA/TP–2015-218674 (Corrected Copy)
NESC-RP-13-00884

Spin Forming Aluminum Crew Module (CM) Metallic Aft Pressure Vessel Bulkhead (APVBH) – Phase II

Eric K. Hoffman and Marcia S. Domack
Langley Research Center, Hampton, Virginia

Pablo D. Torres and Preston B. McGill
Marshall Space Flight Center, Huntsville, Alabama

Wesley A. Tayon
Langley Research Center, Hampton, Virginia

Jay E. Bennett
Johnson Space Center, Houston, Texas

Joseph T. Murphy
Lockheed Martin Space Systems Company, New Orleans, Louisiana

January 2015

NASA STI Program . . . in Profile

Since its founding, NASA has been dedicated to the advancement of aeronautics and space science. The NASA scientific and technical information (STI) program plays a key part in helping NASA maintain this important role.

The NASA STI program operates under the auspices of the Agency Chief Information Officer. It collects, organizes, provides for archiving, and disseminates NASA's STI. The NASA STI program provides access to the NTRS Registered and its public interface, the NASA Technical Reports Server, thus providing one of the largest collections of aeronautical and space science STI in the world. Results are published in both non-NASA channels and by NASA in the NASA STI Report Series, which includes the following report types:

- TECHNICAL PUBLICATION. Reports of completed research or a major significant phase of research that present the results of NASA Programs and include extensive data or theoretical analysis. Includes compilations of significant scientific and technical data and information deemed to be of continuing reference value. NASA counter-part of peer-reviewed formal professional papers but has less stringent limitations on manuscript length and extent of graphic presentations.

- TECHNICAL MEMORANDUM. Scientific and technical findings that are preliminary or of specialized interest, e.g., quick release reports, working papers, and bibliographies that contain minimal annotation. Does not contain extensive analysis.

- CONTRACTOR REPORT. Scientific and technical findings by NASA-sponsored contractors and grantees.

- CONFERENCE PUBLICATION. Collected papers from scientific and technical conferences, symposia, seminars, or other meetings sponsored or co-sponsored by NASA.

- SPECIAL PUBLICATION. Scientific, technical, or historical information from NASA programs, projects, and missions, often concerned with subjects having substantial public interest.

- TECHNICAL TRANSLATION. English-language translations of foreign scientific and technical material pertinent to NASA's mission.

Specialized services also include organizing and publishing research results, distributing specialized research announcements and feeds, providing information desk and personal search support, and enabling data exchange services.

For more information about the NASA STI program, see the following:

- Access the NASA STI program home page at *http://www.sti.nasa.gov*

- E-mail your question to help@sti.nasa.gov

- Phone the NASA STI Information Desk at 757-864-9658

- Write to:
  NASA STI Information Desk
  Mail Stop 148
  NASA Langley Research Center
  Hampton, VA 23681-2199

NASA/TP–2015-218674 (Corrected Copy)
NESC-RP-13-00884

Spin Forming Aluminum Crew Module (CM) Metallic Aft Pressure Vessel Bulkhead (APVBH) – Phase II

Eric K. Hoffman and Marcia S. Domack
Langley Research Center, Hampton, Virginia

Pablo D. Torres and Preston B. McGill
Marshall Space Flight Center, Huntsville, Alabama

Wesley A. Tayon
Langley Research Center, Hampton, Virginia

Jay E. Bennett
Johnson Space Center, Houston, Texas

Joseph T. Murphy
Lockheed Martin Space Systems Company, New Orleans, Louisiana

National Aeronautics and
Space Administration

Langley Research Center
Hampton, Virginia 23681-2199

January 2015

Acknowledgments

The team acknowledges Ryan Cullen, Mark Misiag, James Collins, Richard Morganti, and Geri Hayes of Spincraft for their expertise in spin forming and their dedicated support during the fabrication of the spin formed aft bulkhead evaluated in this study.

Also, the team acknowledges the support of Harold Claytor, Stewart Walker, Jim Baughman, and Joel Alexa of LaRC support contractor AMA and the LaRC Light Alloy Laboratory for their materials processing, mechanical testing, and metallurgical analysis support; and Carlos Castillo, Rolando Padilla, John Savage, and Johnnie West of LaRC for their dedication during specimen fabrication.

The team wishes to acknowledge the support of Lisa Sharff, Charles Kay, David Beaty, Matt Jackson, Tafton Hastings of MSFC engineering support contractor ESSSA/Jacobs, and Wendell DeWeese (MSFC) for their dedicated support for tensile, stress corrosion cracking (SCC), fracture testing, and metallurgical analysis support. The team appreciates the dedicated support of Ayman Girgis (ESSSA/Jacobs) for his tensile and fracture toughness assessment and PoShou Chen (ESSSA/Jacobs) for his microstructural and failure analysis assessment.

Thank you also to Norm Elfer (LM), Steve Gentz (NESC), Lucie Johannes (JSC), Kirby Lawless (NESC), Sandeep Shah (MSFC), and Tim Vaughn (MSFC) for their comprehensive peer review.

Available from:

NASA STI Program / Mail Stop 148
NASA Langley Research Center
Hampton, VA 23681-2199
Fax: 757-864-6500

ERRATA
NASA/TM–2015-218674

Issue Date: 12/04/2015

Revisions were made regarding interpretation of the stress corrosion results. The data generated is insufficient to establish Table ratings according to MSFC-STD-3029. Finding F-6 is modified to correct interpretation of the data and the text modified appropriately for consistence. Changes occur primarily in the Executive Summary, Section 8.5, and Section 10.4. One Finding (F-7) was created using the third bullet of F-6.

Spin Forming Aluminum Crew Module (CM) Metallic Aft Pressure Vessel Bulkhead (APVBH) – Phase II

October 28, 2015

Report Approval and Revision History

NOTE: This document was approved at the October 28, 2015, NRB. This document was submitted to the NESC Director on November 9, 2015, for configuration control.

Approved:	*Original Signature on File*	*11/12/15*
	NESC Director	Date

Version	Description of Revision	Office of Primary Responsibility	Effective Date
1.0	Initial Release	Dr. Robert Piascik, NASA Technical Fellow for Materials, LaRC	11/20/14
2.0	A Supplemental Report has been generated for this report using the same TI # (TI-13-00884_Supplemental Report). The Supplemental Report will be published as NASA-TM-2015-218797. Revisions were made regarding interpretation of the stress corrosion results. The data generated is insufficient to establish Table ratings according to MSFC-STD-3029. Finding F-6 is modified to correct interpretation of the data and the text modified appropriately for consistence. Changes occur primarily in the Executive Summary, Section 8.5, and Section 10.4. One Finding (F-7) was created using the third bullet of F-6.	Dr. Robert Piascik, NASA Technical Fellow for Materials, LaRC	10/28/15

Table of Contents

List of Figures

List of Tables

Technical Assessment Report

1.0 Notification and Authorization

The principal focus of this project was to assist the Multi-Purpose Crew Vehicle (MPCV) Program in developing a spin forming fabrication process for manufacture of the Orion crew module (CM) aft pressure vessel bulkhead. The spin forming process will enable a single piece aluminum (Al) alloy 2219 aft bulkhead resulting in the elimination of the current multiple piece welded construction, simplify CM fabrication, and lead to an enhanced design. Phase I (NASA TM-2014-218163 (1)) of this assessment explored spin forming the single-piece CM forward pressure vessel bulkhead.

The Orion MPCV Program and Lockheed Martin (LM) recently made two critical decisions relative to the NESC Phase I work scope: (1) LM selected the spin forming process to manufacture a single-piece aft bulkhead for the Orion CM, and (2) the aft bulkhead will be manufactured from Al 2219.

Based on the Program's new emphasis related to the spin forming process, the NESC was asked to conduct a Phase II assessment to assist in the LM manufacture of the aft bulkhead and to conduct a feasibility study into spin forming the Orion CM cone.

This activity was approved on June 19, 2013. Dr. Robert Piascik, NASA Technical Fellow for Materials at the Langley Research Center (LaRC), was selected to lead this assessment. The project plan was approved by the NASA Engineering and Safety Center (NESC) Review Board (NRB) on July 18, 2013.

The primary stakeholders for this assessment were the NASA and LM MPCV Program offices. Additional benefactors are commercial launch providers developing CM concepts.

2.0 Signature Page

Submitted by:

Team Signature Page Added - 11/23/15

Dr. Robert S. Piascik Date

Significant Contributors:

Mr. Michael D. Squire Date

Ms. Marcia S. Domack Date

Mr. Eric K. Hoffman Date

Signatories declare the findings, observations, and NESC recommendations compiled in the report are factually based from data extracted from program/project documents, contractor reports, and open literature, and/or generated from independently conducted tests, analyses, and inspections.

3.0 Team List

Name	Discipline	Organization
Core Team		
Robert Piascik	NESC Lead	LaRC
Michael Squire	NESC Deputy Lead	LaRC
Marcia Domack	Project Technical Lead	LaRC
Eric Hoffman	Project Aft Bulkhead Lead	LaRC
Jay Bennett	Materials & Processes	JSC
Peter Curreri	Project Coordinator at MSFC	MSFC
Preston McGill	Fracture Toughness Assessment	MSFC
Joseph Murphy	Materials and Processing	LM
Roger Reinmuller	Materials and Processing	LM
Wesley Tayon	Metallurgical Analysis	LaRC
Pablo Torres	Stress Corrosion Testing and Analysis	MSFC
Consultants		
Mark Cantrell	M&P Lead for Orion	LM
Stephen Hales	Physical Metallurgy	LaRC
Lucie Johannes	Welding/Manufacturing	JSC
Mike Smiles	MAF Processing	SSC
John Wagner	Manufacturing and Physical Metallurgy	LaRC
Administrative Support		
Linda Anderson	MTSO Program Analyst	LaRC
Linda Burgess	Planning and Control Analyst	LaRC/AMA
Terri Derby	Project Coordinator	LaRC/AMA
Jeffrey Hisey	Contracting Officer	LaRC
Erin Moran	Technical Writer	LaRC/AMA

3.1 Acknowledgements

The team acknowledges Ryan Cullen, Mark Misiag, James Collins, Richard Morganti, and Geri Hayes of Spincraft for their expertise in spin forming and their dedicated support during the fabrication of the spin formed aft bulkhead evaluated in this study.

Also, the team acknowledges the support of Harold Claytor, Stewart Walker, Jim Baughman, and Joel Alexa of LaRC support contractor AMA and the LaRC Light Alloy Laboratory for their materials processing, mechanical testing, and metallurgical analysis support; and Carlos Castillo, Rolando Padilla, John Savage, and Johnnie West of LaRC for their dedication during specimen fabrication.

The team wishes to acknowledge the support of Lisa Sharff, Charles Kay, David Beaty, Matt Jackson, Tafton Hastings of MSFC engineering support contractor ESSSA/Jacobs, and Wendell

DeWeese (MSFC) for their dedicated support for tensile, stress corrosion cracking (SCC), fracture testing, and metallurgical analysis support. The team appreciates the dedicated support of Ayman Girgis (ESSSA/Jacobs) for his tensile and fracture toughness assessment and PoShou Chen (ESSSA/Jacobs) for his microstructural and failure analysis assessment.

Thank you also to Norm Elfer (LM), Steve Gentz (NESC), Lucie Johannes (JSC), Kirby Lawless (NESC), Sandeep Shah (MSFC), and Tim Vaughn (MSFC) for their comprehensive peer review.

4.0 Executive Summary

The objective of this project was to assist the Multi-Purpose Crew Vehicle (MPCV) Program in developing a spin forming fabrication process for the manufacture of the Orion crew module (CM) aft pressure vessel bulkhead (APVBH) and evaluate the feasibility for manufacture of a single-piece cone. The spin forming process would enable a single-piece aluminum (Al) alloy 2219 aft bulkhead and single-piece cone resulting in the elimination of the current multiple piece welded construction, simplify CM fabrication, and lead to an enhanced design. The objectives of this two-part study were to: (1) spin form a full scale generic aft bulkhead component and characterize its properties as a pathfinder for the Lockheed-Martin (LM) Orion CM, and (2) develop a first-of-a-kind thick-component (6 inches thick) spin forming process for the manufacture of a single piece integrally-machined CM cone that would accommodate all design features (i.e., integral stiffeners, window frames, etc.). This report will focus on the aft bulkhead portion of this study only. The cone feasibility study determined that the benefits of a single-piece cone fabricated using spin forming were not sufficient to warrant proceeding with fabrication and testing. The single-piece cone feasibility study will be described in a supplement to this report.

The NESC Phase I activity, Spin Forming Aluminum Crew Module (CM) Forward Pressure Vessel Bulkhead (FPVBH) (1), demonstrated the feasibility of spin forming a single-piece FPVBH using either Al alloys 2219 or 2195. Based on the Phase I feasibility results, the MPCV Program requested that a Phase II spin forming activity be conducted to address specific objectives (processing and preliminary properties) associated with spin forming the aft bulkhead.

The MPCV Program and LM recently made two critical decisions relative to the NESC Phase I work scope: (1) LM selected the spin forming process to manufacture a single-piece aft bulkhead for the Orion CM, and (2) the aft bulkhead will be manufactured from Al 2219. The motivation for the change in manufacturing method included eliminating weld lands, lowering overall weight, simplifying the design, and improving design analysis and fidelity. The change in material was driven by the single-piece aft bulkhead design, which requires a preform thicker than 2 inches in order to accommodate all design features. Al-Li 2195 is limited in thickness to 2 inches or less due to quench rate sensitivity, which results in in-plane and through-thickness mechanical property anisotropy. As a result, the spin formed single-piece aft bulkhead design requires a corresponding change in material to thicker gage Al 2219.

The following tasks were defined to validate the spin forming process feasibility and demonstrate that acceptable material properties are achieved in a fully processed aft bulkhead:

1. Develop process parameters and spin form a pathfinder aft bulkhead representative of the Orion CM geometry using Al 2219.
2. Develop a preliminary properties data base using material from the fully processed Al 2219-T62 pathfinder aft bulkhead regarding:
   a. Microstructure
   b. Mechanical properties (tensile and fracture toughness)
   c. Stress corrosion cracking (SCC)

3. Develop circumferential (aft bulkhead to barrel) friction stir welding (FSW) parameters using material from the pathfinder aft bulkhead (LM activity).

A pathfinder aft bulkhead was successfully fabricated at a spin forming vendor using standard commercial spin forming and heat treatment practices. The curvature and thickness of the pathfinder were representative of and scalable to the Orion CM geometry. The aft bulkhead was fabricated using a single plate of Al 2219 and was fully processed to the T62 temper. Material was provided for metallurgical examination, tensile, fracture toughness, and stress corrosion testing by NASA. Additional material was provided to LM for additional mechanical property testing, self-reacting friction stir weld (SR-FSW) development for the aft bulkhead-to-CM barrel section joint, and structural sub element testing. The goal of these tasks was to address specific MPCV Program needs related to spin forming the Orion CM APVBH. The overall goal was to reduce risk by assessing a new manufacturing method prior to program deployment, provide information to guide first article test and analysis, develop an initial property database, identify preliminary issues or “show stoppers,” and accelerate program implementation.

This NESC assessment included microstructure evaluation, tensile and fracture toughness property testing, and SCC characterization to develop an initial property database for spin formed and heat treated Al 2219. Selected pathfinder regions (acreage locations) were tested to assess property uniformity. The resulting properties were compared to existing databases, such as Metallic Materials Properties Development and Standardization (MMPDS) to determine relative ranking. This study concluded that there were no insurmountable technical issues that precluded spin forming an aft bulkhead. Major findings are as follows:

The microstructure of the aft bulkhead varied both through-thickness and with meridian distance from the pole. The primary differences were grain size, extent of recrystallization, and residual deformation bands. Strain-induced recrystallized microstructures occurred toward the outer mold line (OML) of the aft bulkhead and reflect deformation imparted by the spin forming rollers. The recrystallized region extended through more of the section thickness in regions of greater deformation, specifically farther from the pole. These variations in grain size in the aft bulkhead are indicative of the complex and varied deformation levels associated with the spin forming process, particularly when combined with the plate rolling history and post-forming heat treatment. Material property tests were performed for in-plane orientations (longitudinal (L) and long transverse (LT)) only at the mid-plane (t/2 where t = thickness) location. Depending on the microstructure developed in a first article produced by LM for Orion, testing may be warranted at other through-thickness positions, particularly those biased toward the OML.

Tensile properties of the spin formed Al 2219-T62 aft bulkhead material were comparable to the MMPDS design properties for T62 wrought plate and other fabricated products in the T6 temper, such as spin formed domes, forgings and rolled rings. Tensile strength increased slightly, but measurably with distance from the pole and was uniform about the circumference. The short transverse (ST) tensile properties were notably greater than those for the other orientations L, LT, and 45º to the ST (ST45)), but elongations were about half. The tensile properties were lower than for Al 2219-T851 and T87 plate, as expected due to the increased precipitation strengthening in T8 temper wrought products that is imparted by the cold work prior to artificial aging.

Fracture toughness values were in-family with conventional Al 2219 tempers and product forms, and the typical variation with orientation was observed. Toughness values were higher for the spin formed material compared with Al 2219–T87 plate, which is expected for the strength levels measured). For 2xxx series Al alloys, strength and toughness are inversely proportional (i.e., T8 tempers achieve higher strength, but lower toughness. In-plane (L-T and T-L) toughness values were relatively constant for a given orientation and did not vary significantly across the aft bulkhead acreage. Toughness in the T-L orientation did decrease slightly with distance from the pole, which is in agreement with the trend noted for tensile strength. The test results showed high toughness values, high toughness-to-yield strength (YS) ratios, and rising R-curve behavior, which suggests excellent damage tolerance capability of the aft bulkhead material. In order to more fully characterize the damage tolerance capability of the material, the NESC team recommends conducting fatigue crack growth rate and surface crack tension testing on the aft bulkhead material.

Stress corrosion resistance varied somewhat with location in the aft bulkhead and more significantly with orientation. The primary data of interest is the 30-day alternate immersion exposure. Results from this test method and test duration are typically the basis for handbook and table ratings for SCC resistance. The L and LT orientations were significantly more resistant to SCC than the ST orientation. No failures occurred for the LT orientation, even at the highest stress levels, and all specimens had passing post-exposure residual strength levels. Susceptibility to SCC in the ST orientation varied with location in the aft bulkhead with the highest SCC resistance occurring at the rim. Regions near the pole and some in the membrane had moderate SCC resistance. One SCC failure of an ST specimen from a membrane location occurred at a low enough exposure stress level to warrant concern, and if validated through more extensive testing would result in a low SCC resistance rating for the spin formed aft bulkhead material. More importantly, the allowable design stress would need to be reduced.

However, some important points must be noted regarding the SCC data. The aft bulkhead tests followed MSFC test standard MSFC-STD-3029 in which the exposure stress levels are based on the measured strength of the material. Handbook values are based on standards that use MMPDS A-basis allowables to determine exposure stress levels. Actual strength is always higher than the allowables due to statistical knockdown; consequently, the aft bulkhead specimens were exposed to higher stress levels than handbook data being used for comparison. Al 2219 is considered an isotropic material with properties in the L, LT, and ST orientations generally agreeing within less than 5%. The ST YS in the aft bulkhead was 10% greater than that for L and LT. While it is unclear whether the high ST YS is inherent in the plate used in fabrication of the spin forming blank or is related to the spin forming process, the high ST YS of the aft bulkhead material further increased the exposure stress levels. The MSFC standard is realistic in that actual material strength will govern the performance of fabricated hardware. However, the difference in exposure stress levels makes interpretation of the aft bulkhead data more difficult.

The test duration specified by MSFC-STD-3029 is an additional deviation from other SCC test practices and standards. One disadvantage of the 3.5% NaCl alternate immersion test is that severe pitting may develop in the test specimens. As per ASTM G47, such pitting in tensile specimens with relatively small cross-sections can markedly reduce the effective cross-sectional area and result in net sectional stresses greater than nominal gross section stress. The end result is that the pitting may interfere with the valid evaluation of the SCC resistance of the material. For this reason, ASTM G47 and G64 recommend a 10-day alternate immersion exposure period for 2xxx series Al alloys when tested in the ST orientation and a 40-day exposure period when tested in the L and LT orientations. These exposure periods are believed to be long enough to detect susceptibility to intergranular SCC yet short enough to avoid excessive pitting that can lead to failure by another mechanism. General pitting, which served as initiation sites for SCC, was noted in the aft bulkhead material following 30-day alternate immersion exposure. The NESC team recommends that further evaluation of the aft bulkhead material be evaluated at shorter exposure times.

For alloys requiring microstructural control to avoid susceptibility to SCC, resistance is obtained by using heat treatments that produce uniform precipitation throughout the microstructure. The susceptibility of the Al 2219 aft bulkhead material to SCC is further exacerbated by the T62 temper, which results in a non-uniform distribution of precipitates. Because of the pitting potential and a susceptible heat treat temper to SCC, deployment of this material for the aft bulkhead may require a materials usage agreement (MUA) prior to acceptance for service.

Interpreting the significance of the SCC results was difficult due to the small data sets generated and the limited SCC data available in handbooks and open literature publications for Al 2219-T6. While the SCC results provide insight about the performance of spin formed Al 2219-T62 material, the data sets were insufficient to establish a threshold stress level for SCC, information that is of high importance to the LM Orion design team. The NESC team recommends that additional SCC testing be performed on serial aft bulkheads to define the SCC threshold. Additionally, SCC testing of Al 2219-T6 wrought products should be performed to generate sufficient data to substantiate handbook and table ratings of the SCC resistance of Al 2219. Finally, in order to understand the impact of the SCC susceptibility of the material on fracture toughness and fatigue, the NESC team recommends evaluating environmentally assisted cracking fracture toughness (KEAC) and fatigue ($(da/dN)_{SCC)}$ in the S-T orientation in a 3.5% NaCl solution.

Based upon the findings and observations, recommendations for follow-on testing to be conducted by Orion are made. A supplemental mechanical property test program designed to address key findings and observations is also presented. Due to project milestones and schedule, the results from these supplemental tests were not available in time to be included in this final report, but are provided in a supplemental NESC report, T1-13-00884_Supplemental Report, and published in NASA-TM-2015-218797 (ref. 43).

5.0 Background

The primary structural elements of the Orion welded crew module (WCM), shown in Figure 5.0-1, consist of a single piece forged barrel, a multi-piece cone section, a single piece forward bulkhead, a single piece forward tunnel, integrated forward gussets, and a multi-piece welded aft bulkhead. The aft bulkhead configuration shown is assembled from Al-Li 2195 using one circular and two latitudinal welds. Fabrication of a Al 2219 single-piece aft bulkhead by spin forming, as is now planned by the Orion Program, will eliminate these welds, improving manufacturing efficiency and reducing the risk associated with welded structure.

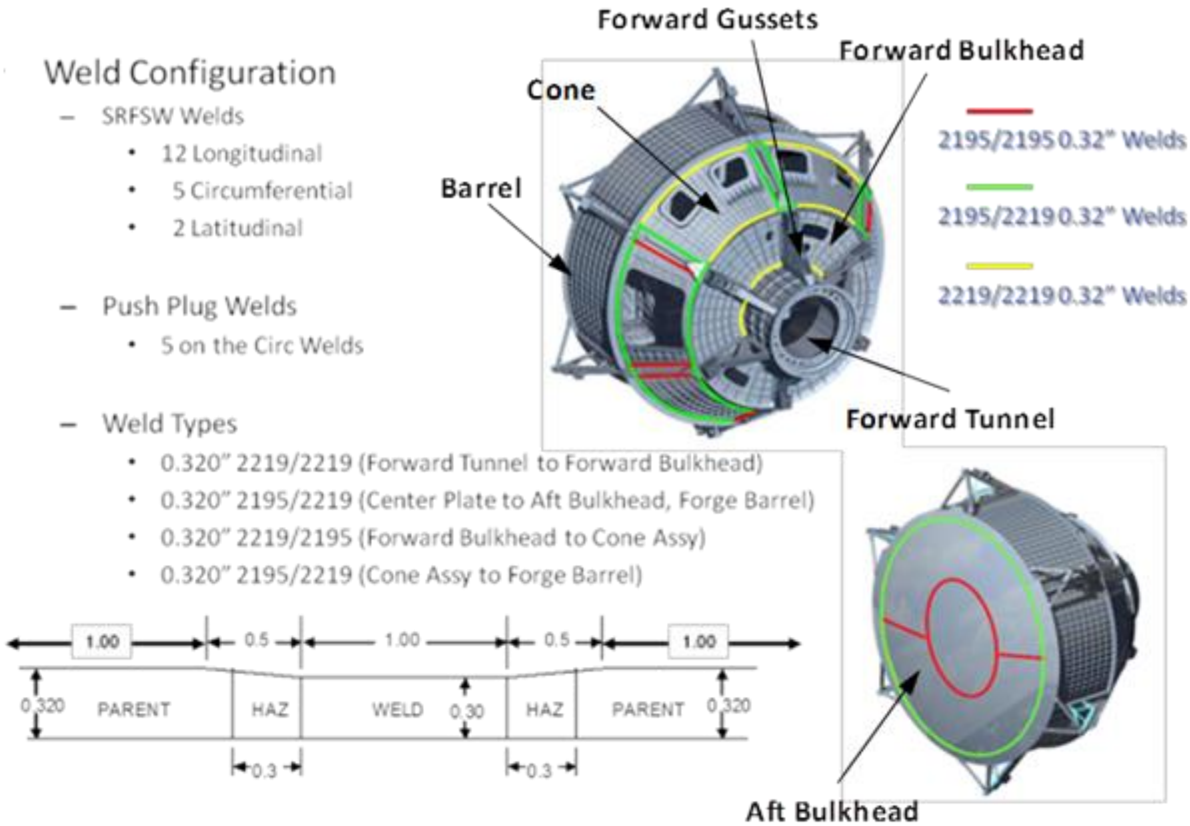

Figure 5.0-1. Welded MPCV CM Configuration

Spin forming is an established commercial metalworking process used in many industries, including fabrication of cryogenic tank domes. In convex spin forming, a circular disc of metal, called the forming blank, and a mandrel, whose shape corresponds to the internal contour of the part to be produced, are mounted in a spinning lathe (Figure 5.0-2). The blank is clamped between mandrel and a follower on the tailstock spindle of the lathe. The mandrel, blank, and follower are then set in rotation. During rotation, a forming roller is used to apply localized pressure to the blank to gradually form it over the mandrel. The size of the part and the thickness and alloy of the forming blank will determine the force required to deform the metal blank to the shape (contour) of the mandrel. Heating of the part during spinning (hot forming) is determined to meet the force requirements and/or the ductility requirements during forming.

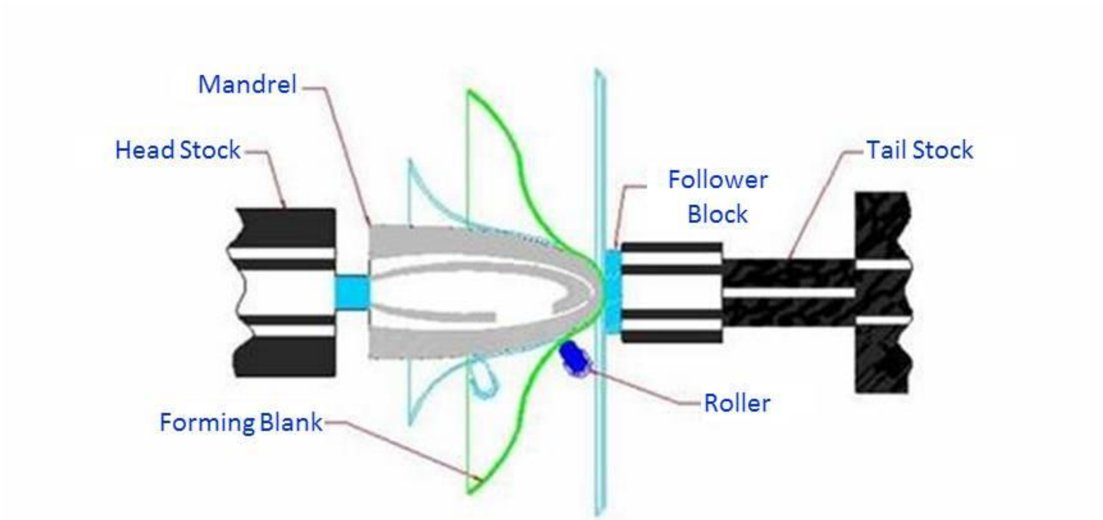

[Credit: Spincraft]

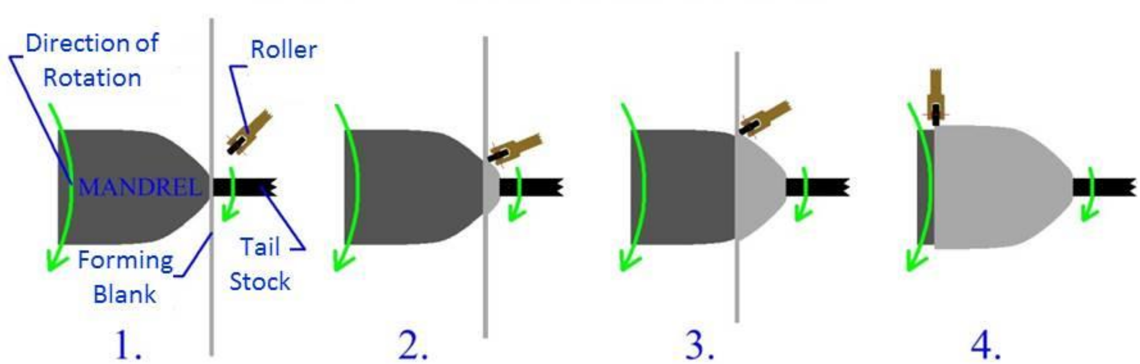

Figure 5.0-2. Schematic of the Metal Spinning Process
[Credit: The Library of Manufacturing – Metal Spinning]

Spin forming is applicable to most malleable metals and can produce a wide range of part sizes; parts can be spun up to 26 feet in diameter and thicknesses of up to 4.5 inches for Al and 1.5 inches in ferrous alloys. Spin forming is particularly adaptable to rotationally symmetric hollow shapes, such as cylinders, cones, and hemispheres and can enable considerable savings in both materials and manufacturing costs compared with other fabrication methods. Benefits include simple and low cost tooling requirements, involving primarily a contoured spinning mandrel, reduced lead times, and increased material yields compared to other forming methods.

The deformation induced during spin forming is complex and non-uniform. During convex spin forming there is generally no deliberate reduction in wall thickness as the material is shaped over the mandrel (2). Through-thickness compressive stresses are generated as a result of pressure from the forming tool as well as the strains induced during forming of the contour. During forming the blank diameter is reduced as material is pushed onto the mandrel, particularly near the rim, consequently the material experiences circumferential compressive stress superimposed on radial tensile stress, which combine to result in nearly constant wall thickness. The tool pressure is fairly uniform from the pole to the rim, but the imposed strain levels likely increase due to the superimposed forming stresses (tangential compressive and radial tensile and compressive) acting on the material, particularly towards the edge of the forming blank. So many process parameters affect material response during spin forming that modeling the process has been unsuccessful. The industrial success of spin forming is based on extensive experience at the vendors.

Producing a single-piece aft bulkhead by spin forming is consistent with design for manufacturing principles that enable lower manufacturing costs by reducing the number of parts and manufacturing steps. Eliminating welds reduces mass by eliminating weld lands and cost because post-weld NDE is no longer required. Spin forming has potential weight and production cost advantages over the current MPCV welded CM design and provides opportunities for improved performance and design margins as a result of design changes made possible using spin forming. A single-piece aft bulkhead also enables a simplified design analysis, which improves the fidelity of analysis and reduces the risk of analysis errors.

The components of the CM are constructed from high strength, heat treatable Al alloys such as Al 2219 and Al-Li 2195 because they offer high strength-to-weight ratios, good fracture and SCC resistance properties, and are weldable via FSW. These alloys are typically used in the T8 heat treat temper, which involves a solution heat treatment, water quench, and cold work to promote precipitation strengthening during subsequent artificial aging heat treatments. The thickness of the aft bulkhead is large enough that uniform cold stretch/work cannot be introduced after solution heat treatment. Consequently, the final heat treat temper for the aft bulkhead is T6 (solution heat treat, water quench, and age), which can result in lower strength, greater potential for pitting corrosion, and greater susceptibility to SCC compared to T8 temper products. In addition, very little data exist in open literature sources on mechanical properties of spin formed products. The spin formed aft bulkhead mechanical properties were compared to existing databases and standards for both T6 and T8 wrought plate and fabricated product forms to assist designers in determining any property knockdowns associated with the spin forming process and to provide fundamental material property data sets for manufacturing trade studies.

Throughout this report the temper designations will follow the Aluminum Association's definitions of T6 being solution heat treated and then artificially aged by the material producer and T62 being solution heat treated and then artificially aged by the user. Furthermore, the aft bulkhead material was also compared to both wrought plate and fabricated products forms in the T851 and T87 temper. T851 temper is solution heat treated, stress-relieved by controlled stretching (permanent set 1.5% to 3% for plate) and then artificially aged while T87 temper is solution heat treated, cold worked approximately 7% and then artificially aged.

See Appendix, Section 20.1, for a full description of the temper designations used in this report.

5.1 Goals and Objectives

The proposed scope of this Phase II project was to spin form an aft bulkhead test article to assess the mechanical properties (e.g., tensile, fracture, and SCC) and to provide representative spin formed material for LM circumferential FSW development. A second objective was to conduct a feasibility study to spin form a 6-inch thick single-piece cone to accommodate integral machining of all required structural elements (i.e., window frames, door hatches, etc.). A closer investigation of the cone region showed that the thickness requirements were approximately 8 inches and spin forming using current capabilities was not feasible; therefore, this objective was cancelled. A summary of the cone feasibility study will be provided in a supplement to this report.

5.2 Spin Formed Aft-Bulkhead Pathfinder

This task included spin forming and heat treating a pathfinder article from a single plate of Al 2219 (1.5 to 2.5-inch thick) with a diameter and curvature similar to the Orion CM aft bulkhead. After fabrication, the pathfinder was sectioned to supply spin formed material to support the two following studies that were conducted in parallel.

i. **Material Property Testing:** The NESC team conducted a microstructure (grain size) evaluation, tensile and fracture toughness property testing, and SCC characterization to develop an initial property database for spin formed and heat treated Al 2219. Selected pathfinder regions (acreage locations) were tested to assess uniformity.

ii. **FSW Developmen**t: The NESC team supplied LM with sufficient spin formed pathfinder material for an initial FSW development study required to optimize the final aft bulkhead pressure vessel circumferential weld. Additional material was supplied to support mechanical property and structural subcomponent testing by the Orion structural design group.

6.0 Aft-Bulkhead Spin Forming Pathfinder:

6.1 Requirements and Specifications

The preliminary design for the Al 2219 Orion aft bulkhead has a 148.8-inch diameter, a 229.3-inch radius of curvature, and a 2.6-inch wall thickness. To meet the assessment objectives, the NESC team conducted a preliminary engineering analysis to assess manufacturing capabilities, tooling requirements, production schedule, and material availability for fabricating an aft bulkhead pathfinder component using spin forming technologies currently employed for the manufacture of Al alloy cryogenic tank dome structures. The funding level and schedule did not support fabrication of tooling (mandrel) required to produce the current Orion design nor could it afford long lead times for material delivery and production schedule openings. Based on this engineering assessment, Spincraft, a division of the Standex International Corporation, of North Billerica, MA, was chosen as the contractor to produce the aft bulkhead pathfinder. Among the large-scale spin forming vendors, it was determined that only Spincraft had both the capability to produce components with the combined thickness and diameter needed to produce a pathfinder component representative of the Orion CM aft bulkhead and had production schedule openings to meet the project schedule. To support the aft bulkhead fabrication, Spincraft used an existing mandrel designed for a commercial customer that had similar size and geometry to the Orion aft bulkhead design. Figure 6.1-1 shows the aft bulkhead pathfinder component that was spin formed at Spincraft with dimensions of 135.5-inch diameter, 204.75-inch radius of curvature, and a wall thickness of 2.3 inches. Due to long material production lead times from Al producers, Spincraft was able to provide a suitably sized Al 2219 plate by diverting a plate from an existing production contract.

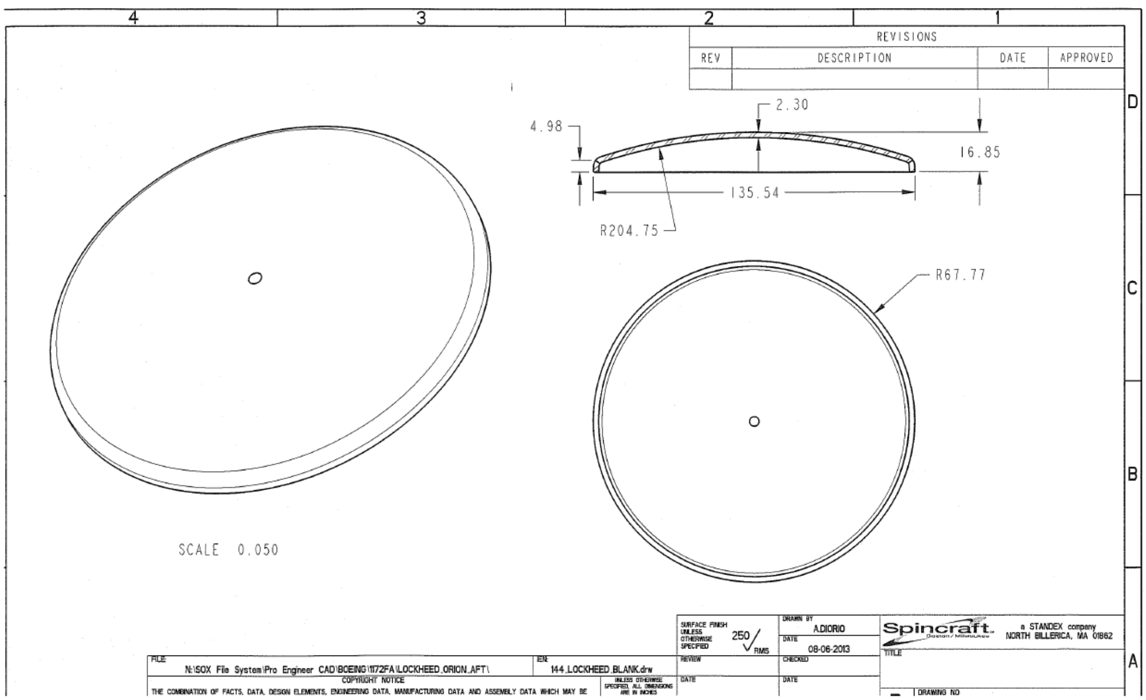

Figure 6.1-1. Proposed aft bulkhead pathfinder configuration. Dimensions are based on existing mandrel at Spincraft.

To support Orion in determining the suitability of the spin forming process for fabricating the aft bulkhead for the Orion CM, a spin formed pathfinder component was fabricated using standard spin forming technologies and practices. The spin formed component was fabricated on a best effort basis using existing commercial tooling and commercially-available materials, and was subjected to standard industry inspections, company proprietary spin forming processing, and post-forming thermal treatments.

Specifically, Spincraft was tasked with fabricating a pathfinder component through the following tasks outlined in the statement of work:

1. Perform a preliminary engineering analysis to assess the tooling requirements for fabricating the pathfinder component using spin forming technologies currently employed for manufacture of launch vehicle upper stage Al alloy cryogenic tank

dome structures. Based on preliminary designs, the component shall have approximate dimensions ranging from 100 to 150 inches diameter at the rim, 200 to 250 inches radius of curvature, and 1.5 to 2.5 inches thick.

2. Identify existing tooling necessary to support spin forming, heat treatment, and machining. Identify and procure Al 2219 plate suitable for manufacturing the pathfinder component.
3. Fabricate the pathfinder component including all preparation of the spin forming blank, spin forming operations, inspections, subsequent heat treatment and machining.
4. After all spin forming and post-fabrication processing is complete, section the pathfinder component and corner drops from the forming blank per NASA-supplied cut plan and ship pieces to NASA LaRC, MSFC, JSC, and LM-MAF.
5. Prepare a final report on the spin formed pathfinder component fabrication to include a detailed description of the tooling and fabrication process and recommendations for further process development.

6.2 Material Specifications

For the commercial production of Al 2219 spin formed components, Spincraft starts with Al 2219-F temper plate that meets material certification specifications in accordance with AMS QQ-A-250/30 (3). For domes of the size required in the aft bulkhead pathfinder, the minimum dimensions required were 2.3 inches thick x 141 inches x 141 inches. The following notes are the material specification standards utilized by Spincraft:

General notes:

1. Chemical composition shall conform to the specified standard.
2. Heat treatment response testing is required to demonstrate compliance to the T62 temper.
3. Plate shall be ultrasonically inspected for internal defects in accordance with AMS-STD-2154, Class A.
4. Plate shall be stretched to an amount necessary to achieve flatness of 1.00 inch in any 72-inch direction.
5. Provide material certification standards confirming the chemical analyses, mechanical property testing after heat treatment, and nondestructive inspection for defects are in compliance with AMS QQ-A-250/30.
6. Heat Lot Number to be marked on the plate surface using black permanent ink (STM0257A37038 or equivalent) in accordance with FED-STD-595.
7. The grain direction is to be identified on each plate by an ink arrow.
8. Water jet cut plate to form a circular blank of approximately 140-inch diameter.

9. Plate will be packaged for shipment in accordance with AMS-QQ-A-250 Level "C".
10. Shipment will include plate corners remaining after cutting circular blank.

7.0 Spin Forming Manufacturing Process

7.1 Manufacturing of Aft Bulkhead

The aft bulkhead was fabricated in accordance with Spincraft's standard practice for Al spin formed domes, process plan 2009FA, and was documented in the final report (4). The processing steps used in the production of the aft bulkhead are as follows:

1. Material procurement
2. Inspection of raw plate
3. Machining and preparation of forming blank
4. Annealing of spin forming blank
5. Spin form process
6. Post-spin forming inspection
7. Heat treatment to the T62 temper
8. Final product inspection
9. Coupon blank machining

7.2 Material Procurement

The Al 2219-F plate material used by Spincraft to spin form the aft bulkhead measured 2.3 inches x 141 inches x 141 inches and was supplied by Alcoa North American Rolled Products – Davenport Works, Davenport, IA. Chemical analysis was performed to determine the composition relative to AMS QQ-A-250/30 specification standards (Table 7.2-1). The plate stock was found to be in compliance with material certification AMS QQ-A-250/30 and of the proper thickness and size. The material certification supplied with the plate is shown in the Appendix (see Section 20.2, Figure 20.2-1).

Table 7.2-1. Chemical Composition, wt %

Heat No. H9134063; Lot No. 446391

	Si	Fe	Cu	Mn	Mg	V	Zn	Ti	Zr	Each	Total	Aluminum
Actuals	0.06	0.14	6.3	0.25	0.01	0.09	0.02	0.04	0.13			Balance

Specification AMS-QQ_A-250/30

	Si	Fe	Cu	Mn	Mg	V	Zn	Ti	Zr	Each	Total	Aluminum
Max	0.20	0.30	6.8	0.40	0.02	0.15	0.10	0.10	0.25	0.05	0.15	
Min			5.8	0.20		0.05		0.02	0.10			Balance

7.3 Inspection of Raw Plate

The incoming inspection of the raw plate consisted of verifying material certification specifications, visual inspection for defects, and measurement of plate size and thickness using an ultrasonic transmission (UT) inspection and pull tape. The incoming plate stock was found to be in compliance to the material certifications and of the proper size and thickness. Thickness of the plate was measured at numerous locations using ultrasonic methods and varied from 2.326 to 2.316 inches. Following inspection, the plate was stamped with the Alcoa plate lot number, Spincraft identification number, and plate rolling direction.

7.4 Machining and Preparation of Forming Blank

Following inspection, the plate was shipped to a waterjet vendor where it was cut into a circular forming blank measuring 140-inch in diameter. It was then re-inspected following return to Spincraft and found to be in compliance.

As per Spincraft's standard practice for spin forming domes without center holes or manways, two central pins were installed in the forming blank to support the blank during spin forming operations.

7.5 Annealing of Spin Forming Blank

The forming blank was given a full anneal in an air furnace to ensure maximum formability and ductility during spin forming operations. This annealing treatment was conducted in accordance with AMS 2770 (5) and consisted of a thermal soak at 775°F ± 25°F for a soak time of 3 hours followed by a furnace cool at 50°F per hour to 500°F, and an air cool to room temperature. The annealing treatment used is the standard practice at Spincraft for spin formed Al 2219 domes.

7.6 Spin Form Process

Spincraft uses the convex spin forming process to manufacture domes and bulkheads (Figure 7.6-1). The sequence for forming a dome from flat plate consists of a series of sequential forming operations, beginning with break forming over a dome-shaped mandrel and then final spinning over the mandrel. In this process, a thick circular blank is rigidly clamped at the pole between a head stock/mandrel assembly and a tail stock, and the assembly is rotated about its central axis. A roller forming tool is used to force the forming blank against the mandrel as it translates from the pole to rim along the outer mold line surface (OML or convex side) of the rotating blank in multiple forming steps. The force of the roller forming tool against the forming blank causes the metal to plastically deform and flow against the mandrel. In the final spin forming operation, the dome or bulkhead is spun against the male tool until the desired surface contour is achieved to create the final dome configuration.

The forming blank was installed on the convex spin forming lathe and spin formed to the contour of the mandrel as per Spincraft's standard production practice. Torches were used to heat the mandrel and forming blank to the forming temperature of 500 to 700°F. Temperatures were monitored with temperature indicating sticks and recorded throughout the spin forming process.

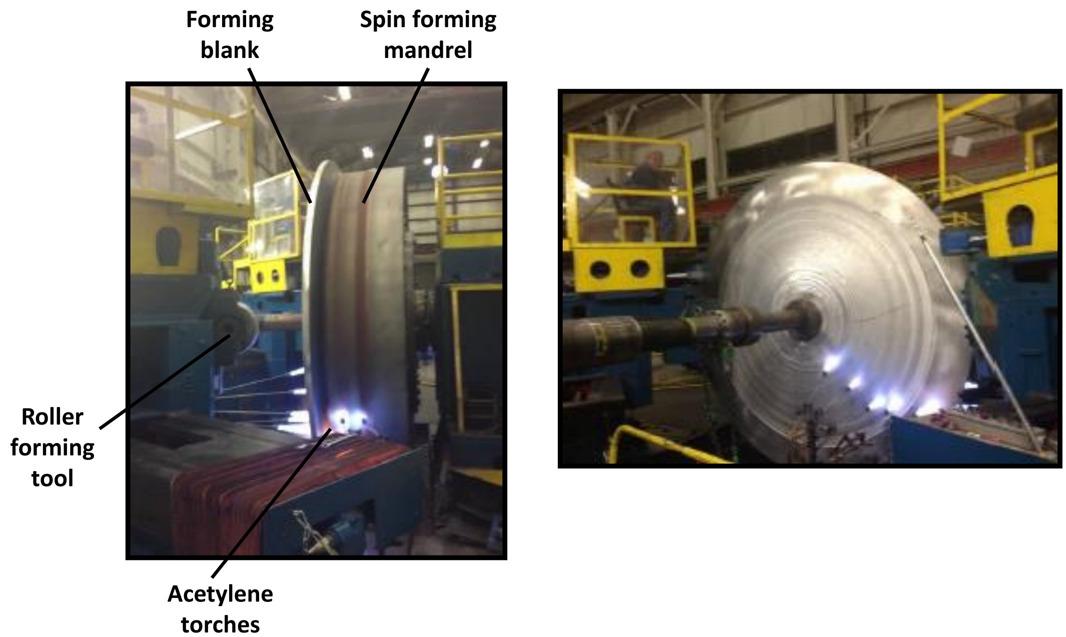

Figure 7.6-1. Convex Spin Forming of the Aft Bulkhead

7.7 Post Spin Forming Inspection

Following spin forming, the aft bulkhead was removed from the tooling and visually inspected for defects. The inner mold line (IML) surface of the aft bulkhead was inspected with forming inspection templates with the same contour shape as the mandrel while the circumference of the aft bulkhead was measured with pi tape to verify that the aft bulkhead was in compliance with the final part contour and diametric specifications. No visible damage or contour deviations were noted.

The thickness of the aft bulkhead was measured using ultrasonic methods at locations along the inspection template noted numerically in Figure 7.7-1. Measurements were made at locations 5 through 20, spaced 4 inches apart along the meridian line, spanning from 4 to 64 inches from the pole. Measurements 12 and 13 were separated by 8 inches. Measurements were made along four meridian lines at 90 degree intervals and results for each meridian and the average are provided in Table 7.7-1 and shown graphically in Figure 7.7-2. The OML surface of the aft bulkhead exhibited a scalloped pattern due to the advance of the forming roller and this is reflected in the fluctuation observed in the plotted data in Figure 7.7-2. Despite the fluctuation in the curve, overall the thickness decreased from pole to rim. The thickness was a maximum within 12 inches of the pole, a minimum at about 54 inches from the pole, and increased again at the rim. The maximum change in thickness was approximately 0.089 inches, which corresponds to a reduction in thickness of less than 4% during spin forming.

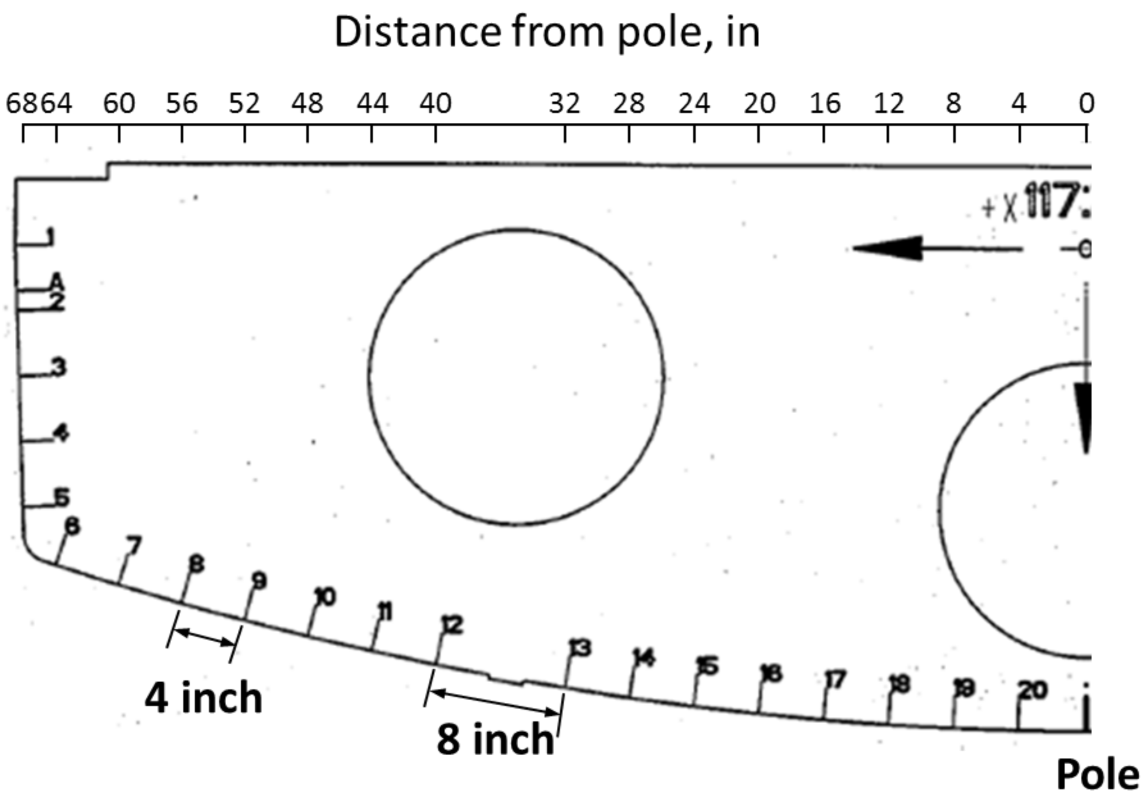

Figure 7.7-1. Schematic of forming inspection template showing numbered locations of ultrasonic thickness measurements. The aft bulkhead was measured at locations 5 through 20, with measurements made every 4 inches along a meridian line.

Table 7.7-1. Ultrasonic Thickness Measurements of the Aft Bulkhead corresponding to Locations 5 through 20 shown in Figure 7.7-1

Template Point	Distance from Pole (in)	UT Thickness Measurements (in)				
		0 deg	180 deg	90 deg	270 deg	Average
20	4	2.311	2.319	2.311	2.310	2.313
19	8	2.310	2.313	2.314	2.309	2.312
18	12	2.315	2.314	2.316	2.318	2.316
17	16	2.294	2.288	2.289	2.286	2.289
16	20	2.291	2.293	2.295	2.295	2.294
15	24	2.303	2.307	2.309	2.308	2.307
14	28	2.275	2.275	2.279	2.275	2.276
13	32	2.272	2.273	2.264	2.270	2.270
12	40	2.239	2.251	2.246	2.236	2.243
11	44	2.272	2.287	2.293	2.282	2.284
10	48	2.262	2.258	2.259	2.244	2.256
9	52	2.224	2.241	2.226	2.238	2.232
8	56	2.245	2.207	2.243	2.212	2.227
7	60	2.274	2.283	2.290	2.277	2.281
6	64	2.276	2.284	2.286	2.273	2.280
5	68	1.965	1.941	1.995	1.948	1.962

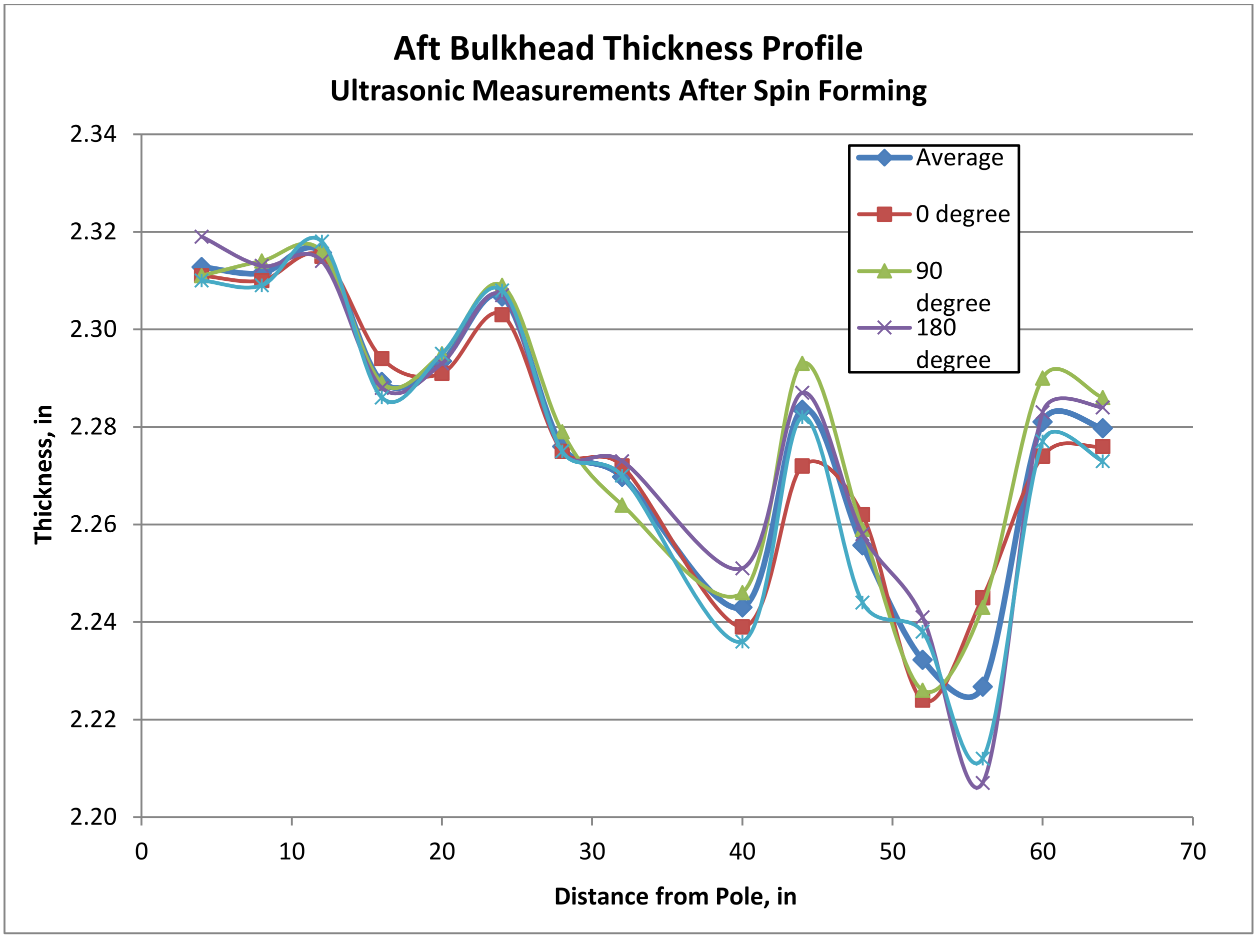

Figure 7.7-2. Thickness Profile of the Aft Bulkhead based on Ultrasonic Thickness Measurements at the Locations shown in Figure 7.7-1

7.8 Heat Treatment to the T62 Temper

Following final spinning, the Al 2219 aft bulkhead pathfinder was solution heat treated, quenched and artificially aged to the T62 temper (Figure 7.8-1). Due to the thickness of the aft bulkhead, uniform cold deformation after solution heat treatment, typically used to produce T8 temper, is not feasible. Therefore, for parts of this size and thickness, Spincraft's manufacturing process can only produce Al spin formed articles in the T62 temper. Thinner spin formed products can be produced in a T8 temper, such as the 0.5-inch-thick Shuttle External tank dome caps, which were spin formed at room temperature in the T37 condition and heat treated to T87. Solution heat treatment, quenching, and artificial aging processes for the aft bulkhead were performed per AMS 2770 specifications. This heat treatment consists of solutionizing at 995°F ± 10°F for a soak time of 3 hours, followed by a quench in 15 to 17% polymer solution type 1/water quench medium (glycol quench). This quench medium provides uniform wetting of the surface and fast, uniform heat transfer thereby reducing distortion problems normally associated with water quenched Al. Normally, following solution heat treatment to the T42 temper, spin formed Al components are installed on a hydraulic straightener and any out-of-round deviations and distortions resulting from the quenching operation are corrected. However, since this spin formed aft bulkhead did not have any finished machining sizing or contour requirements, this processing step was omitted. The aft bulkhead was then artificially aged at 375°F ± 10°F for 36 hours to the T62 temper.

Figure 7.8-1. Aft bulkhead following heat treatment.

7.9 Final Product Inspection

Following final heat treatment, hardness and electrical conductivity inspections were performed per AMS 2658 (6) to verify proper temper. All inspections were compliant to a T62 temper. An outside vendor conducted a laser tracking assessment of both the OML and IML surfaces of the aft bulkhead to confirm that the bulkhead meets the specified contour forming profile. Measurements were made from the pole to the rim at approximately 0.25 inch increments at 5-degree intervals and the results were provided electronically. The laser scan data was analyzed to determine thickness along one meridian line at the same locations as the UT measurements, as illustrated in Figure 7.9-1. The resulting thickness values are shown in Table 7.9-1 and compared with the UT data in Figure 7.9-2. Maximum thickness was at a location of approximately 8 inches from the pole, minimum thickness was at 40 inches, and the overall reduction in thickness was 0.086 inches, values, which agree well with the ultrasonic thickness measurements shown in Table 7.7-1. Figure 7.9-2 illustrates that the laser scan data also exhibits fluctuations related to the surface scalloping.

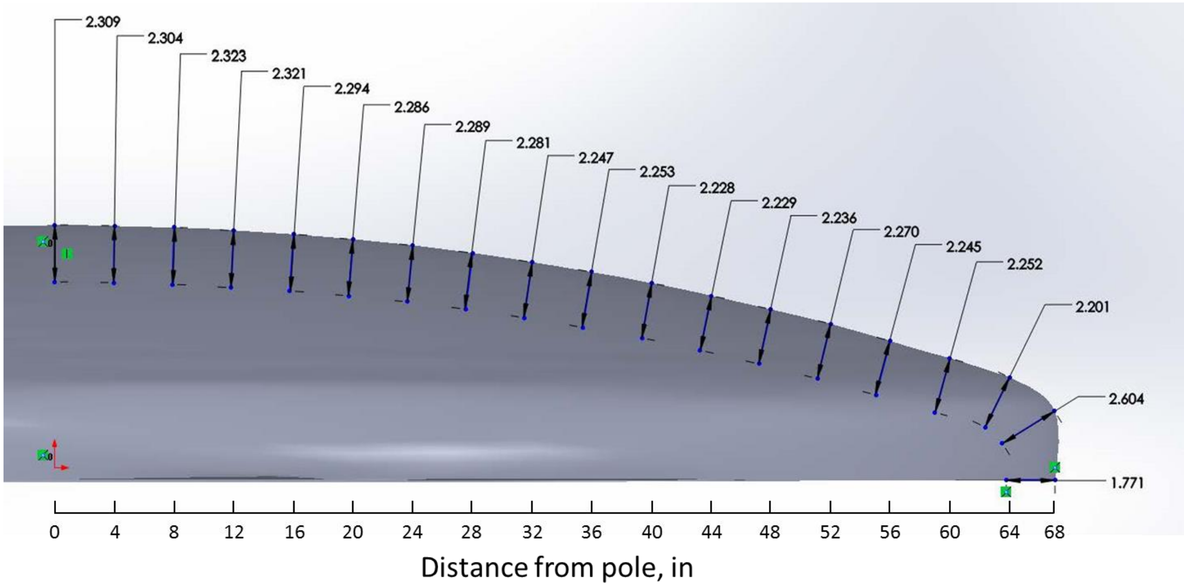

Figure 7.9-1. Section of Laser Scan showing the Locations of Thickness Determinations

Table 7.9-1. Thickness Measurements of the Aft Bulkhead Based on Laser Tracking Scans of the IML and OML

Laser Scan	
Thickness (in)	Distance from Pole (in)
2.309	0
2.304	4
2.323	8
2.321	12
2.294	16
2.286	20
2.289	24
2.281	28
2.247	32
2.253	36
2.228	40
2.229	44
2.236	48
2.270	52
2.245	56
2.252	60
2.201	64
2.604	68

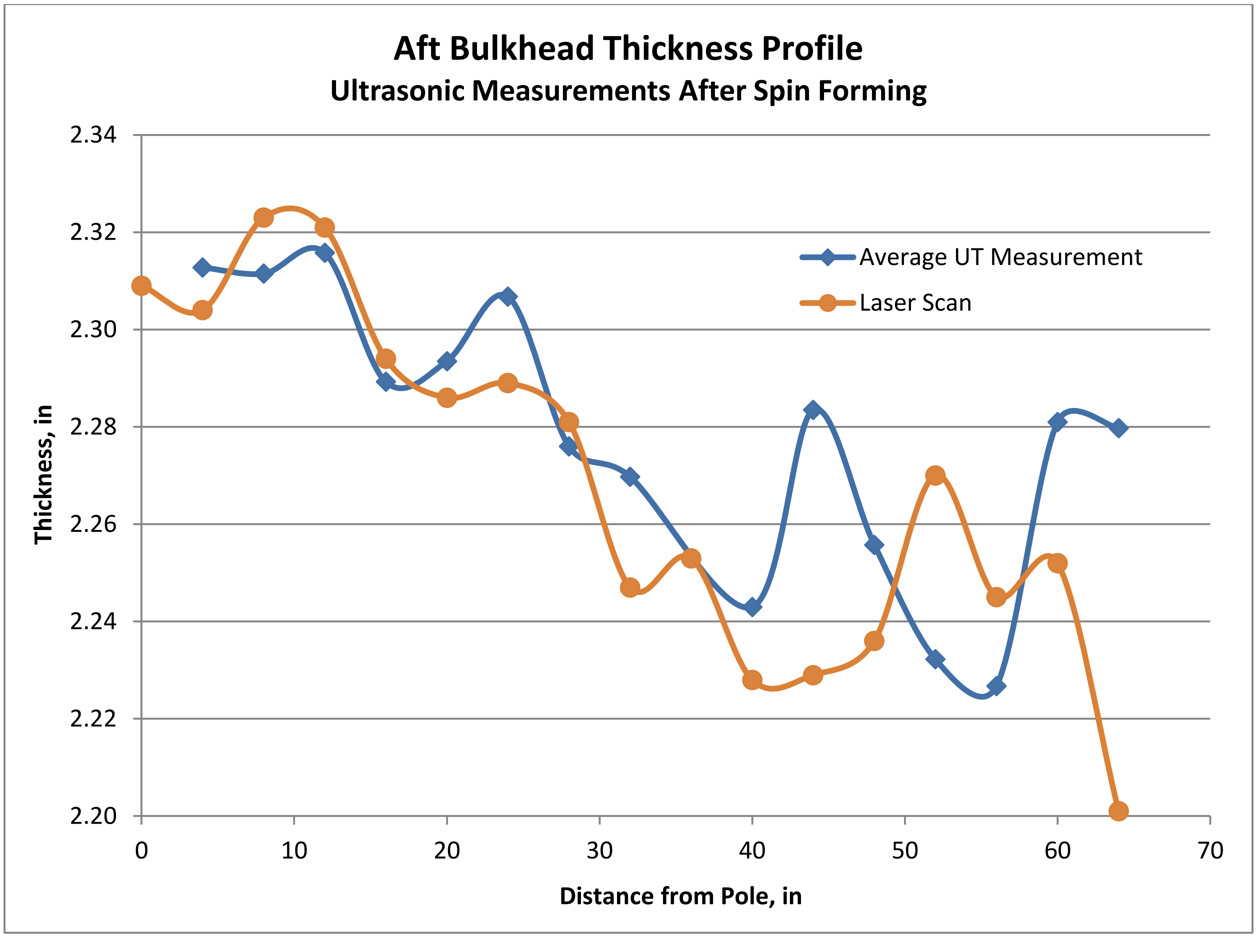

Figure 7.9-2. Thickness Measurements of the Aft Bulkhead determined from the Laser Scan Data compared with the UT Measurements

7.10 Coupon Blank Machining

A coupon cut plan was created prior to spinning the bulkhead and was used as a basis for locating the coupons to be cut for mechanical property testing, metallurgical analysis, and FSW schedule development (Figure 7.10-1). An outside vendor waterjet-machined coupon blanks from representative areas from the pole, membrane, and rim regions, as depicted in the cut plan and Figure 7.10-2.

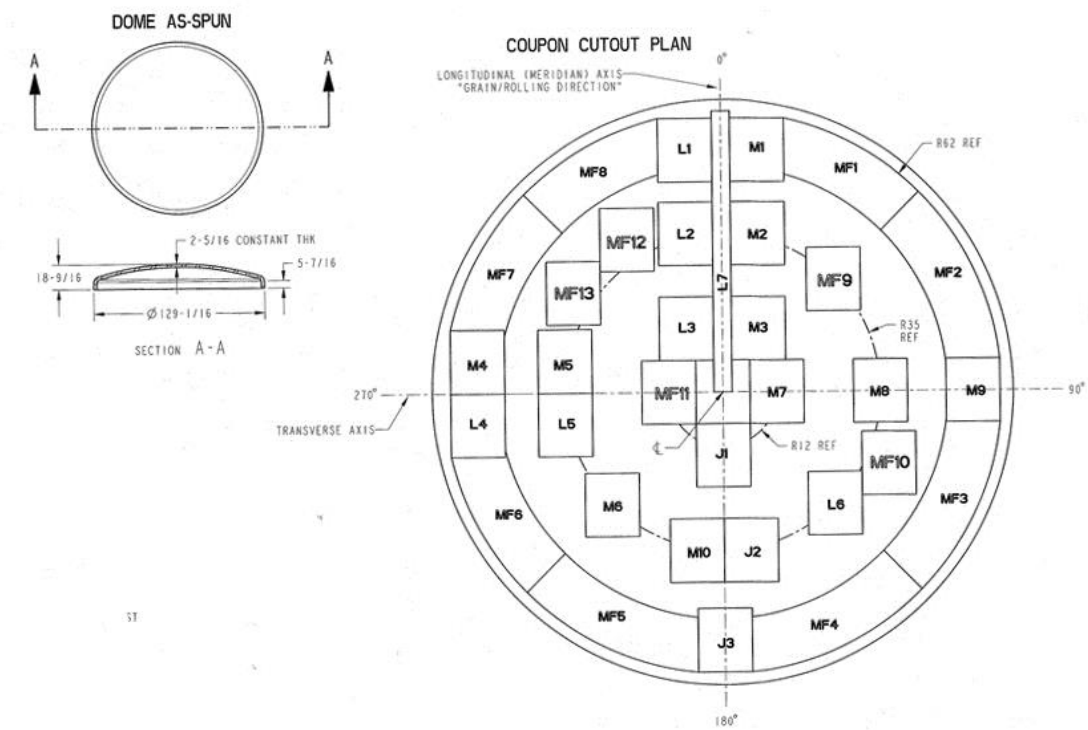

Figure 7.10-1. Aft Bulkhead Coupon Cut Plan

Figure 7.10-2. Aft Bulkhead following Extraction of Coupon Blanks for Test and Analysis

To maintain coupon blank location and orientation reference, every coupon blank was stamped with the identifying blank number, plate rolling direction (within 5 degrees), meridian arc length distance from the central pole, and meridian angle with respect to the original plate rolling direction as depicted in Figure 7.10-3 and Table 7.10-1.

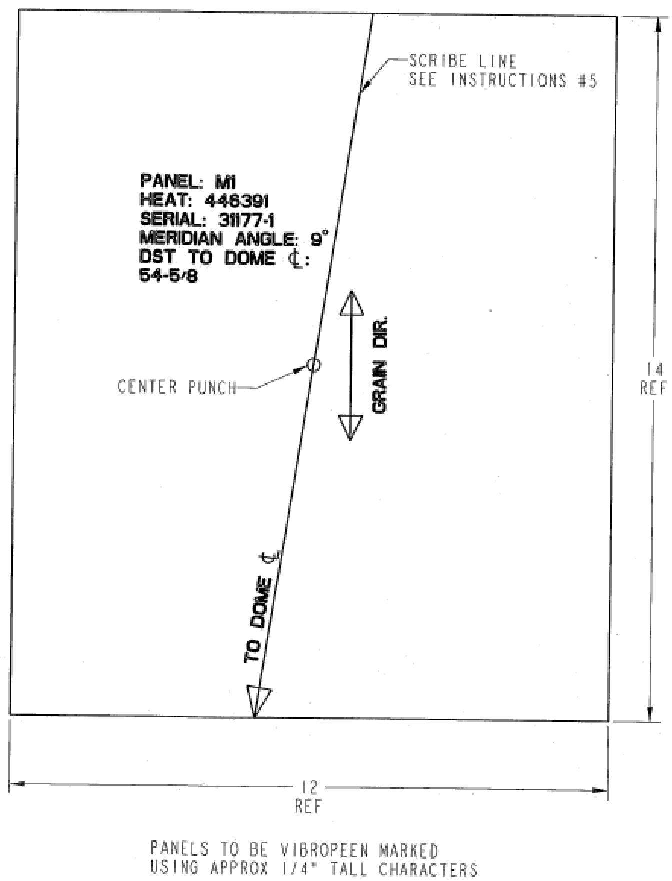

Figure 7.10-3. Coupon Blank Marking Scheme

Table 7.10-1. Location and Orientation of Coupon Blanks

Coupon Blank	Coupon Blank Size		Coupon Center Point	
	Longitudinal Dimension, in.	Transverse Dimension, in.	Meridian Angle , degrees	Arc Length from dome CL in.
M1	14	12	9°	54-5/8
M2	14	12	13°	36
M3	14	12	30°	16-1/8
M4	14	12	277°	55-1/2
M5	14	12	281°	35-7/8
M6	14	12	225°	35-1/8
M7	14	12	90°	12
M8	14	12	90°	35-1/8
M9	14	12	90°	56-1/4
M10	14	12	190°	35-5/8
J1	14	12	180°	12
J2	14	12	170°	35-5/8
J3	14	12	180°	55-5/8
MF9	14	12	45°	35-1/8
MF10	14	12	114°	40-3/8
MF11	14	12	270°	12
MF12	14	12	328°	40
MF13	14	12	304°	39-7/8
L1	14	12	351°	54-5/8
L2	14	12	347°	36
L3	14	12	330°	16-1/8
L4	14	12	259°	55-1/2
L5	14	12	263°	35-7/8
L6	14	12	135°	35-1/8
L7	CL to R62	4	0°	N/A
MF1	N/A	N/A	31°	56-3/4
MF2	N/A	N/A	64°	56-3/4
MF3	N/A	N/A	116°	56-3/4
MF4	N/A	N/A	154°	56-3/4
MF5	N/A	N/A	206°	56-3/4
MF6	N/A	N/A	240°	56-3/4
MF7	N/A	N/A	296°	56-3/4
MF8	N/A	N/A	329°	56-3/4

Additional coupon blanks were waterjet cut from the remnant plate corners remaining after machining of the circular forming blank. To assist in characterizing the effects of spin forming processing on the plate microstructure, test blocks from the remnant plate corners were thermally processed for the same temperature-time combination associated with the various thermal processing steps used in the production of the aft bulkhead (but without any spin form deformation). These thermal processing steps include the starting plate condition (F temper), pre-spin forming full anneal condition (O temper); solution heat treat condition (T4 temper), and the precipitation aged condition (T6 temper). The coupon blanks from the aft bulkhead, remnant plate corner material, and thermally processed test blocks were then shipped to the respective centers for test and analysis as shown in Table 7.10-2.

Table 7.10-2. Coupon Blank Designation, Test Center, and Test Type

Coupon Blank Designation	Test Center	Test Type
L1, L2, L3, L4, L5, L6	LaRC	Tensile
L7, F, O, T4, T6 test blocks	LaRC	Metallurgical analysis
M1, M2, M3, M4, M5, M6	MSFC	Fracture toughness
M7, M8, M9, M10	MSFC	SCC
J1, J2, J3	JSC/KSC	Seacoast exposure SCC[1]
MF1, MF2, MF3, MF4, MF5, MF6 MF7, MF8	MAF	FSW development
MF9, MF10, MF11, MF12, MF13	MAF	Mechanical property and structural subcomponent testing

1 Specimens for seacoast exposure were diverted to laboratory alternate immersion SCC testing at MSFC.

8.0 Aft Bulkhead Test and Analysis

The overall goal of testing and analysis was to examine property uniformity throughout the aft bulkhead and to determine how the properties compared with Al 2219 plate and other formed components. The Spincraft spin forming process cannot impart cold stretch prior to aging, consequently the aft bulkhead was heat treated to the T62 condition. The aft bulkhead mechanical properties were evaluated to determine whether results were comparable (in family) with T6 products. Comparison with Al 2219-T851 plate was made since this is the condition used for elements of the Orion CM that are machined from thick plate and would likely be the condition used if a multi-piece welded Al 2219 aft bulkhead were produced. For cases in which little or no data were available for T851 plate, comparisons were made with T87 plate. Metallurgical analysis and mechanical property (tensile, fracture toughness, stress corrosion) evaluation of the fully processed spin formed Al 2219 aft bulkhead pathfinder component was performed to screen property levels and to provide recommendations to the Orion Program Office regarding implementation of the spin forming fabrication method.

The aft bulkhead was successfully spin formed, heat treated and sectioned for coupon testing. Dimensional analysis was conducted on the completed bulkhead and confirmed that final shape conformed to the manufacturing mandrel and any warping from solution heat treat, quench, or artificial aging was within acceptable manufacturing tolerances. An aft bulkhead coupon cut plan was created prior to spinning the bulkhead and was used as a basis for locating the coupons to be sectioned. Additional metallurgical and fractographic analyses were conducted to gain further insight into the effects of the processing and heat treat practice on the Al 2219 microstructure and resultant mechanical properties.

8.1 Test and Analysis Procedures

The spin formed aft bulkhead dome coupon testing was conducted by NASA LaRC, NASA MSFC, and NASA JSC. Qualifying tests were also conducted by LM-MAF, but are not included in this report due to schedule and mission requirements. Table 7.10-2 shows the test center and test type based upon coupon blank letter and number designations. Further details on the test and analysis procedures are presented in Sections 8.2 through 8.6.

8.2 Metallurgical Analysis

A strip-shaped blank was cut from the fully processed aft bulkhead for metallurgical analysis, spanning from the center of the aft bulkhead to near the rim along the 0° meridian line, noted as L7 in Figure 8.2-1. The blank dimensions were 4 inches in the transverse plate direction and 62 inches along the meridian. Metallurgical samples were extracted at five locations along the strip as shown in Figure 8.2-2.

Samples L7-1 through L7-5 were located at arc length distances from the pole that corresponded approximately to L/8 (8 inches), L/4 (16 inches), L/2 (27 inches), 3L/4 (43 inches), and L (61 inches). Samples were examined using optical microscopy to evaluate variability in grain morphology and degree of recrystallization with distance from the pole and uniformity through the thickness at each location.

The thickness of the L7 strip was measured at locations along the meridian line that corresponded to the locations of the UT measurements and laser scan analysis. Changes in thickness relative to the starting plate thickness were used to estimate the variation in deformation level throughout the aft bulkhead. Vernier calipers with ball end caps were used for these measurements.

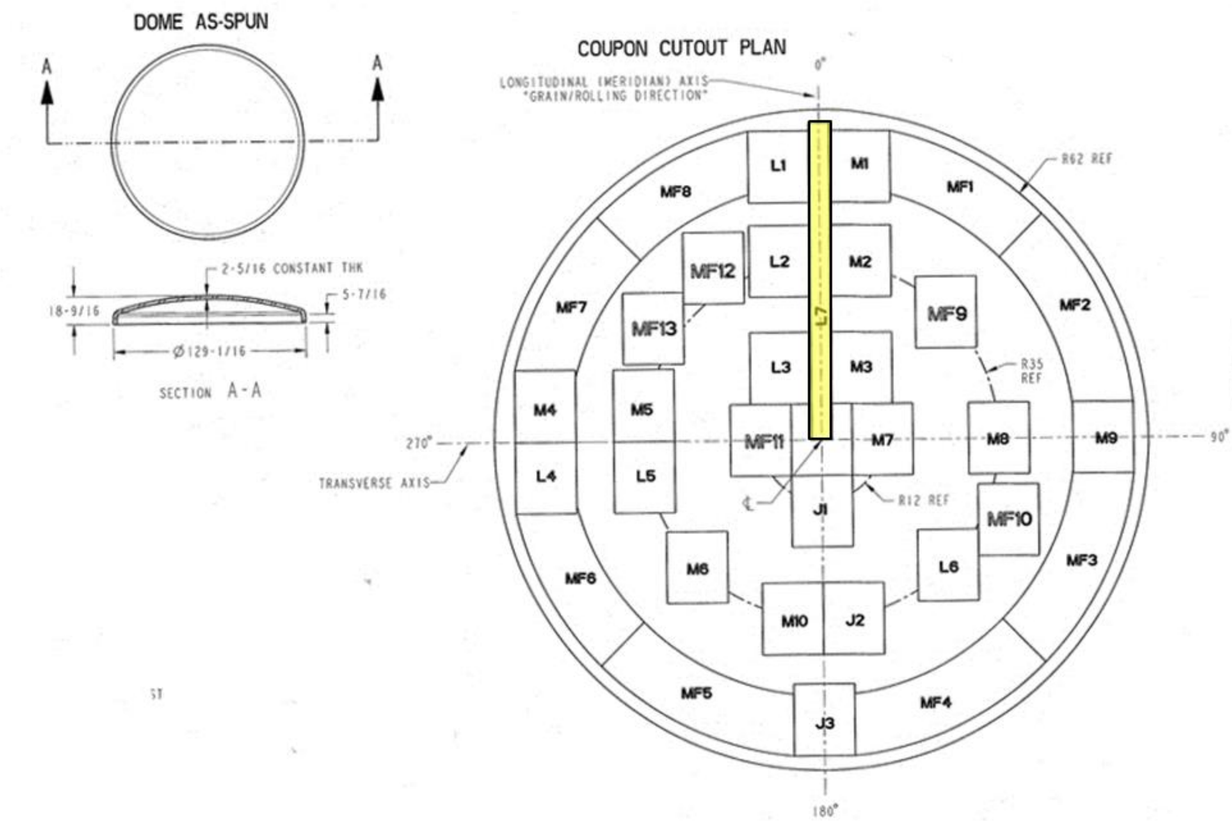

Figure 8.2-1. Aft Bulkhead Cut Plan showing the Location of the Metallurgical Analysis Strip highlighted in Yellow

Additional samples from the supplied starting plate were thermally processed at the time-temperature profiles associated with the various processing steps used in the production of the aft bulkhead (but without any spin forming deformation). Thermal exposures were performed during processing of the aft bulkhead in order to evaluate grain morphology evolution due to thermal processing alone. Samples were examined of the as-received plate (F temper), after the pre-spin forming anneal (O), after solution heat treat and water quench (T4), and after artificial aging (T6). The samples, shown in Figure 8.2-3, were examined using optical microscopy and compared with the aft bulkhead samples.

Samples of the LT-S plane were polished through various grades of SiC paper and then colloidal diamond paste. Following polishing, the samples were etched with Keller's reagent.

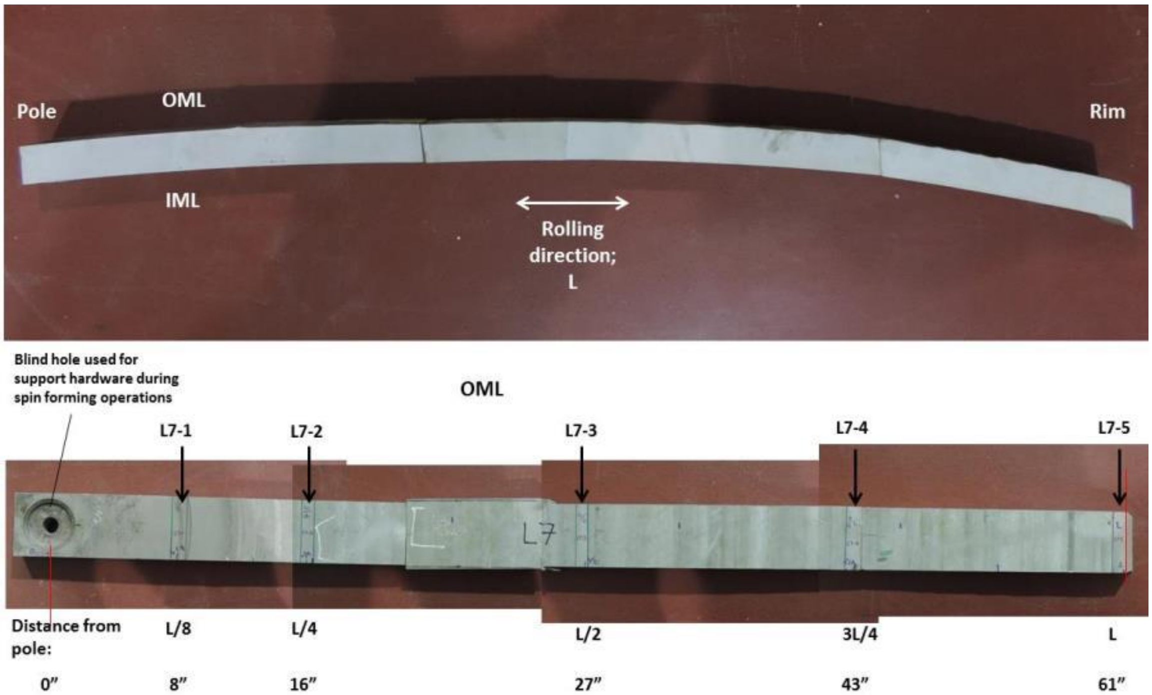

Figure 8.2-2. Metallurgical Analysis Blank showing the Locations of Specimens L7-1 through L7-5

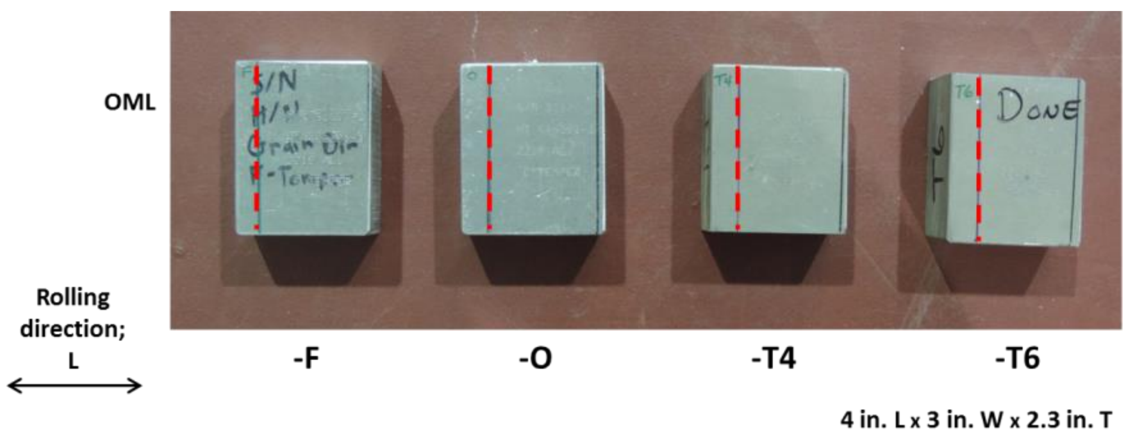

Figure 8.2-3. Thermally Processed Test Blocks

8.3 Tensile Test Procedures

Coupon blanks L1-L6 from the aft bulkhead were provided to NASA LaRC for tensile testing. These blanks were obtained from the locations highlighted in yellow in the aft bulkhead cut plan (Figure 8.3-1) and coupon blank matrix (Table 8.3-1). Additional tensile tests were conducted on coupon blanks M1-M10 provided to NASA MSFC in support of SCC and fracture testing. These coupon blanks are also shown in the accompanying figure and table.

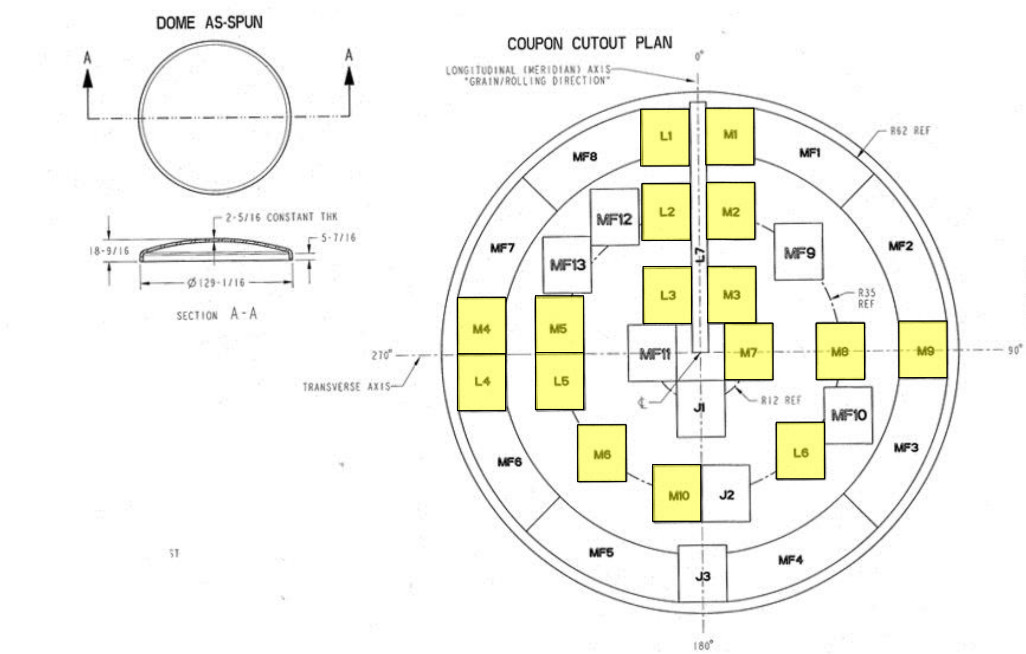

Figure 8.3-1. Aft Bulkhead Cut Plan Showing the Location of the Tensile Coupon Blanks highlighted in Yellow

Table 8.3-1. Tensile Coupon Blank Size, Locations, and Orientations

Coupon Blank	Coupon Blank Size: Long. Dimension, in.	Coupon Blank Size: Transv. Dimension, in.	Coupon Center Point: Meridian Angle , degrees	Coupon Center Point: Arc Length from dome CL in.
L1	14	12	351	54.63
L2	14	12	347	36.00
L3	14	12	330	16.13
L4	14	12	259	55.50
L5	14	12	263	35.88
L6	14	12	135	35.13
M1	14	12	9	54.63
M2	14	12	13	36.00
M3	14	12	30	16.13
M4	14	12	277	55.50
M5	14	12	281	35.88
M6	14	12	225	35.13
M7	14	12	90	12.00
M8	14	12	90	35.13
M9	14	12	90	56.25
M10	14	12	190	35.63

Tensile testing of the spin formed aft bulkhead material was conducted in accordance with ASTM E8 (7). Room temperature tensile characterization was conducted in four grain orientations; L, LT, ST, and 45° to the ST (ST45). These grain orientations were with respect to the original plate rolling direction prior to spin forming. The ST45 orientation is not a typical test orientation for Al alloy plate, but was included for two reasons: (1) there may be regions of the aft bulkhead where service loads are aligned with the ST45 orientation, and (2) metallurgical theory suggests that for some alloys this may be the minimum strength orientation for plate. Two specimen designs were used; one for the L and LT orientations (Figure 8.3-2) and one for the ST and ST45 orientations (Figure 8.3-3). All specimens were machined from the coupon blanks such that the test section was located at the mid-plane thickness (t/2) of the coupon blank. Three replicate tests were conducted for each grain orientation as per the test matrix shown in Table 8.3-2.

Tensile tests were conducted in a servo-hydraulic test machine at a displacement rate of 0.01 in/min (ipm) to specimen failure using the test setup shown in Figure 8.3-4. Back-to-back extensometers with either a 1.000 in (L and LT specimens) or 0.500 in (ST and ST45 specimens) gauge length were used to measure specimen strain response. For tensile tests conducted at NASA MSFC, the displacement rate was 0.05 ipm and only a single 1.000/0.500 in extensometer was used. Ultimate tensile strength (UTS), 0.2% YS, and percent elongation (e) were determined for each test condition. The modulus of elasticity (E) was also calculated from the stress-strain plot and is shown in the results section as a reference value. Figure 8.3-5 shows a typical stress-strain curve for a tensile test.

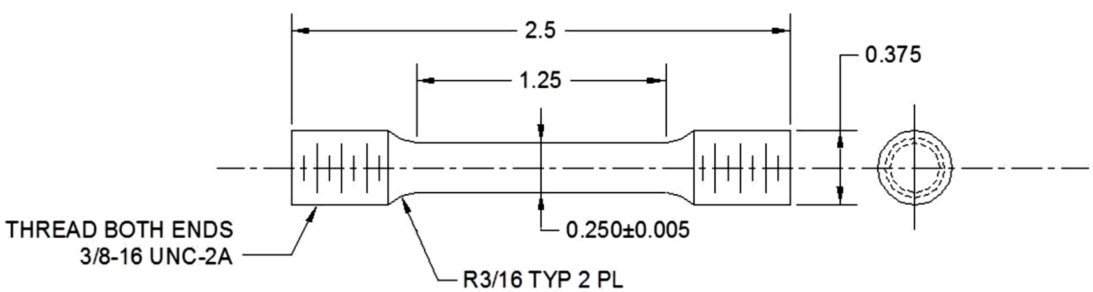

Figure 8.3-2. Round Subsize Tensile Specimen Design used for Testing in the L and LT Orientations

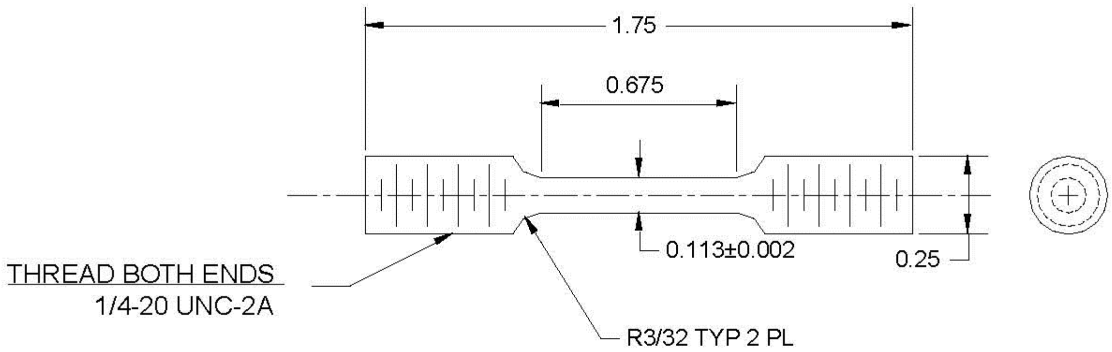

Figure 8.3-3. Round Subsize Tensile Specimen Design used for Testing in the ST and ST45 Orientations

Table 8.3-2. Tensile Test Matrix for the Aft Bulkhead

Coupon Blank	Meridian Angle, degrees	Arc Length from dome CL, in.	Orient.	Specimen Number		
L1	351	54.63	L	T-L1-L-01	T-L1-L-02	T-L1-L-03
			LT	T-L1-LT-04	T-L1-LT-05	T-L1-LT-06
			ST	T-L1-ST-07	T-L1-ST-08	T-L1-ST-09
			ST45	T-L1-ST45-10	T-L1-ST45-11	T-L1-ST45-12
L2	347	36.00	L	T-L2-L-13	T-L2-L-14	T-L2-L-15
			LT	T-L2-LT-16	T-L2-LT-17	T-L2-LT-18
			ST	T-L2-ST-19	T-L2-ST-20	T-L2-ST-21
			ST45	T-L2-ST45-22	T-L2-ST45-23	T-L2-ST45-24
L3	330	16.13	L	T-L3-L-25	T-L3-L-26	T-L3-L-27
			LT	T-L3-LT-28	T-L3-LT-29	T-L3-LT-30
			ST	T-L3-ST-31	T-L3-ST-32	T-L3-ST-33
			ST45	T-L3-ST45-34	T-L3-ST45-35	T-L3-ST45-36
L4	259	55.50	L	T-L4-L-37	T-L4-L-38	T-L4-L-39
			LT	T-L4-LT-40	T-L4-LT-41	T-L4-LT-42
			ST	T-L4-ST-43	T-L4-ST-44	T-L4-ST-45
			ST45	T-L4-ST45-46	T-L4-ST45-47	T-L4-ST45-48
L5	263	35.88	L	T-L5-L-49	T-L5-L-50	T-L5-L-51
			LT	T-L5-LT-52	T-L5-LT-53	T-L5-LT-54
			ST	T-L5-ST-55	T-L5-ST-56	T-L5-ST-57
			ST45	T-L5-ST45-58	T-L5-ST45-59	T-L5-ST45-60
L6	135	35.13	L	T-L6-L-61	T-L6-L-62	T-L6-L-63
			LT	T-L6-LT-64	T-L6-LT-65	T-L6-LT-66
			ST	T-L6-ST-67	T-L6-ST-68	T-L6-ST-69
			ST45	T-L6-ST45-70	T-L6-ST45-71	T-L6-ST45-72
M1	9	54.63	L	CP-406-190	CP-406-192	CP-406-194
			LT	CP-406-195	CP-406-197	CP-406-199
			ST	CP-406-200	CP-406-202	CP-406-204
			ST45	----	----	----
M2	13	36.00	L	CP-406-205	CP-406-207	CP-406-209
			LT	CP-406-210	CP-406-212	CP-406-214
			ST	CP-406-215	CP-406-217	CP-406-219
			ST45	----	----	----
M3	30	16.13	L	CP-406-220	CP-406-222	CP-406-224
			LT	CP-406-225	CP-406-227	CP-406-229
			ST	CP-406-230	CP-406-232	CP-406-234
			ST45	----	----	----
M4	277	55.50	L	CP-406-235	CP-406-237	CP-406-239
			LT	CP-406-240	CP-406-242	CP-406-244
			ST	CP-406-245	CP-406-247	CP-406-249
			ST45	----	----	----
M5	281	35.88	L	CP-406-250	CP-406-252	CP-406-254
			LT	CP-406-255	CP-406-257	CP-406-259
			ST	CP-406-260	CP-406-262	CP-406-264
			ST45	----	----	----
M6	225	35.13	L	CP-406-265	CP-406-267	CP-406-269
			LT	CP-406-270	CP-406-272	CP-406-274
			ST	CP-406-275	CP-406-277	CP-406-279
			ST45	----	----	----
M7	90	12.00	L	----	----	----
			LT	CP-406-1	CP-406-11	CP-406-21
			ST	CP-406-22	CP-406-32	CP-406-42
			ST45	----	----	----
M8	90	35.13	L	----	----	----
			LT	CP-406-43	CP-406-53	CP-406-63
			ST	CP-406-64	CP-406-74	CP-406-84
			ST45	----	----	----
M9	90	56.25	L	----	----	----
			LT	CP-406-85	CP-406-95	CP-406-105
			ST	CP-406-106	CP-406-116	CP-406-126
			ST45	----	----	----
M10	190	35.63	L	CP-406-127	CP-406-137	CP-406-147
			LT	CP-406-169	CP-406-179	CP-406-189
			ST	CP-406-148	CP-406-158	CP-406-168
			ST45	----	----	----

Figure 8.3-4. Tensile Test Load Stand, Specimen, and Instrumentation

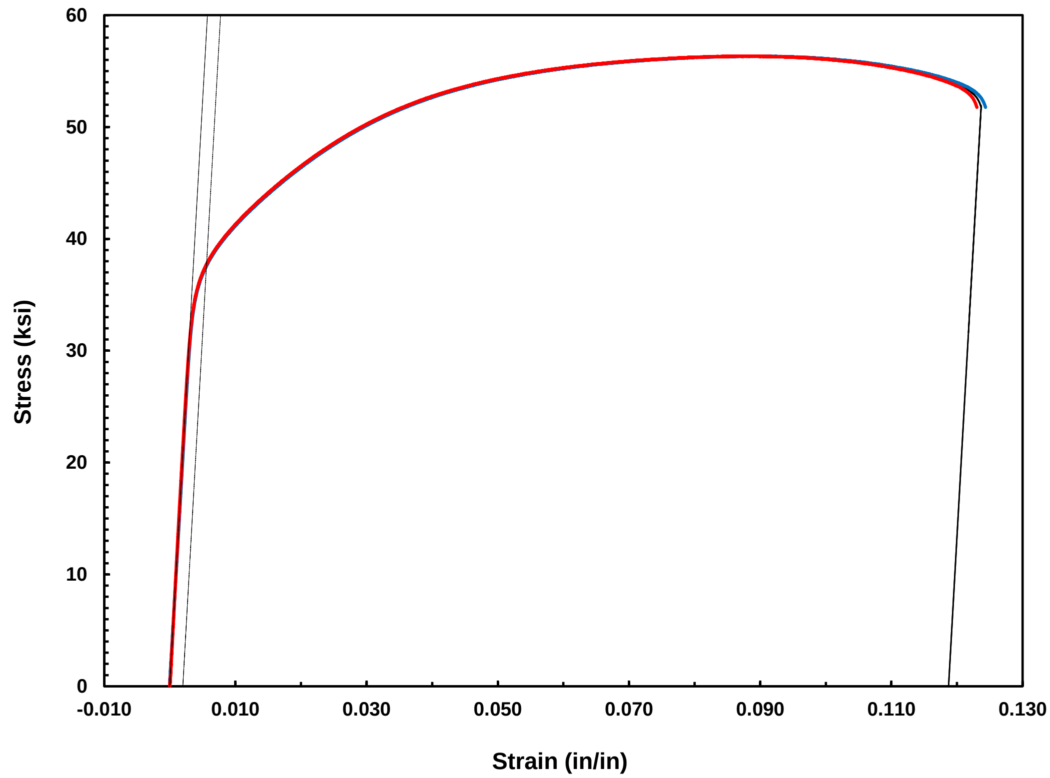

Figure 8.3-5. Typical Stress-Strain Curve for the Spin Formed Al 2219-T62 Aft Bulkhead Material in the L Orientation; Coupon Blank L2, Specimen T-L2-L-13

8.4 Fracture Toughness Test Procedures

Coupon blanks from the aft bulkhead were provided to NASA MSFC for fracture toughness testing. These blanks were identified as M1, M2, M3, M4, M5, and M6 and were obtained from the locations highlighted in yellow in the aft bulkhead cut plan (Figure 8.4-1) and coupon blank matrix (Table 8.4-1).

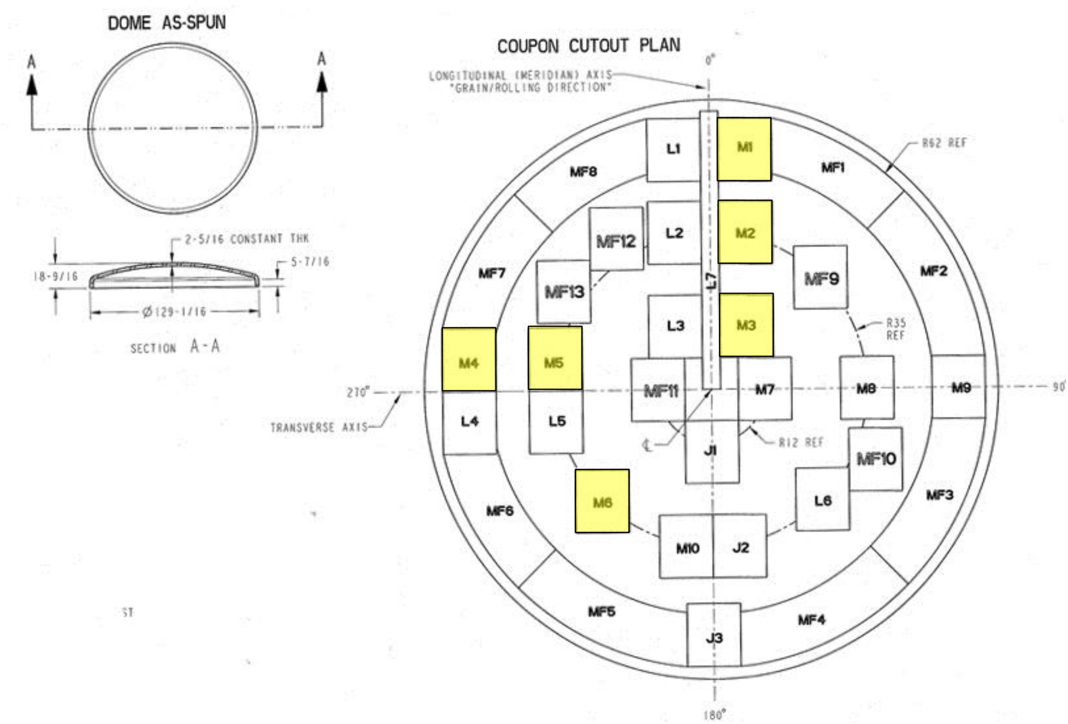

Figure 8.4-1. Aft Bulkhead Cut Plan showing the Location of the Fracture Toughness Coupon Blanks highlighted in Yellow

Table 8.4-1. Fracture toughness Coupon Blank Locations and Orientations

Coupon Blank	Coupon Blank Size		Coupon Center Point	
	Longitudinal Dimension, in.	Transverse Dimension, in.	Meridian Angle , degrees	Arc Length from dome CL in.
M1	14	12	9°	54-5/8
M2	14	12	13°	36
M3	14	12	30°	16-1/8
M4	14	12	277°	55-1/2
M5	14	12	281°	35-7/8
M6	14	12	225°	35-1/8

Fracture toughness testing of the spin formed aft bulkhead material was conducted in accordance with ASTM E1820 (8). Per this test method, the fracture toughness is quantified in terms of J_{IC}, which is a measure of the fracture toughness of the material at the onset of stable crack extension. Fracture toughness characterization was conducted in three grain orientations, L-T, T-L, and S-T. The test orientation designation first identifies the loading direction and is followed by the crack growth orientation as they relate to the grain orientation of the material. The grain orientations are relative to the original grain orientation of the rolled plate prior to spin forming. Fracture toughness was measured using a compact tension (C(T)) specimen configuration.

Two specimen designs were used; one for the L-T and T-L orientations (Figure 8.4-2) and one for the S-T orientation (Figure 8.4-3). All specimens were machined from the coupon blanks such that the test section was located at the mid-plane thickness (t/2) of the coupon blank. Two replicate tests were conducted for each grain orientation as per the test matrix shown in Table 8.4-2. The test apparatus used for fracture toughness testing is shown in Figure 8.4-4.

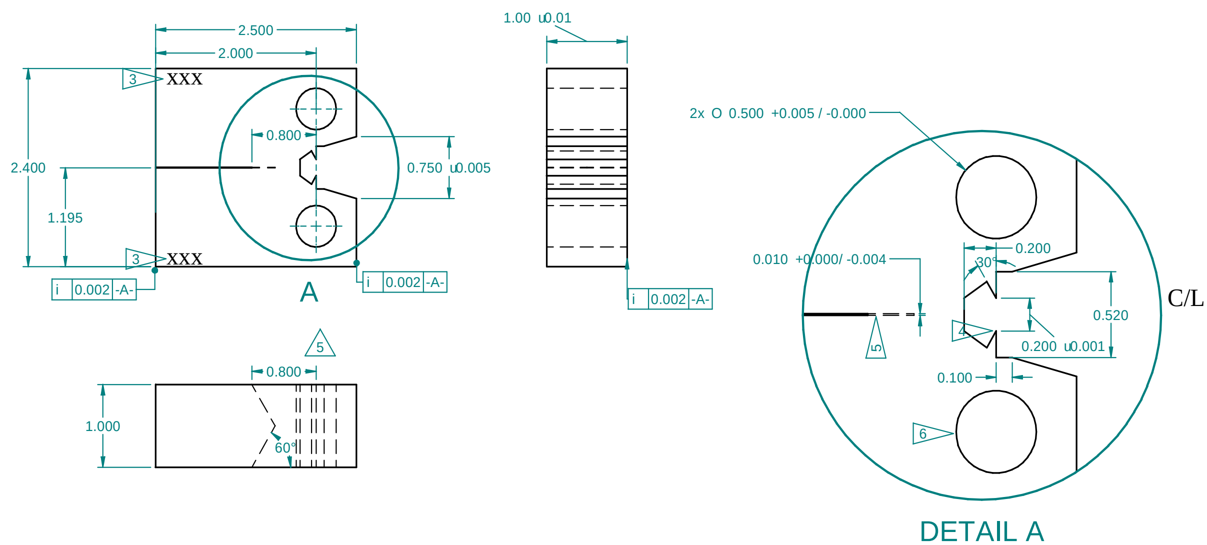

Figure 8.4-2. J_{IC} Fracture Toughness Specimen Design; L-T and T-L Orientations. Drawing No. S-295. All dimensions are in inches.

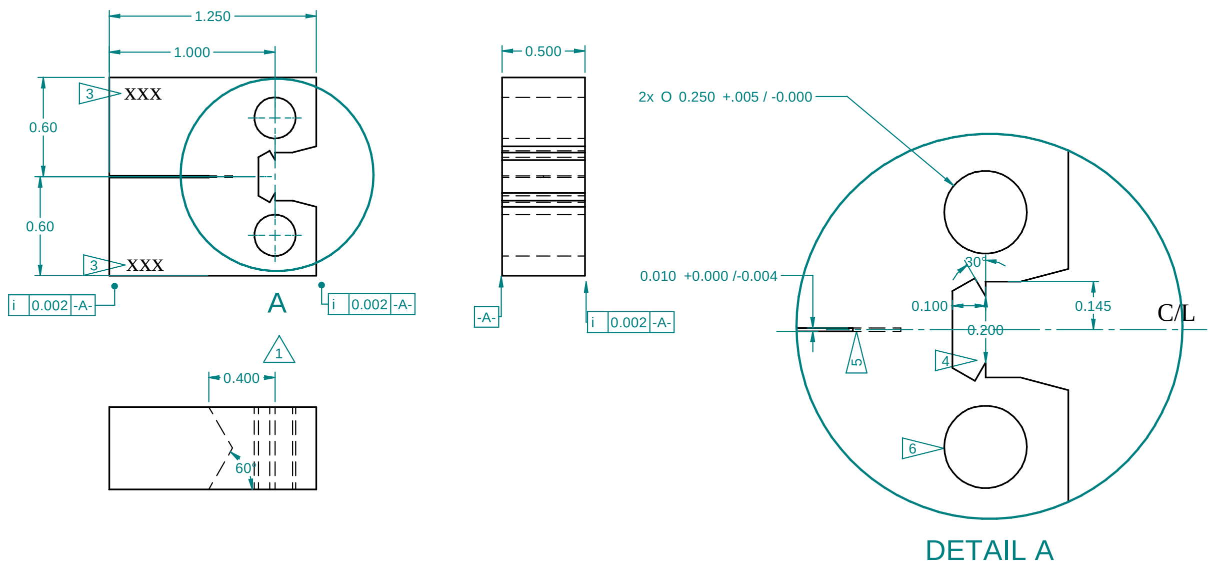

Figure 8.4-3. J_{IC} Fracture Toughness Specimen Design; S-T Orientation. Drawing No. S-294. All dimensions are in inches.

Table 8.4-2. Fracture Test Matrix for the Aft Bulkhead

Specimen ID	Coupon Blank	Orient.
CP-406-191	M1	L-T
CP-406-193	M1	L-T
CP-406-196	M1	T-L
CP-406-198	M1	T-L
CP-406-201	M1	S-T
CP-406-203	M1	S-T
CP-406-206	M2	L-T
CP-406-208	M2	L-T
CP-406-211	M2	T-L
CP-406-213	M2	T-L
CP-406-216	M2	S-T
CP-406-218	M2	S-T
CP-406-221	M3	L-T
CP-406-223	M3	L-T
CP-406-226	M3	T-L
CP-406-228	M3	T-L
CP-406-231	M3	S-T
CP-406-233	M3	S-T
CP-406-236	M4	L-T
CP-406-238	M4	L-T
CP-406-241	M4	T-L
CP-406-243	M4	T-L
CP-406-246	M4	S-T
CP-406-248	M4	S-T
CP-406-251	M5	L-T
CP-406-253	M5	L-T
CP-406-256	M5	T-L
CP-406-258	M5	T-L
CP-406-261	M5	S-T
CP-406-263	M5	S-T
CP-406-266	M6	L-T
CP-406-268	M6	L-T
CP-406-271	M6	T-L
CP-406-273	M6	T-L
CP-406-276	M6	S-T
CP-406-278	M6	S-T

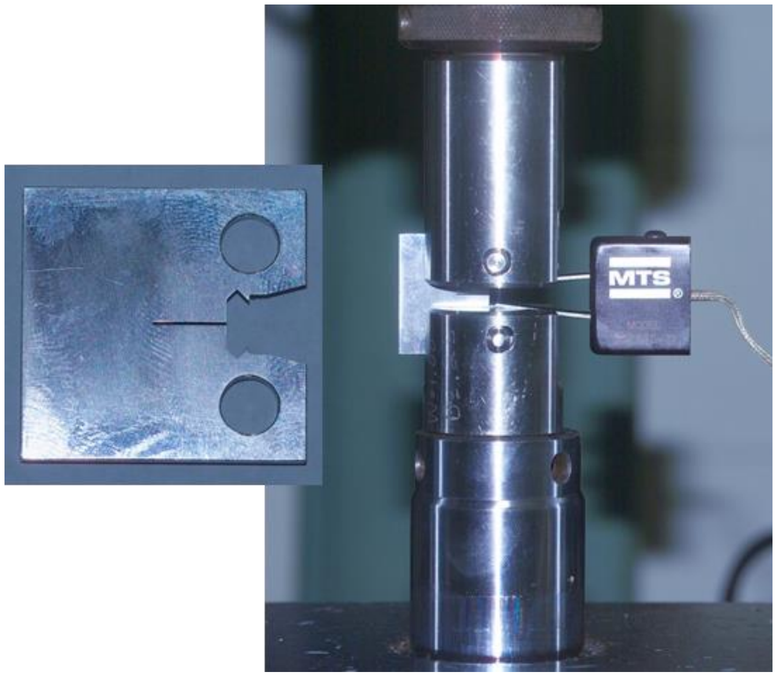

Figure 8.4-4. J_{IC} Fracture Toughness Specimen and Test Apparatus

Following machining, the C(T) specimen was cyclically loaded in tension to generate a fatigue precrack. The specimen was then tested per ASTM E1820 using the unloading compliance method for calculating crack length. A crack-mouth opening displacement gauge (COD) was used for measuring load-line displacement. The load and COD data was then used to generate a resistance curve, or R-curve, for each specimen that describes J (in-lbf/in^2) versus crack extension. An illustrative R-curve is shown in Figure 8.4-5. The critical J value, or J_{IC}, is taken where the crack extension reaches 0.008 inches. This is considered the onset of tearing. Data beyond the critical value provides insight into the ability of the material to tear (crack extension) in a stable manner. Critical J values can be converted to K values (crack tip stress intensity, ksi$\sqrt{\text{in}}$) to support linear elastic fracture analysis. In the event the material displays unstable fracture, data from the ASTM E1820 test can be used to evaluate the critical crack tip stress intensity value (K_{IC}). A typical R-curve for the spin formed aft bulkhead material is shown in Figure 8.4-6. Also, a typical post-test specimen fracture surface is shown in Figure 8.4-7. Significant features along the fracture surface are noted in Figure 8.4-7.

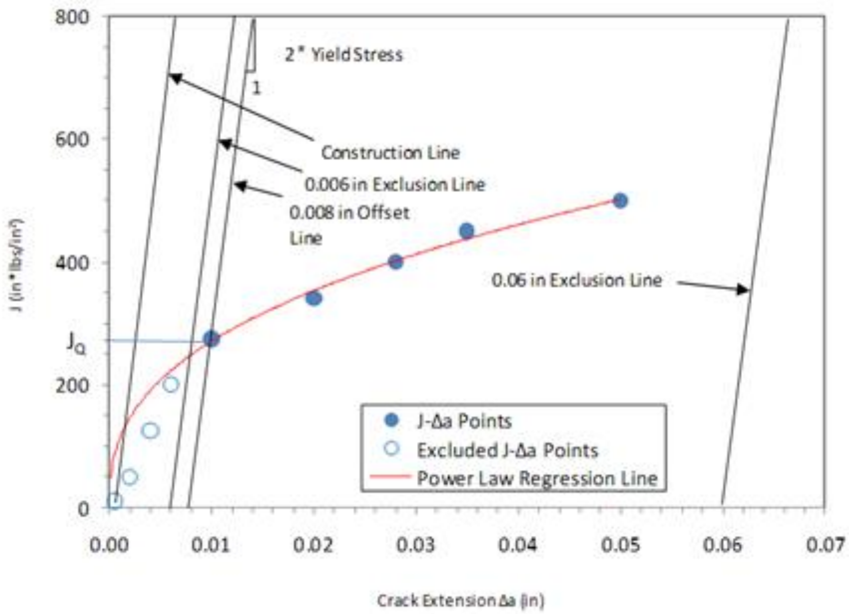

Figure 8.4-5. J_{IC} Fracture Toughness R-Curve Plot

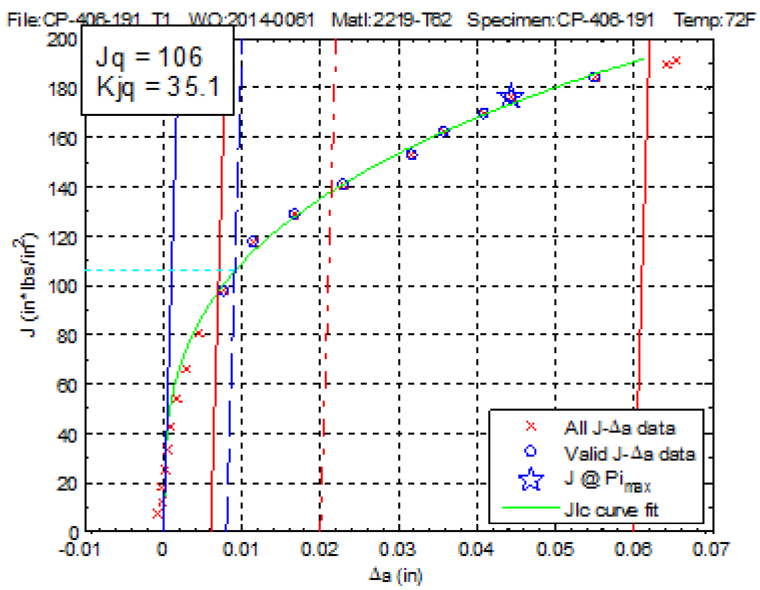

Figure 8.4-6. Typical J_{IC} Fracture Toughness R-Curve Plot
Plot shown is for specimen CP-406-191 from coupon blank M1 in the L-T orientation.

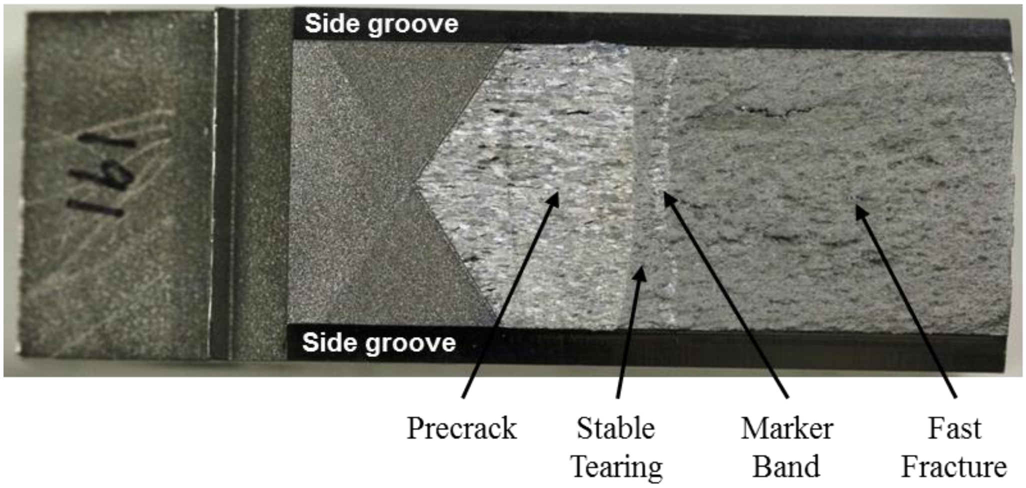

Figure 8.4-7. Typical Cross-Sectional Fracture Surface of a J_{IC} Fracture Toughness Specimen (specimen shown is CP-406-191 from coupon blank M1 in the L-T orientation)

8.5 Stress Corrosion Test Procedures

Coupon blanks M7, M8, M9, and M10 from the aft bulkhead were provided to NASA MSFC for SCC testing. These blanks were obtained from the locations highlighted in yellow in the aft bulkhead cut plan (Figure 8.5-1) and coupon blank matrix (Table 8.5-1). For each coupon blank, 21 LT and 21 ST tension specimens were machined per the ASTM E8 small-size round tension test specimen design shown in Figure 8.5-2. In addition, 21 L tension specimens were machined from coupon blank M10. These specimen orientations were with respect to the original plate rolling direction. The coupon blank cut plans for these tension specimens are shown in Figures 8.5-3 through 8.5-6. Three specimens from each set of 21 were used to obtain baseline tensile data to establish applied stress levels for SCC testing; the remaining 18 were used for SCC testing. Specimen design and test procedures for these baseline tensile tests are discussed in Section 8.3.

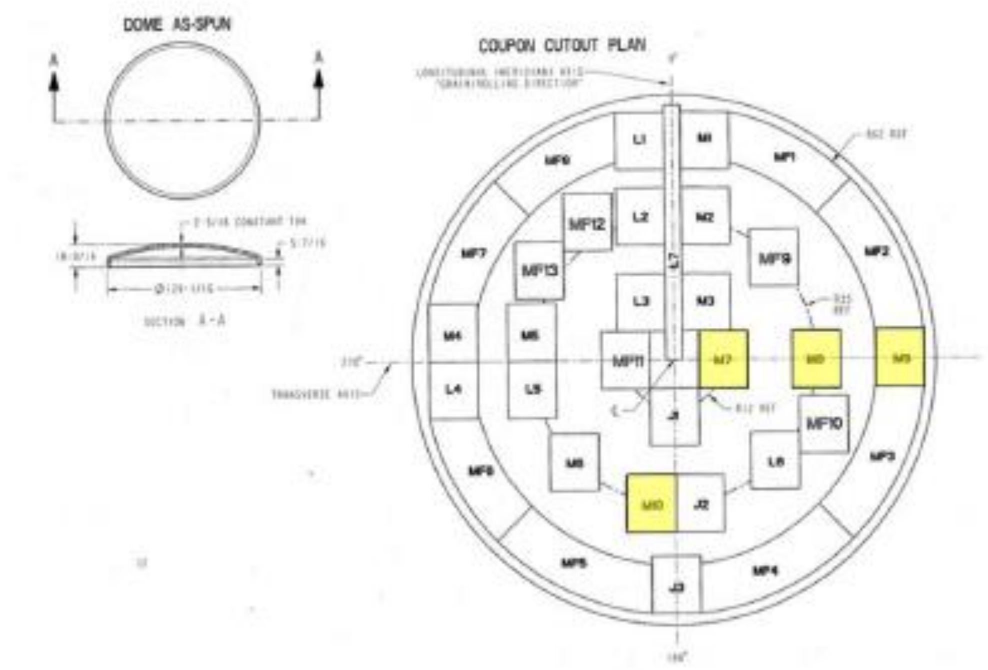

Figure 8.5-1. Aft Bulkhead Cut Plan showing the Location of the SCC Coupon Blanks highlighted in Yellow

Table 8.5-1. SCC Coupon Blank Locations and Orientations

Coupon Blank	Longitudinal Dimension, in.	Transverse Dimension, in.	Meridian Angle, degrees	Center Point Arc Length, in.
M7	14	12	90°	12.00
M8	14	12	90°	35.13
M9	14	12	90°	56.25
M10	14	12	190°	35.63

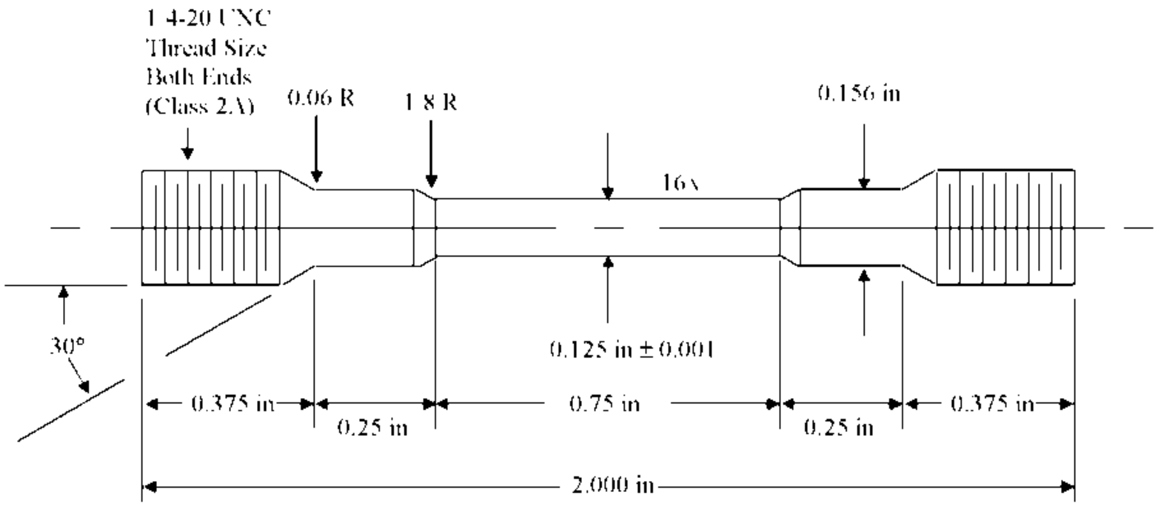

NOTES:

1. Tolerances: ± 0.005 inch, except otherwise specified.
2. Surface finish: 16√ for the reduced section, 32√ for the rest.
3. Thread dimensions must be as specified. Measurement by fabricator is mandatory.
4. No undercutting of radii permitted.
5. Gage section to be concentric with axis within 0.002 inch TIR and parallel.
6. No file marks or nicks permitted within gage section.
7. Center-drilling permissible (both ends). May use a #1 size max. Chamfer diameter not to exceed 0.100 inch.
8. Break sharp edges.
9. The reduced section may have a gradual taper from the ends toward the center with the ends not more than 0.005 inch larger diameter than the center.

Figure 8.5-2. Round Sub-Size Tensile Specimen Design used for SCC Testing

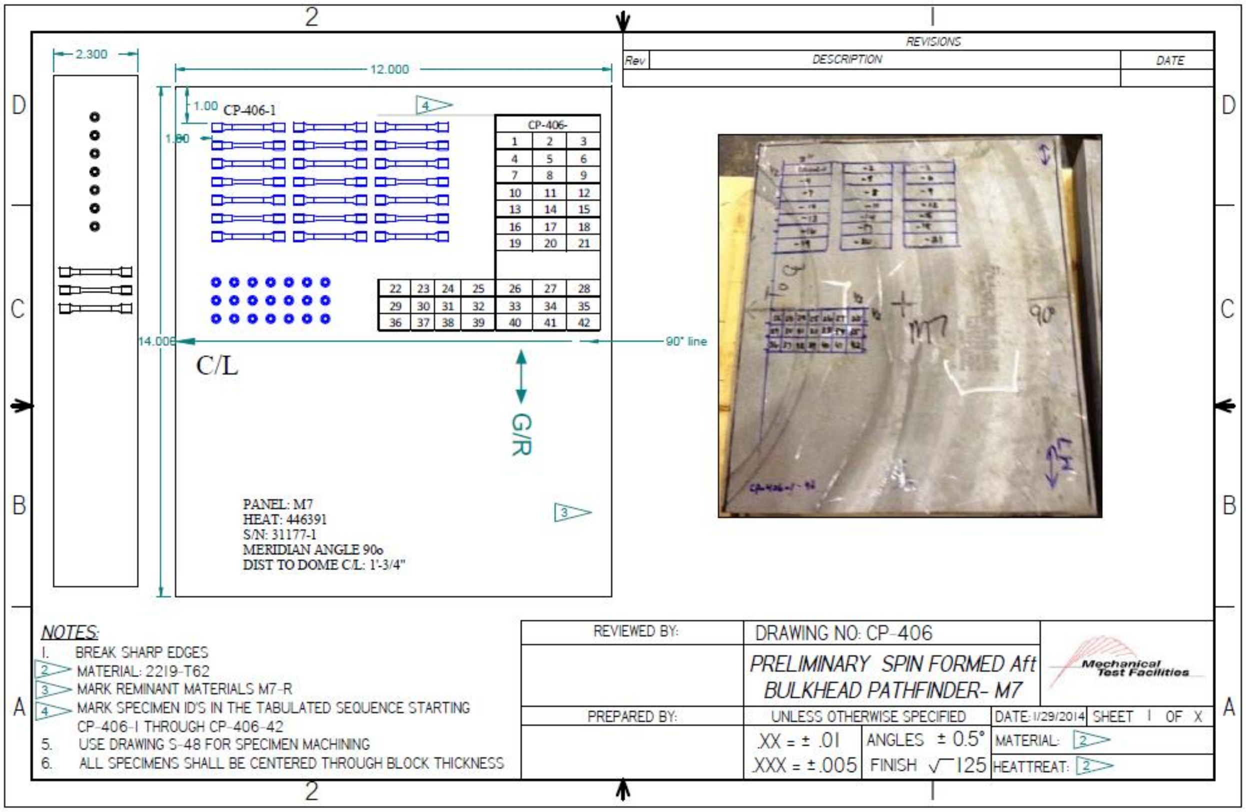

Figure 8.5-3. Cut Plan for Machining SCC Specimens from Coupon Blank M7 (specimens CP-406-1 through CP-406-42)

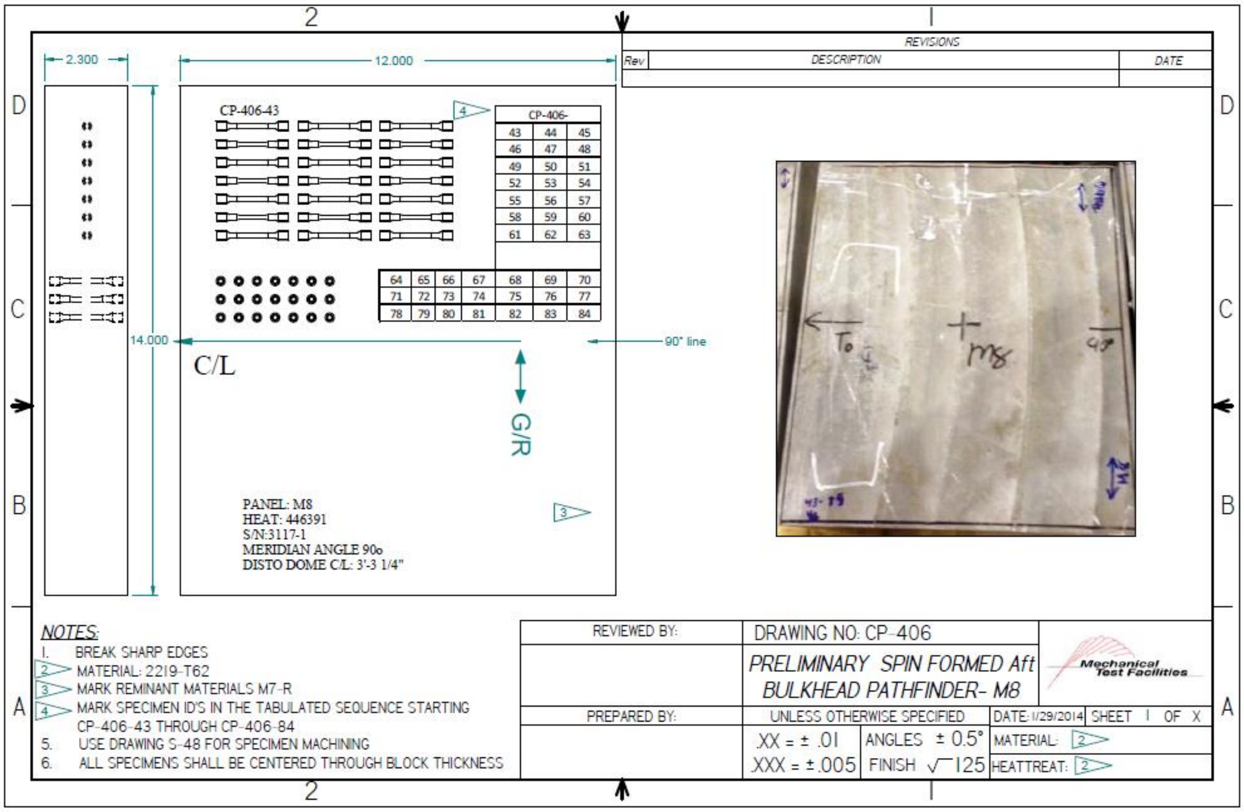

Figure 8.5-4. Cut Plan for Machining SCC Specimens from Coupon Blank M8 (specimens CP-406-43 through CP-406-84)

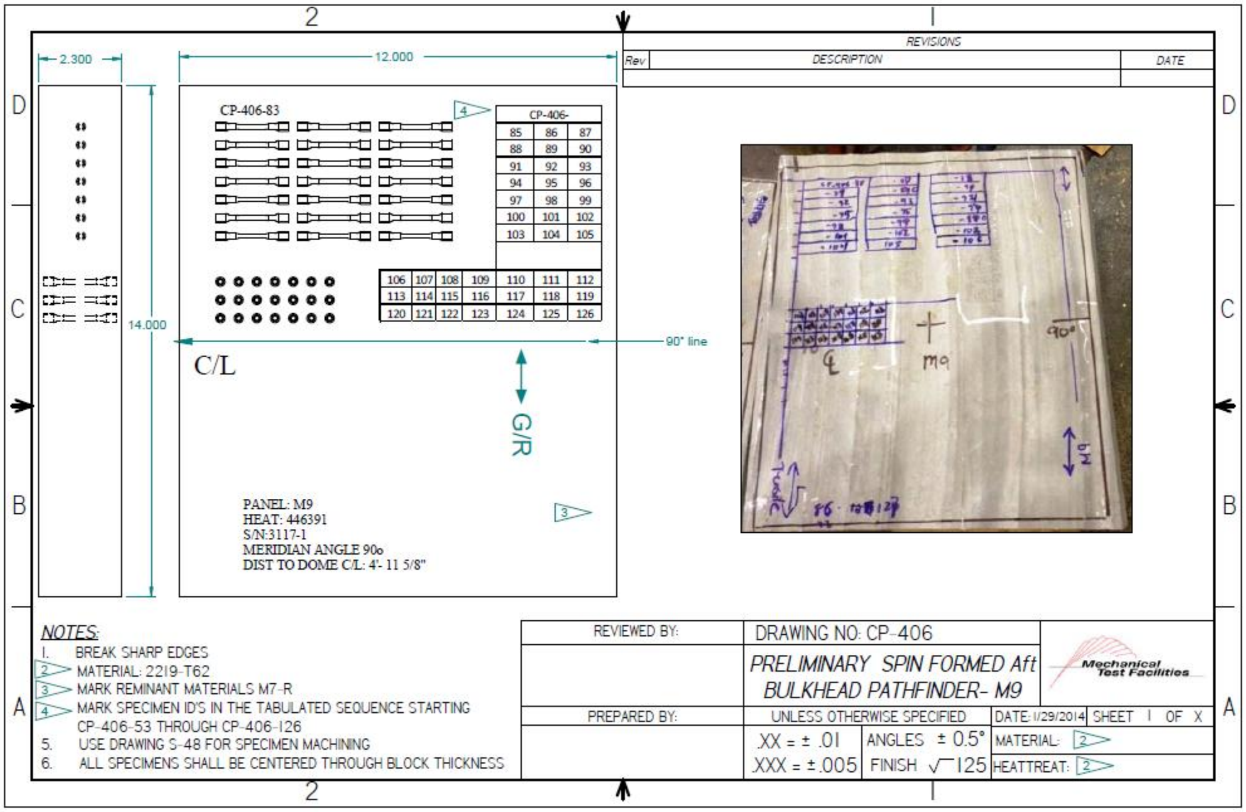

Note: This sequence starts with CP-406-85, not CP-406-83 as stated in the drawing, or CP-406-53 as stated in note 4.

Figure 8.5-5. Cut Plan for Machining SCC Specimens from Coupon Blank M9 (specimens CP-406-85 through CP-406-126)

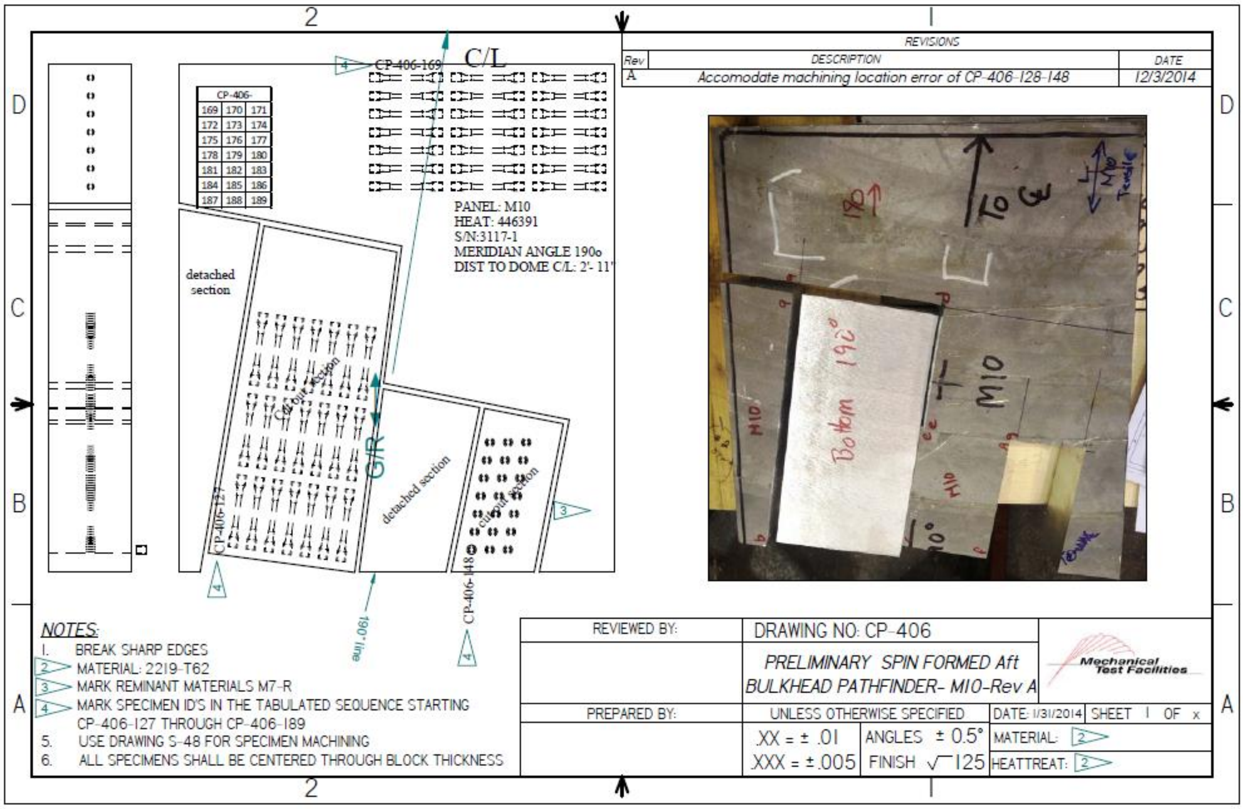

Note: The sequence for the ST specimens starts with CP-406-148 through CP-406-168. A set of 21 longitudinal specimens was also fabricated from this coupon blank, and that sequence starts with CP-406-127 through CP-406-147. The sequence for the LT specimens is as shown in the table (CP-406-169 through CP-406-189.

Figure 8.5-6. Cut Plan for Machining SCC Specimens from Coupon blank M10 (specimens CP-406-127 through CP-406-189)

The SCC testing and analysis were performed in accordance with MSFC-STD-3029, which provides guidelines for the selection of metallic materials for stress corrosion resistance and is the standard for Space Flight Hardware. The SCC specimens were tested using the direct tension loading method as described in ASTM G49 (9). The LT and ST SCC specimens were stressed in tension to 0, 50-, 75-, and 90% of the average YS measured from baseline tensile tests of the aft bulkhead and subjected to alternate immersion exposure in a 3.5% NaCl solution for test durations of 30 and 90 days per ASTM G44 (10). The L SCC specimens from coupon blank M10 were also stressed in tension to 0-, 50-, 75-, and 90% of the YS, but were subjected to salt spray exposure for test durations of 30 and 90 days per ASTM B117 (11). Three replicate specimens were tested for each stress level, test duration, and exposure environment per the SCC test matrices, as shown in Table 8.5-2 through Table 8.5-5. Figure 8.5-7 shows the stressing device, extensometer, stressing frames, and representative SCC specimens. The alternate immersion test apparatus and salt spray chamber are shown in Figure 8.5-8.

Table 8.5-2. 30-Day SCC Test Matrix for the Spin Formed Aft Bulkhead Al 2219-T62 Material Test Environment: 3.5% NaCl alternate immersion per ASTM G44

Coupon Blank	Meridian Angle	Orientation	Stress Level % YS	Number of Replicates
M7	90°	LT	0	3
			50	3
			75	3
			90	3
		ST	0	3
			50	3
			75	3
			90	3
M8	90°	LT	0	3
			50	3
			75	3
			90	3
		ST	0	3
			50	3
			75	3
			90	3
M9	90°	LT	0	3
			50	3
			75	3
			90	3
		ST	0	3
			50	3
			75	3
			90	3
M10	190°	LT	0	3
			50	3
			75	3
			90	3
		ST	0	3
			50	3
			75	3
			90	3

Table 8.5-3. 90-Day SCC Test Matrix for the Spin Formed Aft Bulkhead Al 2219-T62 Material. Test Environment: 3.5% NaCl alternate immersion per ASTM G44

Coupon Blank	Meridian Angle	Orientation	Stress Level % YS	Number of Replicates
M7	90°	LT	0	3
			75	3
		ST	0	3
			75	3
M8	90°	LT	0	3
			75	3
		ST	0	3
			75	3
M9	90°	LT	0	3
			75	3
		ST	0	3
			75	3
M10	190°	LT	0	3
			75	3
		ST	0	3
			75	3

Table 8.5-4. 30-Day SCC Test Matrix for the Spin Formed Aft Bulkhead Al 2219-T62 Material Test Environment: 5% salt spray per ASTM B117

Coupon Blank	Meridian Angle	Orientation	Stress Level % YS	Number of Replicates
M10	190°	L	0	3
			75	3

Table 8.5-5. 90-Day SCC Test Matrix for the Spin Formed Aft Bulkhead Al 2219-T62 Material Test Environment: 5% salt spray per ASTM B117

Coupon Blank	Meridian Angle	Orientation	Stress Level % YS	Number of Replicates
M10	190°	L	0	3
			50	3
			75	3
			90	3

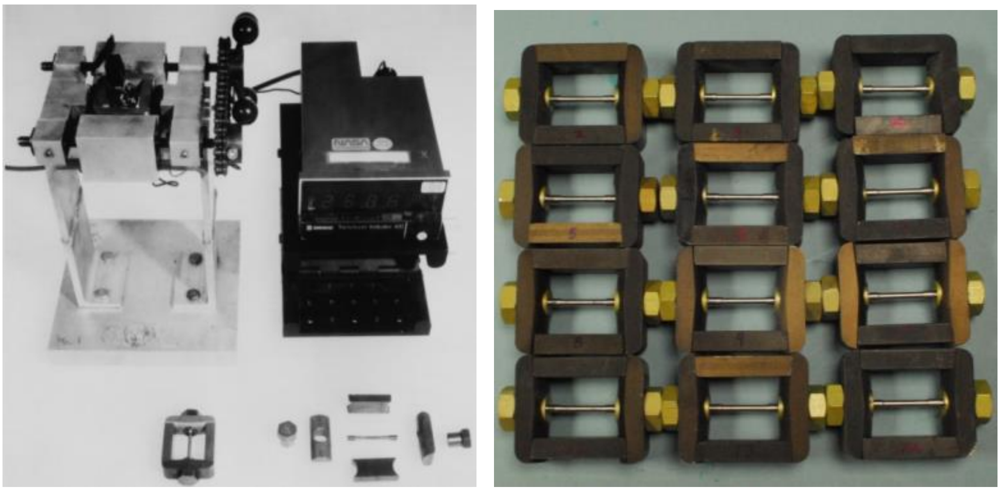

(a) (b)

Figure 8.5-7. (a) Stressing Device and (b) Representative Stressed Specimens and Stressing Frames

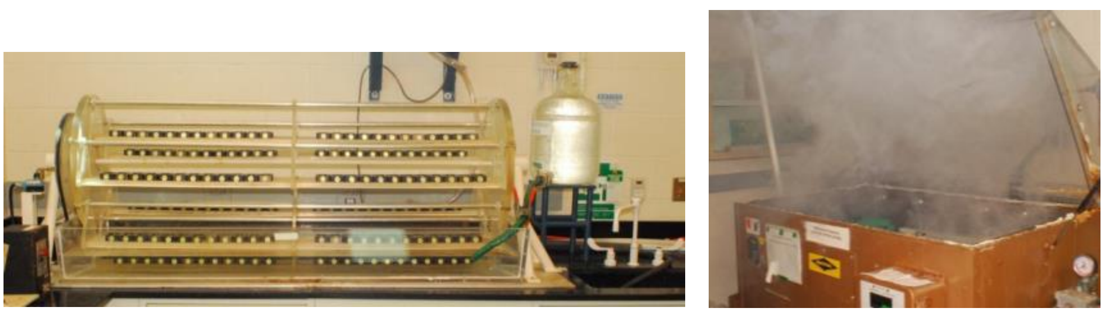

(a) (b)

Figure 8.5-8. (a) Alternate Immersion Test Apparatus and (b) Salt Spray Chamber

Specimens were considered to have failed during the SCC test if one or more of the specimens fractured during exposure or exhibited cracking during post-exposure visual examination. If any failures occurred, then that specimen was sectioned and the morphology of the fracture examined. If no failures occurred for a given test condition, then one specimen from the set was subjected to metallographic examination while the remaining two specimens were tensile tested to failure to determine residual tensile strength. Two measures were used to evaluate the residual tensile strength of the surviving specimens: the percent tensile strength retained, which compares the residual tensile strength of the exposed specimens to typical tensile properties of unexposed specimens; and the residual strength ratio, which compares the residual tensile strength of specimens exposed with and without an applied stress.

The percent tensile strength retained provides a measure of the residual load carrying ability of the specimen as compared to unexposed specimens and is an indication of the reduction in specimen cross-sectional area, not a change in strength of the material. Loss in cross-sectional area can be due to general corrosion, pitting, and stress corrosion. Metallurgical examination is required to confirm the type of corrosion. For the specimens tested with an applied stress, the reduction in tensile strength is the combined effect of stress and the corrosive environment. For the specimens tested with no applied stress the reduction is the effect of the corrosive environment only. The percent tensile strength retained for each exposed specimen was calculated as follows:

$$\text{Percent Tensile Strength Retained} = (UTS_f/UTS_i) \times 100$$

where:

UTS_f = Residual strength of the exposed specimen (failure load/original specimen cross-sectional area)
UTSi = Average ultimate tensile strength for the unexposed specimens.

The residual strength ratio provides a more direct indication of the effect of applied stress during exposure and therefore a method to separate the effects of general corrosion and pitting from stress corrosion. The UTS_S and UTS_0 are calculated based on original specimen cross-sectional area, and provide an indication of the loss in area due to stress corrosion and general corrosion, respectively. For this study, specimens with residual strength ratios of less than 0.75 were considered failures. The residual strength ratio for each specimen that was exposed with an applied stress was calculated as follows:

$$\text{Residual Strength Ratio} = UTS_s/UTS_0$$

where:

UTSs = Residual strength of stressed and exposed specimen
UTS_0 = Averaged residual strength of non-stressed and exposed specimens

One goal of MSFC-STD-3029A is to establish ratings for SCC resistance. The table rating requirements are shown below for reference. It should be noted that while table ratings are important, for design purposes a threshold stress level for SCC must be identified to establish maximum allowable service stress levels. Also, the data generated in this study provide insight to the SCC resistance of the spin formed Al 2219-T6 material, but are not sufficient to define a threshold value or establish table ratings.

Table I Requirements

Alloys, tempers, and weldments in Table I are considered highly resistant to SCC in 3.5% NaCl alternate immersion or 5% salt spray. An alloy or weldment can be added to this table if no stress corrosion failures occur on specimens stressed to 75% of the YS within 30 days of exposure.

Table II Requirements

Alloys, tempers, and weldments in Table II are considered moderately resistant to SCC in 3.5% NaCl alternate immersion or 5% salt spray. An alloy or weldment is added to this table if no stress corrosion failures occur on specimens stressed to 50% of the YS within 30 days of exposure.

Table III Requirements

Alloys, tempers, and weldments in Table III are considered to have low resistance to SCC in 3.5% NaCl alternate immersion or 5% salt spray. They are placed in this table if stress corrosion failures occur on specimens stressed to 50% of the YS within 30 days of exposure.

8.6 Seacoast Exposure SCC Test Plan

While the 3.5% NaCl solution alternate immersion test provides a comprehensive screening method for accelerated stress corrosion testing of high-strength Al alloy product forms, a disadvantage of the test is that severe pitting may develop in the specimens (13). Such pitting in tension specimens with relatively small cross-section can markedly reduce the effective cross-sectional area and produce a net section stress greater than the nominal gross section stress, resulting in either: (1) fracture by mechanical overload of a material that is not susceptible to SCC; or (2) SCC of a material at an actual stress higher than the intended nominal test stress. The occurrence of either of these phenomena might then interfere with a valid evaluation of materials with relatively high resistance to stress corrosion. As a result, seacoast exposure SCC testing was proposed as a complementary screening test in this project. Seacoast exposure SCC testing, which is performed in a natural outdoor environment and requires longer test durations than the standard accelerated corrosion tests performed in a laboratory, is more representative of the intended service environment

Three coupon blanks from the aft bulkhead were provided to NASA JSC for seacoast exposure SCC testing at NASA KSC. These blanks were identified as J1, J2, and J3 and were obtained from the locations highlighted in yellow in the aft bulkhead cut plan (Figure 8.6-1) and coupon blank matrix (Table 8.6-1). For each coupon blank, 9 short transverse (ST) tension specimens were machined per the ASTM E8 small-size round tension test specimen design (Figure 8.6-2**)**. This specimen orientation is with respect to the original plate rolling direction. Specimens were machined such that the gage section was located at the mid-plane thickness (t/2) of the coupon blank.

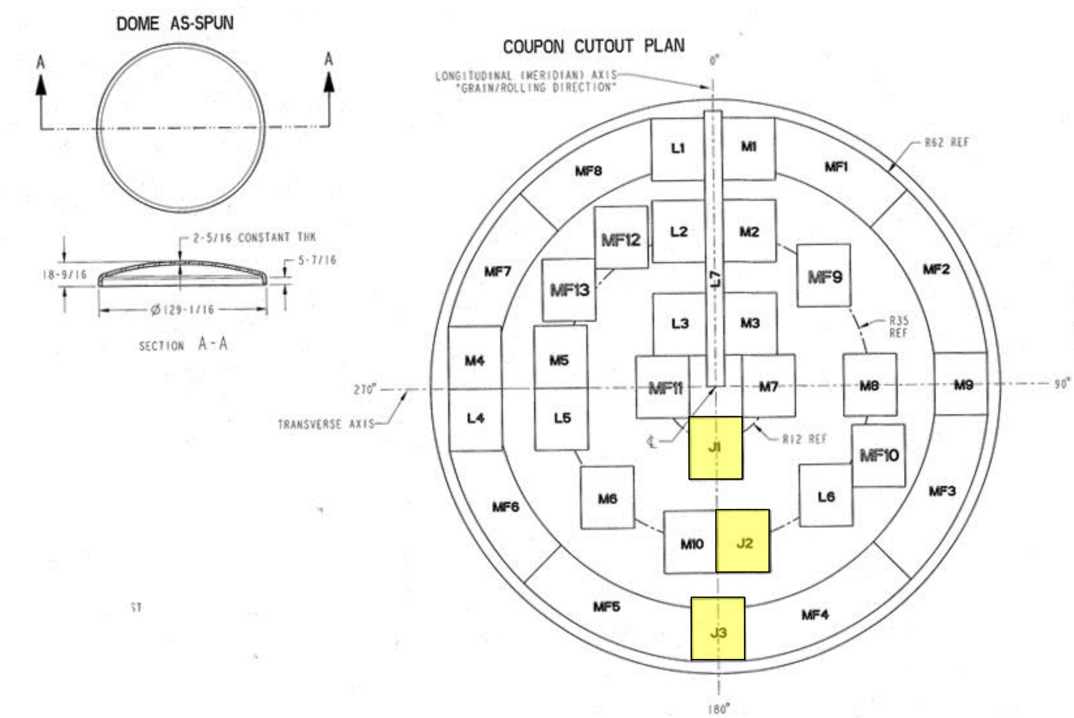

Figure 8.6-1. Aft Bulkhead Cut Plan showing the Location of the Seacoast Exposure SCC Coupon Blanks highlighted in Yellow

Table 8.6-1. Seacoast Exposure SCC Coupon Blank Locations and Orientations.

Coupon Blank	Coupon Blank Size		Coupon Center Point	
	Longitudinal Dimension, in.	Transverse Dimension, in.	Meridian Angle , degrees	Arc Length from dome CL in.
J1	14	12	180°	12
J2	14	12	170°	35-5/8
J3	14	12	180°	55-5/8

NOTE:

Prior to the start of the seacoast exposure SCC tests, the initial laboratory alternate immersion SCC tests results became available. Based upon the 30-day alternate immersion exposure in 3.5% NaCl test results (Section 10.4.1.1), the accelerated test condition provides adequate screening methodology for SCC. Longer test durations of 90 days, however, did lead to severe general corrosion and pitting (Section 10.4.1.2). Consequently, specimens scheduled for seacoast exposure testing in this project were diverted to laboratory alternate immersion testing at MSFC to generate SCC data on more locations in the aft bulkhead and to confirm initial test results. The NESC team recommends that Orion conduct seacoast exposure SCC testing of the first-article aft bulkhead in order to characterize the corrosion performance in the service environment. The following test plans are provided as a guide for the Orion Program if they choose to conduct these tests.

The seacoast exposure SCC specimens should be tested using the direct tension loading method as described in ASTM G49. The specimens should be stressed in tension to 0-, 75-, and 90% of the YS and will be subjected to seacoast exposure for durations of up to 3 years as per ASTM G44. Table 8.6-2 shows a proposed seacoast exposure SCC test matrix. Specimens should be tested in triplicate for each test condition.

Table 8.6-2. Test Matrix for the Seacoast Exposure SCC Tests

Bulkhead Location	Coupon Blank	Meridian Angle	Orient.	Stress Level	# Replicates
Pole	J1	180°	ST	0% YS	3
				75% YS	3
				90% YS	3
Membrane	J2	180°	ST	0% YS	3
				75% YS	3
				90% YS	3
Rim	J3	180°	ST	0% YS	3
				75% YS	3
				90% YS	3

9.0 LM Test Plan

This is a high-level summary of the LM test plan in support of the LM Orion Program. This information is provided for completeness and is intended to indicate the overall scope of the activities. Due to proprietary considerations, results from this work will not be published in this or addendum NESC reports.

The LM test plan focused on two activities; FSW schedule development and complementary mechanical property, and structural subcomponent testing. Further details are provided in Sections 9.1 and 9.2

9.1 Self-Reacting FSW and Friction Pull Plug Weld (FPPW) Development

Coupon blanks from the aft bulkhead were provided to LM-MAF for SR-FSW and FPPW schedule development. These blanks were identified as MF1, MF2, MF3, MF4, MF5, MF6, MF7, and MF8 and were obtained from the arc-shaped segments located at the rim of the aft bulkhead as shown in the aft bulkhead cut plan (Figure 9.1-1) and coupon blank matrix (Table 9.1-1).

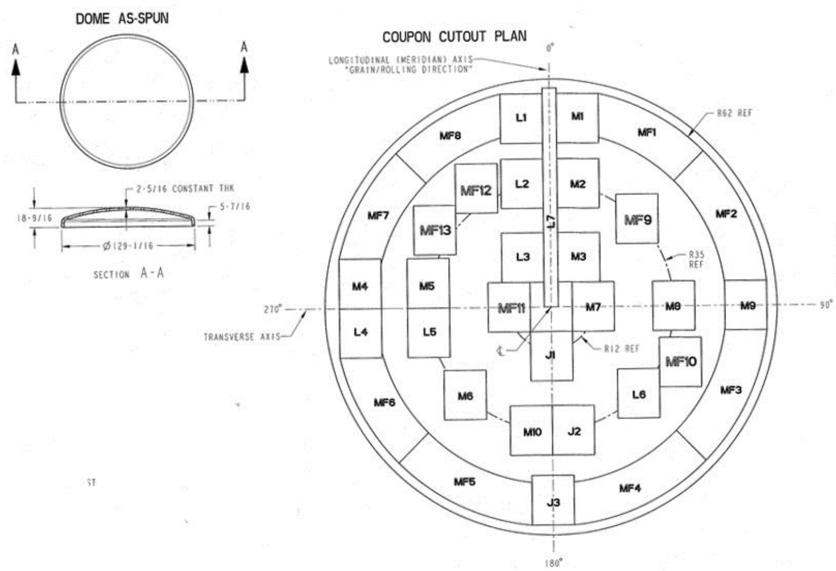

Figure 9.1-1. Aft Bulkhead Cut Plan showing the Location of the FSW and FPPW Schedule Development Coupon Blanks

Table 9.1-1. FSW and FPPW Schedule Development Coupon Blank Locations and Orientations

Coupon Blank	Coupon Blank Size		Coupon Center Point	
	Longitudinal Dimension, in.	Transverse Dimension, in.	Meridian Angle , degrees	Arc Length from dome CL in.
MF1	N/A	N/A	31°	56-3/4
MF2	N/A	N/A	64°	56-3/4
MF3	N/A	N/A	116°	56-3/4
MF4	N/A	N/A	154°	56-3/4
MF5	N/A	N/A	206°	56-3/4
MF6	N/A	N/A	240°	56-3/4
MF7	N/A	N/A	296°	56-3/4
MF8	N/A	N/A	329°	56-3/4

The LM Orion Program was provided with spin formed Al 2219-T62 aft bulkhead material to develop nominal SR-FSW and FPPW weld schedules. The development will be focused on schedules for the Al 2219-T6 plate and Al 2219-T8 forging weld combination that will be utilized on the Orion CM.

The SR-FSW development will generally follow three phases of development. The first phase will follow a design of experiment to evaluate the weldability of the material combination. Evaluation will consist of non-destructive phased array ultrasonic testing (PAUT) inspection, tensile testing, and metallography. Emphasis will be placed on identifying load characteristics and identifying potential nominal weld schedules that show a strength insensitivity to load. The second phase will be a verification step, aimed at characterizing the available operating load ranges and down-selecting a final nominal weld schedule. The final phase will involve sensitivity testing were the selected nominal schedule will be exposed to production-related variables. These verification tests will include, but not be limited to, joint fit-up, tacking, off-set, and clean time. The end of the development cycle will produce a weld schedule that the Orion Program will feel confident about going forward into the production pathfinder activity. The pathfinder activity will be the final step that certifies the weld schedule for use on production flight articles.

The FPPW development will follow a cycle similar to the SR-FSW cycle described above. The initial phase FPPW will be geared towards establishing the boundaries of the FPPW weldable space. These welds will then be evaluated using penetrant and ultrasonic inspection, tensile tests for ultimate strength, YS, elongation, and metallography. The results of the initial welding will be characterized in an attempt to understand the driving factors of FPPW and determine potential nominal FPPW schedules. The second phase will take the selected nominal schedules and run a series of verification tests to characterize the repeatability of the weld schedules performance. The final phase will evaluate sensitivity impacts. Again, these verification tests will include, but not be limited to joint fit-up, alignment, and cleaning. The end of the development cycle will produce a weld schedule that the LM Orion Program feels confident about going forward into the production pathfinder activity. The pathfinder activity will be the final step that certifies the weld schedule for use on production flight articles.

9.2 Mechanical Property and Structural Subcomponent Testing

Coupon blanks from the aft bulkhead were provided to LM-MAF for mechanical property testing in support of the Orion Program. These blanks were identified as MF9, MF10, MF11, MF12, and MF13 and were obtained from the locations highlighted in yellow in the aft bulkhead cut plan (Figure 9.2-1) and coupon blank matrix (Table 9.2-1).

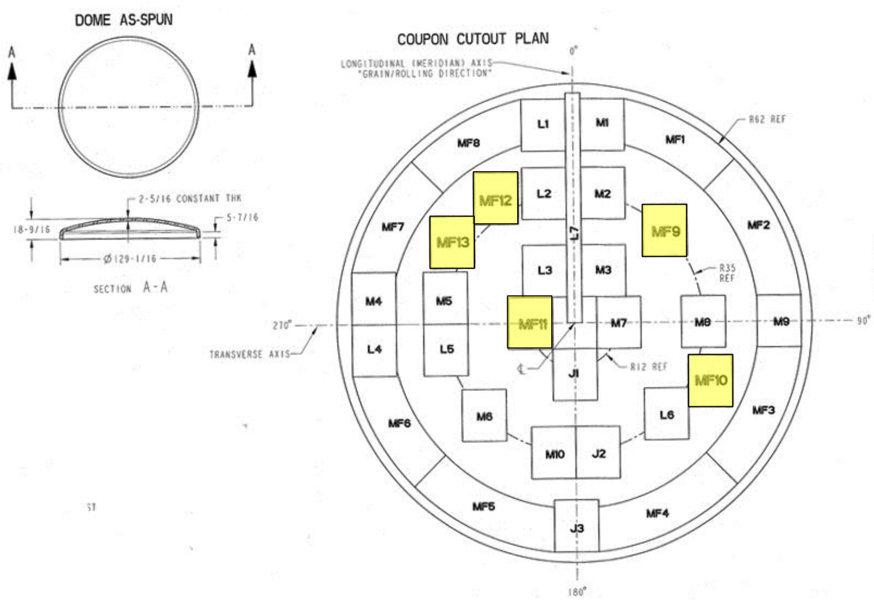

Figure 9.2-1. Aft Bulkhead Cut Plan showing the Location of the Supplemental Mechanical Property Test Coupon Blanks highlighted in Yellow

Table 9.2-1. LM Mechanical Property Test Coupon Blank Locations and Orientations

Coupon Blank	Coupon Blank Size		Coupon Center Point	
	Longitudinal Dimension, in.	Transverse Dimension, in.	Meridian Angle , degrees	Arc Length from dome CL in.
MF9	14	12	45°	35-1/8
MF10	14	12	114°	40-3/8
MF11	14	12	270°	12
MF12	14	12	328°	40
MF13	14	12	304°	39-7/8

The testing program at MAF is designed to complement the mechanical property test data (tensile, fracture, and SCC) being generated by the NESC team and provide additional supporting data to aid the Orion Program in the design of the aft bulkhead. The first objective of these mechanical property tests is to characterize the fatigue properties of the spin formed Al 2219-T62 aft bulkhead material and compare it to existing reference data for both Al 2219-T6 and –T8 product forms. This fatigue testing will include surface flaw testing to a leak condition, using specimens that will be machined to the minimum membrane thickness and crack growth testing in the ST orientation. The second objective is to characterize the aft bulkhead material with bearing and insert pull tests. This testing will utilize special machined specimens that are representative of hardware attachment methods used on the Orion aft bulkhead.

After completion of the NESC test program, the skeletal remains of the spin formed aft bulkhead (Figure 7.10-2) were shipped to LM-MAF for further testing. Planned activities include structural subcomponent testing in which different configurations of the backbone-to-aft bulkhead joint will be tested to simulate the CM internal pressure load (Figure 9.2-2). The goals of these tests are to demonstrate structural performance of the aft bulkhead in the ST direction and to verify bolt and splice plate strength.

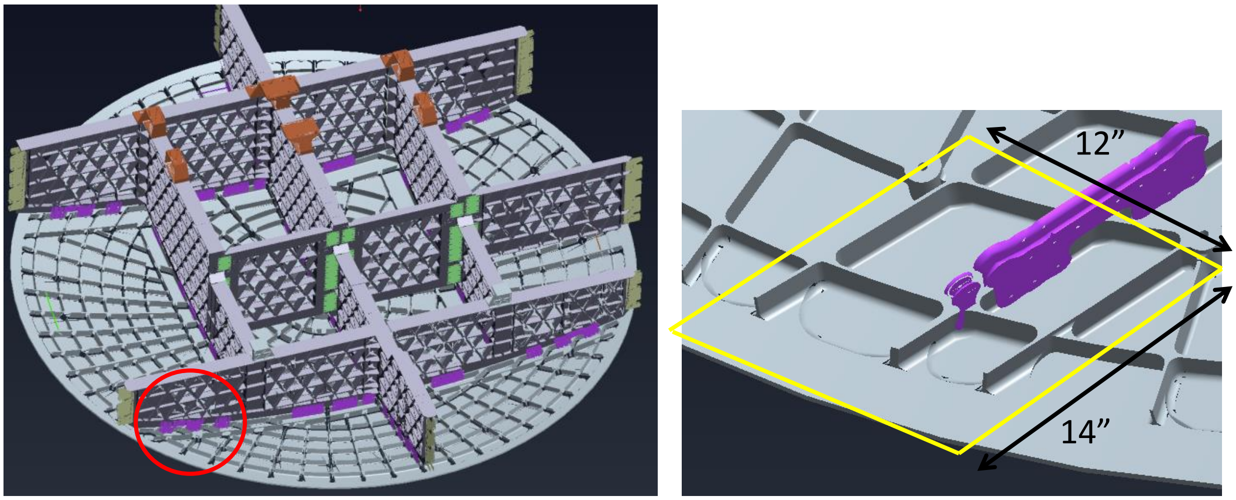

Figure 9.2-2. Schematic showing the Simulated Location for Backbone Panel 6 Connection to Aft Bulkhead Joint

10.0 Results and Discussion

10.1 Metallurgical Analysis

10.1.1 Thickness Measurements

The thickness of the L7 coupon blank was measured at locations along the meridian line that corresponded to the locations of the UT measurements and laser scan analysis. Vernier calipers with ball end caps were used for these measurements and an effort was made to make measurements at the base of the surface scallops. The measurements are summarized in Table 10.1-1 and compared with the UT and laser scan measurements in Figure 10.1-1. The maximum thickness occurred at a distance of 4 inches from the pole, the minimum thickness at 52 inches, and the maximum reduction in thickness was 0.12 inches, values that are fairly consistent with the UT and laser scan results. Thickness measurements from all three sources indicate a 4 to 5% reduction in thickness. Also consistent with the UT and laser scan data, the thickness measured on coupon blank L7 indicates thinning from pole to rim for approximately 50 inches and then thickening to the rim. The L7 thickness profile in Figure 10.1-1 shows minimal fluctuations except toward the rim.

The deformation induced during spin forming is complex and non-uniform. Thickness reduction is a simplified metric used in this analysis to evaluate the variation over the acreage of the aft bulkhead. During convex spin forming there is generally no deliberate reduction in wall thickness as the material is shaped over the mandrel (2). During forming the blank diameter is reduced as material is pushed onto the mandrel, particularly near the rim, consequently the material experiences circumferential compressive stress superimposed on radial tensile stress, which combine to result in nearly constant wall thickness. So many process parameters affect material response during spin forming that modeling the process has been unsuccessful. The industrial success of spin forming is based on extensive experience at the vendors.

Table 10.1-1. Thickness Measurements of Coupon Blank L7 at Distances from the Pole

Thickness Measurements of Coupon Blank L7	
Distance from Pole (in)	Thickness (in)
4	2.319
12	2.318
20	2.290
24	2.287
32	2.245
36	2.253
40	2.275
48	2.221
52	2.204
56	2.270

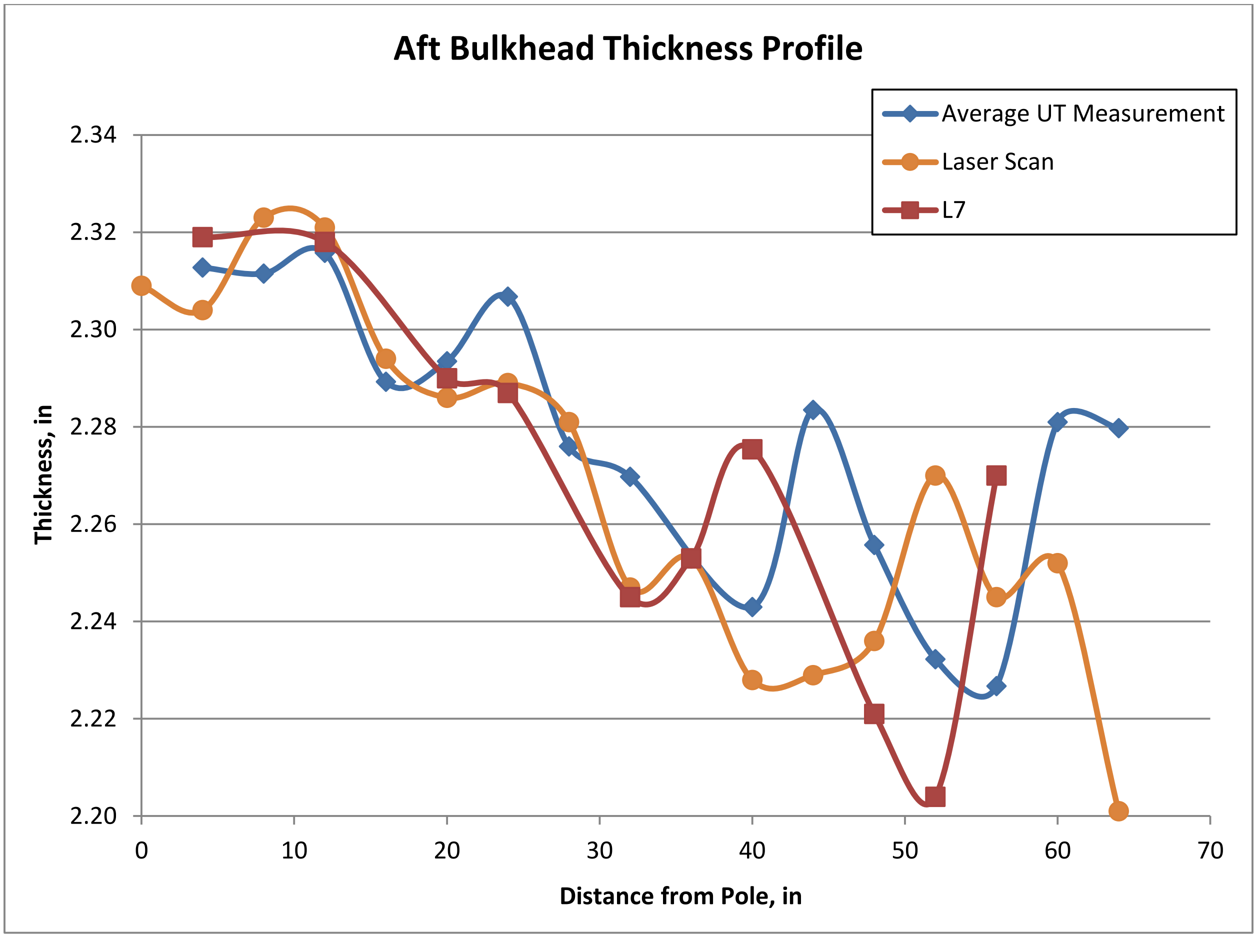

Figure 10.1-1. Thickness Profile of Coupon Blank L7 Compared with the UT and Laser Scan Data

10.1.2 Microstructural Analysis

Through-thickness montages shown in Figure 10.1-2 for samples L7-1 through L7-5 illustrate the variability in grain morphology with both through-thickness location and distance from the pole of the aft bulkhead. The blue lines denote through-thickness locations (t = thickness) that were examined at higher magnification and which are shown in Figure 10.1-3. Specimen L7-1 is located near the pole just inside the innermost forming tool contact area and consequently represents a region that was not deformed by spin forming. The thickness profile of coupon blank L7 indicates that the forming blank was thinned by about 4-5% during spin forming to create the aft bulkhead shape, with the thickness decreasing from pole to a minimum near the rim at a distance of approximately 50 inches from the pole and then increasing in thickness at the rim.

The through-thickness micrographs in Figure 10.1-2 show that as deformation increases, the microstructure changes from a uniform small grain size (L7-1) to a banded microstructure that exhibits regions of larger grain size, most likely due to strain induced recrystallization, primarily towards the OML surface where the forming tool contacts the plate. Notably larger grain size is observed between 3t/4 and 7t/8 starting with L7-2 and more pronounced in L7-3 and L7-4. Macroscopic deformation bands are observed near the OML, particularly in samples L7-3, L7-4, and L7-5.

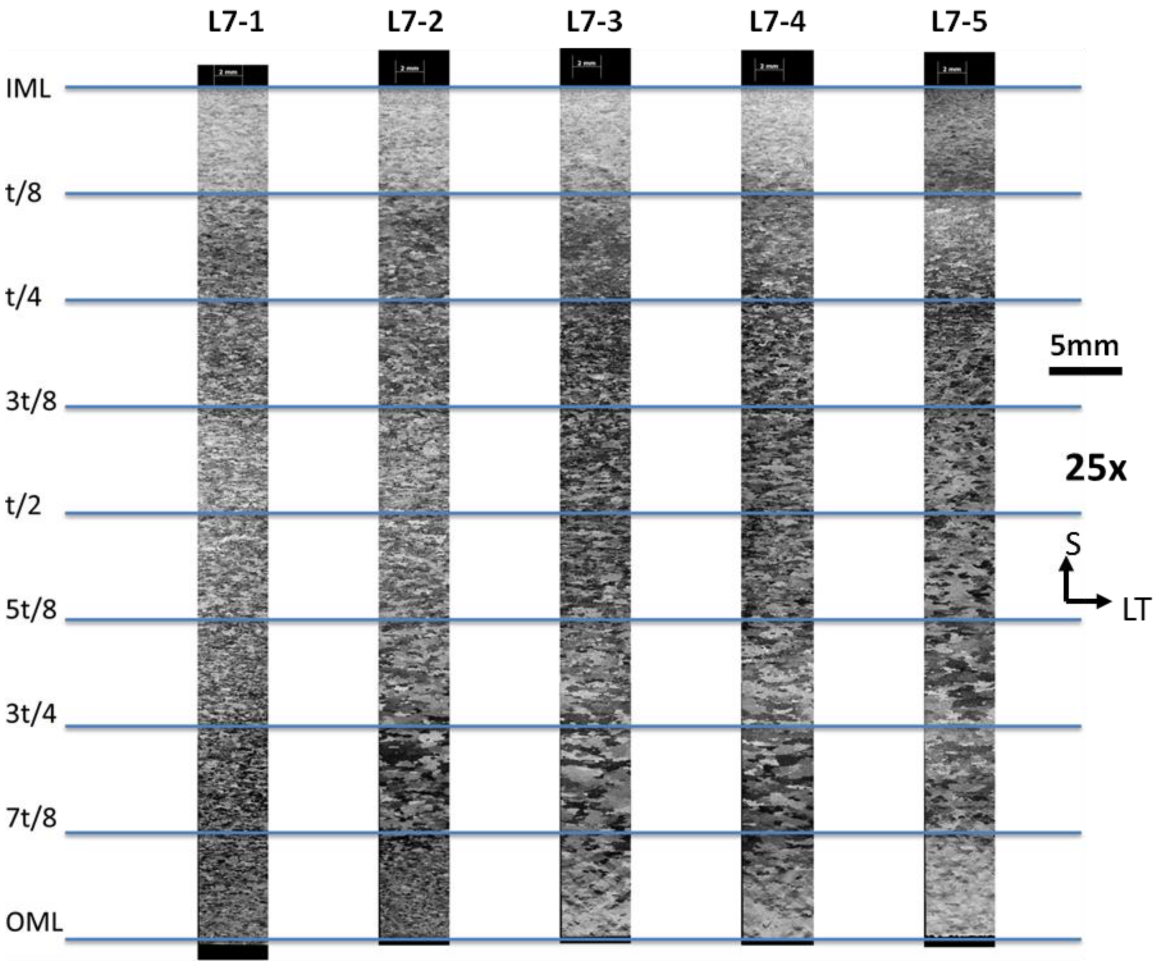

Figure 10.1-2. Through-thickness Microstructures of the Aft Bulkhead at Locations Along the 0° Meridian

Higher magnification micrographs of each through-thickness position for meridian locations L7-1 through L7-5 are summarized in Figure 10.1-3(a-e). All samples exhibit grains slightly elongated in the LT direction. At the L7-1 location ((Figure 10.1-3(a)), no deformation) the grain size and morphology are uniform from IML to OML. All through-thickness positions at L7-1 exhibit precipitation on deformation bands, particularly from 3t/8 to 5t/8. Sections L7-2 through L7-5 exhibit strain induced recrystallization, biased towards the OML and extending from the OML towards the mid-thickness. In sections L7-4 and L7-5, recrystallization occurs from the OML to 3t/8. All through-thickness positions exhibit precipitation on deformation bands, more heavily in the unrecrystallized regions. Aligned precipitation in the recrystallized regions may indicate that the prior deformation history associated with both plate rolling and spin forming is not completely erased during SHT. Alternatively, the alignment may indicate precipitation on slip planes (14), (15), (16).

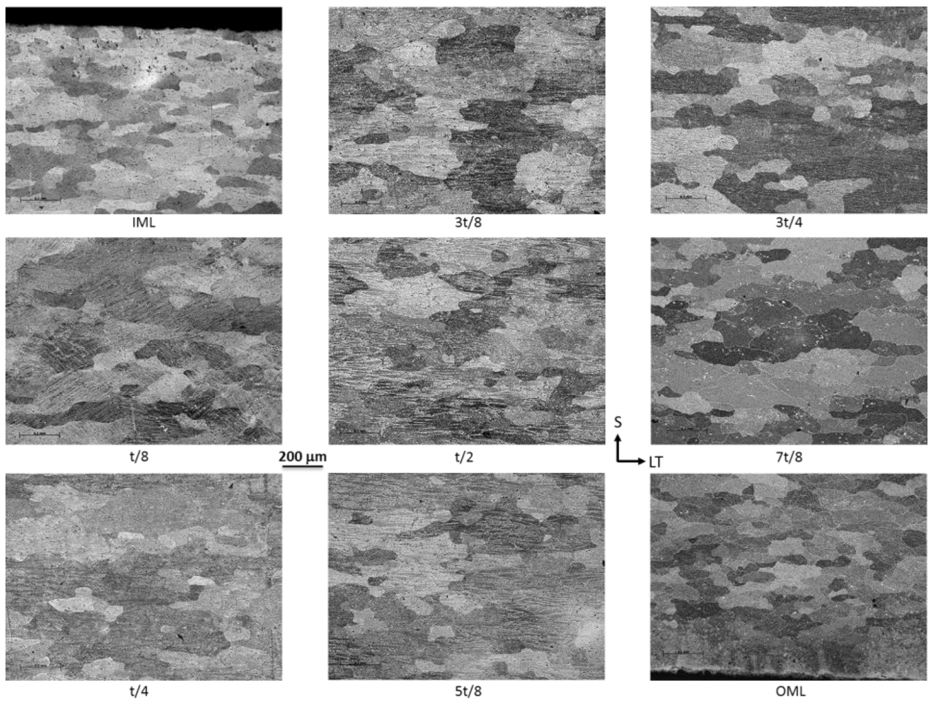

(a) Microstructure at L7-1 (L/8, 8 inches from the pole)

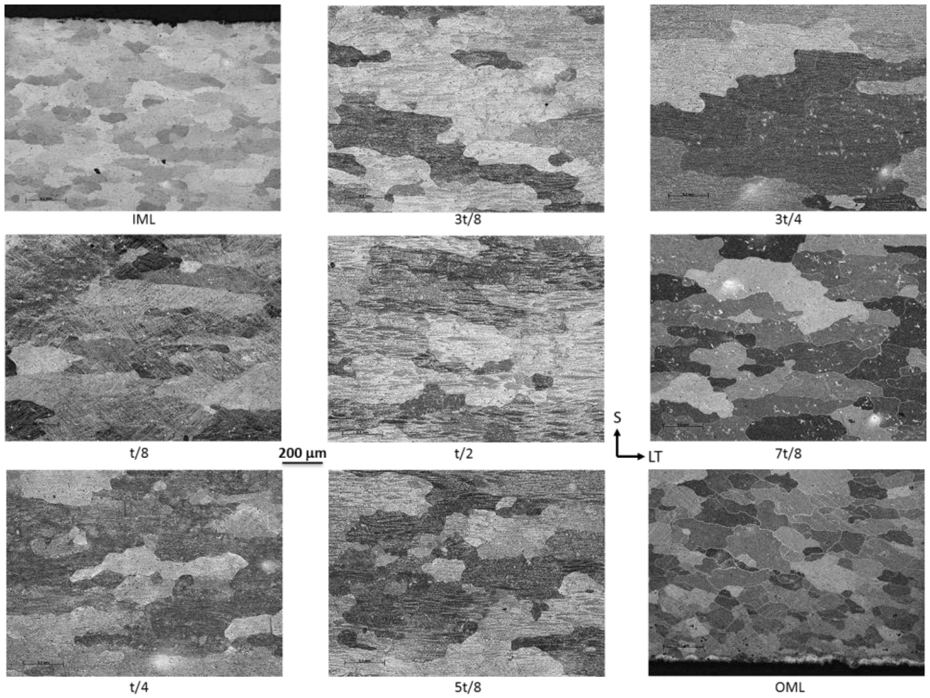

(b) Microstructure at L7-2 (L/4, 16 inches from the pole)

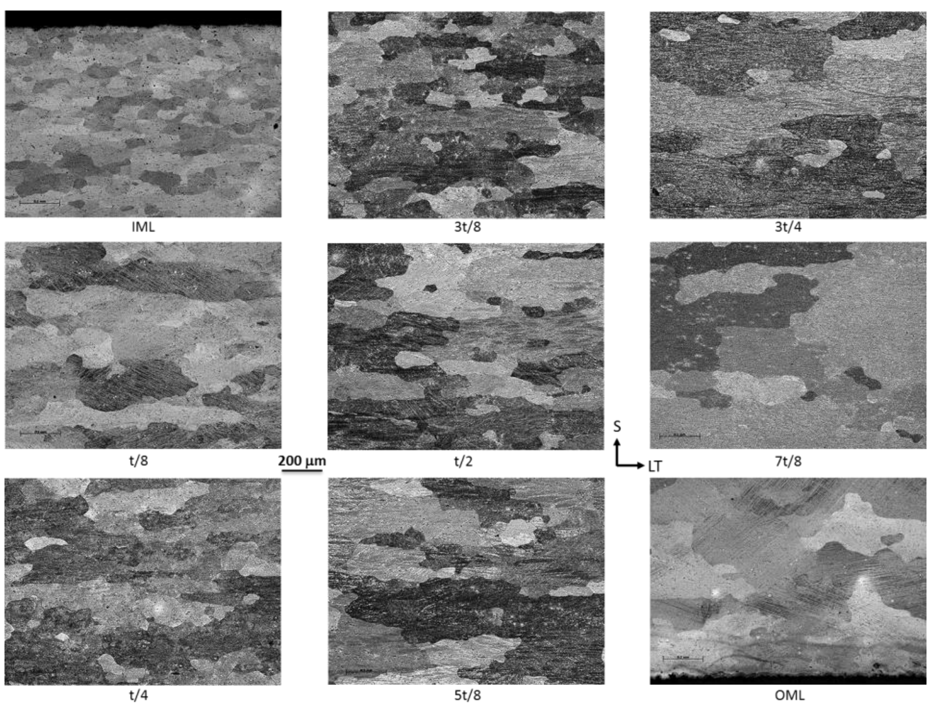

(c) Microstructure at L7-3 (L/2, 27 inches from the pole)

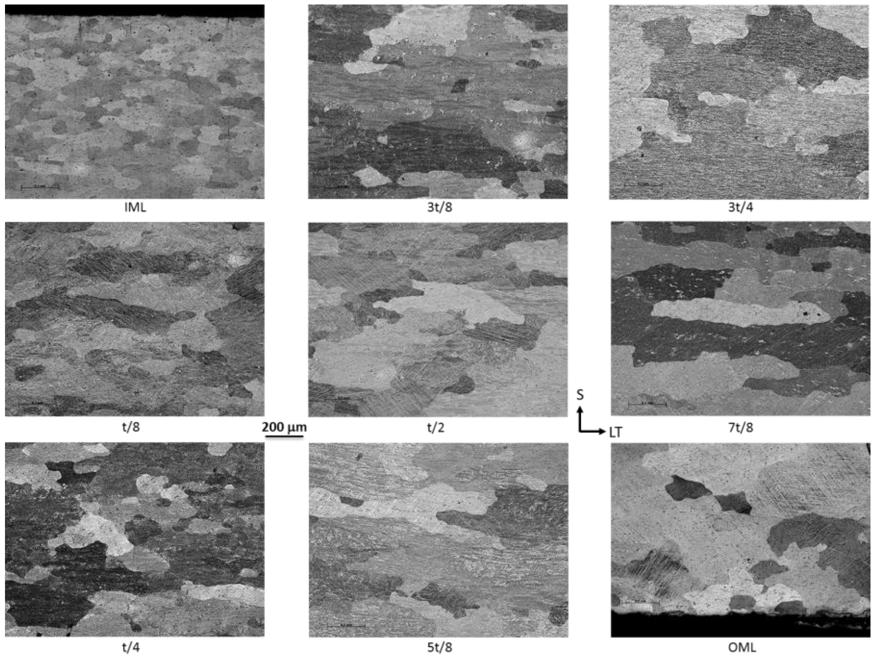

(d) Microstructure at L7-4 (3L/4, 43 inches from the pole)

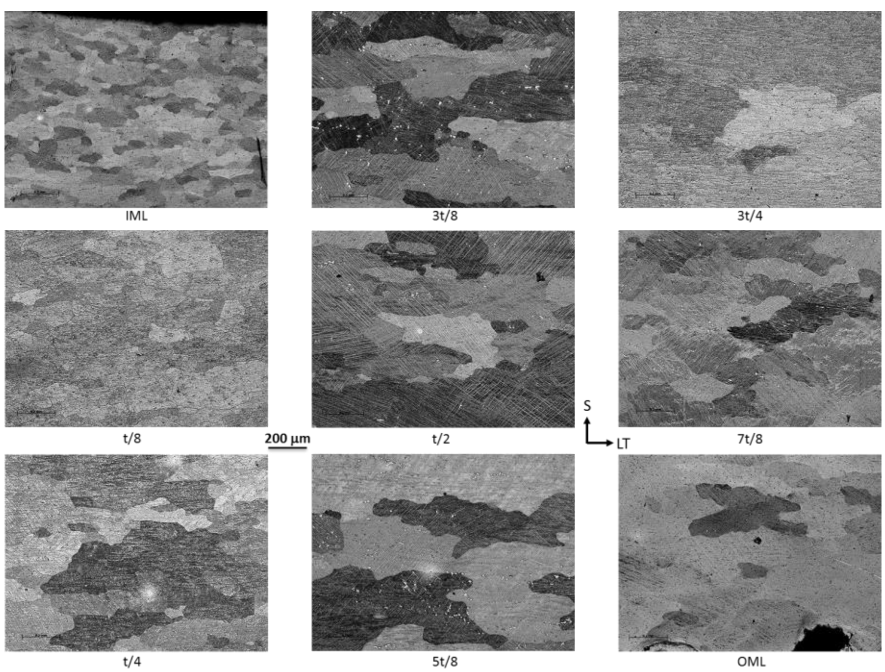

(e) Microstructure at L7-5 (L, 61 inches from the pole)

Figure 10.1-3. Microstructure at the IML, t/8, t/4, 3t/8, t/2, 5t/8, 3t/4, 7t/8, and OML Through-Thickness Positions for (a) L7-1, (b) L7-2, (c) L7-3, (d) L7-4, and (e) L7-5 Locations along the 0° Meridian

Through-thickness micrographs of the thermally processed blocks shown in Figure 10.1-4 for as-received plate (F), after the pre-spin forming anneal (O), after SHT (T4), and after aging (T6). In comparison with the F and O tempers, the T4 and T6 blocks exhibit larger grain size indicative of recrystallization during SHT. In contrast to the fully processed spin formed material shown in Figure 10.1-2 and Figure 10.1-3, the microstructure of the T4 and T6 thermally processed blocks shown in Figures 10.1-5 and 10.1-6 exhibit uniform microstructures with smaller grain sizes indicating that spin forming deformation promotes larger recrystallized grain size. Tracking of the OML and IML surfaces was maintained during spin forming and subsequent thermal processing of the aft bulkhead forming blank for direct comparison with the thermally processed test blocks. Macroscopically, the microstructure of the T6 processed test block is similar to the L7-1 sample from the aft bulkhead (Figure 10.1-2). Higher magnification micrographs of the thickness positions noted in Figure 10.1-4 for the T4 and T6 conditions are shown in Figure 10.1-5. Both conditions exhibit uniform through-thickness microstructure with slightly smaller grain sizes at the OML and IML surfaces. The grain size and morphology in both T4 and T6 conditions are similar to that observed in section L7-1 (Figure 10.1-2(a)) from the aft bulkhead, which did not experience deformation. The T6 test block exhibits precipitation on residual deformation bands similar to those observed in section L7-1, at positions from t/2 to 7t/8, and are similarly much less apparent at the OML and IML.

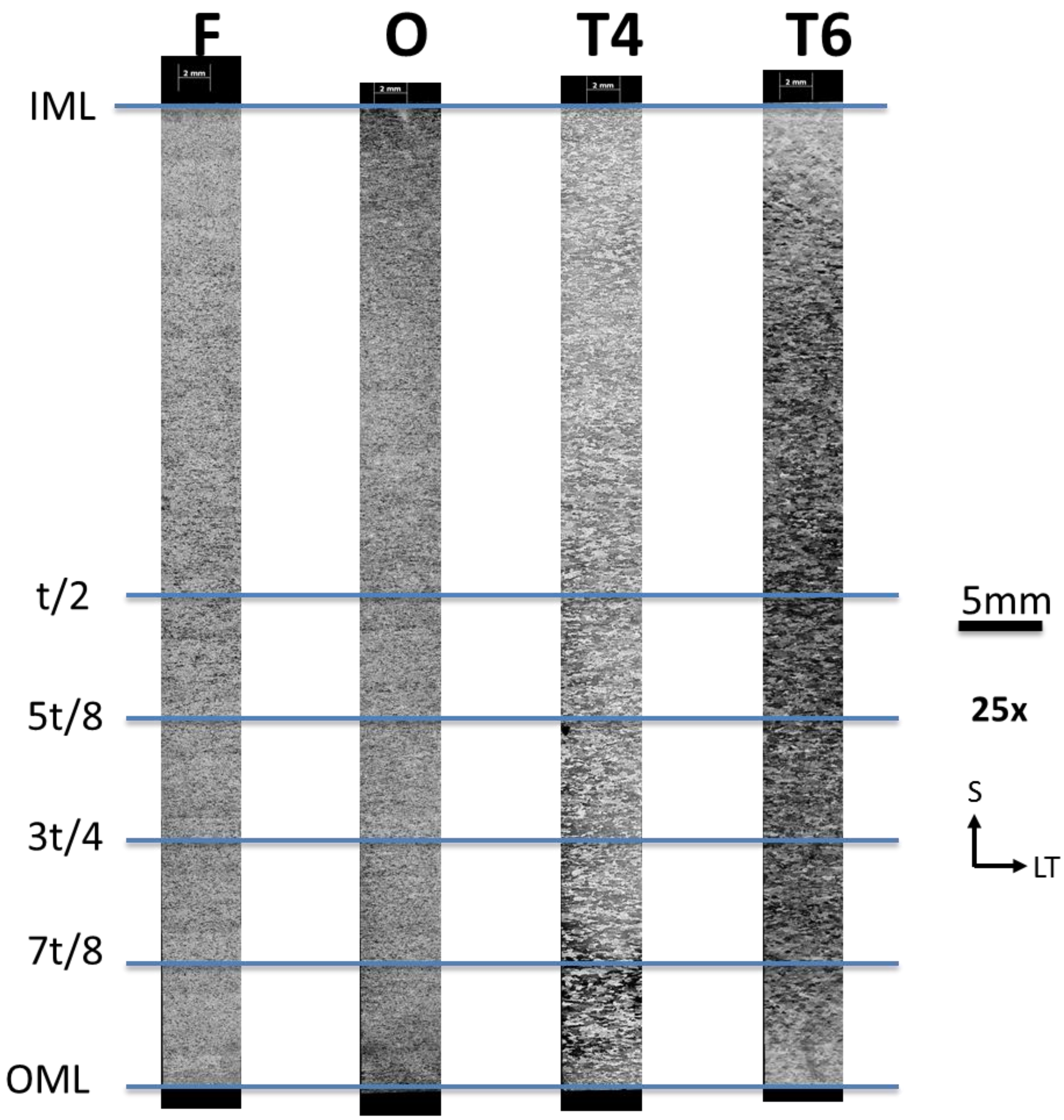

Figure 10.1-4. Through-Thickness Microstructures of the Thermally Processed Test Blocks

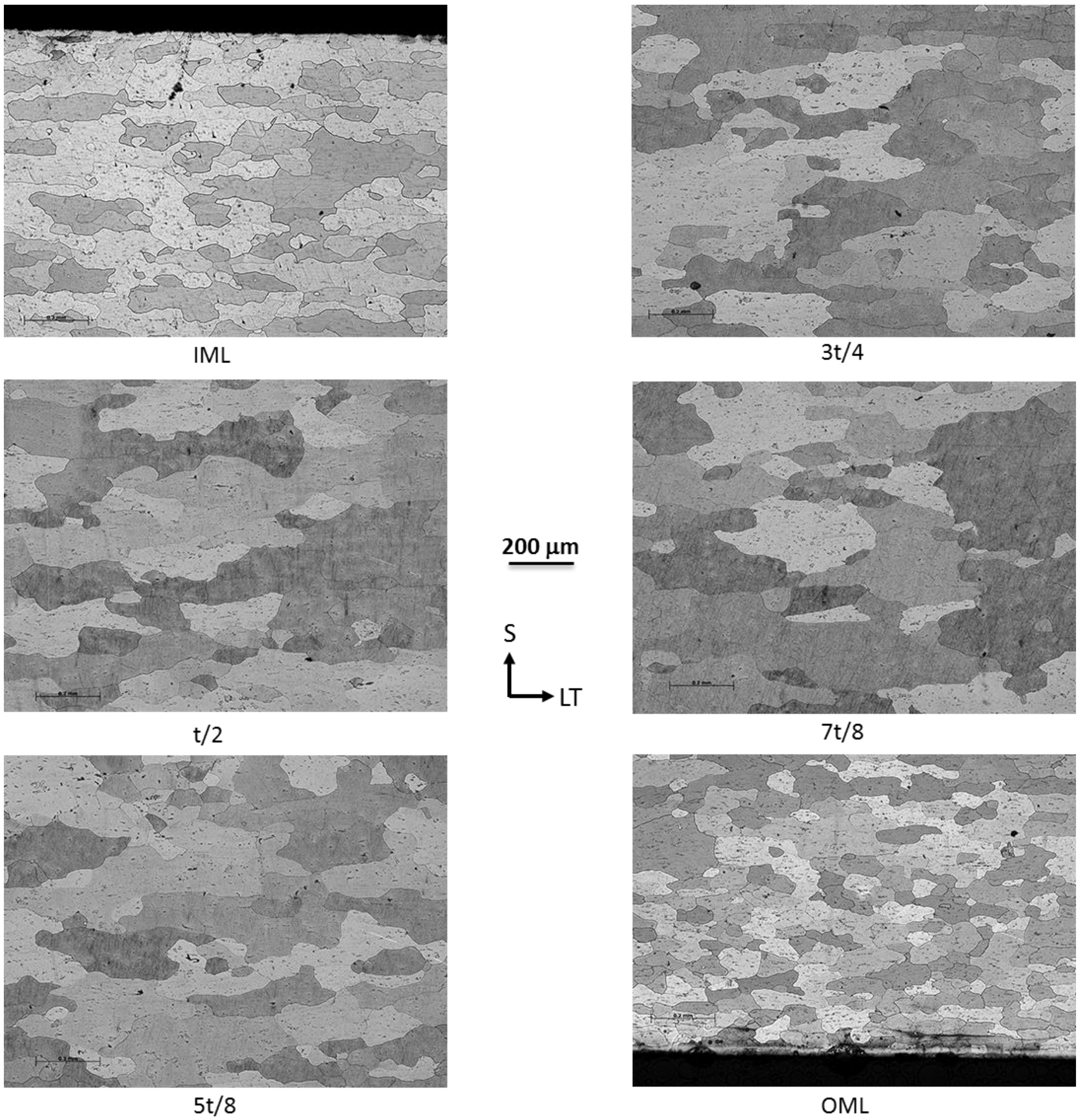

(a) Through-thickness microstructure of the T4 thermally processed test block.

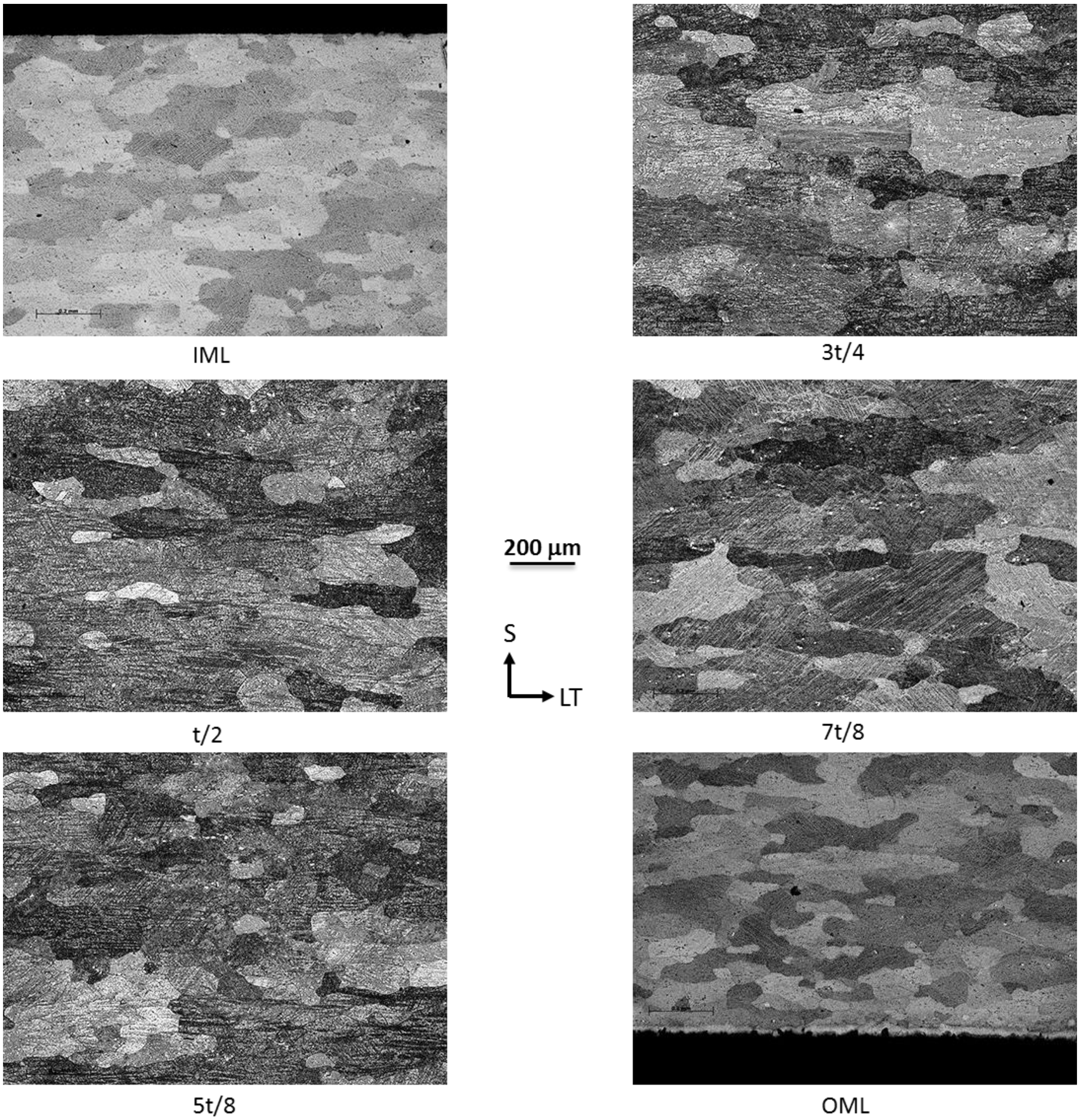

(b) Through-thickness microstructure of the T6 thermally processed test block.

Figure 10.1-5. Microstructure at the IML, t/2, 5t/8, 3t/4, 7t/8, and OML Through-Thickness Positions for the (a) T4 and (b) T6 Thermally Processed Test Blocks

Microstructures of the aft bulkhead sections L7-1 through L7-5 are compared in Figure 10.1-6 with the T6 thermally processed test block at the through-thickness locations IML, t/2, 5t/8, 3t/4, 7t/8, and OML. The grain size and morphology are similar in all samples at the IML (Figure 10.1-6(a)), and also represent the smallest and most equiaxed grain structure at all through-thickness locations. The post-recrystallization grain size varies throughout the L7 meridian locations and through-thickness positions, with larger grain sizes associated with likely regions of higher deformation. Evidence of precipitation on prior deformation bands is noted throughout all samples. At t/2 and 5t/8, the grain size is largest in the L7-4 and L7-5 locations, with L7-1 through L7-3 locations exhibiting similar grain size to that in the T6 test block. At 3t/4, the grain size is similar and notably larger in L7-2 through L7-5 than in L7-1 and T6. At 7t/8 the grain size is largest in L7-3 and L7-4. At the OML, the grain size is notably larger in L7-3 through L7-5 than L7-1 through L7-2 and T6. These variations in grain size in the aft bulkhead sections compared with T6 are indicative of the complex and varied deformation levels associated with the spin forming process, particularly when combined with the plate rolling history and post-forming heat treatment.

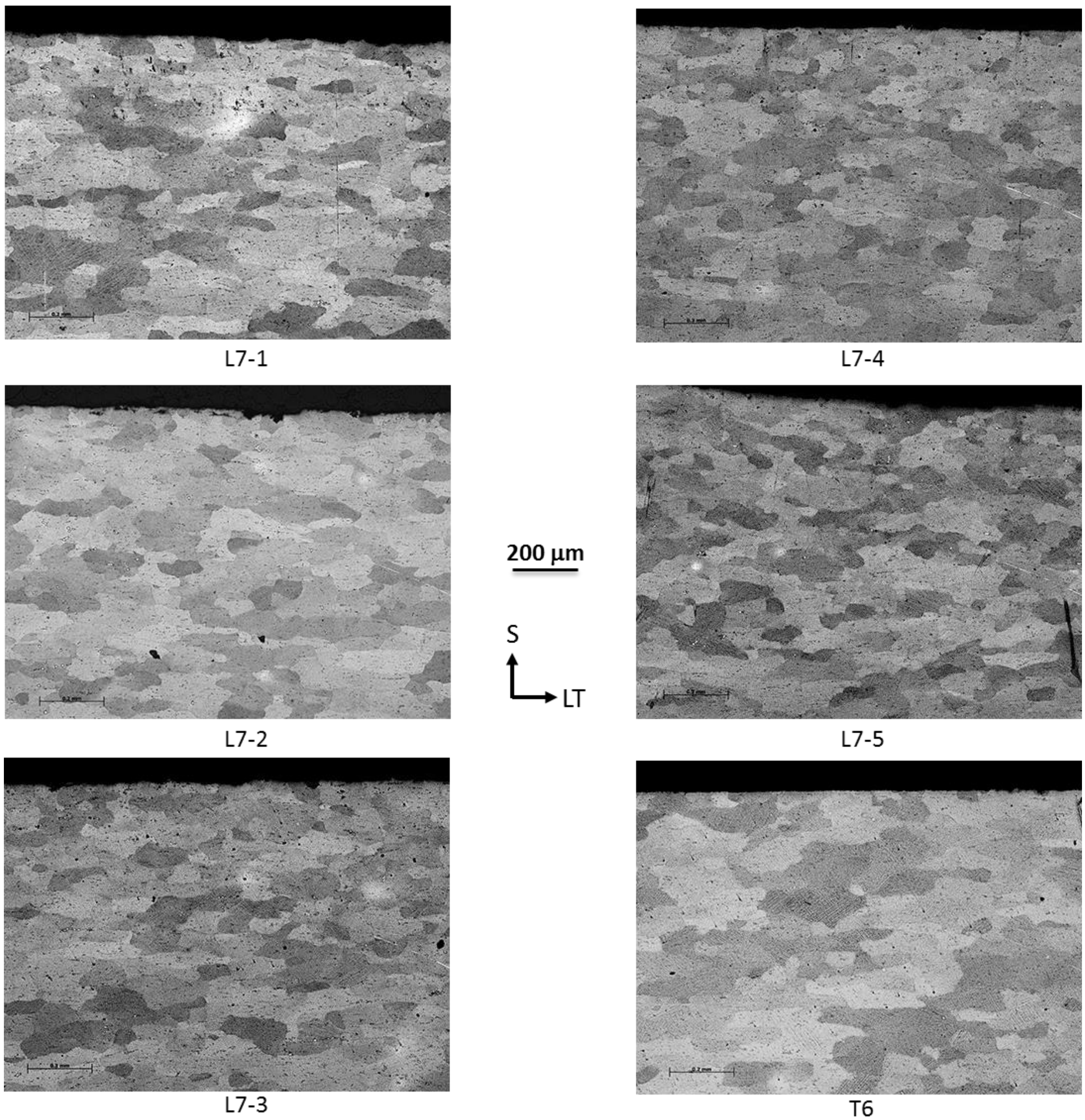

Microstructure of aft bulkhead locations L7-1 through L7-5 compared with the T6 thermally processed test block at (a) IML.

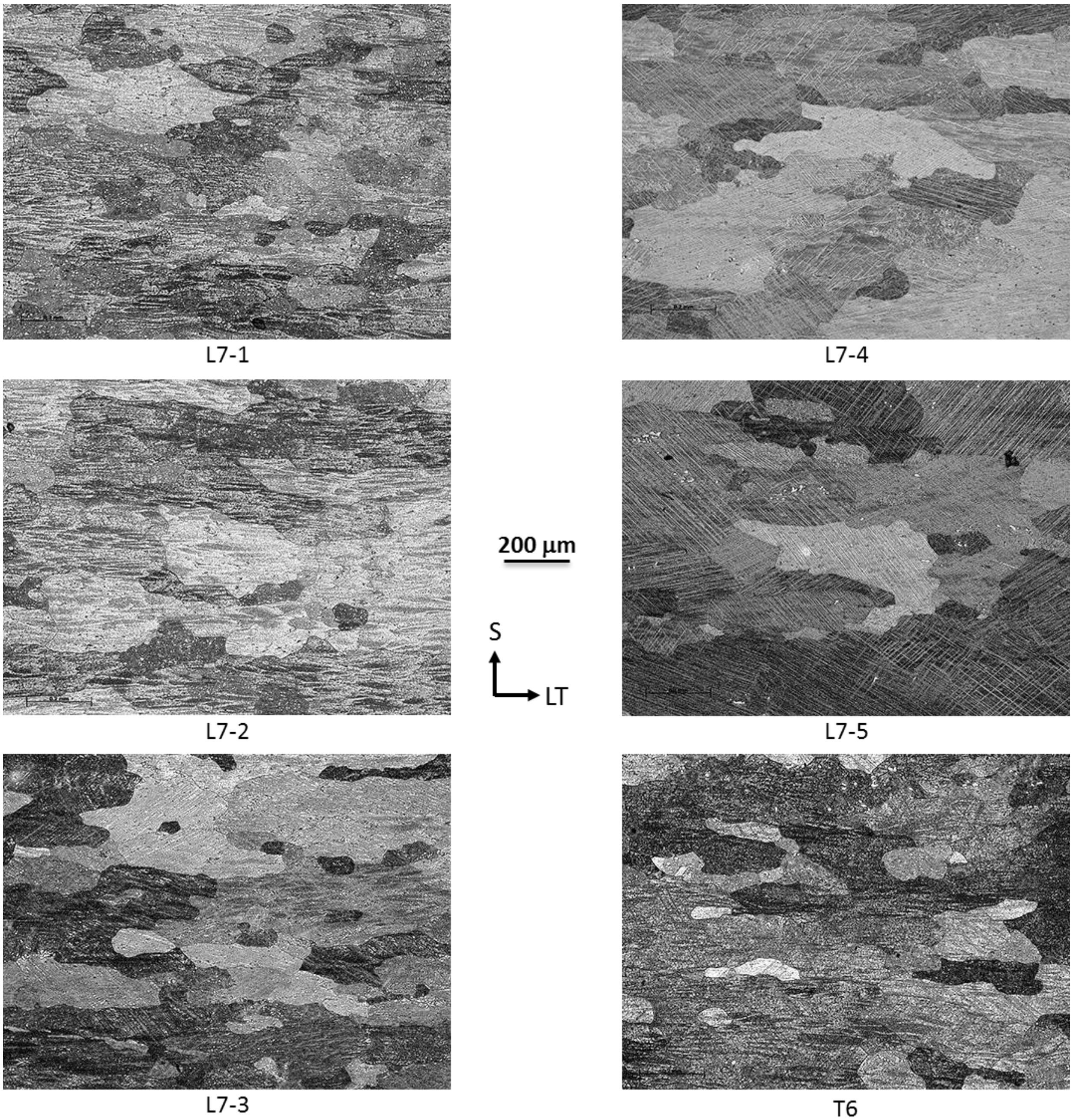

Microstructure of aft bulkhead locations L7-1 through L7-5 compared with the T6 thermally processed test block at (b) t/2.

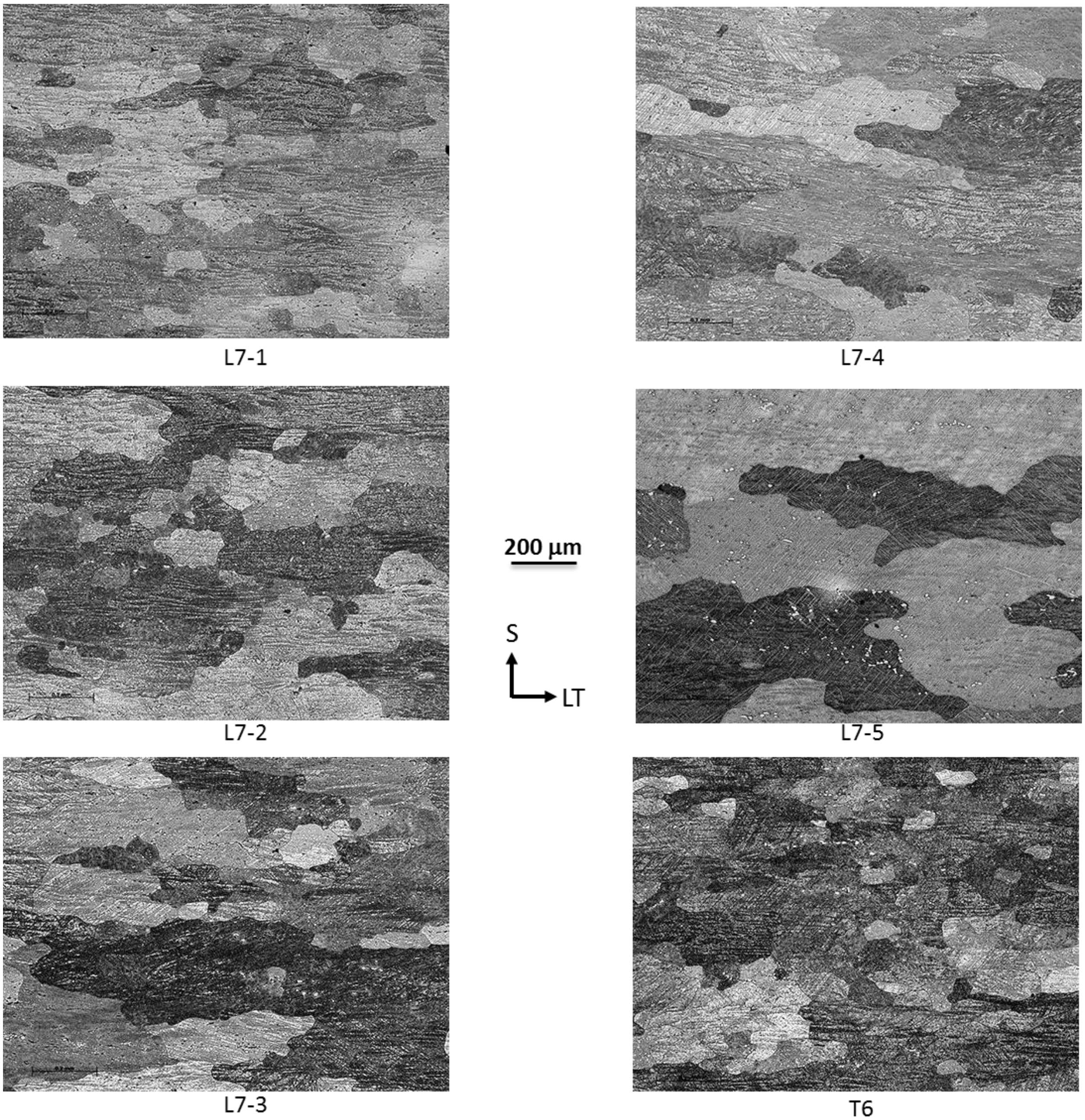

Microstructure of aft bulkhead locations L7-1 through L7-5 compared with the T6 thermally processed test block at (c) 5t/8.

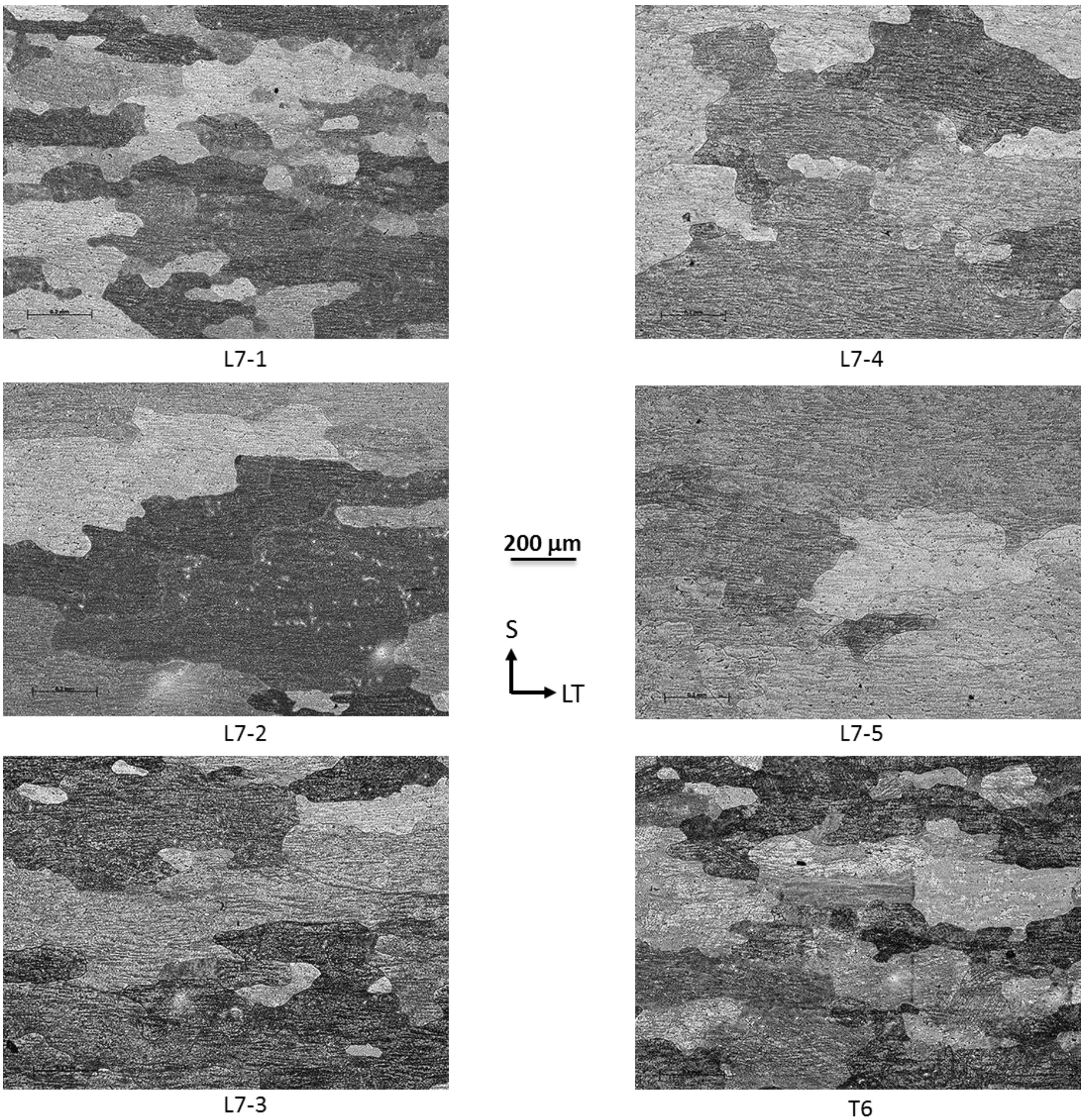

Microstructure of aft bulkhead locations L7-1 through L7-5 compared with the T6 thermally processed test block at (d) 3t/4.

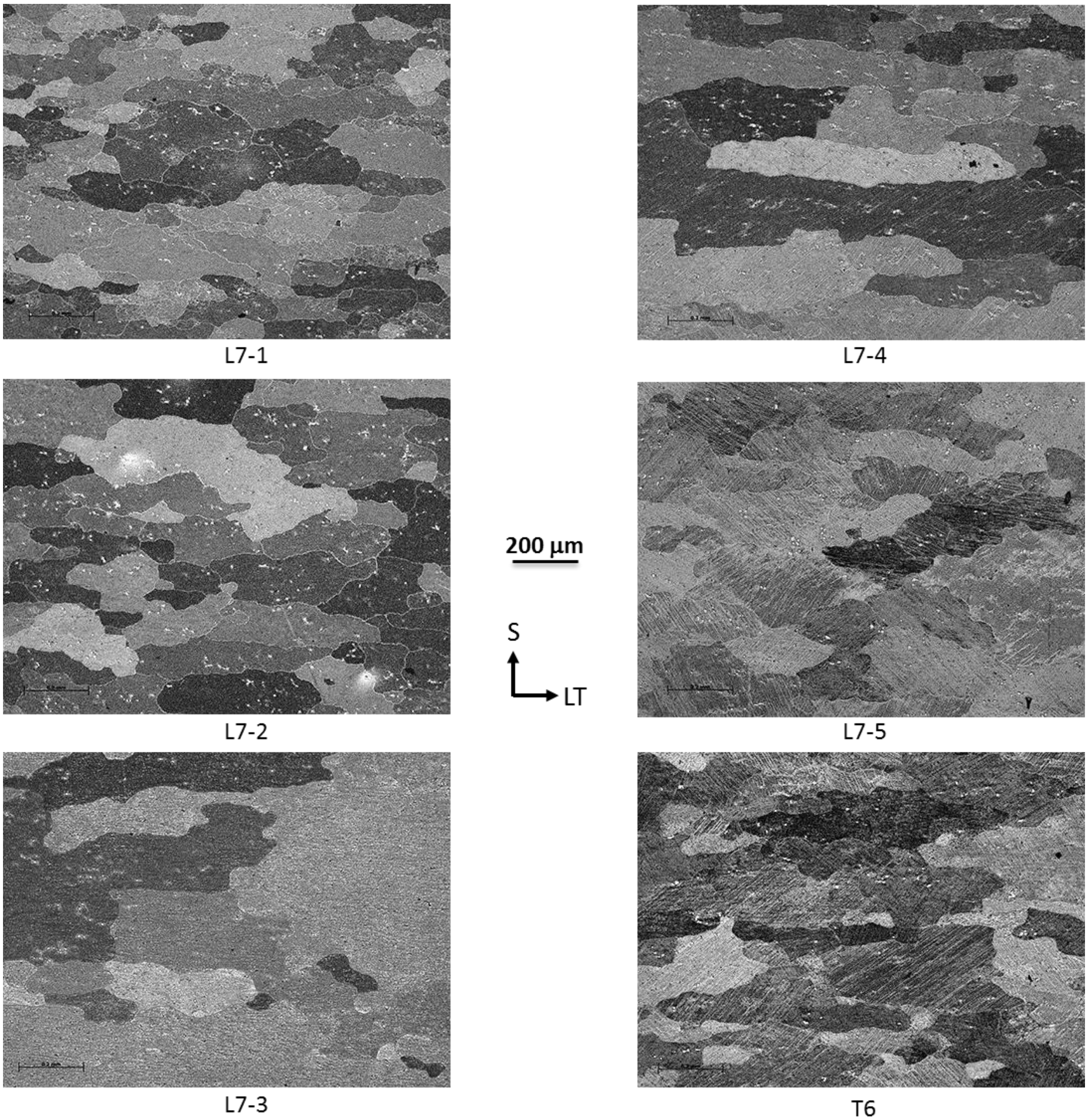

Microstructure of aft bulkhead locations L7-1 through L7-5 compared with the T6 thermally processed test block at (e) 7t/8.

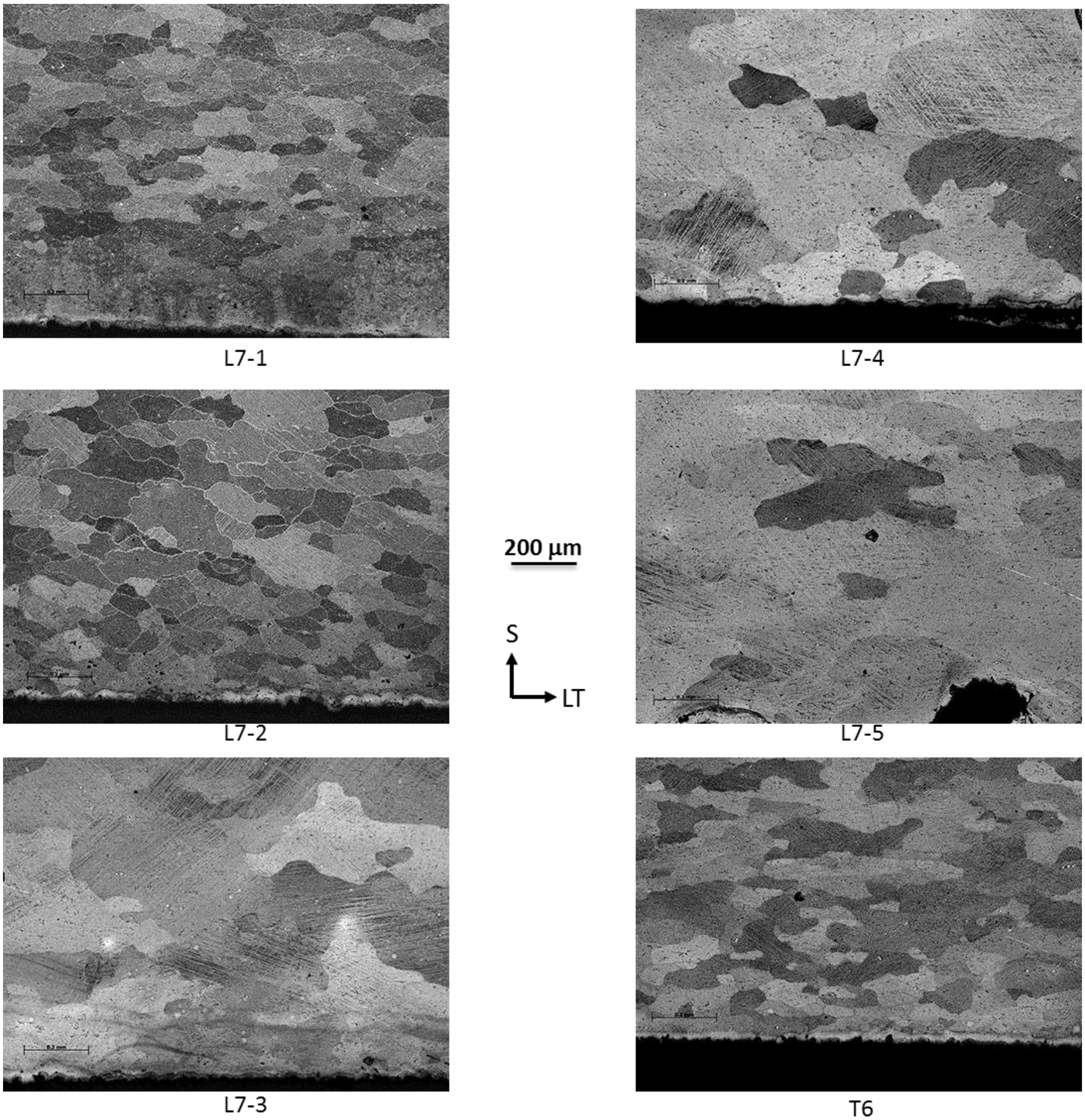

Microstructure of aft bulkhead locations L7-1 through L7-5 compared with the T6 thermally processed test block at (f) OML.

Figure 10.1-6. Microstructure of Aft Bulkhead Locations L7-1 through L7-5 Compared with the T6 Thermally Processed Test Blocks at Through-Thickness Positions (a) IML, (b) t/2, (c) 5t/8, (d) 3t/4, (e) 7t/8, and (f) OML

Various options exist for altering the recrystallization kinetics during spin forming and heat treatment and the resulting recrystallized grain size. These include changing the spin forming temperature, incorporating a recovery anneal, or changing the SHT temperature. A higher spin forming temperature may result in lower retained deformation (reduce stored energy) in the material and thus reduce the driving force for recrystallization during SHT, whereas a lower forming temperature would increase the stored energy and provide more nucleation sites for recrystallization during SHT, which would result in lower overall grain size due to grain boundary impingement. While the change in forming parameters may result in a change in the recrystallization kinetics, they represent a major shift in the established practice for Spincraft and would require substantial empirical development and validation.

Lower SHT temperatures following spin forming would reduce the overall recrystallized grain size due to lower thermal energy for grain growth. Since the objective of the SHT is to put as much solute (alloying additions) as possible into solid solution in order to obtain optimum properties after the final heat treatment process step (aging), adopting a SHT temperature below this range may limit the peak strength that can be achieved during aging. However, depending on service requirements, sufficient strength may be developed. Extending SHT time may provide some property recovery.

A more viable option may be to incorporate a recovery anneal during heat up to the SHT temperature to reduce the driving force for recrystallization. This recovery anneal can be readily incorporated into their standard SHT cycle.

Tensile, fracture, and stress corrosion specimens extracted from the aft bulkhead were located at t/2. The microstructure at t/2 for the aft bulkhead locations L7-1 through L7-5 and the T6 test block shown in Figure 10.1-6(b) exhibit the greatest similarity in grain size and morphology and extent of precipitation on prior deformation bands. Additional specimen testing will be needed to evaluate the effect of the variable microstructures at other through-thickness positions, particularly those biased toward the OML.

F-1. The aft bulkhead microstructure varies both through-thickness and along the meridian arc length positions, with larger grain sizes associated with likely regions of higher deformation.

- Grain size was larger toward the rim and toward the OML surface, likely associated with the combined stresses necessary to shape the material to fit the mandrel.
- These variations in grain size are indicative of the complex and varied deformation levels associated with the spin forming process, particularly when combined with the plate rolling history and post-forming heat treatment.

10.2 Tensile Test Results

Figure 10.2-1 shows the aft bulkhead cut plan with the location of coupon blanks from which tensile specimens were excised for mechanical property testing highlighted in yellow. Coupon blanks L1-L6 were tensile tested at LaRC while coupon blanks M1-M10 were tested at MSFC. Table 10.2-1 shows the size and location of these coupon blanks with respect to the original plate rolling direction and distance from the aft bulkhead pole to the coupon blank center point. These coupon blank locations were designed to determine uniformity of tensile properties throughout the aft bulkhead and were evaluated along selected meridian and circumferential lines.

An additional goal of these tests was to determine how these properties compare to wrought plate in the T6 and T8 tempers and to other fabricated product forms in the T6 temper. These results will assist the Orion designers in assessing the attributes of the spin form fabrication process for the aft bulkhead and identify any deficiencies or "show stoppers" associated with this fabrication process.

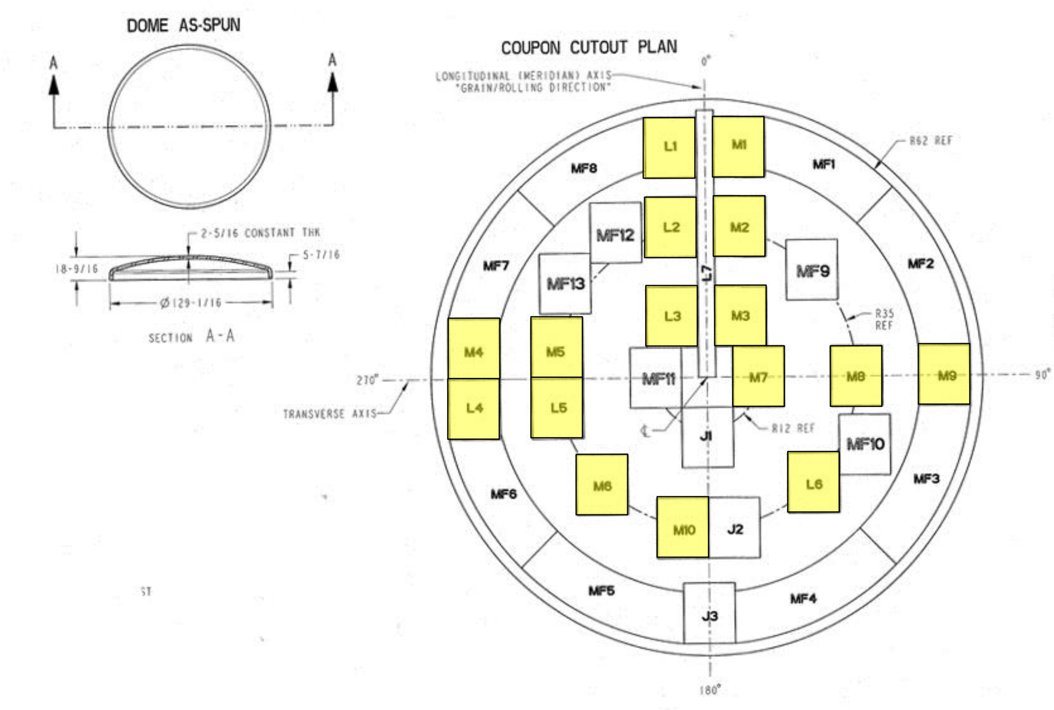

Figure 10.2-1. Aft Bulkhead Cut Plan showing the Location of the tensile Coupon Blanks highlighted in Yellow

Table 10.2-1. Tensile Coupon Blank Locations and Orientations

Coupon Blank	Coupon Blank Size		Coupon Center Point	
	Longitudinal Dimension, in.	Transverse Dimension, in.	Meridian Angle , degrees	Arc Length from dome CL in.
L1	14	12	351°	54-5/8
L2	14	12	347°	36
L3	14	12	330°	16-1/8
L4	14	12	259°	55-1/2
L5	14	12	263°	35-7/8
L6	14	12	135°	35-1/8
M1	14	12	9°	54-5/8
M2	14	12	13°	36
M3	14	12	30°	16-1/8
M4	14	12	277°	55-1/2
M5	14	12	281°	35-7/8
M6	14	12	225°	35-1/8
M7	14	12	90°	12
M8	14	12	90°	35-1/8
M9	14	12	90°	56-1/4
M10	14	12	190°	35-5/8

10.2.1 Uniformity of Tensile Properties

Complete tensile test results for the aft bulkhead are shown in Table 10.2-2 through Table 10.2-5, with individual specimen results for orientations L, LT, ST, and ST45, respectively. The average values and standard deviations for each coupon blank and orientation are shown in Table 10.2-6 - Table 10.2-9. The overall average tensile property values and standard deviations for all coupon blanks tested are shown in Table 10.2-10 for each orientation. Tensile values shown in red were below MMPDS A-basis allowables and will be discussed in Section 10.2.2.

Table 10.2-2. Tensile Properties of the Spin Formed Al 2219-T62 Aft Bulkhead Material, Longitudinal (L) Orientation

Specimen No.	Coupon Blank	Meridian Angle	Orient.	UTS (ksi)	0.2% YS (ksi)	E (Msi)	e 1.00" GL (%)
T-L1-L-1	L1	351°	L	58.75	39.11	10.09	12.90
T-L1-L-2				58.50	39.04	10.19	11.87
T-L1-L-3				58.97	39.22	10.50	12.74
T-L2-L-13	L2	347°	L	56.35	37.66	10.43	12.37
T-L2-L-14				56.56	37.79	10.47	12.68
T-L2-L-15				56.75	37.77	10.40	13.85
T-L3-L-25	L3	330°	L	54.03	36.65	10.40	14.10
T-L3-L-26				53.73	36.63	10.44	13.21
T-L3-L-27				53.41	36.52	10.42	11.92
T-L4-L-37	L4	263°	L	58.26	39.27	10.47	9.28
T-L4-L-38				58.07	38.79	10.48	10.74
T-L4-L-39				57.47	38.36	10.47	10.09
T-L5-L-49	L5	259°	L	----	----	----	----
T-L5-L-50				55.30	37.16	10.48	11.11
T-L5-L-51				56.22	37.61	10.49	11.19
T-L6-L-61	L6	135°	L	56.27	37.62	10.44	11.61
T-L6-L-62				56.27	37.75	10.46	10.54
T-L6-L-63				56.31	37.65	10.47	11.36
CP-406-190	M1	9°	L	59.66	39.48	10.55	11.77
CP-406-192				59.52	39.70	10.38	11.41
CP-406-194				58.36	38.72	11.92	11.30
CP-406-205	M2	13°	L	57.01	38.02	10.30	11.81
CP-406-207				56.95	38.08	10.15	11.64
CP-406-209				57.09	38.02	11.99	11.62
CP-406-220	M3	30°	L	54.93	37.26	10.30	13.74
CP-406-222				55.61	37.51	9.77	13.79
CP-406-224				55.02	37.18	9.38	15.23
CP-406-235	M4	277°	L	59.21	39.51	12.13	10.91
CP-406-237				59.93	39.78	9.75	11.41
CP-406-239				58.20	38.60	11.42	13.12
CP-406-250	M5	281°	L	58.49	38.44	9.59	11.38
CP-406-252				58.25	38.19	11.04	12.01
CP-406-254				56.79	37.48	10.75	12.47
CP-406-265	M6	225°	L	57.66	38.46	9.88	12.37
CP-406-267				57.54	38.14	9.88	12.41
CP-406-269				58.12	38.33	10.38	13.26
----	M7	90°	L	----	----	----	----
----				----	----	----	----
----				----	----	----	----
----	M8	90°	L	----	----	----	----
----				----	----	----	----
----				----	----	----	----
----	M9	90°	L	----	----	----	----
----				----	----	----	----
----				----	----	----	----
CP-406-127	M10	190°	L	58.48	38.99	9.92	14.37
CP-406-137				56.88	38.13	10.74	11.53
CP-406-147				55.79	37.65	10.24	12.32

Table 10.2-3. Tensile Properties of the Spin Formed Al 2219-T62 Aft Bulkhead Material, Long-Transverse (LT) Orientation

Specimen No.	Coupon Blank	Meridian Angle	Orient.	UTS (ksi)	0.2% YS (ksi)	E (Msi)	e 1.00" GL (%)
T-L1-LT-4	L1	351°	LT	57.64	38.33	10.44	10.63
T-L1-LT-5				57.75	38.55	10.48	10.11
T-L1-LT-6				57.86	38.67	10.38	10.14
T-L2-LT-16	L2	347°	LT	56.33	37.49	10.38	10.73
T-L2-LT-17				56.46	37.56	10.39	10.12
T-L2-LT-18				56.10	37.35	10.44	10.61
T-L3-LT-28	L3	330°	LT	53.77	36.58	10.40	10.66
T-L3-LT-29				53.78	36.69	10.37	9.36
T-L3-LT-30				54.16	36.76	10.42	10.38
T-L4-LT-40	L4	263°	LT	56.38	38.34	10.46	7.85
T-L4-LT-41				56.69	38.33	10.37	7.99
T-L4-LT-42				57.10	38.41	10.40	8.63
T-L5-LT-52	L5	259°	LT	55.26	37.11	10.37	10.08
T-L5-LT-53				54.99	36.92	10.41	11.00
T-L5-LT-54				55.21	37.02	10.39	11.48
T-L6-LT-64	L6	135°	LT	56.37	37.42	10.41	12.98
T-L6-LT-65				56.11	37.41	10.43	11.87
T-L6-LT-66				56.27	37.66	10.41	10.48
CP-406-195	M-1	9°	LT	58.59	38.69	11.66	9.79
CP-406-197				58.53	38.71	11.06	10.09
CP-406-199				58.59	38.68	10.29	10.27
CP-406-210	M-2	13°	LT	57.49	38.03	9.38	10.49
CP-406-212				56.90	37.44	10.00	10.70
CP-406-214				57.48	38.00	10.67	11.17
CP-406-225	M-3	30°	LT	55.43	37.34	10.06	11.41
CP-406-227				55.33	37.08	10.10	12.36
CP-406-229				54.44	36.96	10.84	10.98
CP-406-240	M-4	277°	LT	58.93	38.80	11.37	10.20
CP-406-242				60.02	39.58	10.34	10.92
CP-406-244				58.14	38.88	10.13	9.21
CP-406-255	M-5	281°	LT	56.71	37.42	9.90	11.30
CP-406-257				56.82	37.48	10.02	10.87
CP-406-259				56.25	37.30	10.43	10.92
CP-406-270	M-6	225°	LT	56.50	37.45	10.94	10.36
CP-406-272				56.95	37.77	9.60	10.85
CP-406-274				56.72	37.54	9.82	10.64
CP-406-1	M7	90°	LT	53.77	36.29	9.71	10.25
CP-406-11				54.57	37.02	10.04	10.64
CP-406-21				54.07	36.60	10.15	10.86
CP-406-43	M8	90°	LT	57.61	38.57	10.64	9.67
CP-406-53				56.96	38.72	10.14	9.35
CP-406-63				58.79	39.05	10.66	10.36
CP-406-85	M9	90°	LT	59.71	39.50	9.77	8.78
CP-406-95				59.04	39.53	10.28	8.64
CP-406-105				60.00	40.01	10.87	8.95
CP-406-169	M10	190°	LT	54.37	36.93	10.06	9.63
CP-406-179				56.41	38.35	10.54	11.31
CP-406-189				56.88	38.32	9.83	9.51

Table 10.2-4. Tensile Properties of the Spin Formed Al 2219-T62 aft Bulkhead Material, Short Transverse (ST) Orientation

Specimen No.	Coupon Blank	Meridian Angle	Orient.	UTS (ksi)	0.2% YS (ksi)	E (Msi)	e 0.50" GL (%)
T-L1-ST-7	L1	351°	ST	57.56	44.16	10.21	4.77
T-L1-ST-8				58.06	44.78	10.32	4.47
T-L1-ST-9				58.34	44.48	10.26	4.94
T-L2-ST-19	L2	347°	ST	56.96	43.13	10.13	4.41
T-L2-ST-20				57.64	43.17	10.37	5.09
T-L2-ST-21				58.37	44.08	10.40	5.16
T-L3-ST-31	L3	330°	ST	57.77	43.39	10.34	5.33
T-L3-ST-32				57.86	43.96	10.45	4.87
T-L3-ST-33				58.06	43.65	10.33	5.95
T-L4-ST-43	L4	263°	ST	58.58	44.89	10.33	4.17
T-L4-ST-44				59.29	45.20	10.39	5.13
T-L4-ST-45				59.19	44.70	10.36	5.63
T-L5-ST-55	L5	259°	ST	57.74	44.21	10.48	4.63
T-L5-ST-56				56.87	44.13	10.36	3.99
T-L5-ST-57				57.11	43.59	10.37	4.85
T-L6-ST-67	L6	135°	ST	57.24	43.79	10.27	4.74
T-L6-ST-68				57.66	43.85	10.35	4.78
T-L6-ST-69				58.44	44.36	10.38	5.07
CP-406-200	M-1	9°	ST	58.62	38.32	10.95	4.28
CP-406-202				62.08	37.82	10.58	5.35
CP-406-204				59.87	36.53	9.59	5.13
CP-406-215	M-2	13°	ST	59.52	41.96	9.14	4.61
CP-406-217				60.49	41.44	9.46	4.62
CP-406-219				59.37	40.68	10.08	4.53
CP-406-230	M-3	30°	ST	56.21	37.64	9.72	5.08
CP-406-232				57.12	37.77	10.57	3.93
CP-406-234				57.90	36.50	10.26	4.04
CP-406-245	M-4	277°	ST	58.50	38.08	10.52	4.80
CP-406-247				60.28	39.54	10.21	4.14
CP-406-249				61.48	39.88	9.24	5.70
CP-406-260	M-5	281°	ST	58.61	38.52	10.14	3.77
CP-406-262				64.14	39.42	9.91	4.55
CP-406-264				56.71	38.10	9.75	3.54
CP-406-275	M-6	225°	ST	56.89	40.83	10.53	3.34
CP-406-277				59.36	40.08	8.76	4.77
CP-406-279				59.27	40.06	10.09	4.38
CP-406-22	M7	90°	ST	58.15	43.76	10.39	4.9
CP-406-32				57.24	42.23	9.52	4.68
CP-406-42				58.21	43.61	9.76	4.83
CP-406-64	M8	90°	ST	58.13	42.59	9.84	4.38
CP-406-74				58.94	44.48	9.39	4.05
CP-406-84				59.00	44.11	9.76	5.29
CP-406-106	M9	90°	ST	60.87	45.55	9.33	4.49
CP-406-116				61.20	43.63	9.01	4.36
CP-406-126				57.50	43.80	9.44	3.52
CP-406-148	M10	190°	ST	59.44	44.57	9.98	4.76
CP-406-158				59.59	44.79	10.04	5.01
CP-406-168				59.92	43.88	10.34	4.73

Table 10.2-5. Tensile Properties of the Spin Formed Al 2219-T62 Aft Bulkhead Material, Short Transverse 45° (ST45) Orientation

Specimen No.	Coupon Blank	Meridian Angle	Orient.	UTS (ksi)	0.2% YS (ksi)	E (Msi)	e 0.50" GL (%)
T-L1-ST45-10	L1	351°	ST45	53.14	43.44	10.81	2.99
T-L1-ST45-11				49.34	37.53	10.62	2.82
T-L1-ST45-12				52.14	36.77	10.50	4.10
T-L2-ST45-22	L2	347°	ST45	54.36	38.00	10.73	5.01
T-L2-ST45-23				53.63	38.06	10.60	4.70
T-L2-ST45-24				54.01	39.28	10.82	4.58
T-L3-ST45-34	L3	330°	ST45	53.24	38.94	10.64	4.41
T-L3-ST45-35				52.85	40.71	10.31	3.25
T-L3-ST45-36				55.23	43.64	10.79	4.13
T-L4-ST45-46	L4	263°	ST45	51.76	38.65	10.84	3.33
T-L4-ST45-47				51.74	36.03	10.73	4.47
T-L4-ST45-48				49.80	36.38	10.50	3.38
T-L5-ST45-58	L5	259°	ST45	53.94	38.39	10.77	4.80
T-L5-ST45-59				53.76	37.82	10.87	4.80
T-L5-ST45-60				53.29	37.42	10.61	5.04
T-L6-ST45-70	L6	135°	ST45	55.52	47.54	10.91	2.64
T-L6-ST45-71				55.85	47.49	11.07	2.79
T-L6-ST45-72				54.30	38.62	10.90	4.48

Table 10.2-6. Average Tensile Properties and Standard Deviations of the Spin Formed Al 2219-T62 Aft Bulkhead Material, Longitudinal (L) Orientation

Coupon Blank	Orient.	UTS (ksi)	0.2% YS (ksi)	E (Msi)	e 1.00" GL (%)	
L1	L	58.74	39.12	10.26	12.5	Average
		0.23	0.09	0.21	0.56	Std Dev.
L2	L	56.55	37.74	10.44	12.97	
		0.2	0.07	0.03	0.78	
L3	L	53.72	36.6	10.42	13.08	
		0.31	0.07	0.02	1.1	
L4	L	57.93	38.81	10.47	10.04	
		0.41	0.45	0.01	0.73	
L5	L	55.76	37.38	10.48	11.15	
		0.65	0.32	0.01	0.05	
L6	L	56.28	37.68	10.46	11.17	
		0.03	0.07	0.02	0.56	
M1	L	59.18	39.3	10.95	11.49	
		0.71	0.51	0.84	0.24	
M2	L	57.02	38.04	10.81	11.69	
		0.07	0.03	1.02	0.1	
M3	L	55.19	37.32	9.82	14.25	
		0.37	0.17	0.46	0.85	
M4	L	59.11	39.29	11.1	11.81	
		0.86	0.62	1.22	1.16	
M5	L	57.84	38.04	10.46	11.95	
		0.92	0.5	0.77	0.55	
M6	L	57.77	38.31	10.04	12.68	
		0.31	0.16	0.29	0.5	
M10	L	57.05	38.26	10.3	12.74	
		1.35	0.68	0.41	1.47	

Table 10.2-7. Average Tensile Properties and Standard Deviations of the Spin Formed Al 2219-T62 Aft Bulkhead Material, Long Transverse (LT) Orientation

Coupon Blank	Orient.	UTS (ksi)	0.2% YS (ksi)	E (Msi)	e 1.00" GL (%)	
L1	LT	57.75	38.52	10.43	10.29	Average
		0.11	0.17	0.05	0.29	Std Dev.
L2	LT	56.3	37.47	10.41	10.49	
		0.18	0.11	0.03	0.32	
L3	LT	53.9	36.68	10.4	10.13	
		0.23	0.09	0.03	0.69	
L4	LT	56.72	38.36	10.41	8.16	
		0.36	0.04	0.04	0.41	
L5	LT	55.16	37.02	10.39	10.85	
		0.15	0.1	0.02	0.71	
L6	LT	56.25	37.5	10.42	11.77	
		0.13	0.14	0.01	1.25	
M1	LT	58.57	38.69	11	10.05	
		0.03	0.01	0.69	0.24	
M2	LT	57.29	37.82	10.01	10.79	
		0.34	0.33	0.64	0.35	
M3	LT	55.07	37.13	10.34	11.58	
		0.55	0.2	0.44	0.7	
M4	LT	59.03	39.09	10.61	10.11	
		0.94	0.43	0.66	0.86	
M5	LT	56.59	37.4	10.11	11.03	
		0.3	0.09	0.28	0.24	
M6	LT	56.72	37.59	10.12	10.61	
		0.22	0.17	0.72	0.25	
M7	LT	54.14	36.64	9.97	10.58	
		0.4	0.37	0.23	0.31	
M8	LT	57.79	38.78	10.48	9.79	
		0.93	0.25	0.29	0.52	
M9	LT	59.58	39.68	10.31	8.79	
		0.49	0.29	0.55	0.16	
M10	LT	55.89	37.87	10.14	10.15	
		1.33	0.81	0.36	1.01	

Table 10.2-8. Average Tensile Properties and Standard Deviations of the Spin Formed Al 2219-T62 Aft Bulkhead Material, Short Transverse (ST) Orientation

Coupon Blank	Orient.	UTS (ksi)	0.2% YS (ksi)	E (Msi)	e 0.50" GL (%)	
L1	ST	57.99	44.48	10.26	4.73	Average
		0.4	0.31	0.05	0.24	Std Dev.
L2	ST	57.65	43.46	10.3	4.89	
		0.7	0.54	0.15	0.41	
L3	ST	57.9	43.67	10.37	5.38	
		0.14	0.29	0.07	0.54	
L4	ST	59.02	44.93	10.36	4.98	
		0.39	0.25	0.03	0.74	
L5	ST	57.24	43.98	10.4	4.49	
		0.45	0.34	0.07	0.45	
L6	ST	57.78	44	10.33	4.87	
		0.61	0.31	0.06	0.18	
M1	ST	60.19	37.55	10.37	4.92	
		1.75	0.93	0.7	0.57	
M2	ST	59.79	41.36	9.56	4.59	
		0.61	0.65	0.48	0.05	
M3	ST	57.08	37.3	10.19	4.35	
		0.85	0.7	0.43	0.63	
M4	ST	60.09	39.17	9.99	4.88	
		1.5	0.96	0.66	0.78	
M5	ST	59.82	38.68	9.93	3.96	
		3.86	0.68	0.2	0.53	
M6	ST	58.51	40.32	9.8	4.16	
		1.4	0.44	0.92	0.74	
M7	ST	57.87	43.2	9.89	4.8	
		0.54	0.84	0.45	0.11	
M8	ST	58.69	43.73	9.66	4.57	
		0.49	1	0.24	0.64	
M9	ST	59.86	44.33	9.26	4.12	
		2.05	1.06	0.22	0.53	
M10	ST	59.65	44.41	10.12	4.83	
		0.25	0.47	0.19	0.15	

Table 10.2-9. Average Tensile Properties and Standard Deviations of the Spin Formed Al 2219-T62 Aft Bulkhead Material, Short Transverse 45° (ST45) Orientation

Coupon Blank	Orient.	UTS (ksi)	0.2% YS (ksi)	E (Msi)	e 0.50" GL (%)	
L1	ST45	51.54	39.25	10.65	3.30	Average
		1.97	3.65	0.16	0.69	Std Dev.
L2	ST45	54.00	38.44	10.72	4.77	
		0.36	0.73	0.11	0.22	
L3	ST45	53.77	41.10	10.58	3.93	
		1.28	2.37	0.25	0.61	
L4	ST45	51.10	37.02	10.69	3.73	
		1.13	1.42	0.17	0.65	
L5	ST45	53.66	37.88	10.75	4.88	
		0.33	0.49	0.13	0.14	
L6	ST45	55.22	44.55	10.96	3.30	
		0.81	5.13	0.10	1.02	

Table 10.2-10. Average Tensile Properties and Standard Deviation Values for the Spin Formed Al 2219-T62 aft Bulkhead Material

Orient.	UTS (ksi)	0.2% YS (ksi)	E (Msi)	e 1.00" GL (%)	
L	57.12	38.17	10.46	12.14	Average
	1.64	0.86	0.59	1.23	Std Dev.
LT	56.67	37.89	10.35	10.32	
	1.67	0.90	0.42	1.02	
ST*	58.69	42.16	10.05	4.66	
	1.54	2.67	0.47	0.56	
ST45*	53.22	39.71	10.72	3.98	
	1.76	3.51	0.18	0.84	

* = 0.50" GL

The trends observed in the aft bulkhead tensile results, based on the average tensile values shown in Table 10.2-10, are representative of the trends observed for each coupon blank. Average tensile strengths and elongation values are essentially equivalent for the L and T orientations. Of note, however, is that the UTS and YS are highest in the ST orientation, by approximately 3% for UTS and 10% for YS as compared to the L and LT orientations. The ST UTS and YS values were greater than those for the ST45 orientation by approximately 10% and 6%, respectively.

The UTS was lowest for the ST45 orientation, but YS was higher than for the L and T orientations. Elongation values in the ST orientation were about half those for the L and LT orientations. The average elongation value was lowest for the ST45 orientation, but was still nearly 4%. It is unclear whether the measured ST properties are unique to this plate or are the result of the spin forming deformation.

To evaluate the variability in tensile properties in the aft bulkhead the average tensile test results were superimposed on the aft bulkhead cut plan as shown in Figure 10.2-2 through Figure 10.2-5 for each orientation. Trends were evaluated as a function of meridian angle and distance from the pole. Tensile values shown in red fell below MMPDS A-basis design allowables. There appears to be a trend of increasing tensile strength from pole to rim for the L and LT orientations, but uniform properties about circumferential lines. Along the 0° to 180° meridian line, which is parallel to the original plate rolling direction, for the L and LT orientations, the coupon blanks furthest from the pole (L1, M1) exhibit both higher UTS and YS by 1.5 to 2 ksi than coupon blanks at the mid arc length (L2, M2) and become progressively lower in strength as one gets closer to the pole (L3, M3). The same trend appears at the opposing 180° meridian in coupon blank M10. Similar property trends exist along the 90° to 270° meridian line. Conversely, for a given meridian distance, tensile properties are uniform as one translates through the 0° to 360° meridian angles along circumferential lines (for example, meridian distance 35 inches, M2-L6-M10-M6-L5-M5-L2). These trends are not as systematic for the ST and ST45 due to greater scatter in the values for each coupon blank for these orientations. Table 10.2-8 and Table 10.2-9 illustrate the greater standard deviations for these orientations.

To verify whether these trends are statistically significant, the individual tensile test results were plotted as a function of distance from the pole and meridian angle in Figure 10.2-6 through Figure 10.2-17. Also shown in these plots for reference are the MMPDS A-basis design allowables. Figure 10.2-6 and Figure 10.2-7 show tensile properties for the L and LT orientations along the 0° to 180° meridian line. The tensile data shows a clear trend of increasing strength with arc length distance from the pole for both of these orientations. The scatter in results for each coupon blank is less than the difference between populations of data clusters. Figure 10.2-8 and Figure 10.2-9 confirm that the trend is similar for the 90° - 270° meridian line. Similar plots for the ST and ST45 orientations, shown in Figure 10.2-10 through Figure 10.2-13 illustrate the larger scatter in this data and inability to discern any definitive trend.

Plots of tensile data as a function of meridian angle at a distance of 35 inches from the pole, shown in Figure 10.2-14 through Figure 10.2-17, confirm that the tensile data is uniform for a given circumferential line. The scatter in the L and LT data (Figure 10.2-14 and Figure 10.2-15) is sufficiently small that the tensile properties are considered constant about this circumferential line. Scatter in the ST orientation (Figure 10.2-16) is greater than that in L and LT, but the data still reflect uniformity with meridian angle. The scatter in the ST45 data (Figure 10.2-17) is small with the exception of the YS at 135 degrees and the amount of data is much less than for the other orientations, but the data is reasonably uniform with meridian angle.

While this trend of increasing strength with arc length distance from the pole has been observed, budget and schedule prevent further studies on this matter. General metallurgical theory suggests that this trend may be related to the level of deformation imparted during spin forming both as a result of pressure from the forming tool as well as the strains induced during forming of the contour. The tool pressure is fairly uniform from the pole to the rim, but the imposed strain levels likely increase due to the superimposed forming stresses (tangential compressive and radial tensile and compressive) acting on the material, particularly towards the edge of the forming blank (2). However, these deformation strains should be relieved and the microstructure should undergo recovery during the high temperature solution heat treatment.

One additional source of deformation may be related to the distortion and residual stress resulting from the quench following solution heat treatment. Because of the potential for non-uniform deformation through-thickness, it is recommended that additional tensile tests be conducted to evaluate through-thickness positions other than t/2.

Variations in grain size described in Section 10.1 were attributed to the variation in forming stresses. All of the tensile tests were performed at the t/2 through-thickness position. The microstructure is fairly constant at t/2 throughout the regions examined in the aft bulkhead (Figure 10.1-6b) in terms of grain size and indications of residual deformation; however, there may be subtle variations that could explain the trends observed in the tensile properties. Other thickness positions exhibit greater variations, such as near the OML (Figure 10.1-6f). Of greater importance may be the effect of through-thickness grain size variations (See Figure 10.1-3a-e) on tensile properties. The through-thickness variation in microstructure should be examined for all spin formed components fabricated from Al 2219-T62 and tensile testing designed to sample the range of grain sizes.

F-2. Tensile tests designed to determine tensile property uniformity over the aft bulkhead acreage noted that the tensile properties varied with location in the aft bulkhead.

- For the L and LT orientations, a trend of increasing tensile and YS with arc length distance from the pole was evident.
- Conversely, the properties were uniform in the circumferential direction.
- The ST tensile properties were notably greater than those for the other orientations (L, LT, ST45), but elongations were about half.

O-1. The rationale for the variations in tensile properties with location in the aft bulkhead was not fully characterized. The microstructure at the through-thickness location tested (t/2) was more uniform throughout the aft bulkhead than at other locations.

R-1. The microstructural variability of the Orion first article spin formed aft bulkhead should be determined and mechanical property testing designed to sample regions of maximum and minimum grain size in order to evaluate the effect of variable microstructures, if observed. (***F-1, F-2, O-1***)

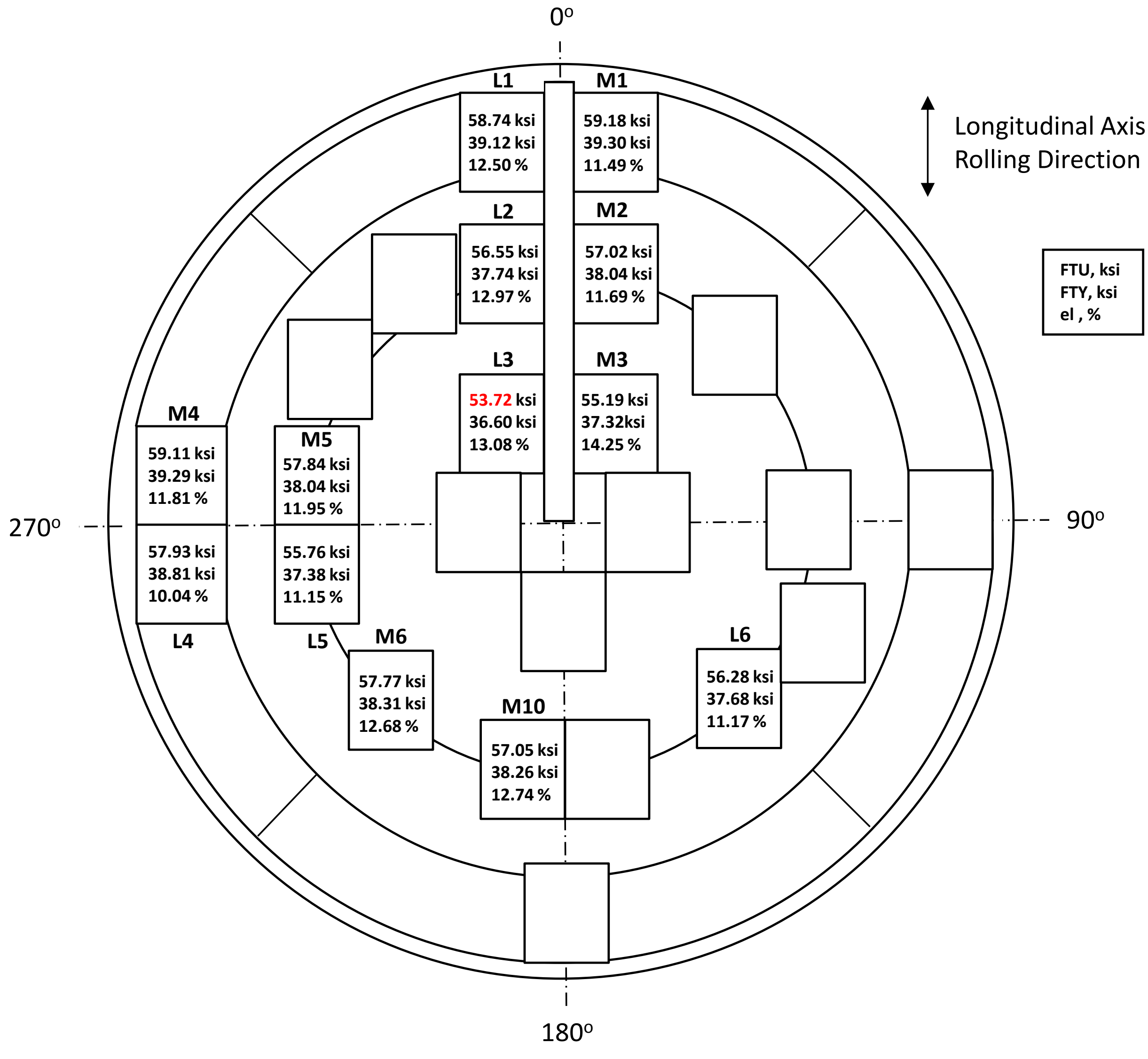

Figure 10.2-2. Average Longitudinal (L) Tensile Properties Superimposed on the Aft Bulkhead Cut Plan

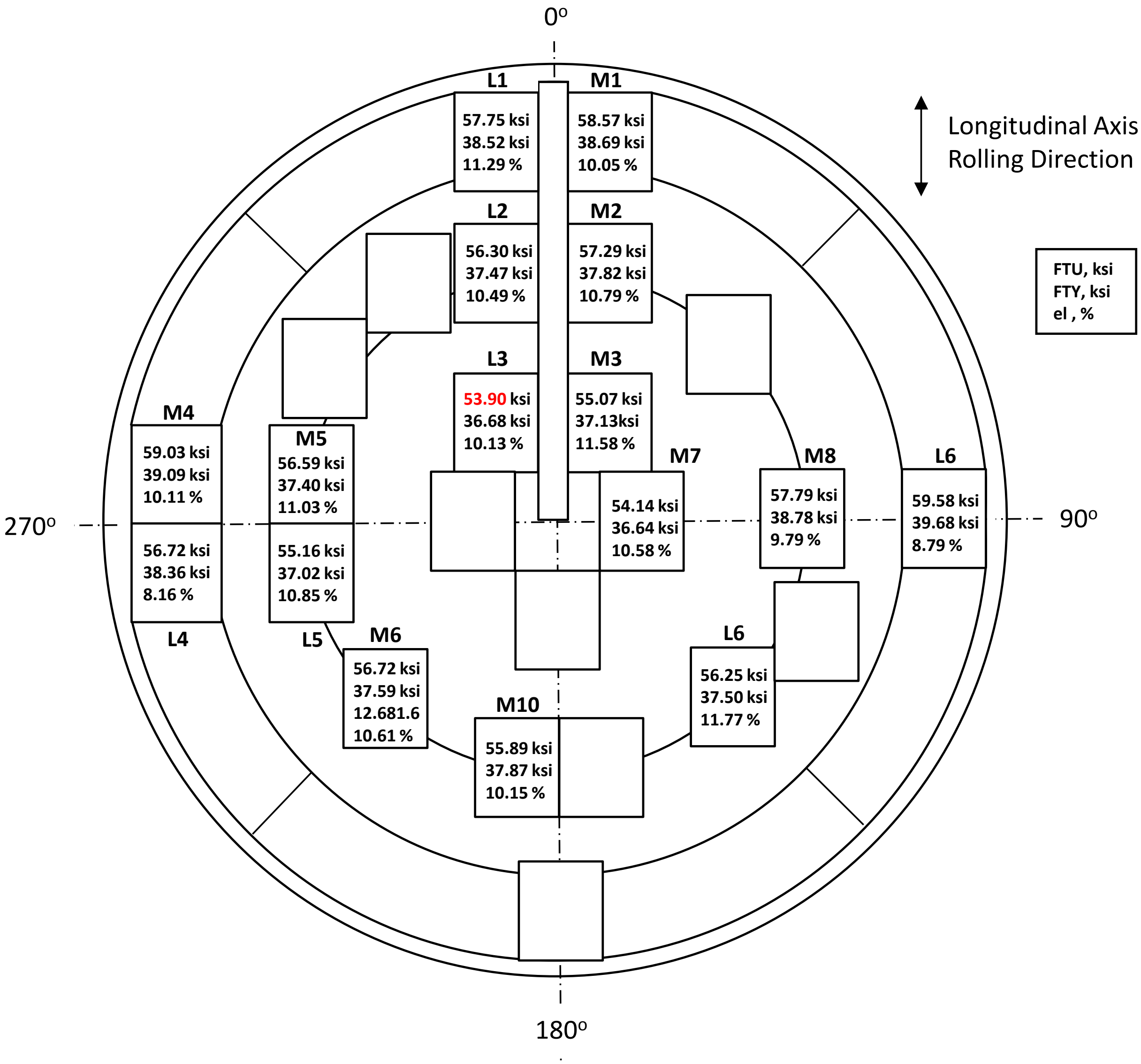

Figure 10.2-3. Average Long Transverse (LT) Tensile Properties Superimposed on the Aft Bulkhead Cut Plan

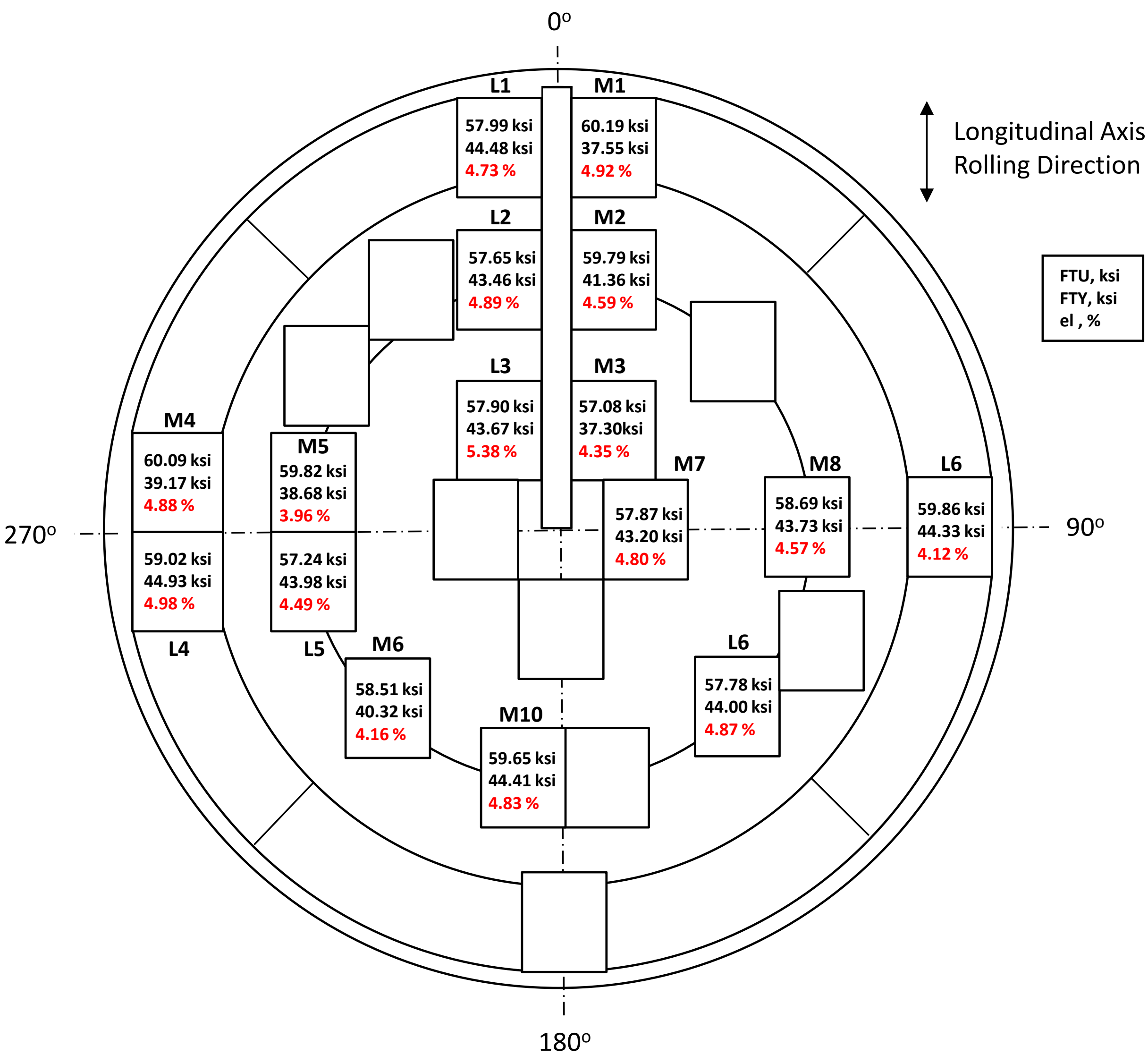

Figure 10.2-4. Average Short Transverse (ST) Tensile Properties Superimposed on the Aft Bulkhead Cut Plan

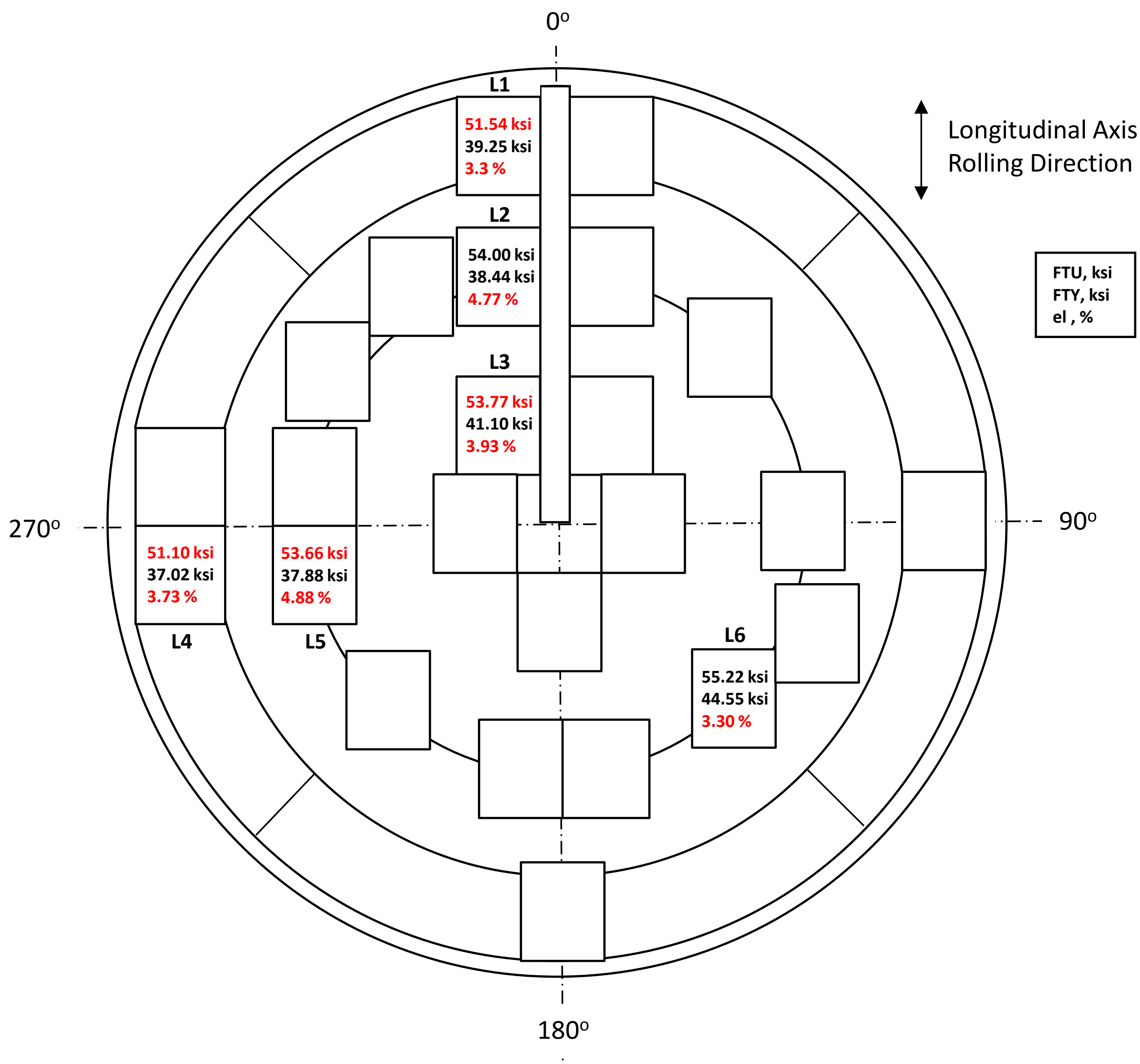

Figure 10.2-5. Average Short Transverse 45° (ST45) Tensile Properties Superimposed on the Aft Bulkhead Cut Plan

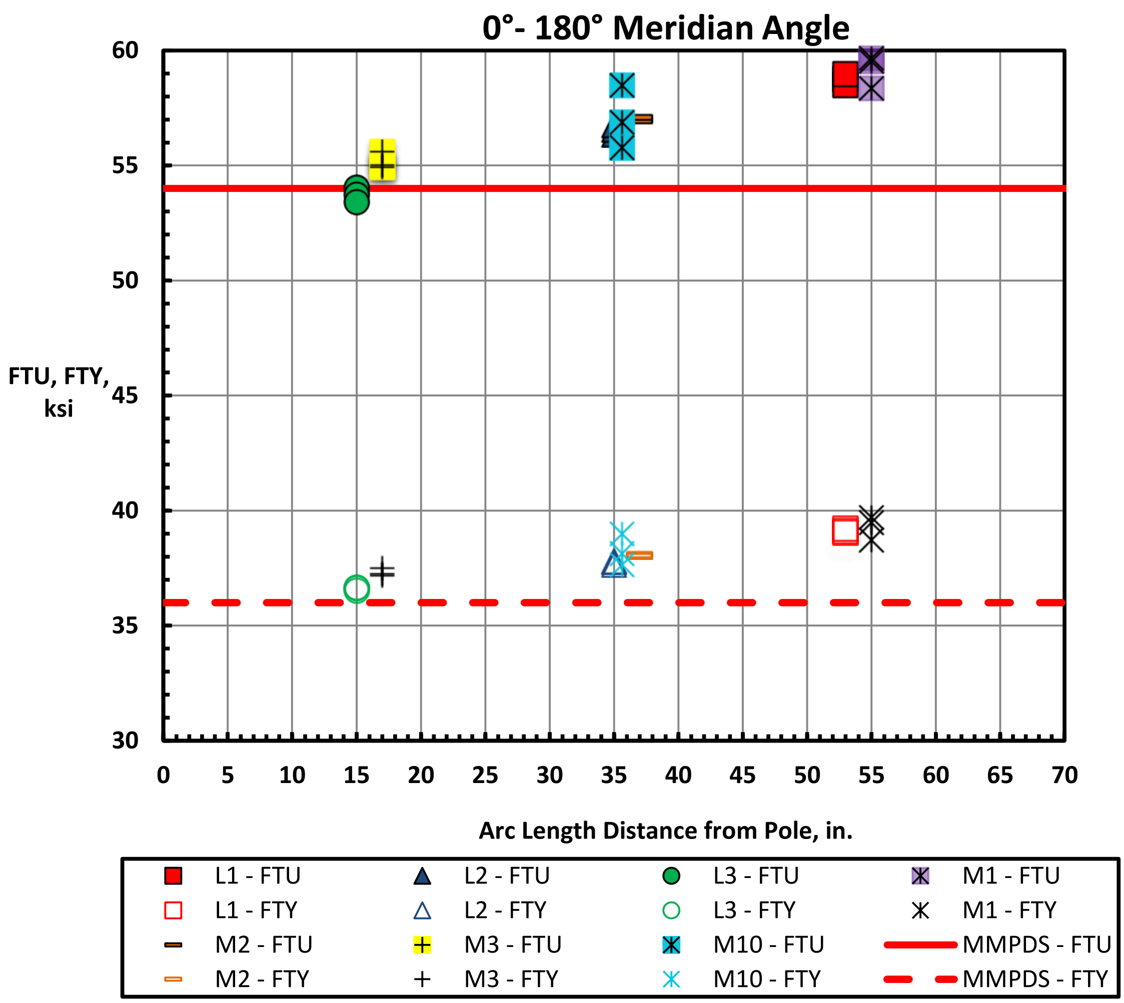

Figure 10.2-6. Longitudinal (L) Tensile Properties of the Spin Formed Al 2219-T62 Aft Bulkhead Material as a Function of Arc Length Distance from the Pole along the 0° to 180° Meridian Angle

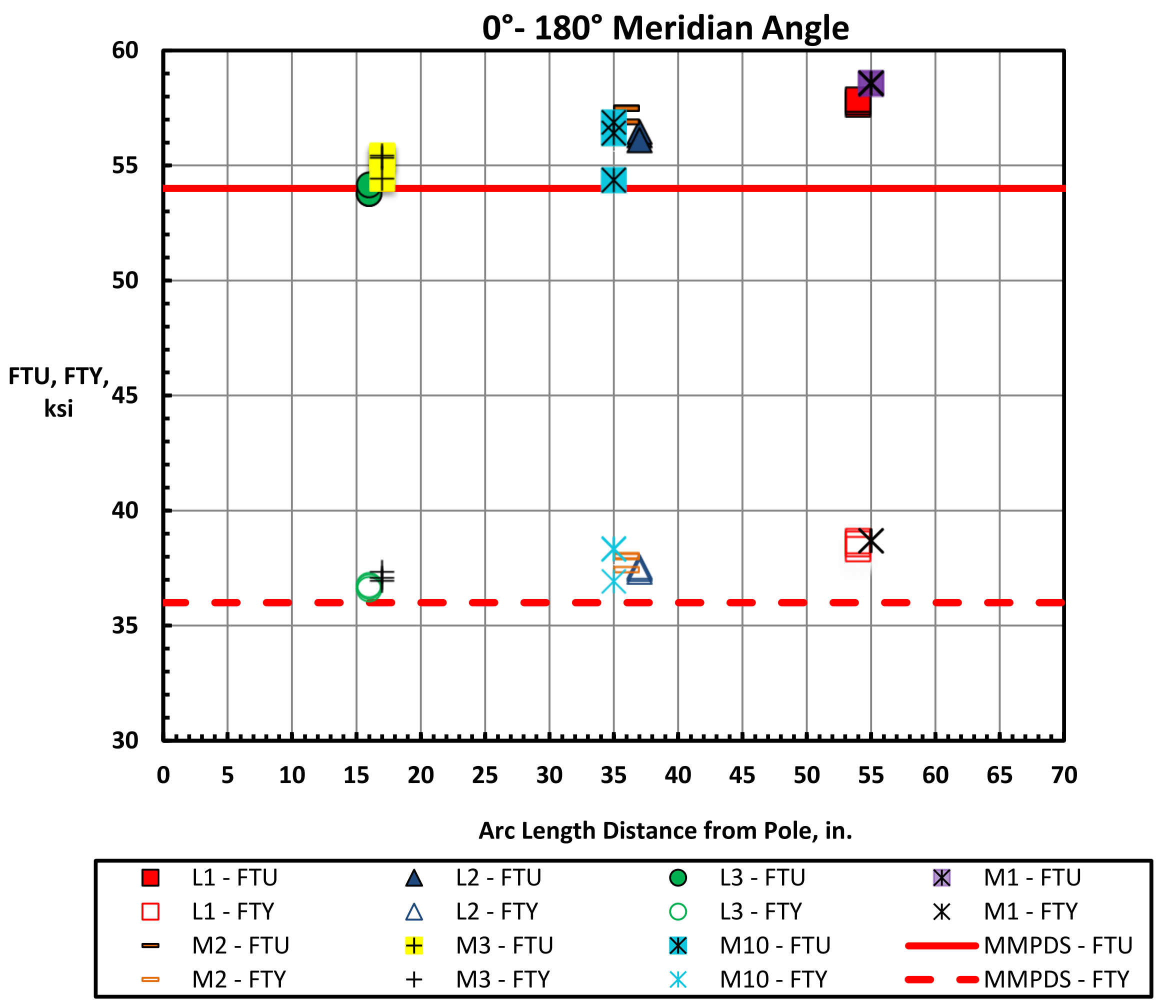

Figure 10.2-7. Long Transverse (LT) Tensile Properties of the Spin Formed Al 2219-T62 Aft Bulkhead Material as a Function of Arc Length Distance from the Pole along the 0° to 180° Meridian Angle

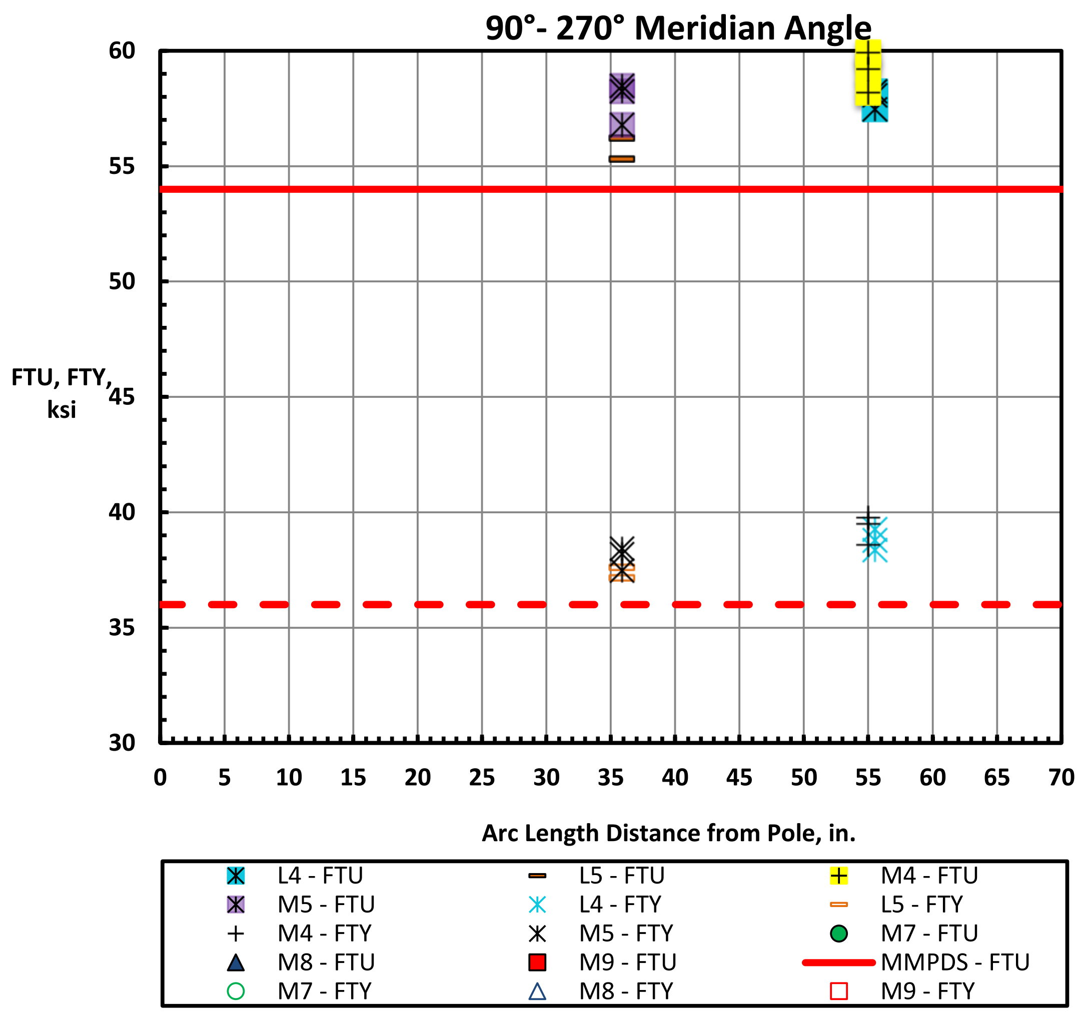

Figure 10.2-8. Longitudinal (L) Tensile Properties of the Spin Formed Al 2219-T62 Aft Bulkhead Material as a Function of Arc Length Distance from the Pole along the 90° to 270° Meridian Angle

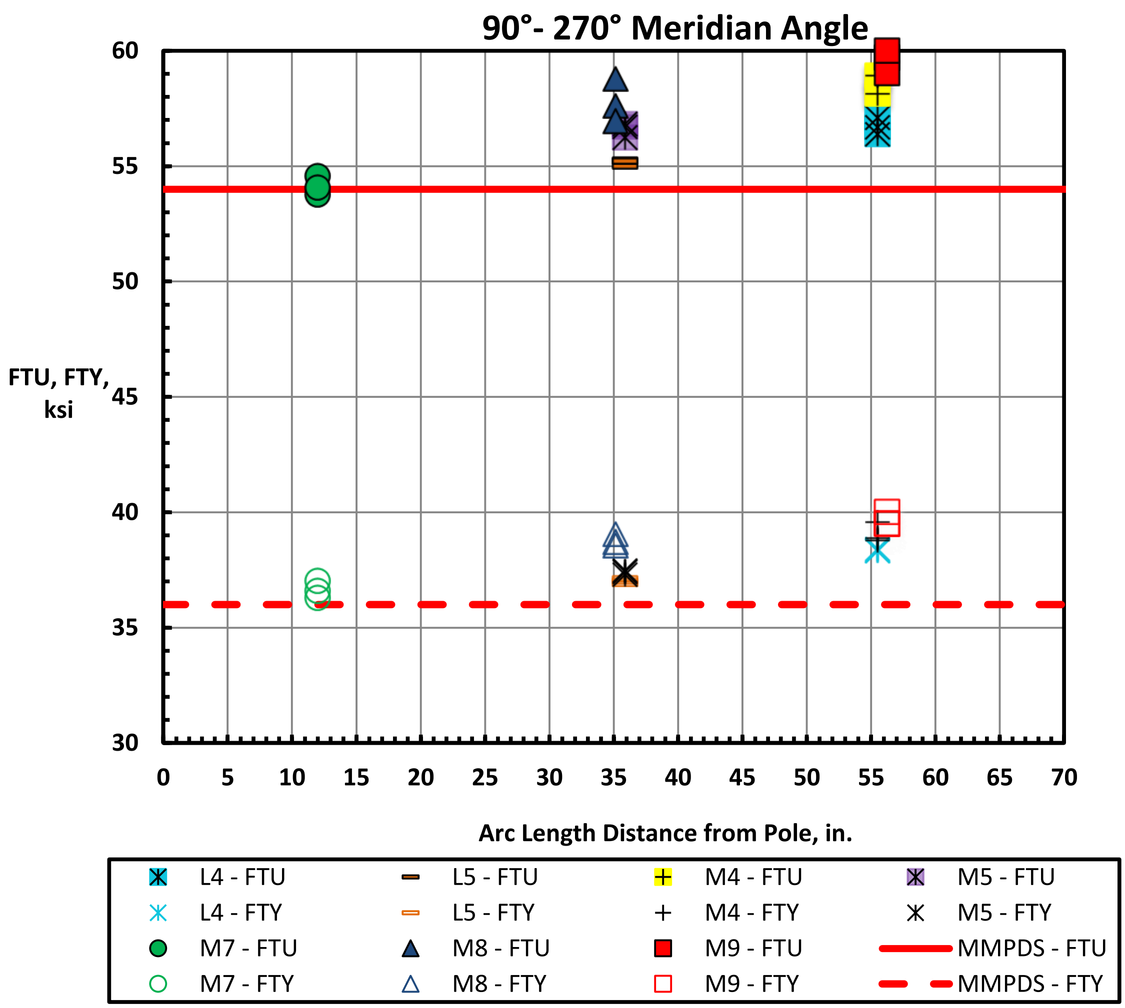

Figure 10.2-9. Long Transverse (LT) Tensile Properties of the Spin Formed Al 2219-T62 Aft Bulkhead Material as a Function of Arc Length Distance from the Pole along the 90° to 270° Meridian Angle

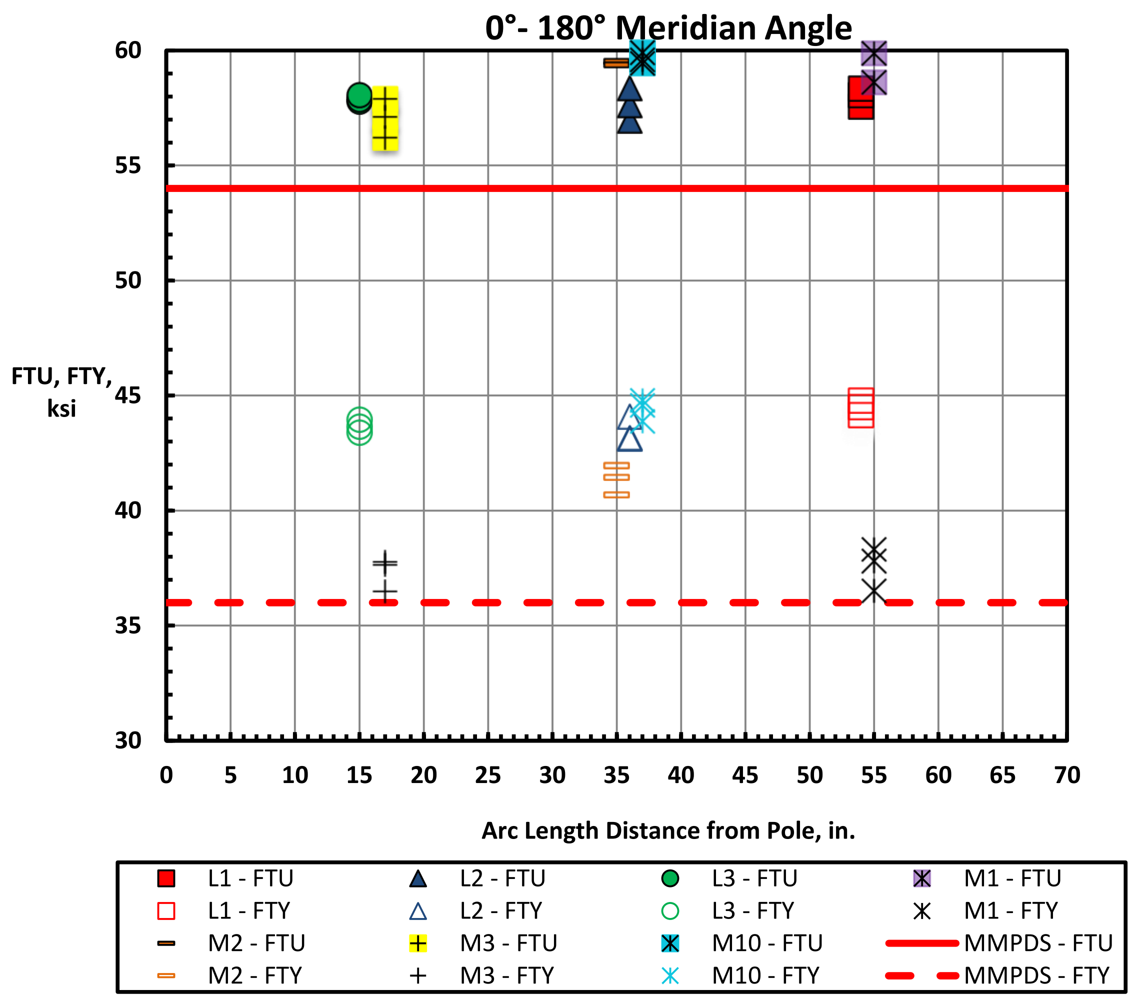

Figure 10.2-10. Short Transverse (ST) Tensile Properties of the Spin Formed Al 2219-T62 Aft Bulkhead Material as a Function of Arc Length Distance from the Pole along the 0° to 180° Meridian Angle

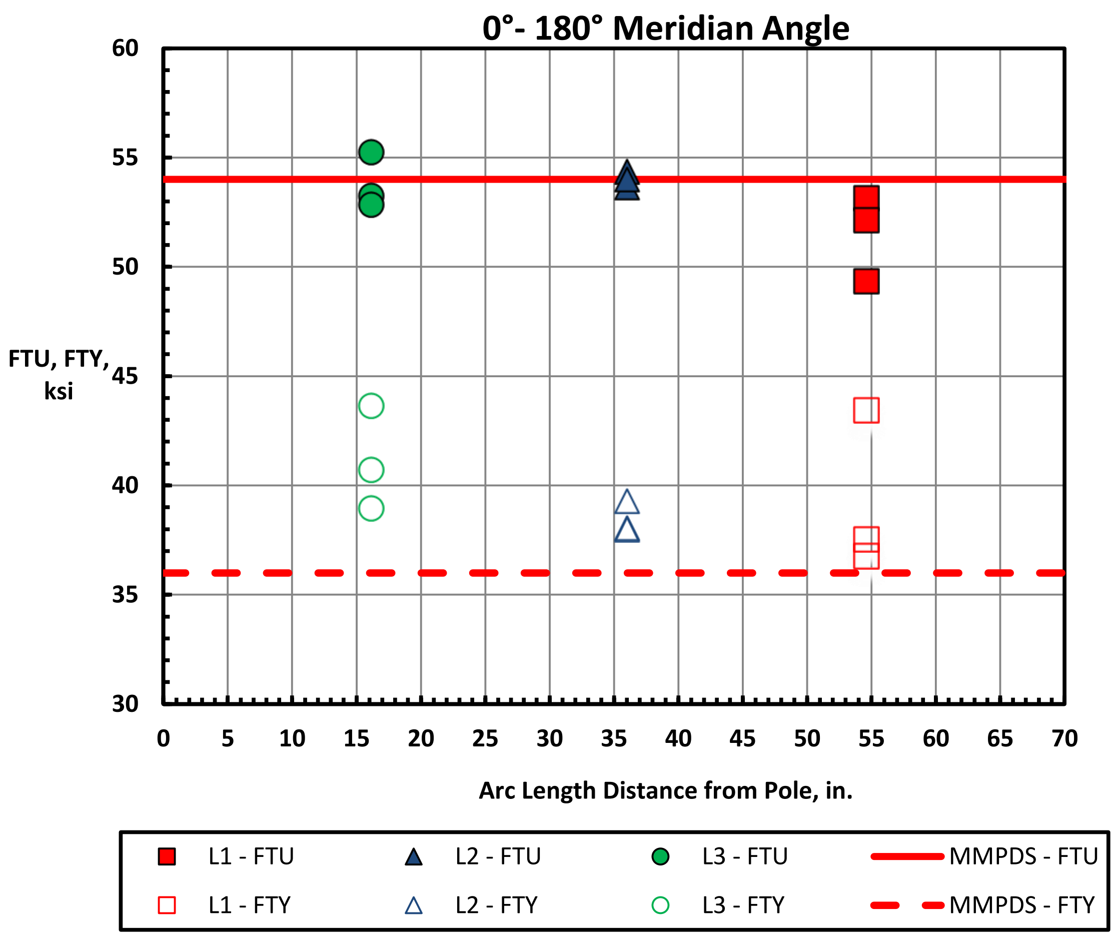

Figure 10.2-11. Short Transverse 45º (ST45) Tensile Properties of the Spin Formed Al 2219-T62 Aft Bulkhead Material as a Function of Arc Length Distance from the Pole along the 0° to 180° Meridian Angle

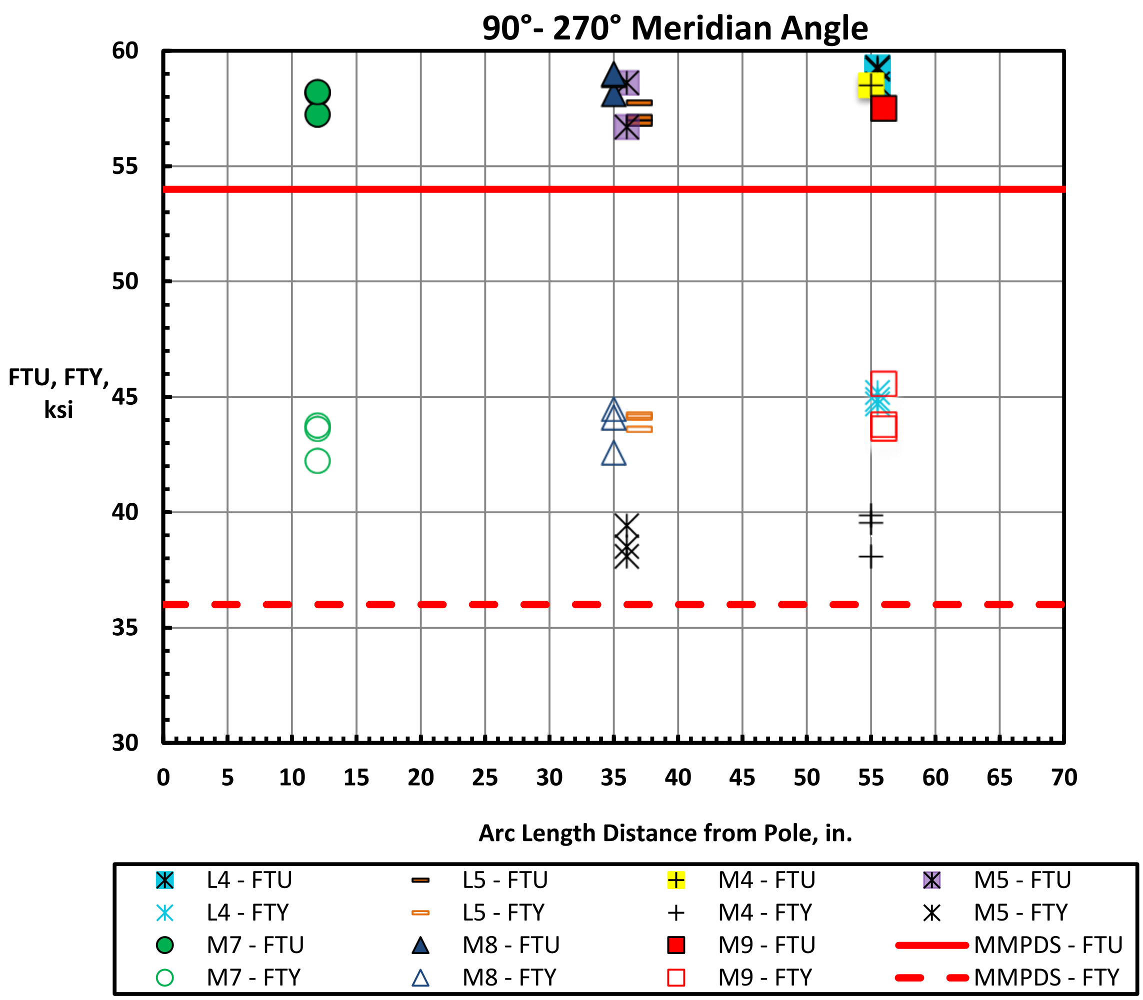

Figure 10.2-12. Short Transverse (ST) Tensile Properties of the Spin Formed Al 2219-T62 Aft Bulkhead Material as a Function of Arc Length Distance from the Pole along the 90° to 270° Meridian Angle

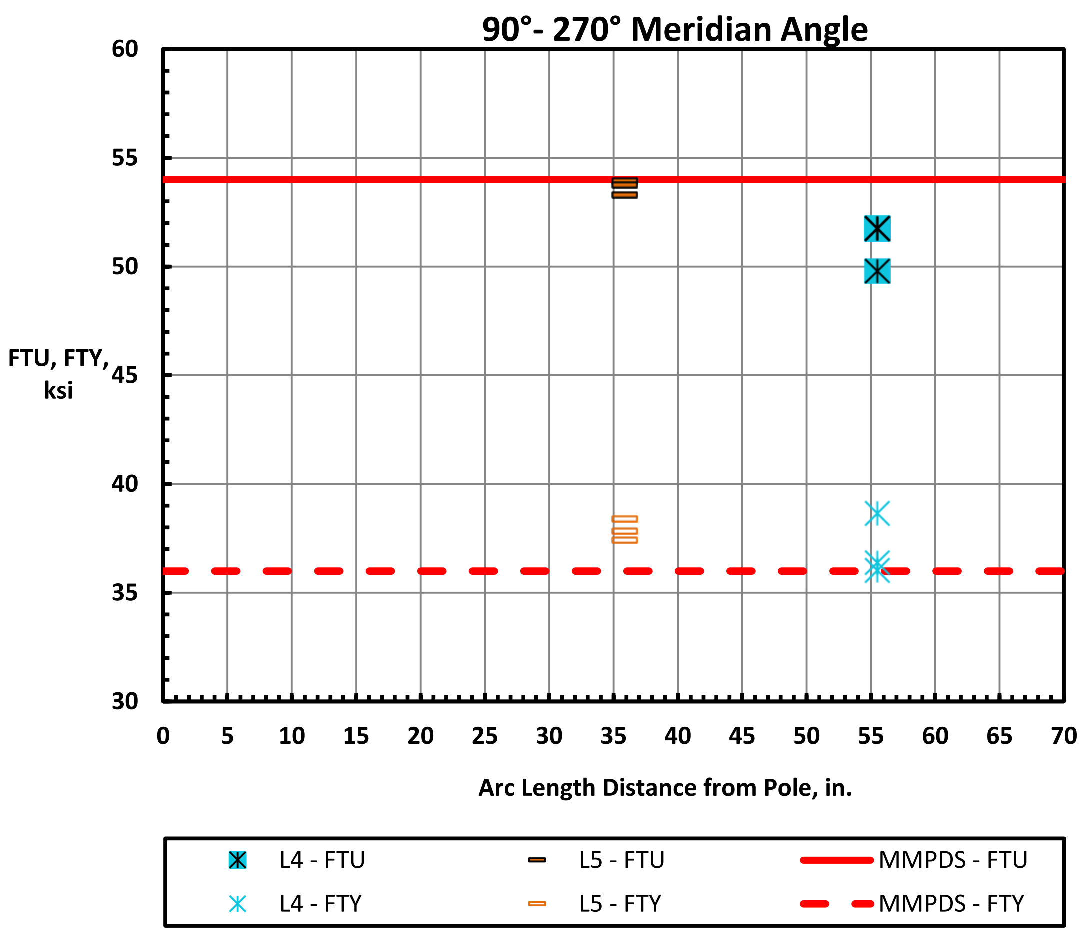

Figure 10.2-13. Short Transverse 45º (ST45) Tensile Properties of the Spin Formed Al 2219-T62 Aft Bulkhead Material as a Function of Arc Length Distance from the Pole along the 90° to 270° Meridian Angle

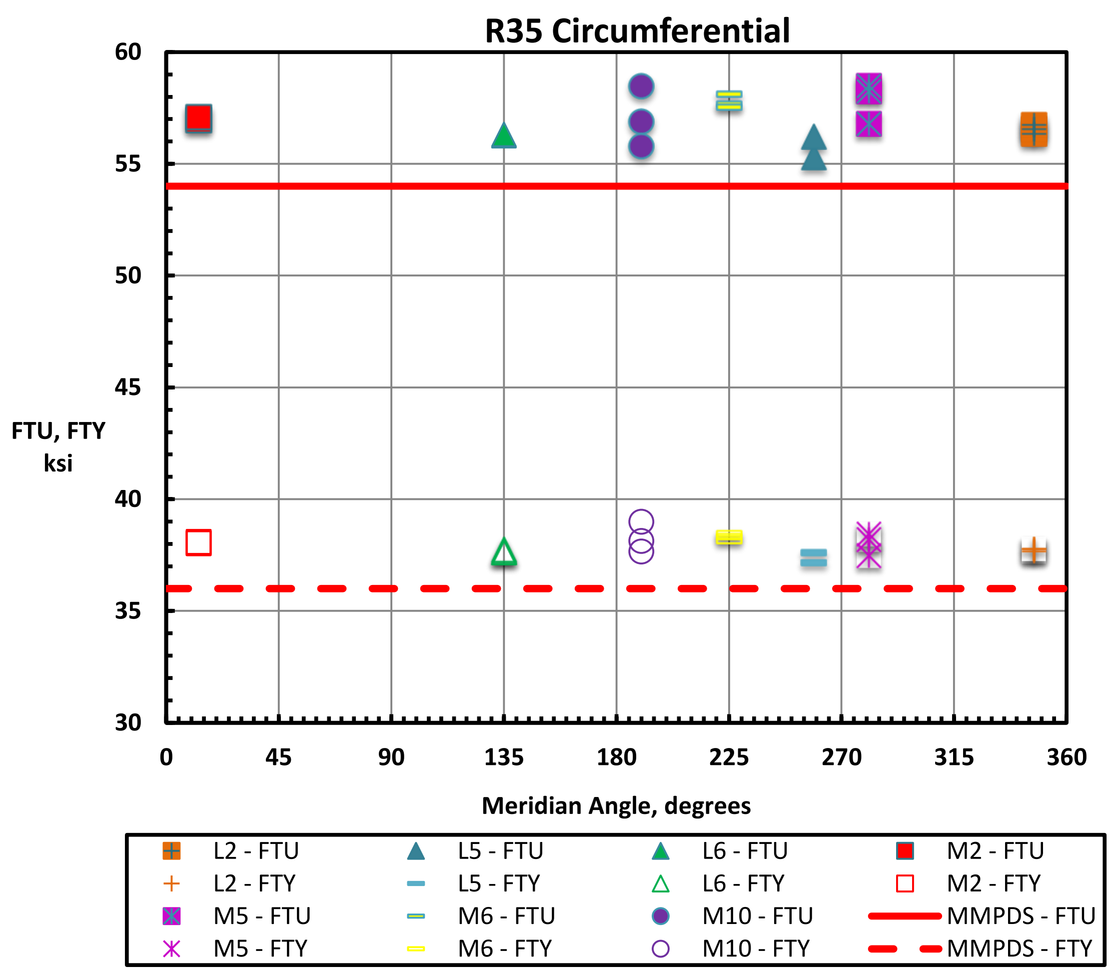

Figure 10.2-14. Longitudinal (L) Tensile Properties of the Spin Formed Al 2219-T62 Aft Bulkhead Material as a Function of Meridian Angle along the R35 Circumferential Arc Length

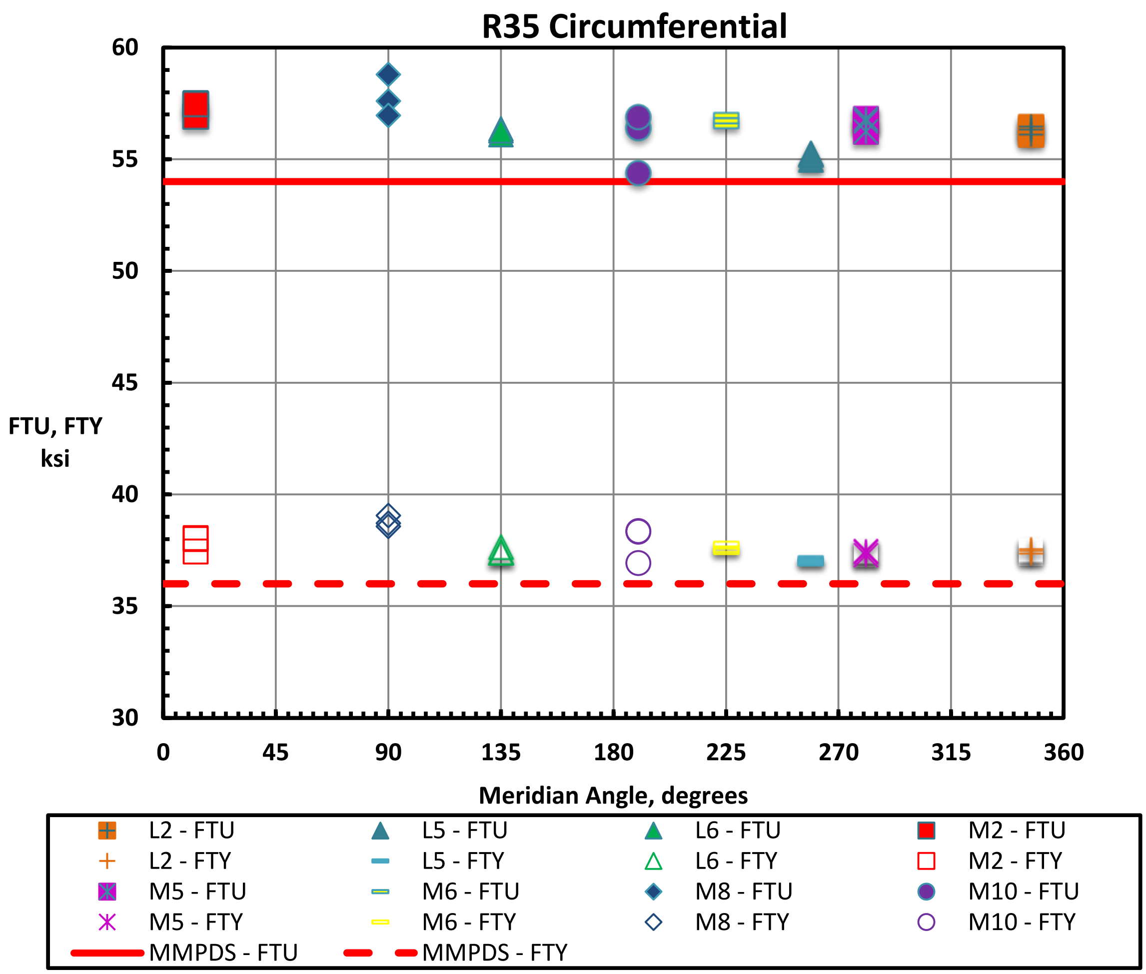

Figure 10.2-15. Long Transverse (LT) Tensile Properties of the Spin Formed Al 2219-T62 Aft Bulkhead Material as a Function of Meridian Angle along the R35 Circumferential Arc Length

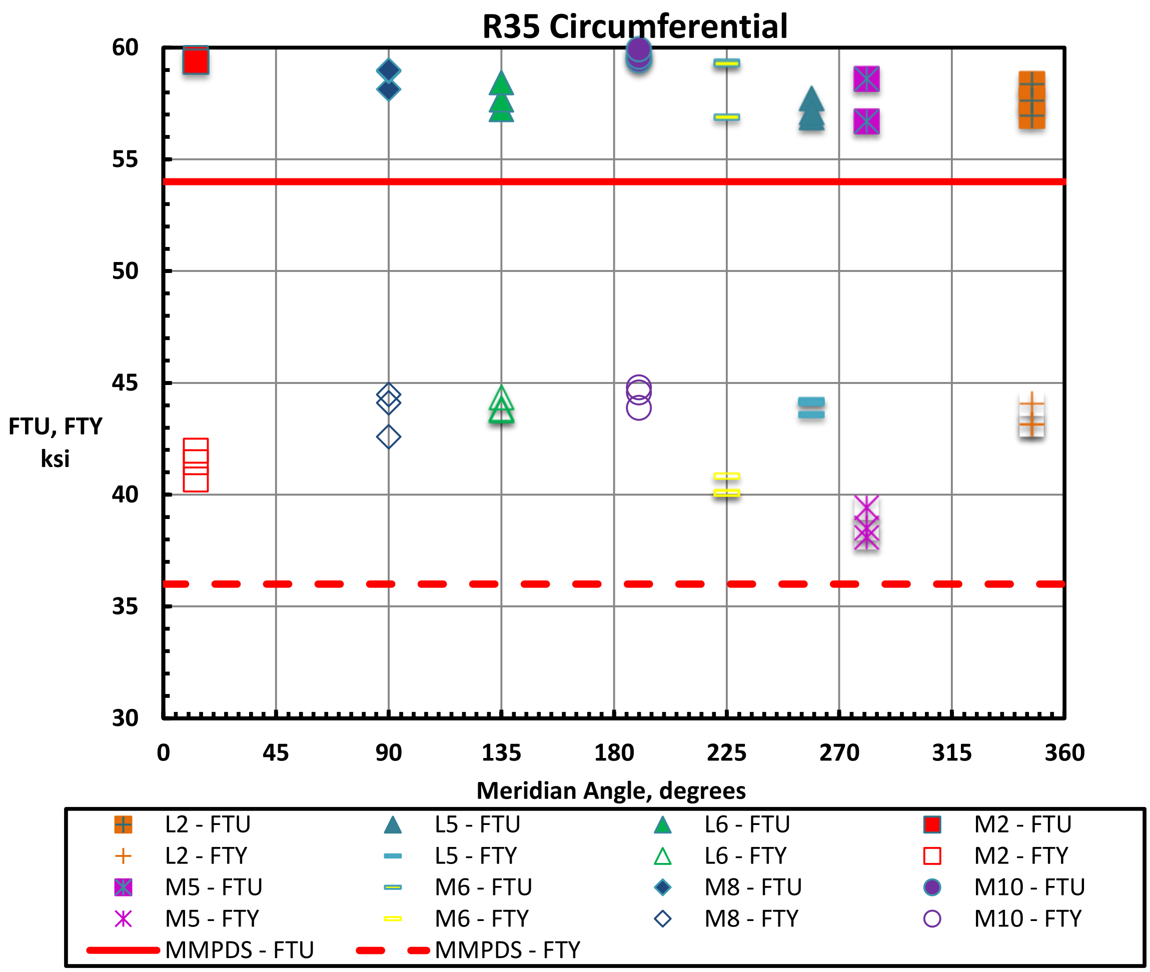

Figure 10.2-16. Short Transverse (ST) Tensile Properties of the Spin Formed Al 2219-T62 Aft Bulkhead Material as a Function of Meridian Angle along the R35 Circumferential Arc length

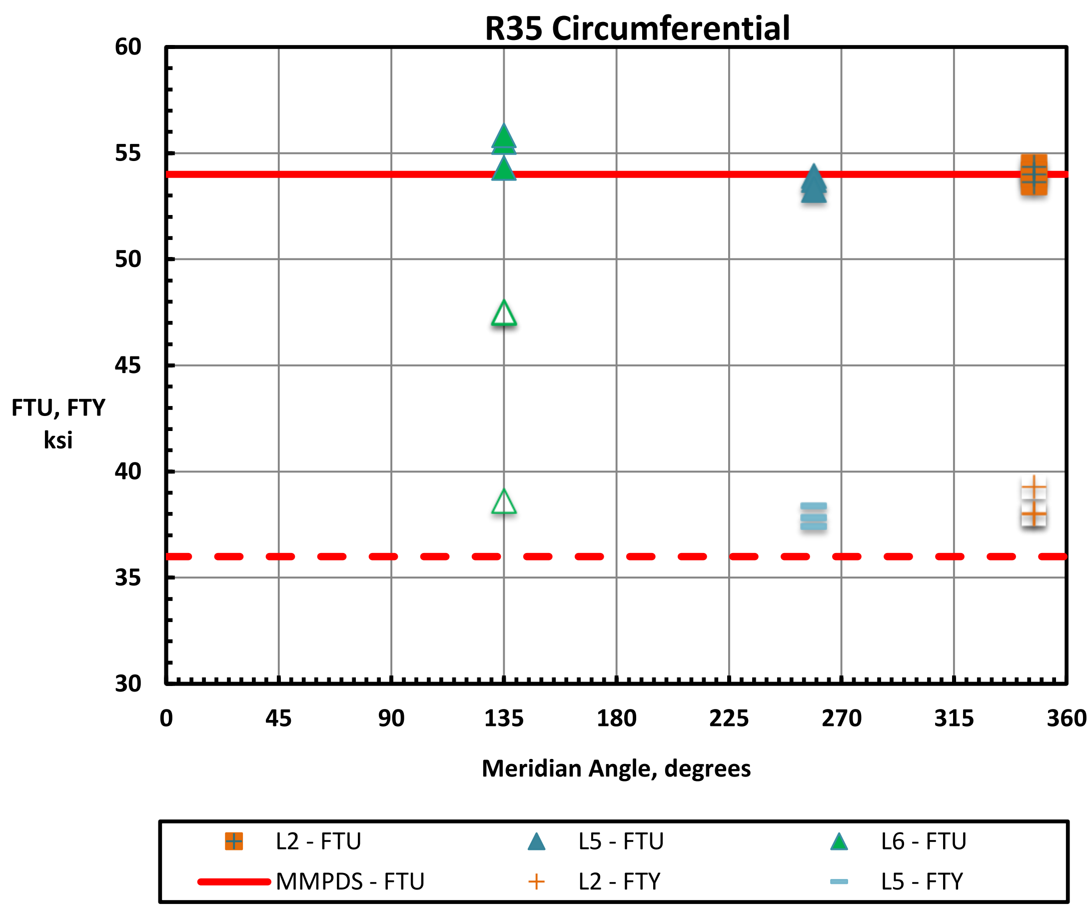

Figure 10.2-17. Short Transverse 45° (ST45) Tensile Properties of the Spin Formed Al 2219-T62 Aft Bulkhead Material as a Function of Meridian Angle along the R35 Circumferential Arc Length

10.2.2 Comparison with Handbook Data and Other T6 and T8 Products

The average tensile properties of the spin formed aft bulkhead shown in Table 10.2-10 were compared with data from numerous sources to assess the effects of spin forming when compared with rolled plate and other formed products heat treated to the T6 temper. Limited data were found in handbooks and open literature publications for Al 2219-T6 products so a variety of product forms were used in this evaluation. Comparisons were also made with T8 products to determine the reduction in tensile properties that designers will need to accommodate if spin forming is adopted for the aft bulkhead. In most cases, data for 2219-T6 and T8 products were available for L and T orientations; however, very little data were available for the ST orientation and no published values were available for the ST45 orientation.

For comparison with wrought plate products, the MMPDS A- and B-basis design properties (17) and the Aluminum Association's typical properties (18) for wrought Al 2219-T62, T851, and

T87 plate are shown in Table 10.2-11 and Table 10.2-12, respectively. It is recognized that in this study typical properties of the aft bulkhead are compared with statistically derived allowables; however, these represent the material properties typically used by designers and provide an indication of whether the aft bulkhead properties will have the properties assumed in the design. It is also noteworthy that the ST orientation data from the aft bulkhead was compared with L and LT allowables since there are no allowables for the ST orientation specified in MMPDS. Typical tensile properties for spin formed Al 2219-T62 products were obtained from three sources for direct comparison to determine whether the aft bulkhead was “in family” with similar products. These included the FPVBH demonstration article presented in Table 10.2-13 (1), (19), (20); domes produced for NASA’s Cryogenic Propellant Storage and Transfer (CPST) Program (Table 10.2-14) (21); and other domes produced for commercial customers (Table 10.2-15) (22). For comparison with other fabricated product forms, minimum tensile properties for Al 2219-T6 forgings and rolled or forged rings are shown in Table 10.2-16 (23).

Based on the overall averages (Table 10.2-10), tensile strengths of the aft bulkhead in the L and LT orientations were about 5% higher than the MMPDS A-basis allowables for T62 plate (Table 10.2-11). The ST properties were even higher with UTS 8% and YS 15% higher than the L and LT orientation allowables. The elongation values exceeded the design values. The L and LT strengths were slightly lower, but within 5% of typical values reported by the Aluminum Association (Table 10.2-12). Al 2219 is generally considered an isotropic material with properties in the L, LT, and ST orientations generally agreeing within less than approximately 5% (see Table 10.2-11 and Table 10.2-16). The ST YS in the aft bulkhead was 10% greater than for L and T. It is unclear whether the higher ST YS is inherent in the plate used in fabrication of the spin forming blank or is related to the spin forming process.

Individual specimen results and average values for each coupon blank were compared with MMPDS A-basis allowables to determine whether there were any regions of concern in the aft bulkhead. Values below MMPDS are highlighted in red in Tables 10.2-2 through 10.2-10 for individual specimens, averages for the coupon blanks, and the overall average. To illustrate the aft bulkhead locations that have strength or elongation values below MMPDS, those values are shown in red in Figures 10.2-2 through 10.2-5. In addition, the MMPDS value is shown on the data plots in Figures 10.2-7 through 10.2-15. Two of three L and LT specimens from coupon blank L3, which is near the pole, exhibit UTS values just below the MMPDS A-basis UTS. This is reflected in the coupon blank average UTS; however, the overall average L and LT UTS is well above the MMPDS value. Strength values for the ST orientation were above, but elongations below MMPDS values at all locations. For the ST45 orientation, all elongation values and all except one UTS value were below MMPDS. All YS values for all locations and orientations were above the MMPDS YS.

The tensile properties of the aft bulkhead agreed well with the typical properties for other Al 2219-T62 spin formed products. The aft bulkhead strength levels were slightly lower than the spin formed FPVBH and the domes produced for the CPST Program and commercially by Spincraft. The L and LT UTS and YS were within 3% and 6%, respectively, of values for the FBVBH (Table 10.2-13). The UTS was about 5% lower and YS 10% lower than the CPST and

Spincraft domes (Table 10.2-14 and Table 10.2-15). Conversely, the ST tensile properties of the aft bulkhead were higher than those of the CPST domes. The UTS was about 2% higher and the YS 5% higher than the values for the CPST domes. The variations in tensile strength may be related to the amount of deformation related to forming these different geometries. The FPVBH experienced some thinning during spin forming and the complex geometry likely generated greater deformation. While some details of the Spincraft domes are proprietary it was confirmed that the domes were of larger scale than the aft bulkhead and had a complex thickness profile. The deformation was likely lower in the aft bulkhead than the FPVBH and Spincraft domes due to the gradual curvature and comparatively simple geometry of the aft bulkhead.

Tensile strengths in the L and LT orientation compared well with minimum values for hand and die forgings and rolled or forged rings (Table 10.2-16), with some values higher and some lower, but all within 5% of the published minimums. However, strengths in the ST orientation were 10 to 15% higher than values for hand forgings. Typical elongation values were higher in all comparisons.

The L and LT tensile properties of the spin formed aft bulkhead are consistent (in family) with wrought plate and other fabricated product forms in the T62 temper. Orion design trade studies use the MMPDS A-basis values for T62 wrought plate to analyze the benefits of spin forming the aft bulkhead because design values do not exist for spin formed products. The tensile results of this aft bulkhead should build confidence in the spin forming fabrication method. Currently, some elements of the Orion CM are multi-piece welded construction of machined thick Al 2219-T851 plate. The tensile properties of the spin formed aft bulkhead are lower than for T851 plate (Table 10.2-11 and Table 10.2-12) as expected due to the increased precipitation strengthening in T851 wrought products that is imparted by the 1.5 to 3.0% cold stretch prior to artificial aging. The thick-plate convex spin forming process cannot accommodate stretch or cold work thus only T6 final temper can be produced. The properties of the spin formed aft bulkhead are comparable to T62 plate and other wrought products. The UTS values in the L and LT orientations of the aft bulkhead are about 10% lower than MMPDS A-basis allowables for T851 plate (Table 10.2-11) and 15% less than typical values (Table 10.2-12). The YS values in both orientations are about 20% lower than the MMPDS A-basis allowables and 30% lower than typical values. It should be recognized that, based on MMPDS A-basis values, the UTS and YS of T62 plate are lower than for T851 plate by 10% and 30%, respectively, and lower than for T87 plate by 17% and 40%, respectively. The lower tensile strength of the spin formed Al 2219-T62 aft bulkhead material compared with Al 2219-T851 and T87 plates is due differences in material temper and not the spin forming process.

F-3. The tensile properties of the spin formed Al 2219-T62 aft bulkhead material were typical for established Al 2219-T62 products.

- Tensile properties were comparable to the MMPDS design properties for T62 wrought plate and other fabricated products in the T6 temper, such as spin formed domes, forgings and rolled rings.
- Tensile properties were lower than those for Al 2219-T851 and T87 plate, as expected due to the increased precipitation strengthening in T8 temper wrought products that is imparted by the cold stretch/work prior to artificial aging.
- The lower tensile strength of the spin formed Al 2219-T62 aft bulkhead material compared with Al 2219-T851 and T87 plate is due to differences in material temper and not the spin forming process.

O-2. Limited data was available in handbooks or open literature publications for Al 2219-T6 material for comparison with the aft bulkhead properties, consequently it was difficult to assess the aft bulkhead in the context of other commercial Al 2219-T6 products.

- Tensile data were unavailable in handbooks or open literature publications for the ST and ST45 orientations, consequently these properties could only be assessed in comparison with established values for the L and LT orientations.

R-2. Additional testing should be performed on first article and initial serial production aft bulkhead components to generate data to populate the material property database for Al 2219-T6 spin formed products. (***O-2***)

- Tensile testing should be continued until sufficient data is generated to demonstrate consistency in material properties and build confidence that the spin forming process is reproducible.

Table 10.2-11. Design Tensile Properties of Al 2219-T62, T851 and T87 Sheet and Plate (17)

Specification	AMS-QQ-250/30, AMS 4031		AMS-QQ-250/30, AMS 4599											
Form	Sheet and Plate													
Temper	T62		T851											
Thickness, in	0.020-2.000		0.250 - 1.000		1.001 - 2.000		2.001 - 3.000		3.001 - 4.000		4.001 - 5.000		5.001 - 6.000	
Basis	A	B	A	B	A	B	A	B	A	B	A	B	A	B
Mechanical Properties:														
F_{tu}, ksi														
L	54	55	61	62	61	62	----	----	----	----	----	----	----	----
LT	54	55	62	63	62	63	62	63	60	61	59	60	57	58
F_{ty}, ksi														
L	36	37	47	48	47	48	----	----	----	----	----	----	----	----
LT	36	37	46	47	46	47	45	46	44	45	43	44	42	43
e, % (S-basis)														
LT	d	----	8	----	7	----	6	----	5	----	5	----	4	----
E, 10^3 ksi	10.5													

d T62: 0.250-1.000 in: 8%; 1.001-2.000 in.: 7%

Specification	AMS-QQ-250/30, AMS 4031		AMS-QQ-250/30, AMS 4613											
Form	Sheet and Plate													
Temper	T62		T87											
Thickness, in	0.020-2.000		0.250 - 1.000		1.001 - 1.500		1.501 - 2.000		2.001 - 3.000		3.001 - 4.000		4.001 - 5.000	
Basis	A	B	A	B	A	B	A	B	A	B	A	B	A	B
Mechanical Properties:														
F_{tu}, ksi														
L	54	55	63	64	63	64	63	64	63	64	61	62	----	----
LT	54	55	64	65	64	65	64	65	64	65	62	63	61	62
ST	----	----	----	----	----	----	59	60	56	57	52	53	----	----
F_{ty}, ksi														
L	36	37	50	51	50	51	50	51	50	51	49	50	----	----
LT	36	37	51	52	51	52	51	52	51	52	51	51	49	50
ST	----	----	----	----	----	----	51	52	50	51	48	49	----	----
e, % (S-basis)														
LT	d	----	7	----	6	----	6	----	6	----	4	----	3	----
E, 10^3 ksi	10.5													

d T62: 0.250-1.000 in: 8%; 1.001-2.000 in.: 7%

Table 10.2-12. Typical Tensile Properties of Al 2219-T62, T851, and T87 Sheet and Plate (18)

	UTS (ksi)	YS (ksi)	E (Msi)	e (%)
2219-T62	58	40	10.5	12
2219-T851	66	50	10.5	12
2219-T87	68	56	10.5	10

Table 10.2-13. Average Tensile Properties for the Spin Formed Al 2219-T62 FPVBH Material (1), (19), (20)

Location	Orient.	UTS (ksi)	0.2% YS (ksi)	E (Msi)	e (%)	
Pole	L	60.05	40.8	10.6	9.25	Average
		0.92	0.71	0.71	1.06	Std Dev.
	LT	60.65	40	10.85	9	
		0.21	0.14	0.78	1.41	
Cone	L	57.53	40.53	10.03	9.25	
		0.67	2.08	0.22	0.96	
	LT	58.05	40.73	10.1	10.63	
		0.59	1.64	0.22	1.7	
Barrel	L	57.3	40.45	9.85	6.5	
		0.14	0.64	0.21	2.12	
	LT	56.95	39.6	9.55	13	
		0.07	0.85	0.78	0	

All coupon blank locations	L	58.29	40.59	10.16	8.33	Average
		1.53	0.18	0.39	1.59	Std Dev.
	LT	58.55	40.11	10.17	10.88	
		1.9	0.57	0.65	2.01	

Table 10.2-14. Tensile Properties of Spin Formed Al 2219-T62 Domes for the CPST Program (21)

Dome S/N	Specimen ID	Location	Orient.	Condition*	Source	UTS, ksi	YS, ksi	e, %
31140-1	31140-1-P2-L	pole	in-plane (L)	T62	LAT	59.0	41.0	12
31140-2	31140-2-P2-L	pole	in-plane (L)	T62	LAT	60.0	42.2	13
31140-3	31140-3-P2-L	pole	in-plane (L)	T62	LAT	60.0	41.7	13
31140-1	31140-1-P1-LT	pole	in-plane (LT)	T62	LAT	60.5	42.0	10
31140-2	31140-2-P1-LT	pole	in-plane (LT)	T62	LAT	60.5	41.1	11
31140-3	31140-3-P1-LT	pole	in-plane (LT)	T62	LAT	60.0	43.6	11
31140-1	120551001	pole	in-plane	T62	MSFC	57.0	35.4	10.4
31140-1	120551005	pole	in-plane	T62	MSFC	57.5	39.0	11.7
31140-1	120551003	pole	ST	T62	MSFC	57.1	37.8	4.2
31140-2	120551013	pole	in-plane	T62 + SR	MSFC	57.3	35.8	10.1
31140-2	120551017	pole	in-plane	T62 + SR	MSFC	56.7	39.6	11.2
31140-2	120551015	pole	ST	T62 + SR	MSFC	59.3	41.3	3.9
31140-1	31140-1-E2-L	rim	in-plane (L)	T62	LAT	59.5	41.9	11
31140-2	31140-2-E2-L	rim	in-plane (L)	T62	LAT	60.5	42.2	11
31140-3	31140-3-E2-L	rim	in-plane (L)	T62	LAT	59.5	41.4	12
31140-1	31140-1-E1-LT	rim	in-plane (LT)	T62	LAT	59.0	41.5	11
31140-2	31140-2-E1-LT	rim	in-plane (LT)	T62	LAT	58.5	41.3	11
31140-3	31140-3-E1-LT	rim	in-plane (LT)	T62	LAT	59.0	40.6	11
31140-1	120551021	rim	in-plane	T62 + SR	MSFC	57.1	35.4	10.6
31140-1	120551023	rim	in-plane	T62 + SR	MSFC	59.4	38.9	9.3
31140-1	120551019	rim	ST	T62 + SR	MSFC	55.4	40.0	4.0
31140-2	120551009	rim	in-plane	T62 + SR	MSFC	58.4	39.0	12.3
31140-2	120551011	rim	in-plane	T62 + SR	MSFC	58.8	40.9	9.9
31140-2	120551007	rim	ST	T62 + SR	MSFC	58.3	41.3	4.9

LAT lot acceptance test
SR Stress relief thermal cycle at 300°F ± 15°F for 8 hours

Table 10.2-15. Typical tensile properties of spin formed Al 2219-T62 domes commercially produced by Spincraft. Also shown for comparison is the Alcoa plate lot certification tensile properties. (22).

Spincraft Dome S/N	Alcoa Plate Lot H/N	Orient.	Alcoa Plate Lot Cert. Data UTS (ksi)	Alcoa Plate Lot Cert. Data YS (ksi)	Alcoa Plate Lot Cert. Data EL4D (%)	Spin Formed Dome – Polar Tensile Coupons UTS (ksi)	Polar YS (ksi)	Polar EL4D (%)	Spin Formed Dome – Equator Tensile Coupons UTS (ksi)	Equator YS (ksi)	Equator EL4D (%)
31152-1	660931-1	LT	58.9	41.0	11.1	59.0	42.7	12.0	59.0	41.3	10.0
		L	58.5	40.6	11.5	60.0	43.4	13.0	59.0	41.6	12.0
31152-2	660941-1	LT	59.2	40.7	11.1	60.5	43.9	10.0	60.5	41.7	9.0
		L	59.3	40.8	11.3	60.0	42.9	10.0	59.0	40.4	10.0
31153-2	478411-1	LT	59.7	40.8	11.8	60.5	44.0	13.0	60.5	42.4	10.0
		L	60.0	41.0	10.6	60.5	44.3	11.0	59.5	42.1	10.0
31153-3	660951-1	LT	58.5	40.8	11.7	59.5	42.5	10.0	60.0	42.5	10.0
		L	58.7	41.0	11.8	59.5	42.8	12.0	59.5	42.8	10.0
31172-1R	528431-1	LT	60.9	42.0	8.2	55.8	37.7	13.0	60.1	43.4	8.5
		LT	60.3	41.5	8.5	58.3	38.5	11.0	59.8	42.7	10.0
		L	------	------	------	56.9	40.4	12.0	58.8	43.9	10.0
		L	------	------	------	57.7	39.3	14.0	59.7	42.4	11.0
31163-1	414091-1	LT	60.9	41.9	10.7	62.5	45.3	11.0	60.0	42.1	11.0
		LT	61.3	41.8	10.2	61.5	43.4	10.0	60.0	42.1	11.0
		L	------	------	------	60.5	43.3	10.0	59.5	41.7	11.0
		L	------	------	------	61.0	43.5	11.0	59.5	42.0	11.0
31163-2	414081-1	LT	59.7	40.6	11.1	60.0	42.9	10.0	58.0	41.8	8.0
		LT	59.6	40.8	11.0	59.5	42.3	10.0	58.5	41.7	10.0
		L	------	------	------	60.5	42.9	10.0	57.5	41.4	8.0
		L	------	------	------	59.5	42.3	10.0	58.0	40.8	10.0

		Orient.	UTS (ksi)	YS (ksi)	EL4D (%)	Polar UTS (ksi)	Polar YS (ksi)	Polar EL4D (%)	Equator UTS (ksi)	Equator YS (ksi)	Equator EL4D (%)
	Average	LT	59.9	41.2	10.5	59.7	42.3	11.0	59.6	42.2	9.8
	Std. Dev.		0.93	0.55	1.24	1.83	2.40	1.25	0.85	0.61	0.98
	Average	L	59.1	40.9	11.3	59.6	42.5	11.3	59.0	41.9	10.3
	Std. Dev.		0.68	0.19	0.51	1.32	1.52	1.42	0.73	1.00	1.06

Table 10.2-16. Minimum Tensile Properties for Al 2219-T6 Forgings and Rolled or Forged Rings (23)

Die Forgings

Minimum tensile properties

Orient.	UTS ksi	0.2% YS ksi	e % in 4D
L	58.0	38.0	8
LT	56.0	36.0	4

Hand Forgings

Minimum tensile properties

Orient.	UTS ksi	0.2% YS ksi	e % in 4D
L	58.0	40.0	6
LT	55.0	37.0	4
ST	53.0	35.0	2

Rolled or Forged Rings

Minimum tensile properties

Orient.	UTS ksi	0.2% YS ksi	e % in 4D
Tangential	56.0	40.0	6
Axial	55.0	37.0	4

10.2.3 Tensile Fractography

Representative tensile specimens were chosen for examination of the fracture surfaces with a combination of macroscopic and microscopic techniques. Macroscopic evaluation was performed with a digital camera and stereo microscope. Microscopic examination was conducted via scanning electron microscopy. Eighteen specimens were tested for the L, LT, ST, and ST45 orientations. All specimens were inspected visually after failure and representative samples were selected for more detailed examination to evaluate fracture morphology.

Three specimens representing the typical tensile failures observed for the L and LT orientations are shown in Figure 10.2-18. In general, the fracture surfaces as seen from the top-view in Figure 10.2-18 appear similar with macroscopic dimples, which indicate a ductile fracture mode. In all cases the specimens exhibited strain bands, which can be seen in the side view in Figure 10.2-19. Differences in the overall fracture path were observed as can be seen in the side-view of the fracture surfaces, with specimens exhibiting two slant fracture modes: full-slant or double-slant tensile fracture, both of which are typical of tensile fractures in Al plate. Of the 18 L orientation tensile specimens, 13 failed with a full-slant fracture at approximately 45 degrees to the tensile axis (see Figure 10.2-18 middle, specimen L2-L-14), while 5 failed in a generally double-slant pattern along with each slant oriented approximately 45 degrees to the tensile axis (see Figure 10.2-18 left, specimen L1-L-3). For the LT orientation, seventeen failed along a single, 45-degree slant (see Figure 10.2-18 right, specimen L2-LT-16) and only one failed in a double-slant manner. Nearly all of the ST and ST45 samples failed in the full-slant fracture mode; the remaining few were somewhat flatter slant fractures. The alignment of the fracture surface at roughly ±45 degrees to the tensile axis is common in ductile failures along the macroscopic plane(s) of maximum shear stress. Macroscopically, the tensile specimens exhibited features considered typical of ductile failure along planes of maximum shear stress, primarily as full-slant failures with some double-slant failures.

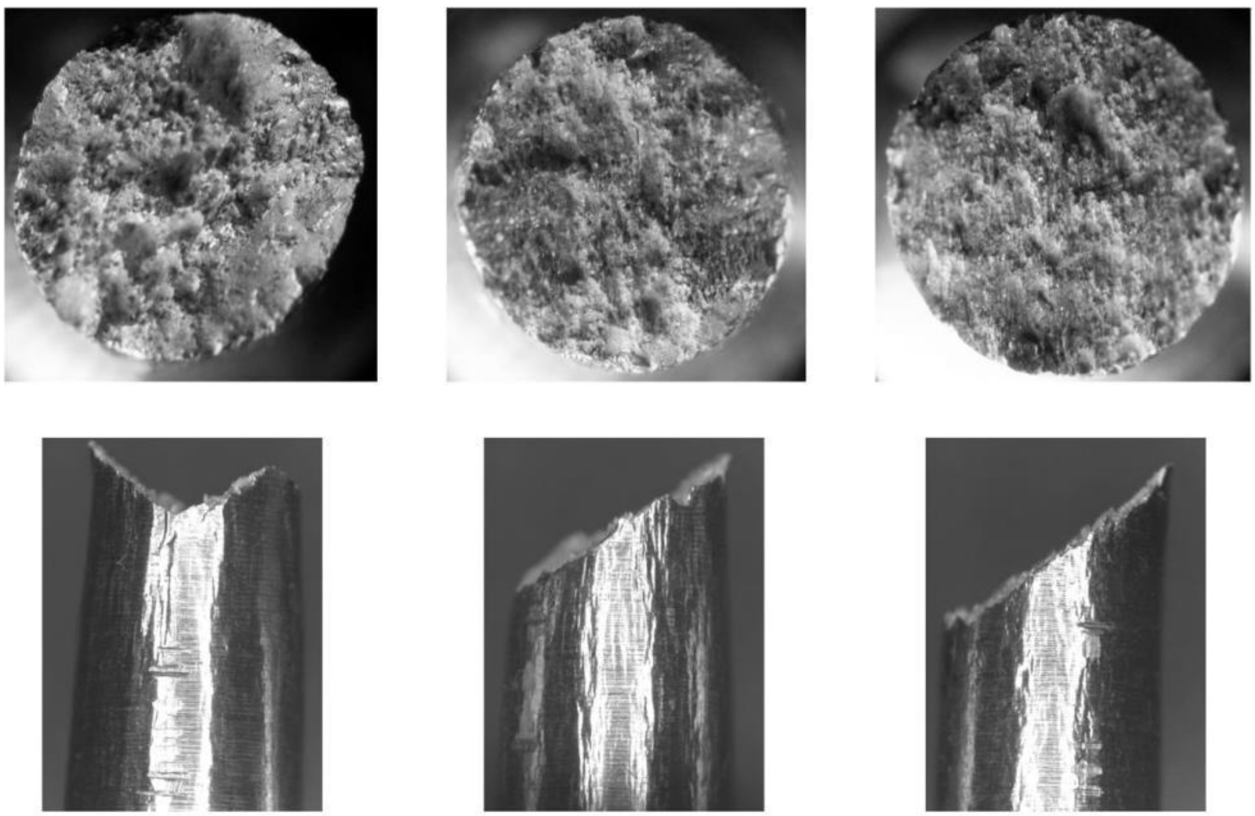

L1 – L - 3 **L2 – L - 14** **L2 – LT - 16**

Figure 10.2-18. Representative Macroscopic View of the Fracture Surfaces from the top and side views for Tensile Specimens L1-L-3 (left), L2-L-14 (middle), and L2-LT-16 (right)

At the microscopic level, all three specimens shown in Figure 10.2-18 were found to exhibit similar features and are representative of all L and LT specimens tested. Hence, only SEM images are presented for one of the specimens, L2-L-14. In Figure 10.2-19, SEM images at sequentially higher magnifications (progressing clockwise from top right as indicated by the arrows) are shown. In Figure 10.2-19a, the entire surface is captured at low-magnification, revealing a fibrous appearance with noticeable ridges and valleys, which is typical of fracture in Al alloy plate. The fibrous features are associated with transgranular fracture of elongated grains in rolled plate and the ridges with transition between grains. At 50x (Figure 10.2-19b), regions of transgranular microvoid coalescence are observed along with regions of lower ductility fracture and small delaminations, features that generally correlated with grain size. Higher magnification (500x, Figure 10.2-19c) confirms that all regions exhibit microvoid coalescence consistent with ductile fracture, with dimple sizes larger in the regions of transgranular fracture. At 2,000x (Figure 10.2-19d), dimples ranging from sub-micron size to approximately 5 µm are observed. Overall, fractography indicates the L and LT tensile specimens failed in a typical, ductile manner, which correlates well with the elongation values measured during the tensile tests.

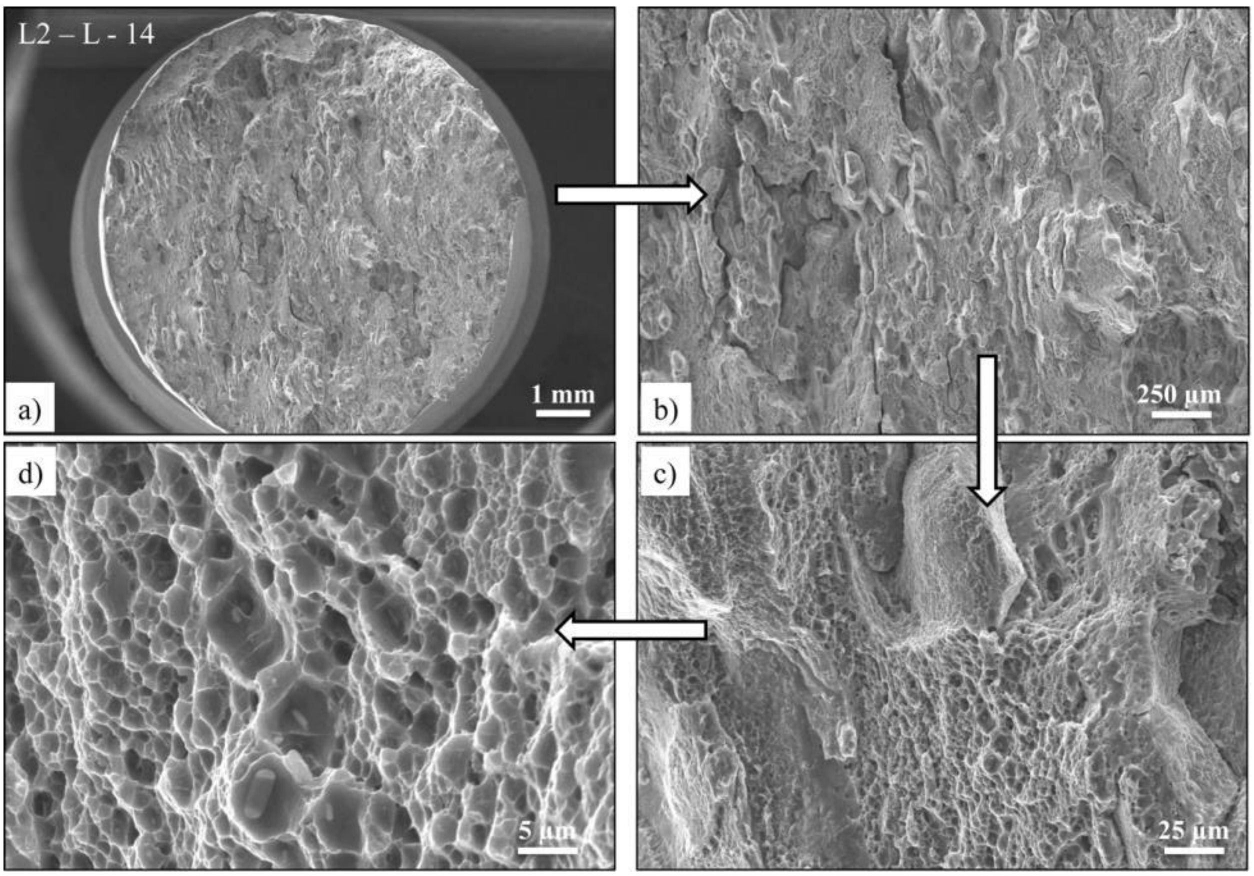

Figure 10.2-19. SEM Images of the Fracture Surface of Tensile Specimen L2-L-14 at a) 14x; b) 50x; c) 500x and d) 2,000x Magnifications

SEM fractography results are shown in Figure 10.2-20 and Figure 10.2-21 for representative ST and ST45 specimens. The ST fracture surface shown in Figure 10.2-20 represents the flatter slant fracture mode. Low magnifications (views a and b) exhibit a stepwise fracture surface illustrating propagation on elongated grain boundaries. Higher magnification (view c) reveals shallow microvoid coalescence initiated at constituent particles, often presented as clusters and stringers of smaller particles (view (d)). The ST45 fracture surface shown in Figure 10.2-21 exhibits some fibrous texture associated with transgranular crack propagation, but without the pronounced ridges and valleys noted on the L and LT fracture surfaced. Large microvoids are noted, again forming at constituent particle populations; however, more colonies of small microvoids are noted than in the ST fracture. The features noted in the ST and ST45 fractures are consistent with the lower ductility levels measured during tensile tests when compared with the L and LT orientations.

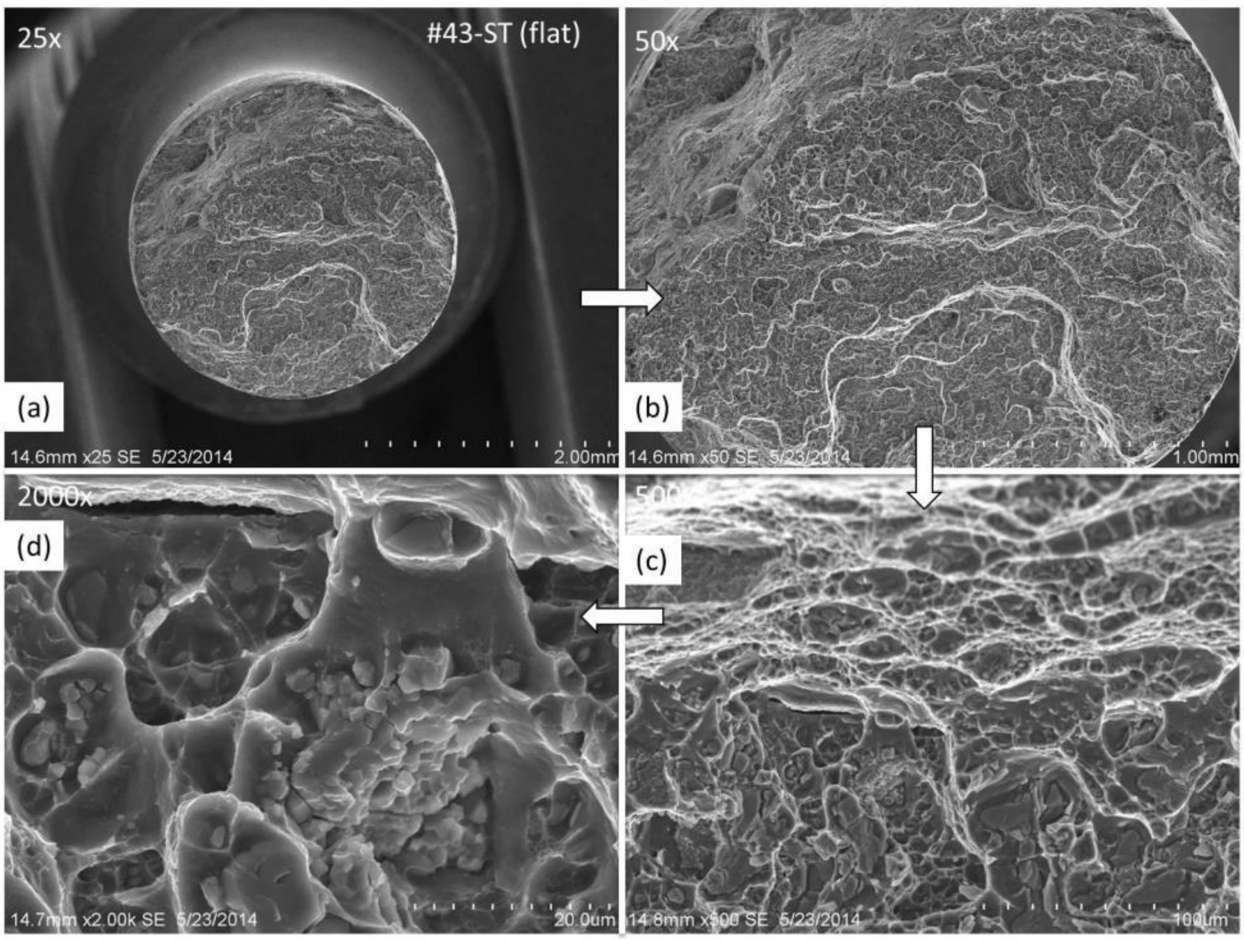

Figure 10.2-20. SEM Images of the Fracture Surface of Tensile Specimen ST-43 at (a) 25x; (b) 50x; (c) 500x; and (d) 2,000x Magnifications

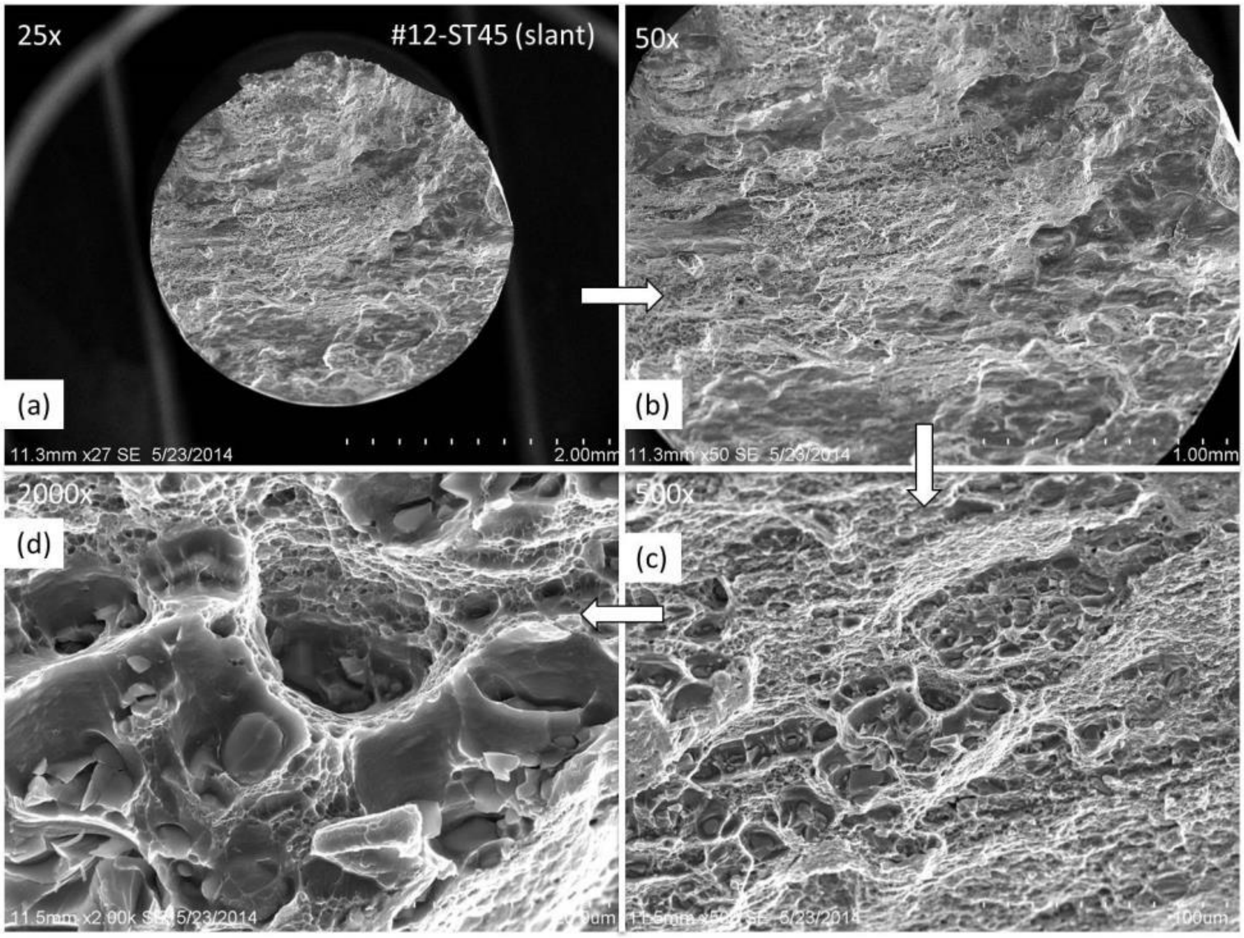

Figure 10.2-21. SEM Images of the Fracture Surface of Tensile Specimen ST45-12 at (a) 25x; (b) 50x; (c) 500x; and (d) 2,000x Magnifications

10.3 Fracture Toughness Test Results

Figure 10.3-1 shows the aft bulkhead cut plan with the location of coupon blanks from which fracture specimens were excised for fracture toughness testing highlighted in yellow. Table 10.3-1 shows the size and location of these coupon blanks with respect to the original plate rolling direction and distance from the aft bulkhead pole to the coupon blank center point. These coupon blank locations were designed to determine uniformity of fracture properties throughout the aft bulkhead and were evaluated along selected meridian and circumferential lines.

An additional goal of these tests was to determine how these properties compare to wrought plate in the T6 and T8 tempers and to other fabricated product forms in the T62 temper. These results will assist the Orion designers in assessing the attributes of the spin form fabrication process for the aft bulkhead and identify any deficiencies or "show stoppers" associated with this fabrication process.

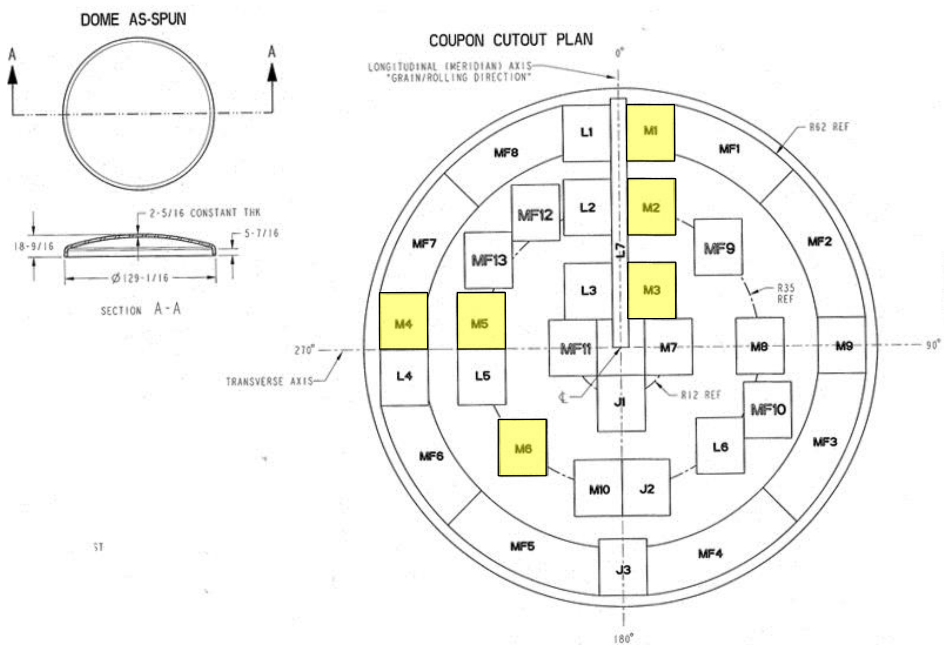

Figure 10.3-1. Aft Bulkhead Cut Plan showing the Location of the Fracture Coupon Blanks highlighted in Yellow

Table 10.3-1. Fracture Toughness Coupon Blank Locations and Orientations

Coupon Blank	Coupon Blank Size		Coupon Center Point	
	Longitudinal Dimension, in.	Transverse Dimension, in.	Meridian Angle , degrees	Arc Length from dome CL in.
M1	14	12	9°	54-5/8
M2	14	12	13°	36
M3	14	12	30°	16-1/8
M4	14	12	277°	55-1/2
M5	14	12	281°	35-7/8
M6	14	12	225°	35-1/8

10.3.1 Uniformity of Fracture Properties

A summary of the fracture toughness test results for the Al 2219-T62 aft bulkhead material is provided in Table 10.3-2. All but five specimens were valid per the ASTM E1820 (8) specification. In each case the invalidity was related to the difference between the estimated crack extension and the measured crack extension. In each case the deviation was considered minor and inconsequential to the toughness results. Comprehensive data analyses are provided in the Appendix (see Section 20.3). Fracture toughness comparisons were based on K_{JIC} values listed in Table 10.3-2.

Table 10.3-2. Summary of Fracture Data for the Spin Formed Al 2219-T62 Aft Bulkhead Material

Specimen ID	Coupon Blank	Orientation	J_{IC} (in-lb/in^2)	K_{JIC} (ksi√in)
CP-406-191	M1	L-T	105.6	35.1
CP-406-193			114.8	36.6
CP-406-196		T-L	91.5*	32.7
CP-406-198			90.6*	32.5
CP-406-201		S-T	62.6	27.0
CP-406-203			62.2	26.9
CP-406-206	M2	L-T	115.1	36.6
CP-406-208			112.8	36.3
CP-406-211		T-L	86.2*	31.7
CP-406-213			91.0	32.6
CP-406-216		S-T	89.9	32.4
CP-406-218			56.0	25.6
CP-406-221	M3	L-T	117.2	37.0
CP-406-223			125.7	38.3
CP-406-226		T-L	84.9	31.5
CP-406-228			93.1	32.9
CP-406-231		S-T	66.0	27.7
CP-406-233			90.7	32.5
CP-406-236	M4	L-T	102.5	34.6
CP-406-238			99.1	34.0
CP-406-241		T-L	86.0	31.7
CP-406-243			93.4*	33.0
CP-406-246		S-T	78.0	30.1
CP-406-248			50.9	24.4
CP-406-251	M5	L-T	108.4	35.5
CP-406-253			107.3	35.4
CP-406-256		T-L	86.3	31.7
CP-406-258			85.6	31.6
CP-406-261		S-T	67.8	28.1
CP-406-263			77.4	30.0
CP-406-266	M6	L-T	118.7	37.2
CP-406-268			114.0	36.4
CP-406-271		T-L	86.5	31.7
CP-406-273			85.0	31.5
CP-406-276		S-T	59.1	26.2
CP-406-278			57.4*	25.9

* Not fully valid J_{IC} value.

The composite fracture data is shown in Figure 10.3-2. This figure reflects all data taken from various locations across the aft bulkhead and is plotted for each orientation. Fracture toughness values vary with orientation as expected. Specifically, toughness in the L-T orientation is higher than toughness in the T-L orientation, which in turn is higher than toughness in the S-T orientation.

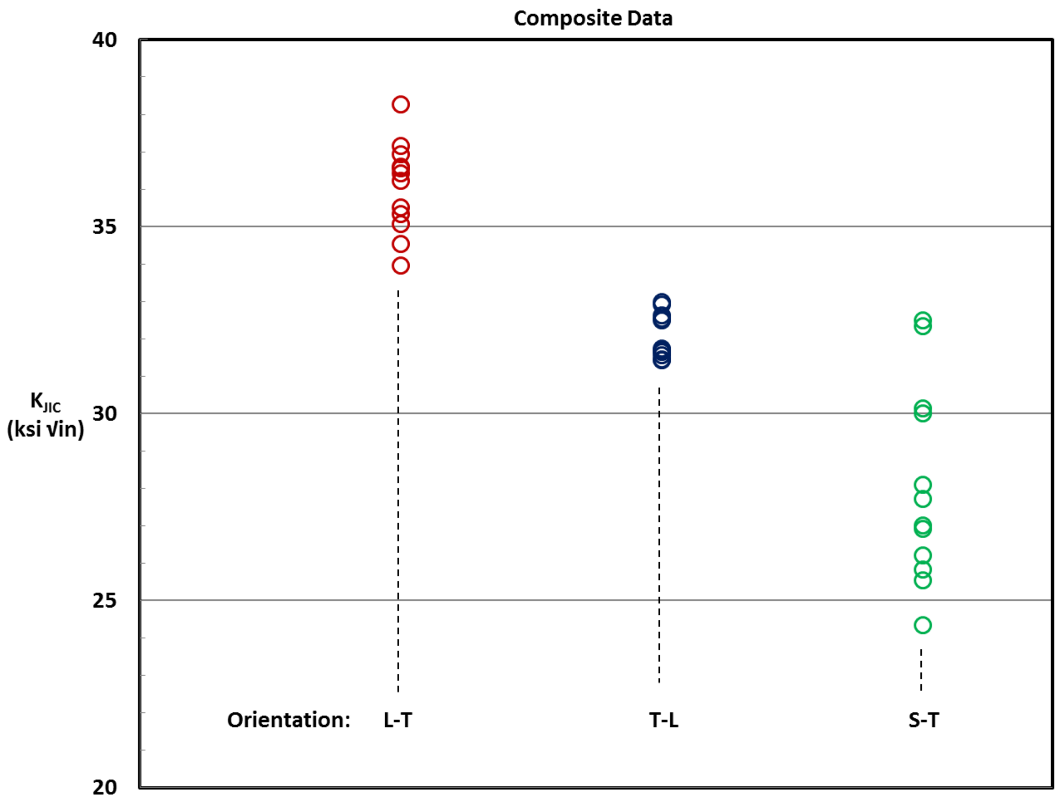

Figure 10.3-2. Fracture Toughness Data as a Function of Orientation

To examine trends in the toughness with respect to location within the aft bulkhead, plots were made along selected meridian angle and circumferential lines as shown in Figure 10.3-3 through Figure 10.3-7. The first plot, shown in Figure 10.3-3, is a composite of all toughness data as a function of orientation and coupon blank ID. For each coupon blank, the local L-T orientation toughness exceeds the T-L and S-T toughness. In blanks M1, M4, M5, and M6, the T-L toughness exceeds the S-T toughness. However, in coupon blanks M2 and M3, the S-T toughness overlaps the T-L toughness. Note that in coupon blanks M1, M2, and M4, the S-T toughness values exhibit a range in values on the order of 20% of their average. Subsequent analysis of data did not identify a trend in the range as a function of coupon blank location. With respect to the range in values for the in-plane orientations, the local L-T toughness values and the T-L toughness values were tightly grouped. The largest range for the local in-plane toughness values was 4%. In general, the data reflect the local toughness pattern that the L-T toughness is greater than the T-L toughness, which is greater than the S-T toughness.

Toughness as a function of arc length distance for the 0º to 180º and 90º to 270º meridian angles is shown in Figure 10.3-4 and Figure 10.3-5, respectively. Along both meridian lines, the L-T orientation toughness shows a slight decrease in toughness from the pole to the rim. The T-L data appear to be uniform across the arc length of the aft bulkhead. The average S-T data exhibit a slight decrease in toughness along the arc length, although the scatter in the S-T data makes it difficult to conclusively describe the trend. The drop in L-T toughness from pole to rim is in contrast to the tensile data, but consistent with such trends in Al wrought products.

Toughness as a function of the meridian angle for circumferential lines of 36-inch and 55-inch arc length is shown in Figure 10.3-6 and Figure 10.3-7, respectively. The L-T and T-L data are uniform. The S-T data also appear uniform, but again, the scatter in the data makes it difficult to definitively identify a trend.

From a damage tolerance perspective, in each orientation, the toughness-to-YS ratios are greater than 60%. For structural designs limited by yield stress margins of safety, this translates into critical flaw sizes that should be readily detectable by conventional non-destructive evaluation techniques.

The fracture toughness of Al alloys is sensitive to many metallurgical parameters, including grain size. Generally, larger grain size microstructures exhibit lower fracture toughness due to preferential fracture paths along large grain boundaries which are often populated by precipitates. The fracture toughness specimens used in this study were machined such that the crack extension region was centered about the mid-plane (t/2) of the aft bulkhead. The microstructure is less variable over the aft bulkhead at the mid-plane as compared with other through-thickness positions which likely contributed to the relatively uniform fracture toughness values. Additional testing is recommended in the large grain regions to assess the effect on fracture toughness.

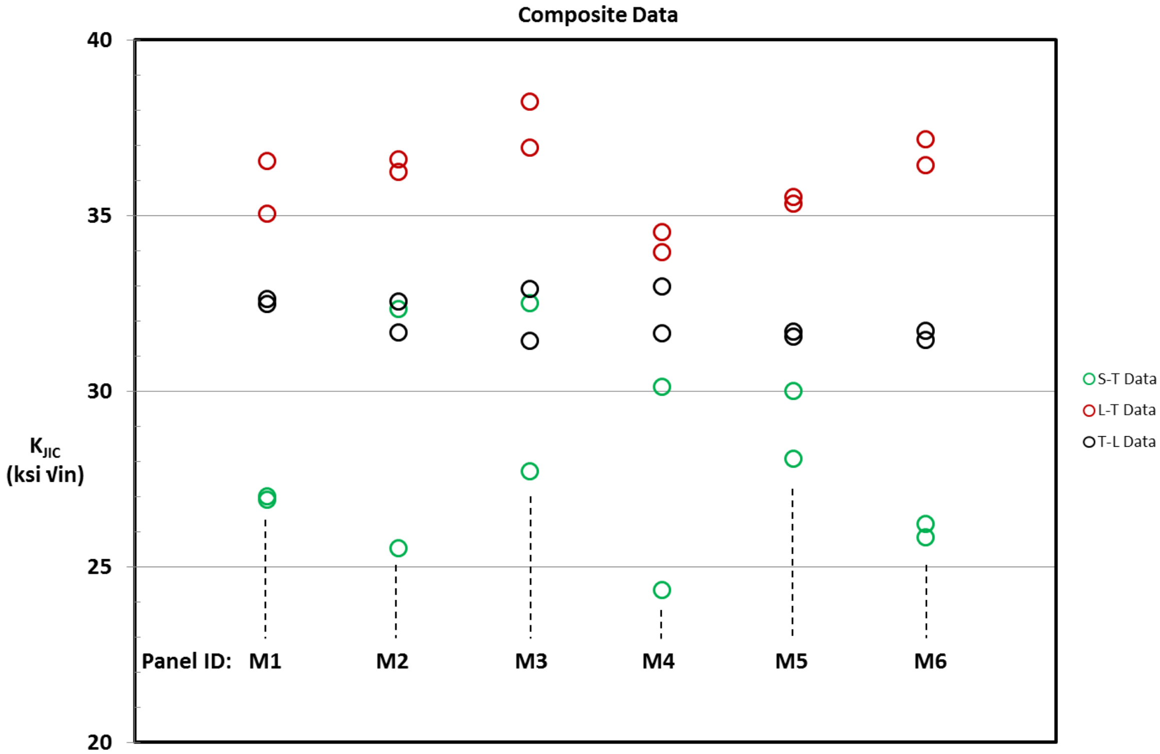

Figure 10.3-3. Fracture Toughness Data as a Function of Coupon Blank Location and Grain Orientation

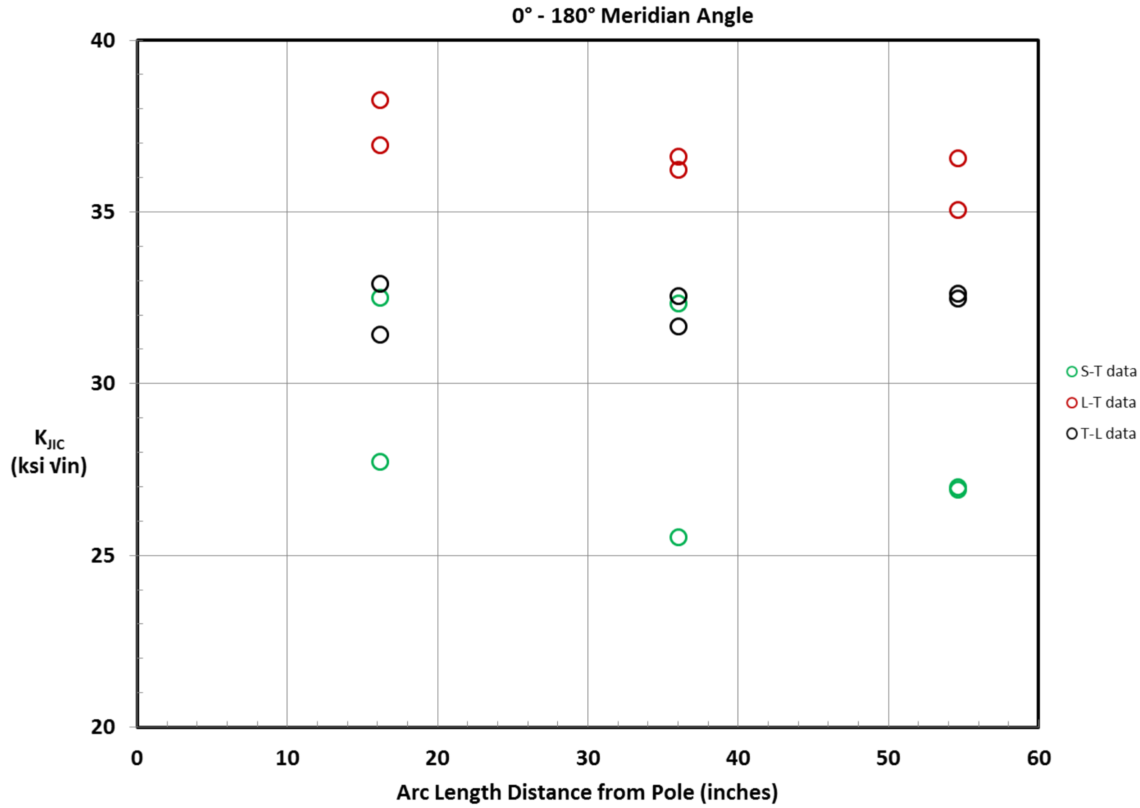

Figure 10.3-4. Fracture Toughness Data as a Function of Arc Length Distance from Pole for the 0° to 180° Meridian

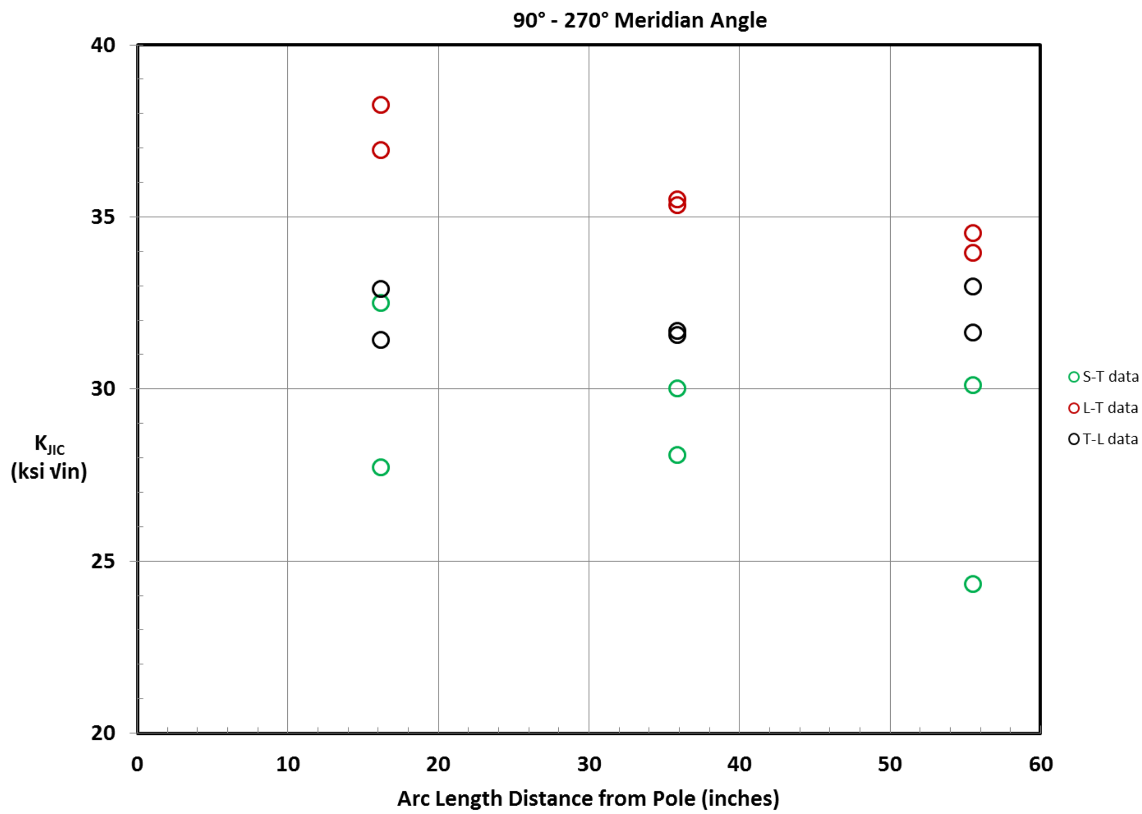

Figure 10.3-5. Fracture Toughness Data as a Function of Arc Length Distance from Pole for the 90° to 270° Meridian

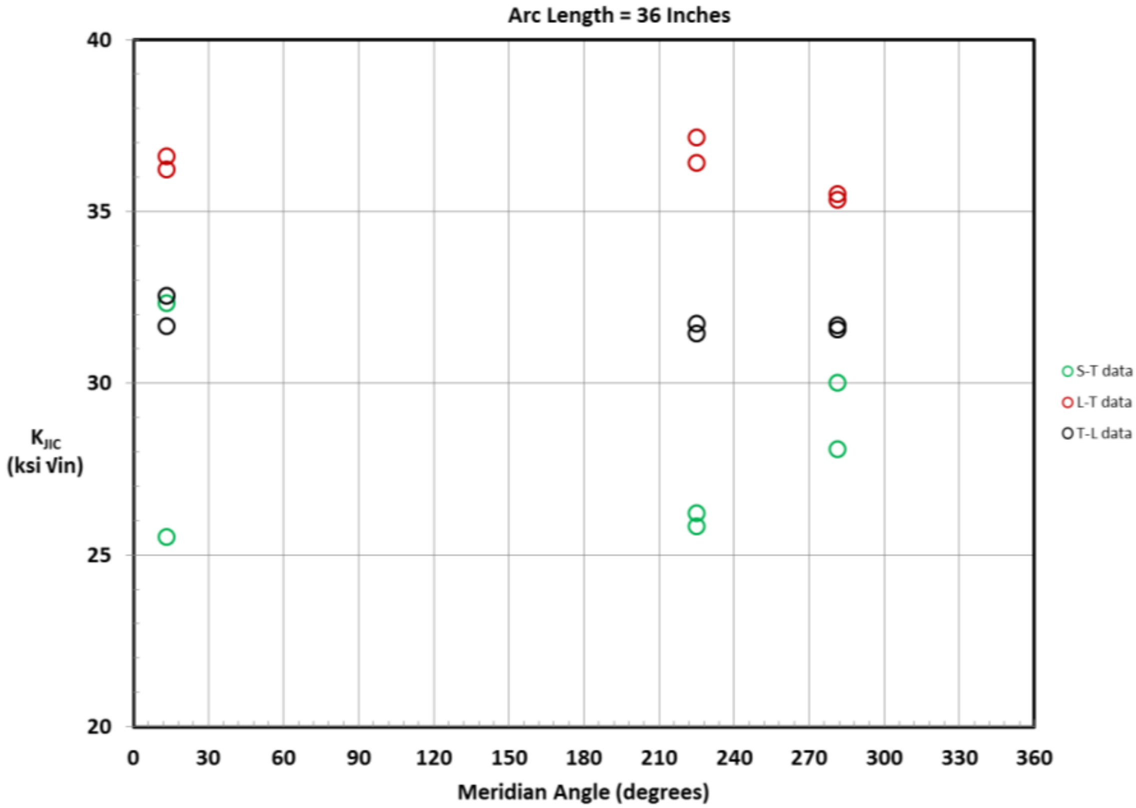

Figure 10.3-6. Fracture Toughness Data as a Function of Meridian Angle for Arc Length Distance of 36 Inches

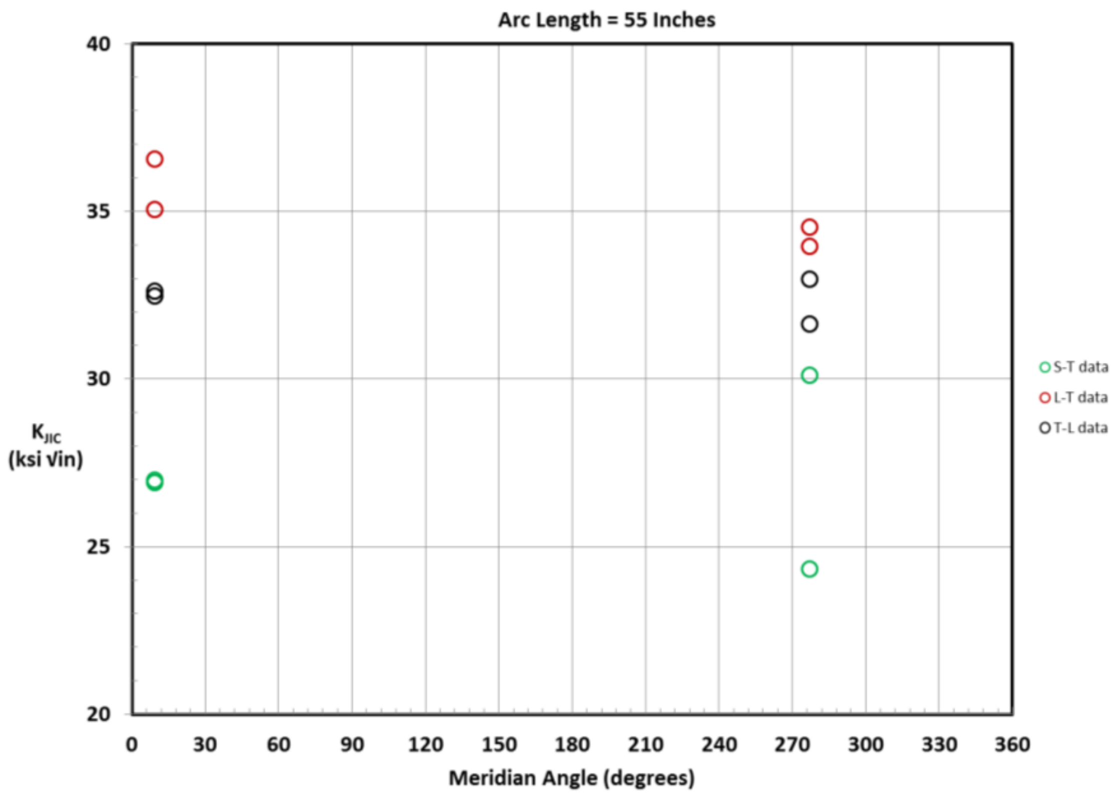

Figure 10.3-7. Fracture Toughness Data as a Function of Meridian Angle for Arc Length Distance of 55 Inches

Another critical element in fracture behavior is the ability of the material to tear in a stable manner. This is generally measured in terms of the fracture toughness (J) versus crack extension (Δa) for the material. This is also known as the resistance or R-curve. The fracture specimens exhibited rising R-curves for all coupon blank locations and test orientations. This reflects ability of the material to tear in a stable manner after crack initiation. Specimens in the L-T orientation tended to have steeper R-curves than specimens in the S-T or T-L orientation. Steeper R-curves reflect greater ability to resist tearing (i.e., the material is less likely to experience unstable crack propagation) (24). Representative R-curves (J vs Δa) are shown in Figures 10.3-8 through 10.3-10. From a damage tolerance perspective, the combination of high toughness and rising R-curve behavior are very positive attributes for the material.

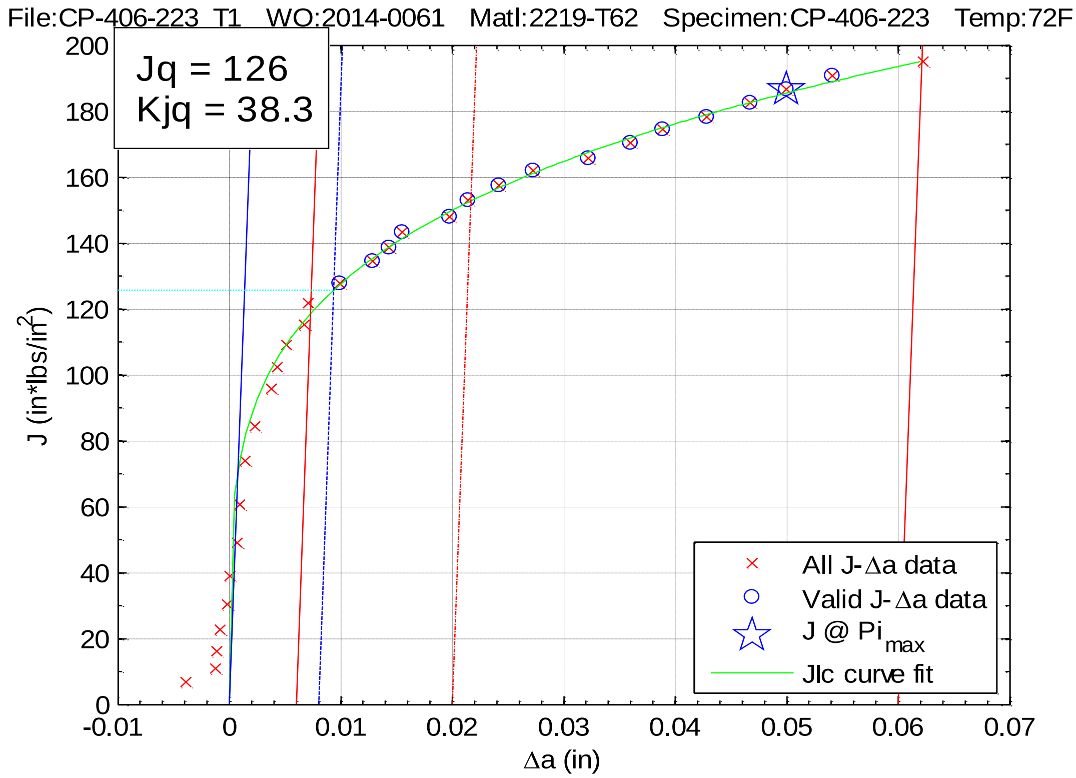

Figure 10.3-8. J-R Curve for Spin Formed Al 2219-T62 Aft Bulkhead Material in the L-T Orientation; Coupon Blank M3, Specimen CP-406-223

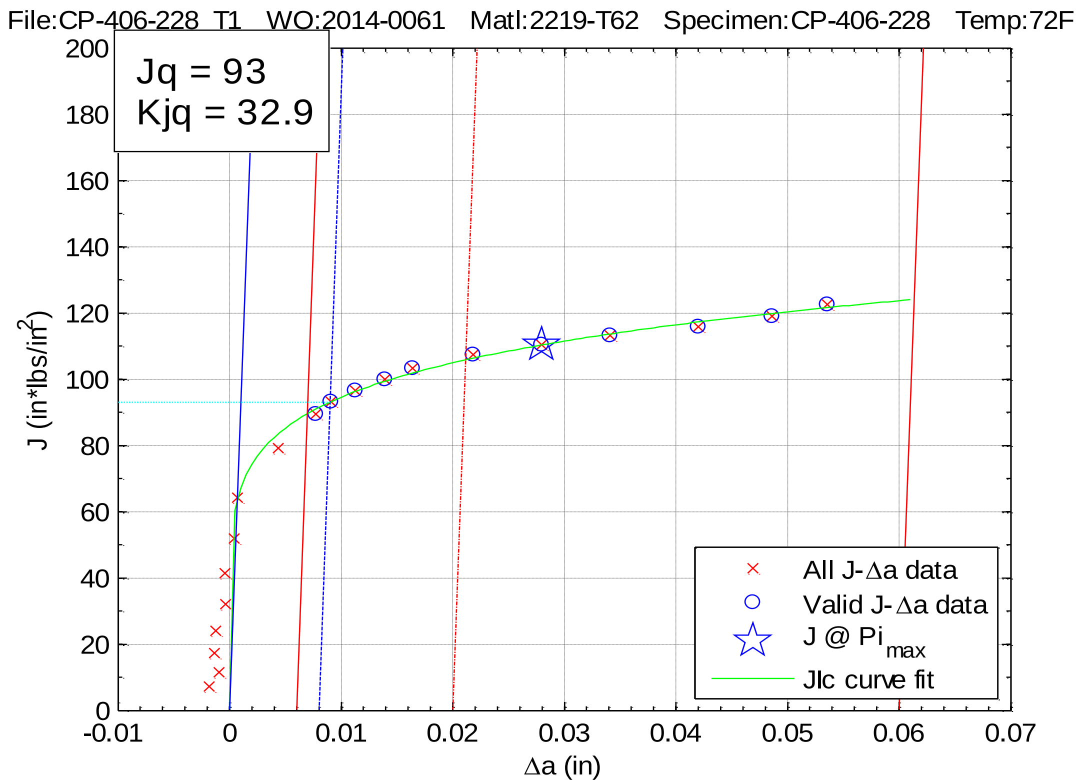

Figure 10.3-9. J-R Curve for Spin Formed Al 2219-T62 Aft Bulkhead Material in the T-L Orientation; Coupon Blank M3, Specimen CP-406-228

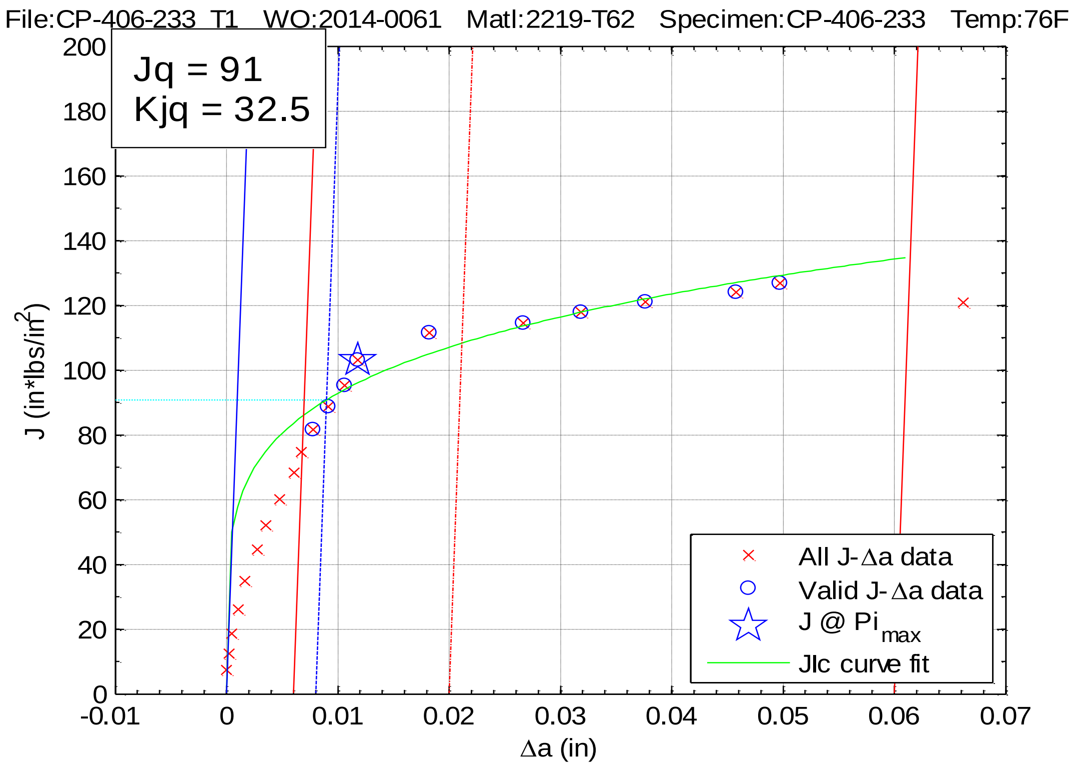

Figure 10.3-10. J-R Curve for Spin Formed Al 2219-T62 Aft Bulkhead Material in the S-T Orientation; Coupon Blank M3, Specimen CP-406-233

F-4. Fracture toughness was uniform with location in the aft bulkhead and indicated excellent damage tolerance capability.

- In-plane (T-L and L-T) toughness values are relatively constant for a given orientation and do not vary significantly across the aft bulkhead acreage.
- Through-thickness (S-T) toughness appears uniform as well, but exhibits significant data scatter for a given bulkhead location.
- Spin formed Al 2219-T62 aft bulkhead material exhibited rising R-curve for all orientations and locations and toughness-to-YS ratios in excess of 60%.
- High toughness values, high toughness-to-YS ratios, and rising R-curve behavior suggest excellent damage tolerance capability for the spin formed Al 2219-T62 aft bulkhead material.

10.3.2 Fractography

Photomicrographs of typical fracture surfaces from compact tension fracture specimens tested in the T-L, L-T, and S-T orientations are shown in Figure 10.3-11 - Figure 10.3-13. For the T-L and L-T orientations (Figure 10.3-11 and Figure 10.3-12), the tearing region is relatively flat and uniform. Conversely, the tearing region for the S-T specimen (Figure 10.3-13) is more irregular and exhibited more topography than the T-L and L-T regions.

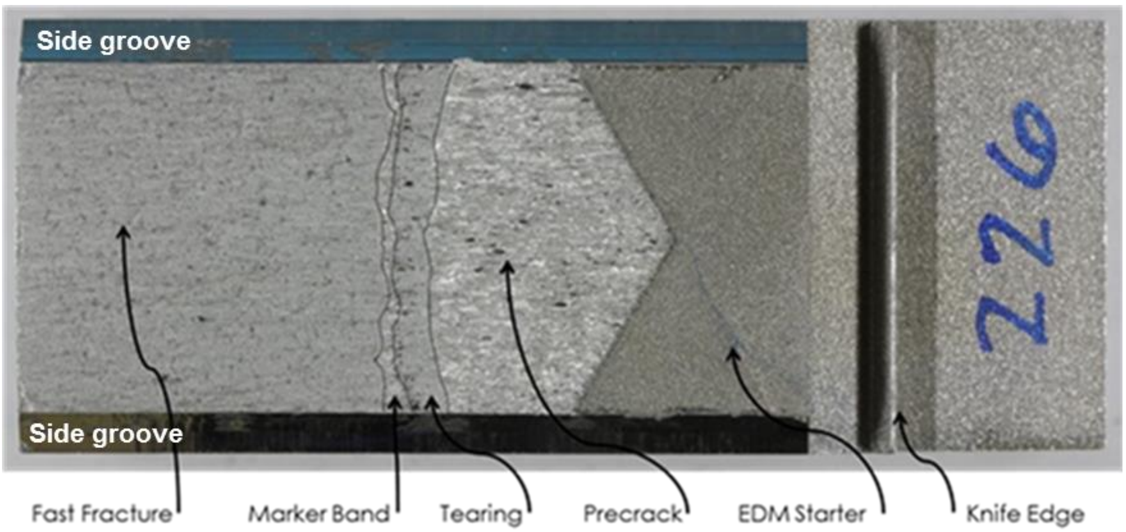

Figure 10.3-11. Photomicrograph of Fracture Surface of T-L Fracture Specimen from Coupon Blank M2

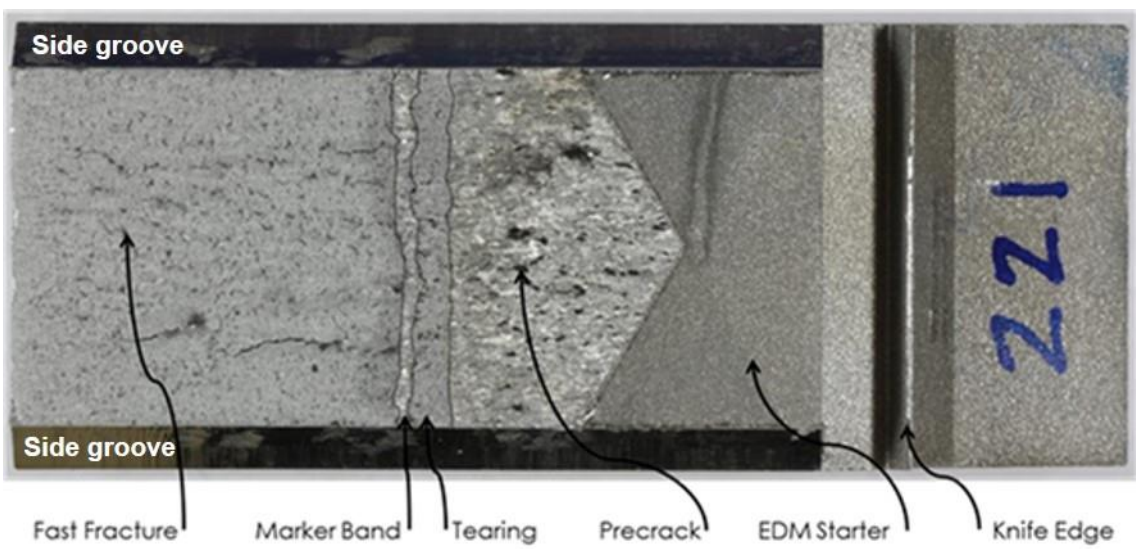

Figure 10.3-12. Photomicrograph of Fracture Surface of L-T Fracture Specimen from Coupon Blank M2

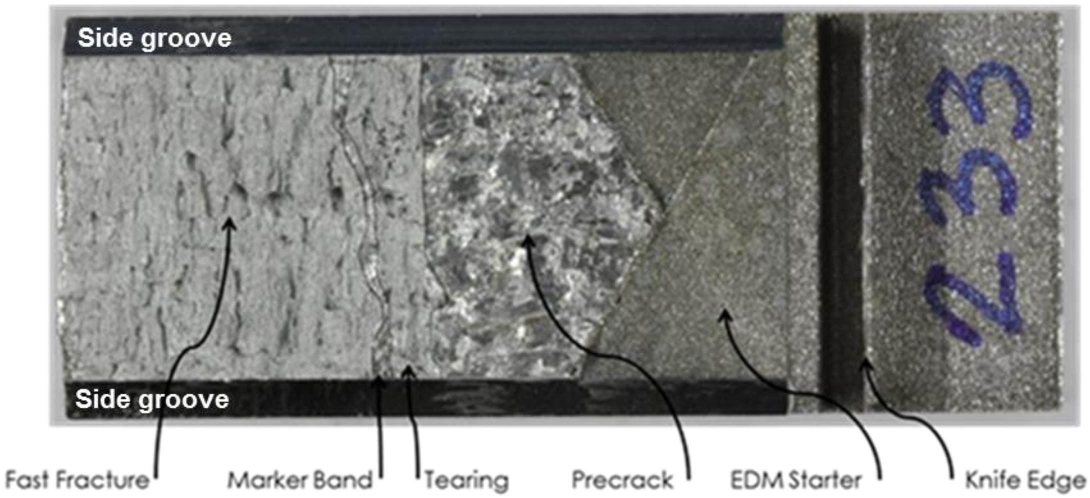

Figure 10.3-13. Photomicrograph of Fracture Surface of S-T Fracture Specimen from Coupon Blank M2

10.3.3 Comparison with Handbook Data and Other T6 and T8 Products

A comparison of fracture toughness behavior between the spin formed Al 2219-T62 aft bulkhead material and Al 2219-T87 plate material in three grain orientations is shown in Figure 10.3-14 (25). As shown in the plot, on average, the spin formed material exhibits higher toughness values than the plate material for each of the orientations. Limited additional data in the T-L orientation was obtained for Al 2219-T62 plate and Al 2219-T851 plate. The data is shown in Figure 10.3-15 (25). Data for Al 2219-T87 plate is repeated from Figure 10.3-14. The T62 spin formed aft bulkhead material toughness is comparable to the toughness in the T62 and T851 plate material. As noted earlier, the T62 spin formed aft bulkhead material toughness is higher than the toughness in the T87 plate material. For the most part, this behavior can likely be attributed to the general behavior of 2000 series Al alloys that reflect an increase in fracture toughness with a decrease in YS (26). In general, per MMPDS-08 (17), the A-Basis YSs for Al 2219-T87 temper is higher than the T851 temper which is higher than the T62 temper.

The fracture parameter K_{JIC} was used in this study to evaluate the fracture toughness of the Al 2219-T6 aft bulkhead. To more fully evaluate damage tolerance fracture toughness with pre-existing surface flaws and fatigue crack, growth rate should be determined. Such damage tolerance testing would typically be required before using a material in fracture critical pressure vessel or structural applications. Crack growth rate testing (27) would provide data to support safe-life assessments based on assumed or NDE based initial flaw sizes. Surface crack toughness testing (28) would provide critical stress intensity data required to evaluate part-through crack toughness of the material. Surface crack and crack growth rate data could be used to evaluate leak or burst behavior of the structure. Collectively, this data could be used to assess damage tolerance of hardware as outlined in NASA-STD-5019, "Fracture Control Requirements for Spaceflight Hardware (29),” and the American Petroleum Institutes’ “Recommended Practice 579 – Fitness-For-Service (30).”

F-5. The fracture toughness of the spin formed Al 2219-T62 aft bulkhead material was typical for established Al 2219-T62 products.

- Fracture toughness values exhibited the typical variation with orientation: L-T orientation > T-L orientation > S-T orientation.
- Fracture toughness was in-family with conventional Al 2219 Al tempers and product forms. Toughness values were comparable to Al 2219-T62 and T851 plate and are greater than for T87 plate, which is consistent with the tensile strength being lower than for T87 plate.

O-2. Limited data was available in handbooks or open literature publications for Al 2219-T6 material for comparison with the aft bulkhead properties, consequently it was difficult to assess the aft bulkhead in the context of other commercial Al 2219-T6 products.

- Fracture toughness data was only available in handbooks and open literature publications for Al 2219-T6 and –T8 plate. No fracture toughness data was publicly available for Al 2219 spin formed products.

O-3. Fracture toughness data suggests excellent damage tolerance in the Al 2219-T6 spin formed material; however, surface crack tension and da/dN testing is necessary to more fully characterize damage tolerance.

R-2. Additional testing should be performed on first article and initial serial production aft bulkhead components to generate data to populate the material property database for Al 2219-T6 spin formed products. (***O-2***)

- Fracture testing should generate data to more substantially populate the K_{JIc} fracture toughness database.

R-3. Perform surface crack tension fracture toughness and fatigue crack growth rate (da/dN) testing in order to fully characterize damage tolerance. ***(O-3)***

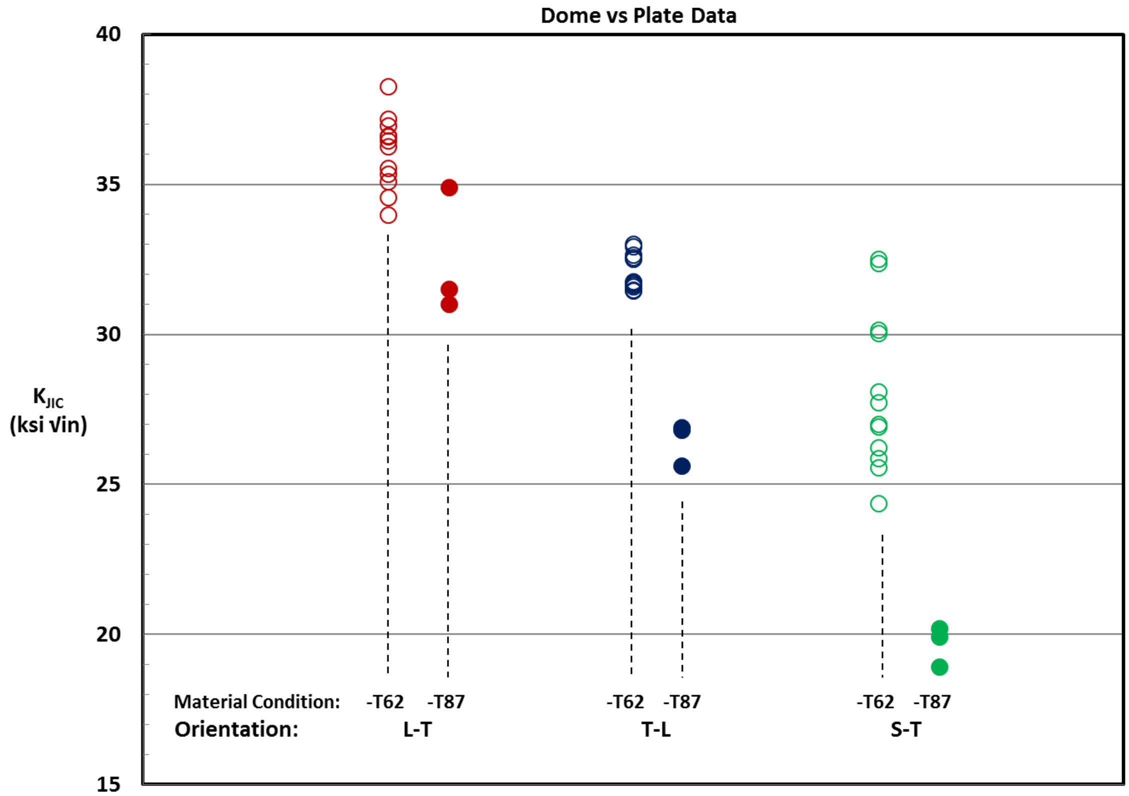

Figure 10.3-14. Fracture Toughness Comparison between Spin Formed Al 2219-T62 Aft Bulkhead Material and Al 2219-T87 Plate (25)

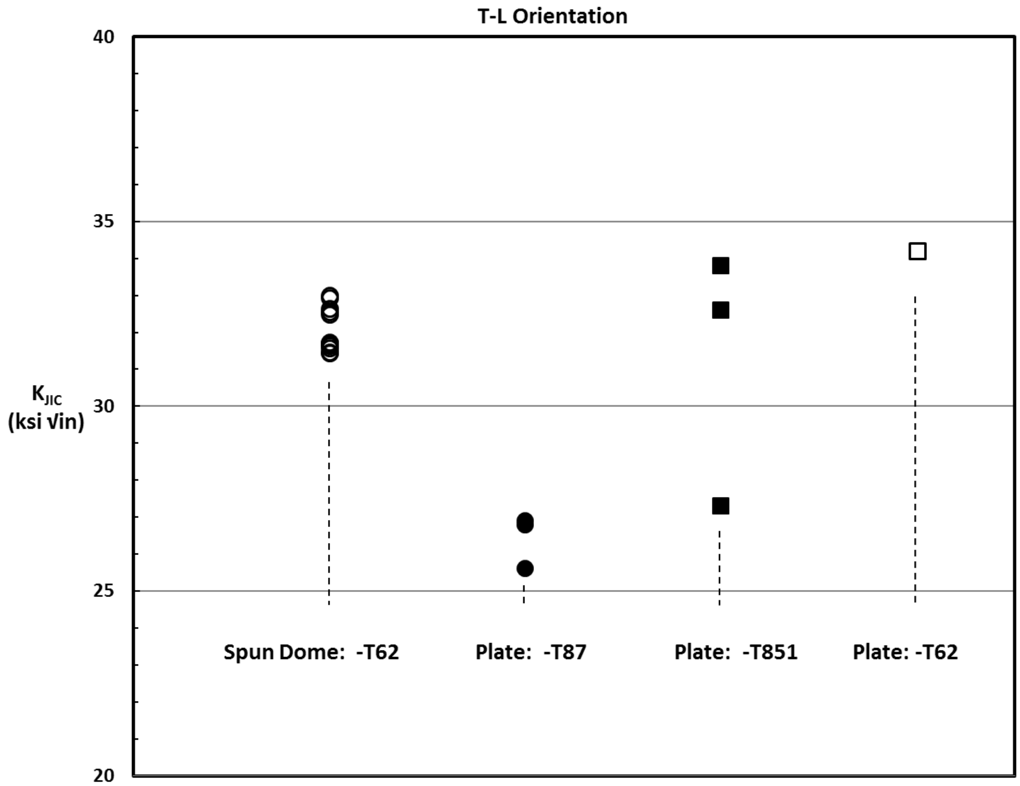

Figure 10.3-15. Fracture Toughness Comparison between Spin Formed Al 2219-T62 Aft Bulkhead Material and other Al 2219 Tempers in the T-L Orientation (25)

10.4 SCC Test Results

Figure 10.4-1 shows the aft bulkhead cut plan with the location of coupon blanks from which specimens were excised for SCC testing highlighted in yellow. Table 10.4-1 shows the size and location of these coupon blanks with respect to the original plate rolling direction and distance from the aft bulkhead pole to the coupon blank center point. These coupon blank locations were designed to determine uniformity of SCC properties throughout the aft bulkhead and were evaluated along selected meridian and circumferential lines.

An additional goal of these tests was to determine how these properties compare to wrought plate in the T6 and T8 tempers and to other fabricated product forms in the T62 temper. These results will assist the Orion designers in assessing the attributes of the spin form fabrication process for the aft bulkhead and identify any deficiencies or "show stoppers" associated with this fabrication process.

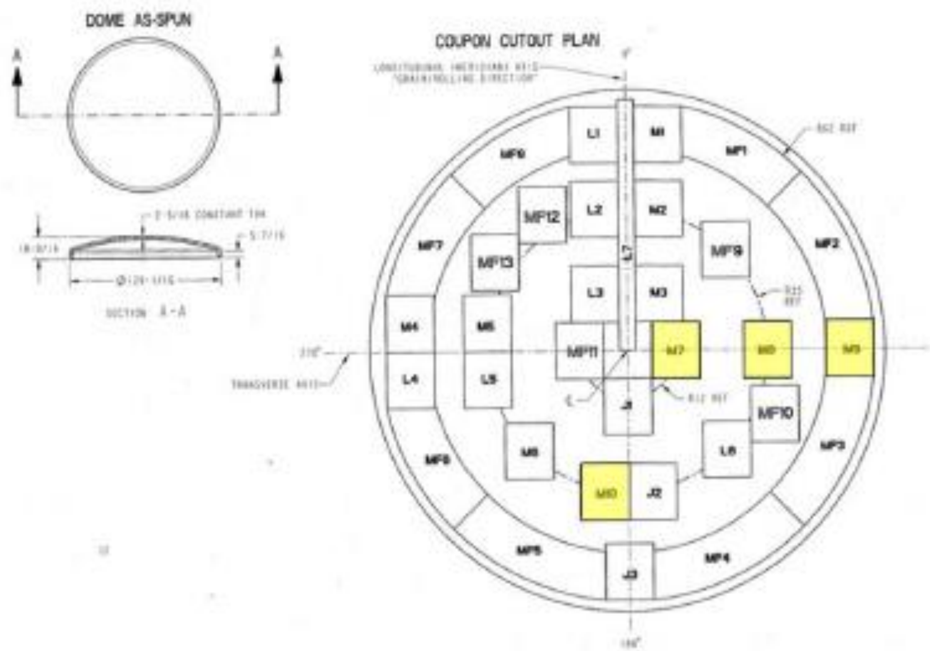

Figure 10.4-1. Aft Bulkhead Cut Plan showing the Location of the SCC Coupon Blanks highlighted in Yellow

Table 10.4-1. SCC Coupon Blank Locations and Orientations

Coupon Blank	Longitudinal Dimension, in.	Transverse Dimension, in.	Meridian Angle, degrees	Center Point Arc Length, in.
M7	14	12	90°	12.00
M8	14	12	90°	35.13
M9	14	12	90°	56.25
M10	14	12	190°	35.63

10.4.1 Alternate Immersion Test Results

10.4.1.1 30-day Alternate Immersion Exposure Test Results

The tests results for the 30-day alternate immersion exposure SCC testing are shown in Table 10.4-2. The baseline tensile data used to establish the applied stress levels for the SCC tests is shown in Table 10.4-3.

LT Specimens:

No SCC failures occurred in the LT specimens after 30-day alternate immersion exposure, even at 90% YS applied stress levels (Table 10.4-2). One of the three replicate specimens from each test group was metallographically examined. Representative photomicrographs at 0 and 90% YS applied stress levels are shown in Figure 10.4-2 through Figure 10.4-5. One 90% YS LT specimen from coupon blank M8 appears to be cracked, as can be observed in specimen #54 (Figure 10.4-3). The 50% and 75% YS LT specimens, although not shown in the figures, did not show cracks.

The remaining two replicate specimens from each test group were tensile tested to determine residual tensile strength remaining after exposure; the results are presented in Table 10.4-4 - Table 10.4-7. The percent tensile strength retained (defined in Section 8.5) ranged from 42 to 71% for the LT specimens. The residual strength ratio (also defined in Section 8.5) for each LT specimen exceeded 0.75, which was defined as the minimum value required to be considered a passing test.

ST Specimens:

Eighteen SCC failures occurred in the reduced section of the ST specimens within 30 days of alternate immersion exposure to 3.5% NaCl (Table 10.4-2). The failures can be divided into groups as follows:

- Nine failures occurred out of 12 specimens tested at 90% YS; three from coupon blank M7, two from M8, one from M9, and three from M10.
- Eight failures out of 12 specimens tested at 75% YS; three specimens from coupon blank M7, three from coupon blank M8, none from coupon blank M9, and two from coupon M10.
- One failure out of 12 specimens tested at 50% YS; one from coupon blank M10.

Metallographic examinations were performed on ST specimens that failed and the control ST specimens that were exposed without stress. Significant pitting corrosion was observed (Figure 10.4-2 - Figure 10.4-5). In addition to pitting, intergranular cracks were also observed on several ST specimens that failed. The cracks were more prominent on the 75 and 90% YS ST specimens, although intergranular cracking was observed on - one 50 % YS specimen. Examples of the most visible cracks are shown in Figure 10.4-2 (specimens #29 (75% YS) and # 34 (90% YS)); Figure 10.4-3 (specimen #73 (75% YS)); and Figure 10.4-5 (specimen #157 (75% YS)). The 50% YS ST specimen that failed in 29 days (Figure 10.4-5, specimen #152) showed intergranular attack, which is associated with stress corrosion on Al alloys. As was the case for all specimens tested, pitting corrosion was also present. This was the only 50% YS specimen that failed within a 30-day period. The 0% YS control ST specimens and the non-failed 50% YS ST specimens were metallographically examined and did not show evidence of SCC. Based on the tabulated data shown in Table 10.4-2 and the metallographic examination, the ST specimens furthest from the pole (coupon blank M9) appear to be less prone to SCC than the other regions.

The residual tensile strength values for the ST specimens that survived the 30 day alternate immersion exposure in 3.5% NaCl are shown in Table 10.4-4 through Table 10.4-7. The percent tensile strength retained for the ST specimens was significantly less than that of the LT specimens and markedly lower in coupon blank M10 compared with ST orientation specimens from the other locations. All of the ST specimens passed the residual strength ratio test except those from coupon blank M10 stressed at 50% YS (see Table 10.4-7). Specimen 153 (50% YS) had a ratio of 0.29 and specimen 154 (50% YS) had a ratio of 0.13.

Overall, SCC susceptibility in the ST orientation varied with the aft bulkhead location. The 90^{o} meridian rim region represented by coupon blank M9 was the most resistant to SCC while the 180^{o} meridian membrane region represented by coupon blank M10 was the least resistant. The remaining 90^{o} meridian pole and membrane regions represented by coupon blanks M7 and M8, respectively, showed intermediate resistance.

10.4.1.2 90-day Alternate Immersion Exposure Test Results

The test results for the 90-day alternate immersion exposure in 3.5% NaCl are presented in Table 10.4-8. The baseline tensile data used to establish the applied stress levels for the SCC tests is shown in Table 10.4-3. Half of the LT specimens and all but one of the ST specimens failed during the 90-day exposure. All the ST specimens stressed to 75% YS failed within the range of 26 to 85 days. Failures also occurred in the LT specimens stressed to 75% YS within the range of 70 to 90 days; two from coupon blank M7, two from coupon blank M8, and three from coupon blank M10. Many ST and LT control specimens (0% YS) failed due to general corrosion within the range of 48 to 90 days. Eleven of them were from the ST direction and five from the LT direction.

Tensile tests were performed on the surviving specimens to determine residual strength; the results are presented in Table 10.4-9. The percent strength retained for the 90-day alternate immersion exposure specimens ranged from 11 to 45%. Most specimens that survived the 90-day SCC exposure test show extremely low load carrying capability.

Metallographic views of representative failed ST and LT specimens are presented in Figure 10.4-6. All failed specimens exhibited severe pitting corrosion with some intergranular cracking.

The severe pitting corrosion and low load carrying capability suggest that the 90-day exposure to 3.5% NaCl is too long and not suitable for the spin formed Al 2219-T62 aft bulkhead material. The 3.5% NaCl alternate immersion exposure should be limited to 30 days. In addition, corrosion protection for this material should be considered when exposed to corrosive environments.

10.4.1.3 Discussion of Alternate Immersion Exposure Test Results

Two of the ST specimens in the 90-day test matrix exposed at 75% of the YS failed before 30 days; consequently, the two data sets were combined and evaluated as 30-day exposure tests. The combined test results show that twenty SCC failures occurred out of a total of 48 ST specimens tested within 30 days of alternate immersion exposure to 3.5% NaCl. The failures can be divided into groups as follows:

- Nine failures occurred out of 12 specimens tested at 90% YS; three from coupon blank M7, two from M8, one from M9, and three from M10.

- Ten failures occurred out of 24 specimens tested at 75% YS; four specimens from coupon blank M7, three from coupon blank M8, none from coupon blank M9, and three from coupon M10.
- One failure out of 12 specimens tested at 50% YS; one from coupon blank M10.

Results from the 30-day exposure tests for specimens exposed at 75% YS and lower are used to establish SCC rankings and table ratings and, while there is not sufficient data to establish these rankings, it is this combined data set that is of primary interest. The ST results have raised some concern and prompted much discussion. Failures occurred in all four locations in the aft bulkhead at the highest exposure stress level (90% of YS) and in most locations when exposed at 75% YS. One specimen failed during exposure at 50% YS. Metallography confirmed that this failure was due to intergranular attack typically associated with SCC and was not due to general corrosion. The significance of the 50% YS stress level failure is that (1) if substantiated by significantly more testing, the resulting ratings will be lower than is currently shown in handbooks for Al 2219-T6, and (2) the design allowable stress level will need to be reduced.

F-6. The SCC resistance of the spin formed Al 2219-T6 material varied with location in the aft bulkhead and in some locations exhibited lower resistance than previously established for Al 2219-T6 material.

- The rim region was the most resistant to SCC and one region in the membrane was the least resistant, exhibiting failure at lower exposure stress levels than typical for Al 2219-T6. The remaining pole and membrane regions showed intermediate resistance.

- The LT orientation appeared to be significantly more resistant to SCC than the ST orientation. Residual strength after exposure was significantly higher for LT specimens than ST specimens.

F-7. The 90-day alternate immersion exposure appears to be too long for the spin formed Al 2219-T62 material since failures can occur by corrosion mechanisms (general and pitting corrosion) different than those for SCC, which can interfere with the SCC evaluation.

10.4.2 Salt Spray Test Results

10.4.2.1 30-day Salt Spray Exposure Test Results

The test results for the L specimens from coupon blank M10 exposed to 5% salt spray are presented in Table 10.4-10. The baseline tensile data used to establish the applied stress levels for the SCC tests is shown in Table 10.4-3. None of the specimens exposed to salt spray and stressed to 0% and 75% YS failed.

Post exposure tensile testing was performed to determine residual strength. The results are presented in Table 10.4-12. The percent tensile strength retained for the 30-day salt spray exposure specimens ranged from 93 to 98% which is significantly greater than the specimens exposed for 30 days to 3.5% NaCl alternate immersion (see Table 10.4-4 through Table 10.4-7).

The superior SCC resistance for the 30-day salt spray testing is likely related to the inherently better SCC resistance in the L orientation.

10.4.2.2 90-day Salt Spray Exposure Test Results

The test results for the L specimens from coupon blank M10 exposed to 5% salt spray are presented in Table 10.4-11. The baseline tensile data used to establish the applied stress levels for the SCC tests is shown in Table 10.4-3. None of the specimens exposed to salt spray and stressed to 0%, 50%, 75%, and 90% YS failed.

Post exposure tensile testing to determine residual strength was performed; the results are presented in Table 10.4-12. The percent tensile strength retained for the 90-day salt spray exposure specimens ranged from 90 to 97%. These specimens retained significantly more of the initial strength than the specimens that survived 90 day 3.5% NaCl alternate immersion exposure (Table 10.4-8). The improved SCC results of the 90-day salt spray testing is likely related to the inherently better SCC resistance in the L orientation.

10.4.3 Comparison with Handbook Data and Other T6 and T8 Products

There is little SCC data available in open literature publications for Al 2219-T6 products in general and none for spin formed components. A review of the available literature for Al 2219-T6 material suggests excellent SCC properties for this material. This is in stark contrast to the SCC ratings determined for the aft bulkhead material in various locations. However, a closer examination of the data and sources reveals that the SCC ratings for Al 2219-T6 were either poorly documented, assumed based on testing of other tempers and exposure conditions, or were based on non-standardized test methodologies. Many of these studies were from the 1960’s and were conducted prior to the established ASTM G44 standard practice for alternate immersion testing.

Alcoa Green Letters 176 and 188 indicate excellent resistance to SCC for Al 2219 in the T62, T6, T81, T851, and T87 tempers, but also indicates that non-standard aging treatments may decrease the resistance of Al 2219 to an unsatisfactory level (31), (32). Similar ratings were published in MSFC-STD-3029. ASTM G64 states that Al 2219-T6 products do not have an assigned rating because the product is not offered commercially (33). However, no specific test data was published in these summary level reports so the sources were reviewed to determine possible explanations for the discrepancy in SCC ratings.

NASA-CR-88110 (34) indicates that rolled rod of alloy Al 2219-T62 demonstrated immunity to SCC in seacoast and industrial atmosphere when stressed to 75% of the actual YS. Results in that document show no failures out of 5 specimens stressed to 75% YS and exposed to alternate immersion for 84 days. It must be mentioned that when that test was performed the alternate immersion test method had not been standardized, and Alcoa used tap water when preparing the test solutions for testing Al 2219-T62. In a meeting that took place at Alcoa and that was documented in Memo 3-4820-194 it was concluded that tap water was causing Alcoa results to be better than results obtained in other laboratories because pH tends to be higher when tap water is used (35). For the current testing, deionized water was used when preparing the 3.5% NaCl solution to comply with ASTM G44. This may have contributed to the lower SCC performance of Al 2219-T62 material from the aft bulkhead when compared to the Alcoa study.

NASA-CR-155461 indicates on page two that Al 2219-T62 would be expected to have a high degree of resistance to SCC (36). A Chapter Prepared for ARPA Handbook indicates a SCC threshold for Al 2219-T62 plate in the ST direction of 32 ksi (37).

The Al 2219-T62 literature search suggests excellent SCC properties for this material. Highly susceptible Al alloys usually start failing within the first or second week of exposure. In the alternate immersion testing of the aft bulkhead material, the specimens survived several weeks of exposure before failures started to occur. This suggests that even though the Al 2219-T62 aft bulkhead material is not highly resistant to SCC, it is not highly susceptible either. Much of the literature data is from tests performed in the 1960's before SCC test techniques had been standardized and may have rendered a slightly elevated rating. It also seems that the excellent results from seacoast and industrial atmospheres had a significant weighting on the established ratings. Based on the paucity of relevant SCC data, the NESC team recommends that Orion conduct further SCC testing of the Al 2219-T62 aft bulkhead material to establish SCC ratings as well as SCC threshold levels.

SCC data on Al-Li 2195-T8 and Al 2219-T87 wrought plate is presented in Table 10.4-14 for comparison. These data were generated at MSFC and most of it was reported in MSFC Memos EH24 (94-107) and EH24 (95-57) (38), (39). MSFC-STD-3029 assigns Al-Li 2195-T8 a Table II rating and Al 2219-T87 a Table I rating. The criteria for the Table ratings are provided in Section 8.5. Table 10.4-14 provides an interpretation of the SCC data in the context of the MSFC-STD-3029 table ratings. A comparison of results for the Al 2219-T62 aft bulkhead (Table 10.4-2) with the 1.7-inch thick Al-Li 2195-T8 plate (Table 10.4-13) indicates similar SCC resistance for these materials. SCC failures in the ST orientation occurred at shorter times for Al-Li 2195-T8 for specimens exposed at 75% and 90% YS. Also noted is that one Al-Li 2195-T8 specimen exposed at 50% YS failed after 31 days, as compared to 29 days for the Al 2219-T62 aft bulkhead. These results suggest that the SCC resistance of the Al 2219-T62 aft bulkhead is comparable to Al-Li 2195-T8 plate.

Comparison of results from the Al 2219-T62 aft bulkhead (Table 10.4-2) with those for Al 2219-T87 plate (Table 10.4-13) reveals that, for the ST orientation, failures occur at shorter exposure times for the aft bulkhead. For the Al 2219-T87 plate, specimens exposed at 75% YS began to fail after 38 days and the 50% YS failures after 41 days. For the Al 2219-T62 aft bulkhead material failures began after 26 days for the 75% YS exposures and the one failure at 50% YS occurred after 29 days exposure. The shorter times to failure indicate that the spin formed Al 2219-T62 aft bulkhead material has inferior SCC properties compared to Al 2219-T87 plate.

O-2. Limited data was available in handbooks or open literature publications for Al 2219-T6 material for comparison with the aft bulkhead properties, consequently it was difficult to assess the aft bulkhead in the context of other commercial Al 2219-T6 products.

- The SCC data for the aft bulkhead provides insight about the SCC resistance of spin formed 2219-T62 material, but is insufficient to establish a threshold stress level.

10.4.4 Discussion of Stress Corrosion Results

SCC tests were performed on material from four coupon blank locations in the aft bulkhead corresponding to the rim (M9), membrane (M8), and pole (M7) along the 90° meridian line, and a second membrane region (M10) located along the 180° meridian line. Both LT and ST orientations were tested using alternate immersion and salt fog for either 30 or 90 day exposures. There were no failures during the salt fog tests and the 90-day alternate immersion results are clouded by general corrosion problems.

The primary data of interest are the 30-day alternate immersion exposure since results from this test method and test duration are typically the basis for handbook and table ratings of SCC resistance. No failures occurred for the LT orientation, even at the highest stress levels, and all specimens had passing post-exposure residual strength levels. The ST results raise some concern. Failures occurred in all four locations in the aft bulkhead at the highest exposure stress level (90% of YS) and in most locations when exposed at 75% YS. One specimen failed during exposure at 50% YS. Metallography confirmed that this failure was due to intergranular attack typically associated with SCC and was not due to general corrosion. The significance of the 50% YS stress level failure is that, if substantiated by significantly more testing, (1) the resulting ratings will be lower than is currently shown in handbooks for Al 2219-T6, and (2) the design allowable stress level will need to be reduced.

There are some important points to make regarding this data. The aft bulkhead tests followed MSFC test standard MSFC-STD-3029 in which the exposure stress levels are based on the measured strength of the material. Handbook values are based on standards that use MMPDS A-basis allowable strengths for plate to determine applied stress levels. Actual strength is always higher than the allowables due to statistical knockdown; consequently the aft bulkhead specimens were exposed at higher stress levels than handbook data being used for comparison. In addition, since there are no allowables for the ST orientation for Al 2219-T6 plate, standards that base exposure stress on allowables use the L orientation allowables regardless of the orientation of the SCC specimen. For the aft bulkhead SCC testing, the ST YS was used to determine the exposure stress. The ST YS was 10% greater than the L YS, which further contributed to the high exposure stress levels.

An additional caveat for these test results is the test duration as specified in MSFC-STD-3029. One disadvantage of the accelerated laboratory 3.5% NaCl alternate immersion test is that severe pitting may develop in the test specimens. As per ASTM G47, such pitting in tensile specimens with relatively small cross-sections can markedly reduce the effective cross-sectional area and result in net sectional stresses greater than nominal gross section stress. The end result is that the pitting may interfere with the valid evaluation of the SCC resistance of the material. For this reason, ASTM G47 and G64 recommend a 10-day alternate immersion exposure period for 2xxx series Al alloys when tested in the ST orientation and a 40-day exposure period when tested in the L and LT orientations. These exposure periods are believed to be long enough to detect susceptibility to intergranular SCC yet short enough to avoid excessive pitting that can lead to failure by another mechanism. General pitting, which served as initiation sites for SCC, was noted in the aft bulkhead material following 30-day alternate immersion exposure. The NESC team recommends that further evaluation of the aft bulkhead material be evaluated at shorter exposure times.

For alloys requiring microstructural control to avoid susceptibility to SCC, resistance is obtained by using heat treatments that produce uniform precipitation throughout the microstructure. The susceptibility of the Al 2219 aft bulkhead material to SCC is further exacerbated by the T62 temper which results in a non-uniform distribution of precipitates. Because of the pitting potential of this material and a susceptible heat treat temper to SCC, deployment of this material for the aft bulkhead may require a MUA prior to acceptance for service.

Alternative explanations for the reduced SCC resistance are that (1) the spin forming process has a negative effect, (2) the SCC properties are typical for T62 temper plate, and (3) that the reduced quench rate associated with the glycol/water mixture reduces the SCC resistance.

Metallurgical theory recognizes that variations in thermal treatments, such as solution heat treatment, quenching, and aging treatment can have marked effects on the SCC resistance of 2xxx series Al alloys. Ideally, all alloying elements should be fully dissolved during solution heat treatment, and the quench cooling rate should be rapid enough to keep them in solid solution. The quench medium for the spin formed aft bulkhead was a 15 to 17% polymer solution (see Section 7.8), which is intended to reduce distortion problems associated with water quenched Al alloys. Although this quench operation is permissible per AMS 2770, a sufficiently rapid quench rate might not be obtained because of the inherent cooling rate limitations of the polymer solution. The slower cooling rate affects the precipitation kinetics during subsequent aging and will lead to less uniform precipitation at and/or adjacent to the grain boundaries and hence this could lower the SCC resistance. Supplemental SCC testing, described in Section 11.3, was performed in an attempt to answer these questions. The results of the supplemental testing are provided in Supplemental Report T1-13-00884_Supplemental report (ref) and published in NASA-TM-2015-218797 (ref. 43).

All SCC test specimens evaluated in this study were machined at the t/2 position through the thickness. The grain size varies less at t/2 with location in the aft bulkhead compared with other through-thickness positions and also represents an intermediate grain size. The SCC properties may be different in locations that have larger grain sizes. Generally, the larger grain size areas may be more prone to SCC than the smaller grain size areas because the larger grain size areas would require less energy for the crack to propagate. In order to determine to what extent the SCC susceptibility varies with grain size grain size additional testing is recommended. Additional specimens should be obtained from the rim at the OML surface, which has been found to have very large grains in comparison to other areas. Successful completion of additional testing will add more confidence for the use of this material.

While the SCC results provide insight into the material behavior, the data sets generated are very small and caution should be exercised in assigning table ratings. Additionally, the LM Orion design team will require definition of a threshold stress level for SCC to bracket service stress limits. There is not sufficient data in this study to define the threshold stress level for SCC. The NESC team recommends that additional SCC testing be performed on the first spin formed aft bulkhead articles fabricated for Orion to define the SCC threshold stress level.

O-4. Questions arose regarding SCC test procedures, particularly the basis for exposure stress level and test duration, which may impact direct comparison of the aft bulkhead SCC results with the very limited handbook and open literature data.

O-5. The SCC tests performed provided an initial indication of the SCC susceptibility of the spin formed Al 2219-T62 material; however, environmentally assisted fracture toughness (KEAC) and fatigue ($(da/dN)_{SCC}$)) in the S-T orientation in a 3.5% NaCl environment is required to understand the impact of the SCC susceptibility on fracture and fatigue.

O-6. The laboratory 30-day alternate immersion accelerated test condition provides adequate screening methodology for SCC; however, longer test durations of 90 days did lead to severe general corrosion and pitting. For determining actual serviceability of the material, other stress corrosion tests should be performed in the intended service environment.

R-2. Additional testing should be performed on first article and initial serial production aft bulkhead components to generate data to populate the material property database for Al 2219-T6 spin formed products. (***O-2***)

- Stress corrosion cracking testing should be continued until sufficient data is generated to establish the SCC threshold stress level.

R-4. Exercise caution in using published handbook and table ratings for the SCC resistance of Al 2219-T6. Handbook and open literature publications should be reviewed in order to substantiate that the SCC test procedures and data generated are directly comparable to the MSFC-STD-3029 standard used in the SCC evaluation of the Al 2219-T62 aft bulkhead **(*O-4*)**

R-5. Perform environmentally assisted fracture toughness (KEAC) and fatigue ($(da/dN)_{SCC}$) tests in the S-T orientation in a 3.5% NaCl environment in order to understand the impact of the SCC susceptibility of the material on fracture toughness and fatigue. (***O-5***)

R-6. Perform seacoast exposure SCC testing to characterize the corrosion performance of the aft bulkhead in the natural service environment. (***O-6***)

Table 10.4-2. 30-day SCC test results for spin formed Al 2219-T62 aft bulkhead material. Test environment: 3.5% NaCl alternate immersion per ASTM G44.

Coupon Blank	Meridian Angle	Orient.	UTS ksi	YS ksi	Stress Level % YS	Stress Level ksi	Failure Ratio	Days to Failure
M7	90°	LT	54.14	36.64	0	0.00	0/3	No failures
					50	18.32	0/3	No failures
					75	27.48	0/3	No failures
					90	32.98	0/3	No failures
		ST	57.87	43.20	0	0.00	0/3	No failures
					50	21.60	0/3	No failures
					75	32.40	3/3	26, 28, 30
					90	38.88	3/3	26, 26, 28
M8	90°	LT	57.79	38.78	0	0.00	0/3	No failures
					50	19.39	0/3	No failures
					75	29.09	0/3	No failures
					90	34.90	0/3	No failures
		ST	58.69	43.73	0	0.00	0/3	No failures
					50	21.87	0/3	No failures
					75	32.80	3/3	27, 30, 30
					90	39.36	2/3	26, 30
M9	90°	LT	59.58	39.68	0	0.00	0/3	No failures
					50	19.84	0/3	No failures
					75	29.76	0/3	No failures
					90	35.71	0/3	No failures
		ST	59.86	44.33	0	0.00	0/3	No failures
					50	22.17	1/3(2)	30(2)
					75	33.25	0/3	No failures
					90	39.90	1/3	26
M10	190°	LT	55.89	37.87	0	0.00	0/3	No failures
					50	18.94	0/3	No failures
					75	28.40	0/3	No failures
					90	34.08	0/3	No failures
		ST	59.65	44.41	0	0.00	0/3	No failures
					50	22.21	1/3(3)	29
					75	33.31	2/3	26, 30
					90	39.97	3/3	29, 29, 30

(1)Exposure started on 3-5-2014 and ended on 4-4-2014.
(2)Invalid failure. Failed in the shoulder (out of the gage length).
(3)The two specimens that did not break apart during exposure did not pass the residual tensile strength ratio test and can also be considered failures.

Table 10.4-3. Baseline tensile properties of spin formed Al 2219-T62 aft bulkhead material. Data is the average of three replicate tests and was used to establish stress levels for the SCC tests.

Coupon Blank	Meridian Angle	Orient.	UTS, ksi	YS, ksi	e, %	RA, %	E, Msi
M7	90°	LT	54.14	36.64	10.58	17.42	9.97
		ST	57.87	43.20	4.80	6.51	9.89
M8	90°	LT	57.79	38.78	9.79	9.52	10.48
		ST	58.69	43.73	4.57	9.89	9.66
M9	90°	LT	59.58	39.68	8.79	16.82	10.31
		ST	59.86	44.33	4.12	6.54	9.26
M10	190°	LT	55.89	37.87	10.15	17.15	10.14
		ST	59.65	44.41	4.83	6.57	10.12
		L	57.05	38.26	12.74	25.78	10.30

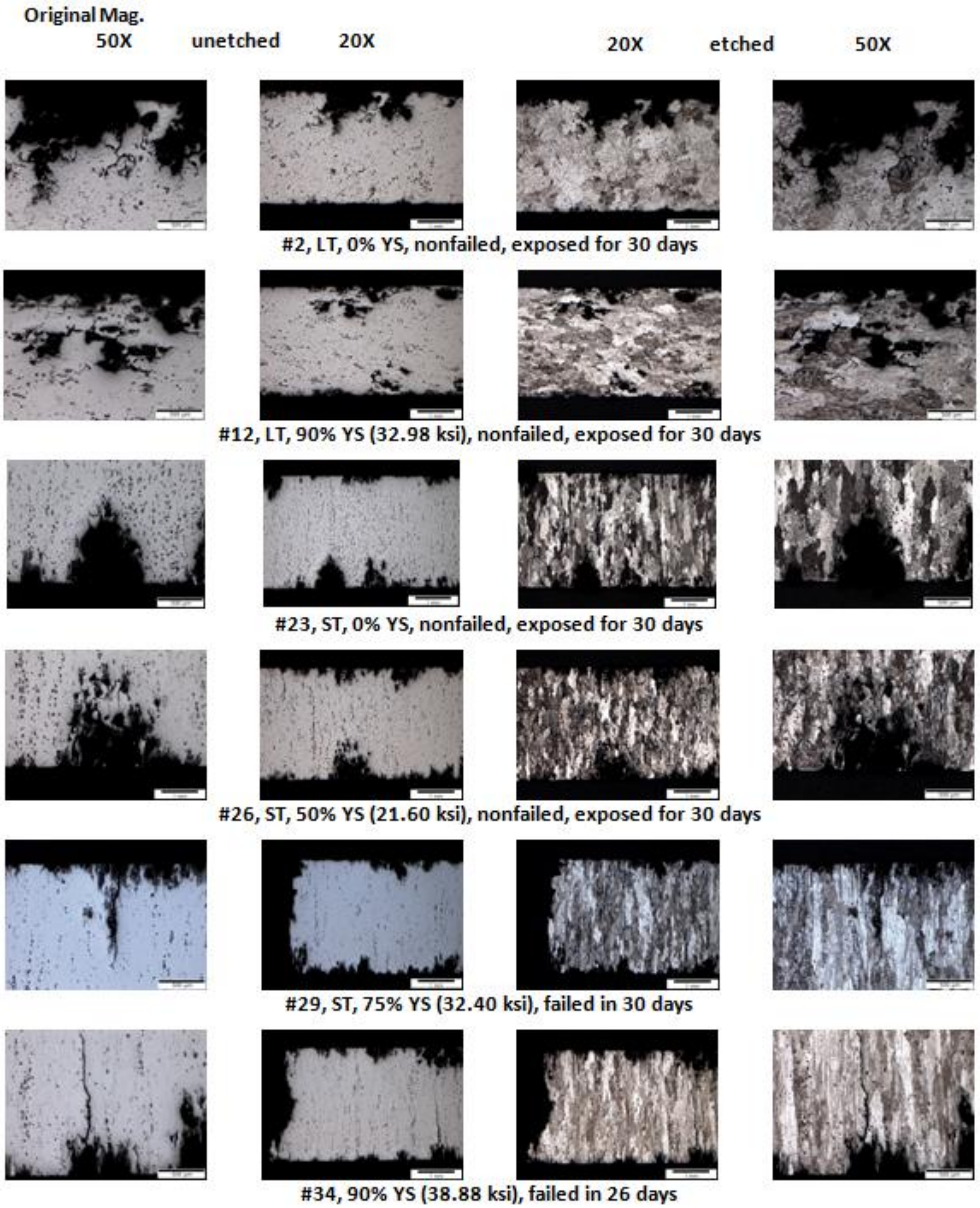

Figure 10.4-2. Photomicrographs of Representative SCC Specimens obtained from Coupon Blank M7 following 3.5% NaCl Alternate Immersion Exposure (30-day test)

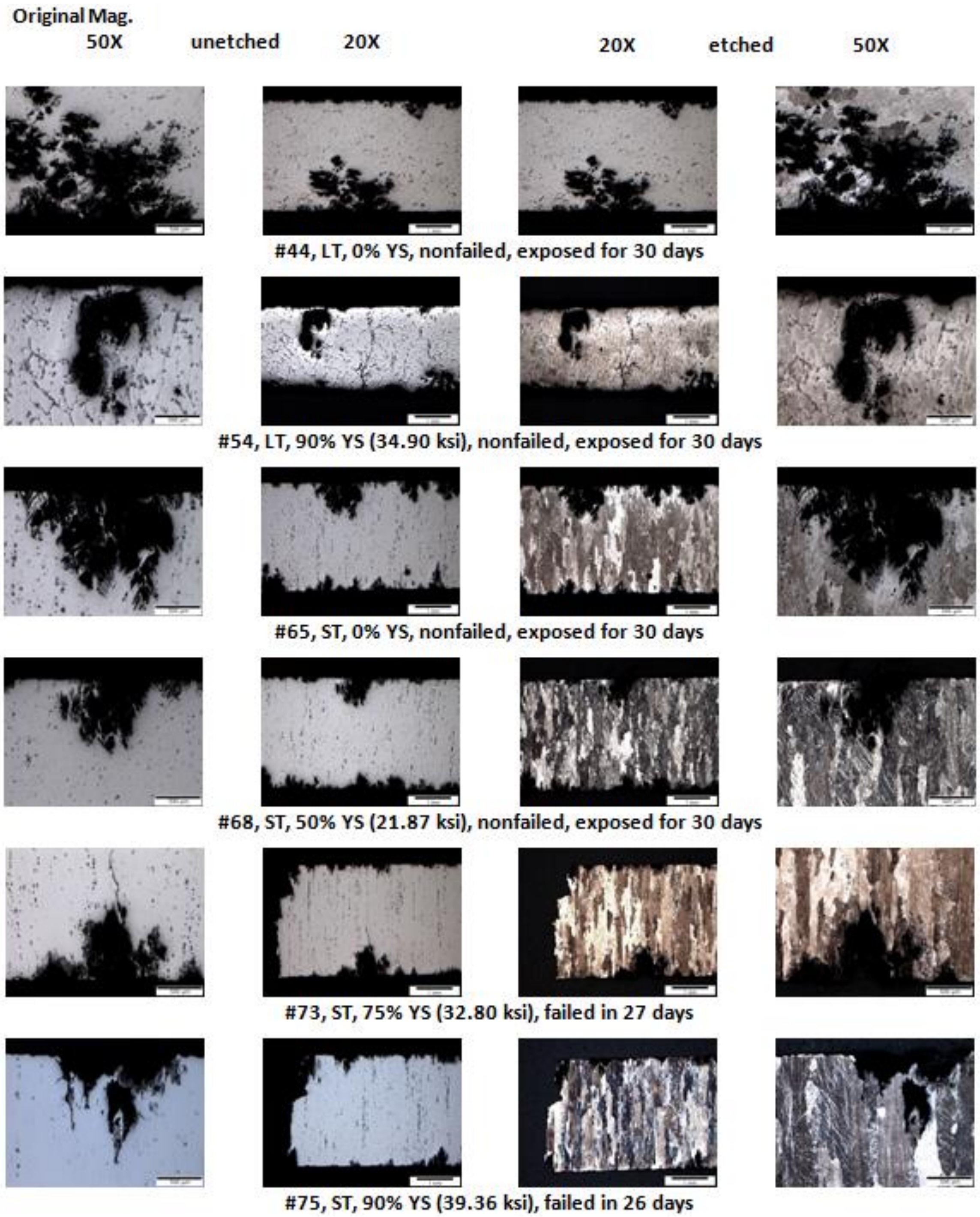

Figure 10.4-3. Photomicrographs of Representative SCC Specimens obtained from Coupon Blank M8 following 3.5% NaCl Alternate Immersion Exposure (30-day test)

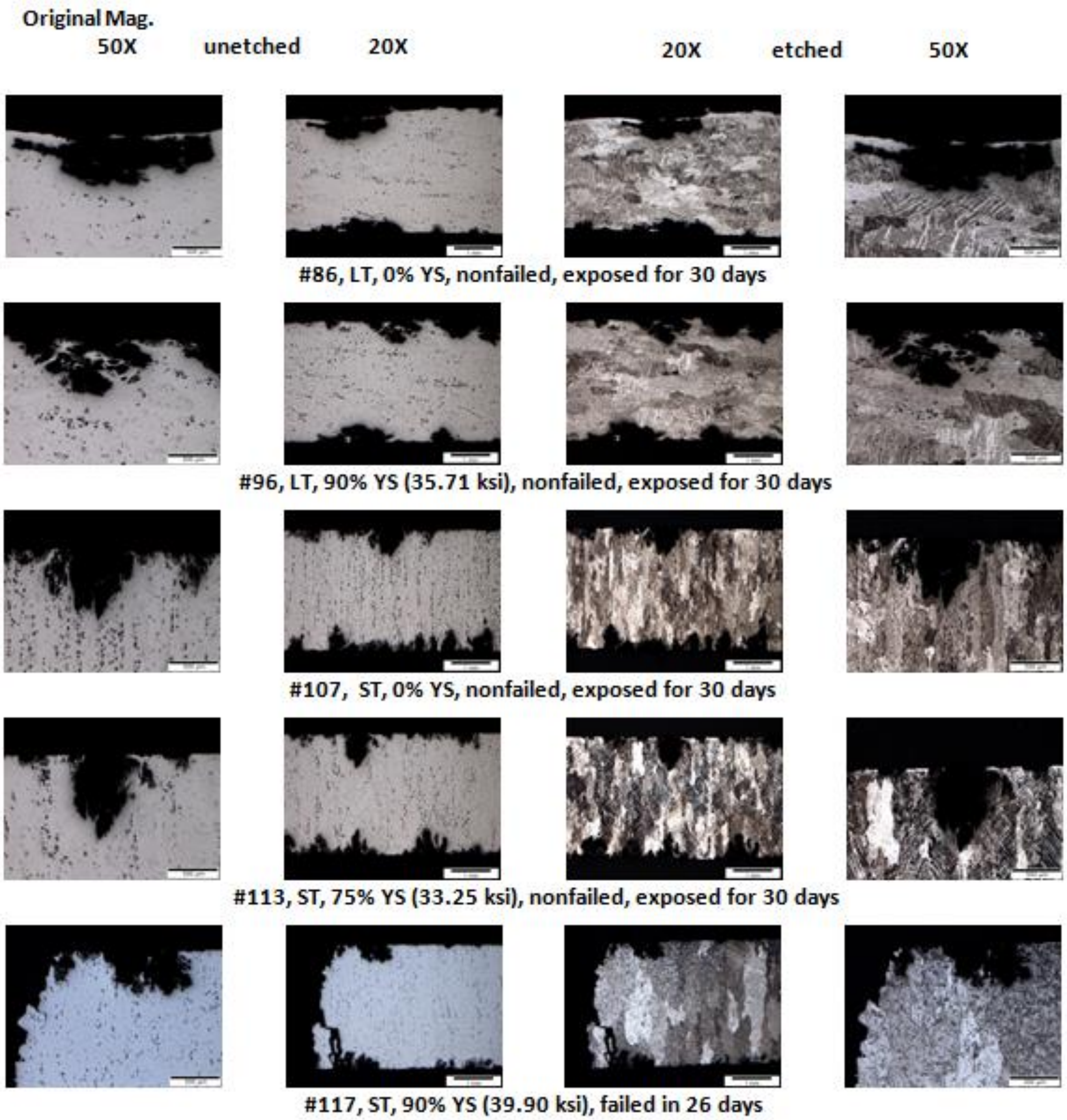

Figure 10.4-4. Photomicrographs of Representative SCC Specimens obtained from Coupon Blank M9 following 3.5% NaCl Alternate Immersion Exposure (30-day test)

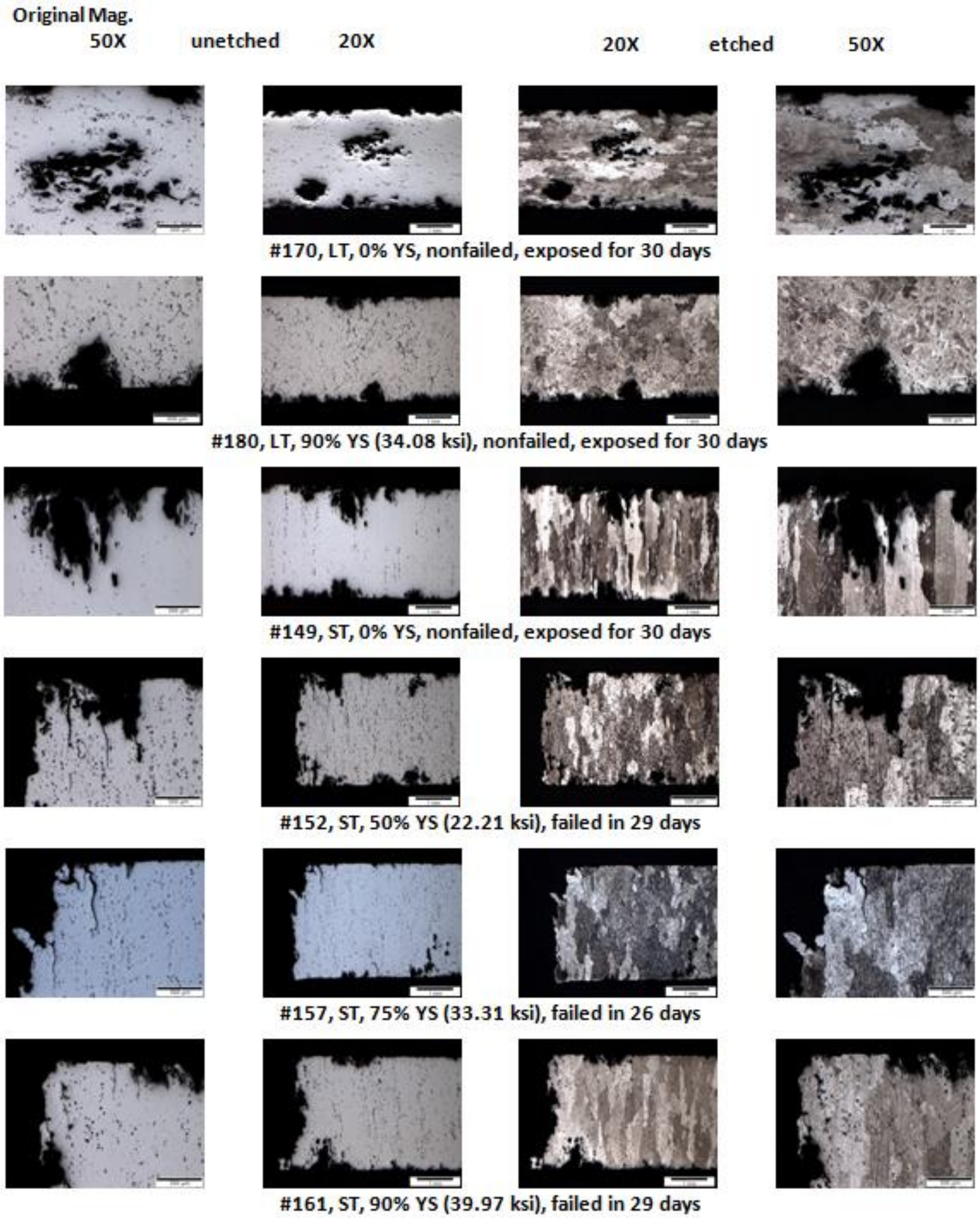

Figure 10.4-5. Photomicrographs of Representative SCC Specimens obtained from Coupon Blank M10 following 3.5% NaCl Alternate Immersion Exposure (30-day test)

Table 10.4-4. Residual Tensile Strength Data for Spin Formed Al 2219-T62 Aft Bulkhead Material following a 30-Day Exposure to 3.5% NaCl Alternate Immersion per ASTM G44

Bulkhead location: coupon blank: M7; meridian angle: 90°; arc length: 12.00 inches

Orient.	Initial UTS, ksi	Specimen Number	Stress Level, % YS	Stress Level, ksi	Residual UTS, ksi	% Strength Retained	Residual (1) Strength Ratio UTS_s/UTS_o	Pass/Fail (2) UTS Ratio Test
LT	54.14	CP-406-3	0	0.00	28.23	52	NA	NA
		CP-406-4	0	0.00	30.98	57	NA	NA
				Avg:	**29.61**	**54.5**		
		CP-406-6	50	18.32	22.75	42	0.77	passed
		CP-406-7	50	18.32	29.65	55	1	passed
		CP-406-9	75	27.48	31.53	58	1.06	passed
		CP-406-10	75	27.48	25.62	47	0.87	passed
		CP-406-13	90	32.98	28.51	53	0.96	passed
		CP-406-14	90	32.98	25.04	46	0.85	passed
ST	57.87	CP-406-24	0	0.00	28.40	49	NA	NA
		CP-406-25	0	0.00	18.61	32	NA	NA
				Avg:	**23.51**	**40**		
		CP-406-27	50	21.60	22.51	39	0.96	passed
		CP-406-28	50	21.60	20.97	36	0.89	passed

(1) UTS_s = residual strength of stressed and exposed specimen
UTS_0 = averaged residual strength of non-stressed and exposed specimens
(2) Passed if ratio≥0.75, failed if ratio <0.75. The 90% YS data is not used for the ratings, but is presented for information.

Table 10.4-5. Residual Tensile Strength Data for Spin Formed Al 2219-T62 Aft Bulkhead Material following a 30-Day Exposure to 3.5% NaCl Alternate Immersion per ASTM G44

Bulkhead location: coupon blank: M8; meridian angle: 90°; arc length: 35.13 inches

Orient.	Initial UTS, ksi	Specimen Number	Stress Level, % YS	Stress Level, ksi	Residual UTS, ksi	% Strength Retained	Residual [(1)] Strength Ratio UTS_s/UTS_o	Pass/Fail [(2)] UTS Ratio Test
LT	57.79	CP-406-45	0	0.00	33.98	59	NA	NA
		CP-406-46	0	0.00	33.23	58	NA	NA
				Avg:	**33.60**	**58.5**		
		CP-406-48	50	19.39	32.54	56	0.97	passed
		CP-406-49	50	19.39	32.68	57	0.97	passed
		CP-406-51	75	29.09	37.74	65	1.12	passed
		CP-406-52	75	29.09	31.38	54	0.93	passed
		CP-406-55	90	34.90	32.84	57	0.98	passed
		CP-406-56	90	34.90	37.41	65	1.11	passed
ST	58.69	CP-406-66	0	0.00	23.25	40	NA	
		CP-406-67	0	0.00	19.44	33	NA	
				Avg:	**21.35**	**36.5**		
		CP-406-69	50	21.87	16.52	28	0.77	passed
		CP-406-70	50	21.87	32.45	55	1.52	passed
		CP-406-77	90	39.36	22.51	38	1.05	passed

(1) UTS_s = residual strength of stressed and exposed specimen
UTS_0 = averaged residual strength of non-stressed and exposed specimens

(2) Passed if ratio≥0.75, failed if ratio <0.75. The 90% YS data is not used for the ratings, but is presented for information.

Table 10.4-6. Residual Tensile Strength Data for Spin Formed Al 2219-T62 Aft Bulkhead Material following a 30-Day Exposure to 3.5% NaCl Alternate Immersion per ASTM G44

Bulkhead location: coupon blank: M9; meridian angle: 90°; arc length: 56.25 inches

Orient.	Initial UTS, ksi	Specimen Number	Stress Level, % YS	Stress Level, ksi	Residual UTS, ksi	% Strength Retained	Residual (1) Strength Ratio UTS_s/UTS_o	Pass/Fail (2) UTS Ratio Test
LT	59.58	CP-406-87	0	0.00	39.10	66	NA	NA
		CP-406-88	0	0.00	39.16	66	NA	NA
				Avg:	**39.13**	**66**		
		CP-406-90	50	19.84	38.96	65	1	passed
		CP-406-91	50	19.84	40.50	68	1.04	passed
		CP-406-93	75	29.76	39.58	66	1.01	passed
		CP-406-94	75	29.76	42.41	71	1.08	passed
		CP-406-97	90	35.71	34.08	57	0.87	passed
		CP-406-98	90	35.71	39.06	66	1	passed
ST	59.86	CP-406-108	0	0.00	26.95	45	NA	NA
		CP-406-109	0	0.00	19.55	33	NA	NA
				Avg:	**23.25**	**39**		
		CP-406-110	50	22.17	28.09	47	1.21	passed
		CP-406-112	50	22.17	19.66	33	0.85	passed
		CP-406-114	75	33.25	24.50	41	1.05	passed
		CP-406-115	75	33.25	27.58	46	1.19	passed
		CP-406-118	90	39.90	24.62	41	1.06	passed

(1) UTS_S = residual strength of stressed and exposed specimen.
UTS_0 = averaged residual strength of non-stressed and exposed specimens.

(2) Passed if ratio≥0.75, failed if ratio <0.75. The 90% YS data is not used for the ratings, but is presented for information.

Table 10.4-7. Residual Tensile Strength Data for Spin Formed Al 2219-T62 Aft Bulkhead Material following a 30-Day Exposure to 3.5% NaCl Alternate Immersion per ASTM G44

Bulkhead location: coupon blank: M10; meridian angle: 190°; arc length: 35.63 inches

Orient.	Initial UTS, ksi	Specimen Number	Stress Level, % YS	Stress Level, ksi	Residual UTS, ksi	% Strength Retained	Residual [(1)] Strength Ratio UTS_s/UTS_o	Pass/Fail [(2)] UTS Ratio Test
LT	55.89	CP-406-171	0	0.00	34.10	61	NA	NA
		CP-406-172	0	0.00	29.47	53	NA	NA
				Avg:	**31.79**	**57**		
		CP-406-174	50	18.94	31.51	56	0.99	passed
		CP-406-175	50	18.94	29.44	53	0.93	passed
		CP-406-177	75	28.40	34.70	62	1.09	passed
		CP-406-178	75	28.40	32.52	58	1.02	passed
		CP-406-181	90	34.08	30.03	54	0.94	passed
		CP-406-182	90	34.08	34.24	61	1.08	passed
ST	59.65	CP-406-150	0	0.00	18.88	32	NA	NA
		CP-406-151	0	0.00	19.36	32	NA	NA
				Avg:	**19.12**	**32**		
		CP-406-153	50	22.21	5.51	9	0.29	failed
		CP-406-154	50	22.21	2.56	4	0.13	failed
		CP-406-155	75	33.31	20.32	34	1.06	passed

(1) UTS_s = residual strength of stressed and exposed specimen
UTS_0 = averaged residual strength of non-stressed and exposed specimens

(2) Passed if ratio≥0.75, failed if ratio <0.75. The 90% YS data is not used for the ratings, but is presented for information.

Table 10.4-8. 90-day SCC test results for spin formed Al 2219-T62 aft bulkhead material. Test environment: 3.5% NaCl alternate immersion per ASTM G44.

Coupon Blank	Meridian Angle	Orient.	UTS, ksi	YS, ksi	Stress Level % YS	Stress Level ksi	Failure Ratio	Days to Failure
M7	90°	LT	54.14	36.64	0	0	3/3(2)	48(2), 90(2)(5), 90(2)(5)
					75	27.48	2/3	76, 90(5)
		ST	57.87	43.2	0	0	3/3(2)	54(2), 64(2), 89(2)
					75	32.4	3/3	26, 33, 33
M8	90°	LT	57.79	38.78	0	0	1/3(2)(5)	90(2)(5)
					75	29.09	2/3(5)	90(5), 90(5)
		ST	58.69	43.73	0	0	3/3(2)	89(2), 90(2)(5), 90(2)(5)
					75	32.8	3/3	33, 64, 83(3)
M9	90°	LT	59.58	39.68	0	0	1/3(2)(5)	90(2)(5)
					75	29.76	0/3	No failures
		ST	59.86	44.33	0	0	2/3(2)	58(2)(4), 90(2)(5)
					75	33.25	3/3	56, 64(3), 85
M10	190°	LT	55.89	37.87	0	0	0/3	No failures
					75	28.4	3/3	70, 74, 74
		ST	59.65	44.41	0	0	3/3(2)	70(2)(4), 89(2), 89(2)
					75	33.31	3/3	26, 54, 70

(1)Exposure started on 3-5-2014 and ended on 6-3-2014.
(2)Failed due to corrosion since this specimen was not loaded.
(3)Failed in the shoulder, out of the reduced section.
(4)Failed in 2 places.
(5)Failed during disassembly.

Table 10.4-9. Residual Tensile Strength Data for Spin Formed Al 2219-T62 Aft Bulkhead Material following a 90-Day Exposure to 3.5% NaCl Alternate Immersion per ASTM G44

Coupon Blank	Orient.	Initial UTS, ksi	Specimen Number	Stress Level		Residual UTS, ksi	% Strength Retained
				% YS	ksi		
M7	LT	54.14	CP-406-20	75	27.48	15.6	29
M8	LT	57.79	CP-406-57	0	0	17.5	30
M8	LT	57.79	CP-406-58	0	0	13.1	23
M8	LT	57.79	CP-406-62	75	29.09	16.4	28
M9	LT	59.58	CP-406-100	0	0	20.7	35
M9	LT	59.58	CP-406-101	0	0	20.2	34
M9	LT	59.58	CP-406-102	75	29.76	13.7	23
M9	LT	59.58	CP-406-103	75	29.76	18.4	31
M9	LT	59.58	CP-406-104	75	29.76	25.6	43
M9	ST	59.86	CP-406-121	0	0	6.3	11
M10	LT	55.89	CP-406-183	0	0	6.0	11
M10	LT	55.89	CP-406-184	0	0	12.0	21
M10	LT	55.89	CP-406-185	0	0	25.2	45

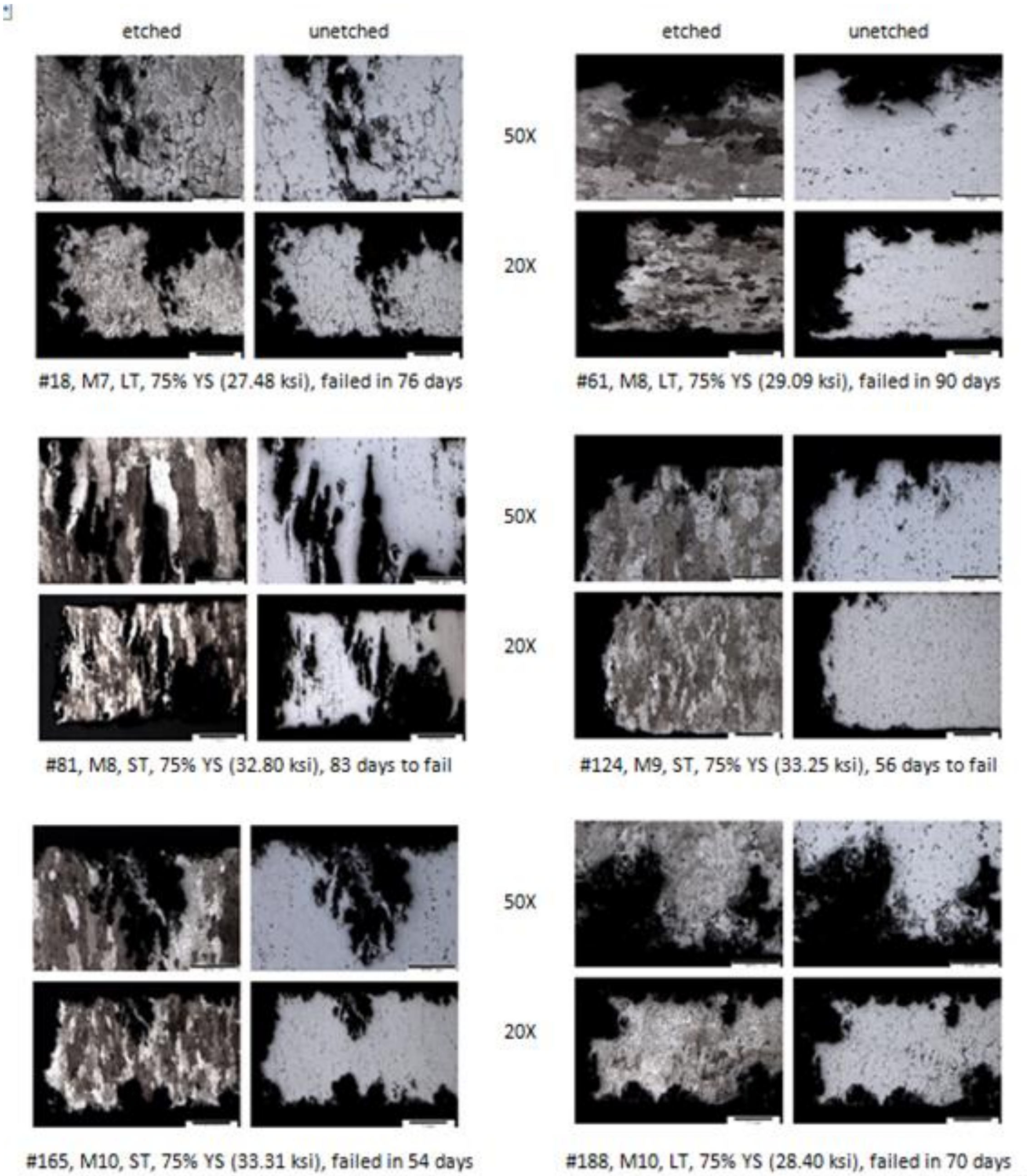

Figure 10.4-6. Photomicrographs of Representative SCC Specimens obtained from Various Coupon Blanks following 3.5% NaCl Alternate Immersion Exposure (90-day test)

Table 10.4-10. 30-day SCC test results for spin formed Al 2219-T62 aft bulkhead material. Test environment: 5% salt fog per ASTM B117.

Coupon Blank	Meridian Angle	Orient.	UTS ksi	YS ksi	Stress Level % YS	Stress Level ksi	Failure Ratio	Days to Failure
M10	190°	L	57.05	38.26	0	0	0/3	No failures
					75	28.70	0/3	No failures

(1) Exposure started on 3-5-2014 and ended on 4-4-2014.

Table 10.4-11. 90-day SCC test results for spin formed Al 2219-T62 aft bulkhead material. Test environment: 5% salt spray per ASTM B117.

Coupon Blank	Meridian Angle	Orient.	UTS ksi	YS ksi	Stress Level % YS	Stress Level ksi	Failure Ratio	Days to Failure
M10	190°	L	57.05	38.26	0	0	0/3	No failures
					50	19.13	0/3	No failures
					75	28.7	0/3	No failures
					90	34.43	0/3	No failures

(1) Exposure started on 3-5-2014 and ended on 6-3-2014.

Table 10.4-12. Residual tensile strength data for spin formed Al 2219-T62 aft bulkhead material following exposure to 5% salt spray per ASTM B117.

Coupon Blank	Orient.	Initial UTS, ksi	Test Duration, Days	Specimen Number	Stress Level		Residual UTS, ksi	% Strength Retained
					% YS	ksi		
M10	L	57.05	30	CP-406-141	0	0	54.3	95
				CP-406-142	0	0	55.8	98
				CP-406-143	0	0	53.2	93
				CP-406-144	75	28.7	53.3	93
				CP-406-145	75	28.7	54.5	96
				CP-406-146	75	28.7	54.6	96
M10	L	57.05	90	CP-406-128	0	0	54.3	95
				CP-406-129	0	0	54.5	96
				CP-406-130	0	0	55.1	97
				CP-406-131	50	19.13	51.5	90
				CP-406-132	50	19.13	51.9	91
				CP-406-133	50	19.13	52.7	92
				CP-406-134	75	28.7	54.7	96
				CP-406-135	75	28.7	53.7	94
				CP-406-136	75	28.7	55.0	96
				CP-406-138	90	34.43	54.5	96
				CP-406-139	90	34.43	51.8	91
				CP-406-140	90	34.43	53.5	94

Table 10.4-13. SCC Test Data for other 2xxx Series Al Alloys for Comparison (38), (39)

Alloy	Heat Treatment	Orient.	UTS, ksi	YS, ksi	Test Environ.	Stress Level, % YS	Stress Level, ksi	Failure Ratio	Days to Failure
2195-T8 (1.7" thick plate)	290°F/16h	ST	86.2	74.1	Alt. Imm.	50	37.1	4/4	31, 40, 41, 69
						75	55.6	4/4	11, 12, 18, 31
						90	66.7	4/4	11, 17, 17, 17
	290°F/20h	ST	89.1	75.7	Alt. Imm.	75	56.8	3/3	27, 30, 31
						90	68.1	3/3	12, 17, 19
					KSC Seacoast	75	56.8	1/3	423
						90	68.1	3/3	315, 454, 513
					High Hum.	75	56.8	0/3	NF in 115 days
						90	68.1	0/3	NF in 115 days
2195-T8 (0.32" thick plate)	320°F/20h	LT	86.4	81.1	Alt. Imm.	50	40.6	0/5	NF in 90 days
						75	60.8	0/5	NF in 90 days
						90	73	3/5	74, 88, 90
2219-T87 (4" thick plate)	350°F/18h	ST[1] (midthick.)	60.7	52	Alt. Imm.	50	26	4/5	41, 52, 58, 62
						75	39	4/5	38, 44, 48, 58, 62
		ST[1] (edge)	63.5	53.3		90	48	12/12	20, 28, 30, 31, 33, 46, 49, 64, 73, 76, 81, 87
		LT	66.4	52.4		50	26.2	0/5	NF in 90 days
						75	39.3	2/5	90, 91

(1)The 2219 ST specimens tested at 50% and 75% YS were obtained from the plate mid-thickness whereas the ST specimens tested at 90% YS were obtained from the plate edge.

Table 10.4-14. Rating of Al 2195-T8 and Al 2219-T87 per MSFC-STD-3029. Based on a 30-day exposure to 3.5% NaCl alternate immersion per ASTM G44.

Alloy	Temper	Rating	Rationale for Rating
2195	T8 (Various conditions)	Table II	5 out of 7 ST specimens failed at 75% YS within 30 days of exposure (11, 12, 18, 27, and 30 days) to 3.5% NaCl alternate immersion. None out of 4 ST specimens failed at 50% YS within 30 days of exposure.
2219	T87	Table I	None out of 5 ST specimens failed at 75% YS within 30 days of exposure to 3.5% NaCl alternate immersion.

Table I = A rating = Highly resistant to SCC in a sodium chloride environment
Table II = B rating = Moderately resistant to SCC in a sodium chloride environment
Table III = C rating = Low resistance to SCC in a sodium chloride environment

11.0 Supplemental Mechanical Test Program

During the execution of the mechanical property testing and analysis of the aft bulkhead, several issues arose which the NESC team attempted to address to assist the Orion designers team in their first article test program. In addition, several findings were observed that the team wished to further analyze to clarify the results. The NESC team proposed a limited number of supplemental tensile, fracture, and SCC tests, which were accepted by the NESC advisory team. Further details on these supplemental tests are addressed in Sections 11.1 through 11.3. Due to project milestones and schedule, the results from these supplemental tests were not available in time to be included in this final report, but will are provided in supplemental report T1-13-00884_Supplemental report and published in NASA-TM-2015-218797 (ref. 43).

11.1 Tensile

Based on the results of the tensile tests performed on the aft bulkhead and the limited amount of handbook data available for interpretation of the results, a limited quantity of additional tensile tests were conducted to address key questions. Table 11.1-1 shows the supplemental tensile test matrix and lists questions being addressed.

Table 11.1-1. Supplemental Tensile Test Matrix

Material Source	Location / Heat Treatment	Orient.	Through-thickness position	# of Specimens	Question Addressed
Aft Bulkhead	L2	L	t/8	3	1. What are the tensile properties at other through-thickness locations in the aft bulkhead? 2. What effect does the inhomogeneous microstructure have on the tensile properties of the aft bulkhead?
			7t/8	3	
		LT	t/8	3	
			7t/8	3	
Typical Plate	SHT + water quench + age, 375°F/36h	L	t/2	3	3. How do the tensile properties of thh aft bulkhead compare to wrought plate? 4. What effect does a slower quench during heat treat processing have on the tensile properties of the material? 5. Are the high ST tensile properties in the aft bulkhead inherent to the plate lot or are they an artifact of spin form processing?
		LT	t/2	3	
		ST	t/2	3	
Modified Plate	SHT + water/glycol quench + age, 375°F/36h	L	t/2	3	
		LT	t/2	3	
		ST	t/2	3	

Based on microstructural characterization of the aft bulkhead, the post-recrystallization grain morphology varies with meridian distance and through-thickness position, with larger grain sizes associated with likely regions of higher deformation. These grain size differences are biased toward the OML, which is in direct contact with the forming tool. To characterize these effects on the tensile properties, tensile specimens from coupon blank L2 (arc length = 36.0 in; meridian angle 347°) were tested at both the t/8 (near the IML surface) and 7/t8 (near the OML surface) through-thickness locations for comparison to tensile test results previously acquired at the t/2 location only. These through-thickness positions showed the most variation in grain size. In addition, the membrane region of the finished machined aft bulkhead will likely be located near the OML surface so tensile properties from this region will be of interest to the Orion designers.

Additional testing was designed to address the heat treat practice used in the processing of the aft bulkhead as described in Section 7.8. The solution heat treat and quench operation used by Spincraft consisted of a quench in a water/glycol mixture which results in a slower overall cooling rate to reduce part distortion and residual stress in the final product. Although this quench operation is permissible per AMS 2770, the slower cooling rate affects the precipitation kinetics during subsequent aging and may impact material properties (40).

Remnant –F temper plate machining drops from the aft bulkhead forming blank were heat treated to the –T62 temper as per AMS 2770. Two heat treat conditions were evaluated: typical plate which was quenched in water following solution heat treatment (SHT) and modified plate which was quenched in a water/glycol mixture similar to that used by Spincraft. Tensile tests were conducted on both heat treated plates to determine if the slower quench rate has any impact on the tensile properties.

The tensile tests of the aft bulkhead revealed that the ST tensile properties were substantially higher than the L and LT orientations (by ~ 4-6 ksi) depending on the aft bulkhead location. The NESC team was not able to find any comparable data for wrought plate or other product forms in the –T62 temper for the ST orientation. A search of the literature for other 2xxx series Al alloys did show that the ST tensile properties are typically lower than the L and LT orientations. Additional tensile tests were conducted in the ST orientation for both heat treated plate conditions and compared to the aft bulkhead tensile test results to determine if the high ST tensile properties are a result of the spin forming processing or are they inherent to the starting material condition and subsequent processing. The ST YS is additionally of interest because this data was used to define the exposure stress levels for the SCC testing and may have resulted in the specimens being exposed at a higher stress level than comparable handbook data.

11.2 Fracture Toughness

Due to the lack of available fracture data in the literature, and in response to the questions regarding plate processing, supplemental fracture toughness tests shown in Table 11.2-1 were performed on the typical and modified plates. Specific questions being addressed by this supplemental fracture toughness testing included whether the spin form processing compromises the fracture toughness of the material and whether the slower quench used during heat treatment of the aft bulkhead has any effect on the fracture toughness compared to the normal water quench rate.

Table 11.2-1. Supplemental Fracture Toughness Test Matrix

Material Source	Location/Heat Treatment	Orient.	Through-thickness position	# of Specimens	Question Addressed
Typical Plate	SHT + water quench + age, 375°F/36h	L-T	t/2	2	1. How does the fracture toughness properties of the aft bulkhead compare to wrought plate? 2. What is the impact of a slower quench rate during heat treat processing have on the fracture toughness of the material?
		T-L	t/2	2	
		S-T	t/2	2	
Modified Plate	SHT + water/glycol quench + age, 375°F/36h	L-T	t/2	2	
		T-L	t/2	2	
		S-T	t/2	2	

11.3 Stress Corrosion

When evaluating the SCC test results and making comparisons with handbook or published data in an attempt to interpret the SCC results, several questions and issues arose. The primary question was whether the failure that occurred in the ST orientation at the exposure stress of 50% YS for coupon blank M10 was an outlier?

A complication that impeded interpreting the results is that there is very little SCC data available for Al 2219-T6 products. In addition, several questions arose regarding the available data for Al 2219-T8 products, both in terms of SCC test practices and the available data to substantiate published ratings. Specifically, what the appropriate basis for the applied stress level should be. There are a number of applicable standards for SCC testing that use different applied stress levels, exposure periods, and criterion ratings. Most are based on MMPDS allowable YS, but the MSFC SCC test standard, MSFC-STD-3029, Revision A, uses typical YS for the product being tested. The ST YS of the aft bulkhead is higher than typical values which may have resulted in a more severe test than the handbook data being used for comparison.

All of the SCC testing procedures used in the evaluation of the aft bulkhead were based on MSFC-STD-3029, Revision A, which is a more conservative test method than ASTM G64 (33). The applied stress levels for the current tests were based on the actual material properties, whereas the handbook data is based on the MMPDS design allowable material properties, which are typically lower than actuals or typicals due to the statistical analysis. Since the susceptibility of metallic materials to stress corrosion tends to increase with the applied stress, the higher reported ST properties in the aft bulkhead result in a more aggressive test condition compared to the reference data in the literature. To address this issue, additional SCC tests were conducted on coupon blank M10 using applied stress levels based on MMPDS A-basis design allowables for Al 2219-T62 plate.

Additional general questions arose regarding how the SCC ratings in published literature were established. What type of SCC data will Orion use to base their design? What is the threshold stress level for SCC for the aft bulkhead? Due to limited funds and schedule, not all of these questions can be addressed in the scope of this supplemental SCC test program.

Table 11.3-1 lists the SCC test matrix, test priorities, and the questions being addressed. These supplemental SCC tests consisted of 30-day alternate immersion in a 3.5% NaCl environment and evaluated only the ST orientation since this was the most susceptible grain orientation to SCC and the orientation of the failures in question. The goal of the supplemental SCC test matrix was to ensure confidence in the data that has been generated, and characterize the aft bulkhead component as best as possible.

Table 11.3-1. Supplemental SCC Test Matrix

Material Source	Location/Heat Treatment	Applied Stress Level, % YS	Applied Stress Level, ksi	Orient.	# of Specimens	# of Specimens per Group	Question Addressed	Priority
Aft Bulkhead	M10	50 based on M10 avg. ST YS	22.2	ST	3	6	Is failure at 50% exposure stress repeatable? Was this data point an outlier or it is representative of this aft bulkhead location?	1
		75 based on M10 avg. ST YS	33.3	ST	3			
Aft Bulkhead	M10	50 based on MMPDS LT YS	18.0	ST	3	6	Does material pass at exposure stress levels based on MMPDS design properties rather than actual material yield strength?	
		75 based on MMPDS LT YS	27.0	ST	3			
Aft Bulkhead	J1	0	0.0	ST	3	9	What is the SCC behavior in other coupon blank locations along a different meridian line? **Note**: These specimens have already been machined and installed in stressing frames.	2
		50 based on MMPDS LT YS	18.0	ST	3			
		75 based on MMPDS LT YS	27.0	ST	3			
Aft Bulkhead	J2	0	0.0	ST	3	9		
		50 based on MMPDS LT YS	18.0	ST	3			
		75 based on MMPDS LT YS	27.0	ST	3			
Aft Bulkhead	J3	0	0.0	ST	3	9		
		50 based on MMPDS LT YS	18.0	ST	3			
		75 based on MMPDS LT YS	27.0	ST	3			
Typical Plate	SHT + water quench + age, 375F/36h	0	0.0	ST	3	9	Does spin forming alter the SCC resistance of plate?	3
		50 based on MMPDS LT YS	18.0	ST	3			
		75 based on MMPDS LT YS	27.0	ST	3			
Modified Plate	SHT + water/glycol quench + age, 375F/36h	0	0.0	ST	3	9	Does the quench rate affect SCC resistance of plate?	
		50 based on MMPDS LT YS	18.0	ST	3			
		75 based on MMPDS LT YS	27.0	ST	3			
CPST Spin Formed Dome	T62	0	0.0	ST	3	9	How does the aft bulkhead compare with other spin formed domes?	
		50 based on MMPDS LT YS	18.0	ST	3			
		75 based on MMPDS LT YS	27.0	ST	3			

The first priority of these supplemental SCC tests was to repeat the tests on coupon blank M10 to determine whether the one failure in the ST orientation that occurred at 50% YS applied stress level was an anomaly. The concern was the viability of the limited data set and its potential impact on the SCC rating. Typically, a larger number of replicate tests are conducted to establish a statistical basis for SCC resistance due to inherent variability in corrosion and stress corrosion testing. The first priority tests repeated the tests for material from coupon blank M10 with the applied stress levels based on the actual test data for the coupon blank to see if the results are repeatable. Additional tests from the same coupon blank were conducted at applied stress levels based on MMPDS design values to determine whether or not the material would pass exposure at lower stress levels.

The second priority tests are in response to input from the LM Orion Program to better understand the SCC resistance throughout the aft bulkhead. The SCC specimens from coupon blank J1, J2, and J3 designated for seacoast exposure SCC testing were re-directed to alternate immersion SCC testing in order to examine more locations in the aft bulkhead. Seacoast exposure SCC testing was proposed in the original test program because of concerns that the alternate immersion test results would become compromised due to general corrosion in the form of pitting thereby rendering the SCC test results invalid. Seacoast exposure SCC testing, which is performed in a natural outdoor environment and requires longer test durations than the standard accelerated corrosion tests performed in a laboratory, is used as a complementary test to alternate immersion. Based on the preliminary alternate immersion SCC test results, the NESC team decided that there was no longer a need to conduct the seacoast exposure SCC testing.

These seacoast exposure SCC specimens had already been machined and loaded in the stressing frames; the only change required was to change the applied stress levels and install them in the alternate immersion test apparatus. For these tests, the applied stress levels were based upon MMPDS A-basis design properties. These specimens offered a ready opportunity to generate the additional data while staying within the prescribed budget and schedule.

The third priority tests were in response to the lack of available SCC data for Al 2219-T6 products. The tests also address whether the lower SCC resistance of the aft bulkhead is inherent in this plate lot or due to the spin forming process. Tests were performed on plate processed to the T62 temper using the typical and modified heat treat procedures to evaluate the effect of spin forming and heat treatment. Remnant spin formed Al 2219-T62 dome material from the CPST Program (21) provided data for a comparable product form. For these tests, the applied stress levels were based upon MMPDS A-basis design properties.

12.0 Findings, Observations, and NESC Recommendations

The following findings, observations, and recommendations are based on the results of a study for which the main objective was to determine whether there are technical obstacles relative to the spin forming a single piece APVHB.

The Phase II M&P studies did not identify any potential insurmountable technical issues that would preclude spin forming the APVBH. The potential benefits of spin forming an Al 2219 APVBH include reduced weight and production costs, which are associated with eliminating welds and weld lands, and improved performance and design margins.

12.1 Findings

The following findings were identified:

F-1. The aft bulkhead microstructure varies both through-thickness and along the meridian arc length positions, with larger grain sizes associated with likely regions of higher deformation.

- Grain size was larger toward the rim and toward the OML surface, likely associated with the combined stresses necessary to shape the material to fit the mandrel.
- These variations in grain size are indicative of the complex and varied deformation levels associated with the spin forming process, particularly when combined with the plate rolling history and post-forming heat treatment.

F-2. Tensile tests designed to determine tensile property uniformity over the aft bulkhead acreage noted that the tensile properties varied with location in the aft bulkhead.

- For the L and LT orientations, a trend of increasing tensile and YS with arc length distance from the pole was evident.
- Conversely, the properties were uniform in the circumferential direction.

- The ST tensile properties were notably greater than those for the other orientations (L, LT, ST45), but elongations were about half.

F-3. The tensile properties of the spin formed Al 2219-T62 aft bulkhead material were typical for established 2219-T62 products.

- Tensile properties were comparable to the MMPDS design properties for T62 wrought plate and other fabricated products in the T6 temper, such as spin formed domes, forgings and rolled rings.
- Tensile properties were lower than those for Al 2219-T851 and T87 plate, as expected due to the increased precipitation strengthening in T8 temper wrought products that is imparted by the cold stretch/work prior to artificial aging.
- The lower tensile strength of the spin formed Al 2219-T62 aft bulkhead material compared with Al 2219-T851 and T87 plate is due to differences in material temper and not the spin forming process.

F-4. Fracture toughness was uniform with location in the aft bulkhead and indicated excellent damage tolerance capability.

- In-plane (T-L and L-T) toughness values are relatively constant for a given orientation and do not vary significantly across the aft bulkhead acreage.
- Through-thickness (S-T) toughness appears uniform as well, but exhibits significant data scatter for a given bulkhead location.
- Spin formed 2219-T62 aft bulkhead material exhibited rising R-curve for all orientations and locations and toughness-to-YS ratios in excess of 60%.
- High toughness values, high toughness-to-YS ratios, and rising R-curve behavior suggest excellent damage tolerance capability for the spin formed Al 2219-T62 aft bulkhead material.

F-5. The fracture toughness of the spin formed Al 2219-T62 aft bulkhead material was typical for established 2219-T62 products.

- Fracture toughness values exhibited the typical variation with orientation: L-T orientation > T-L orientation > S-T orientation.
- Fracture toughness was in-family with conventional Al 2219 Al tempers and product forms. Toughness values were comparable to Al 2219-T62 and T851 plate and are greater than for T87 plate, which is consistent with the tensile strength being lower than for T87 plate.

F-6. The SCC resistance of the spin formed 2219-T6 material varied with location in the aft bulkhead and in some locations exhibited lower resistance than previously established for 2219-T6 material.

- The rim region was most resistant to SCC and one region in the membrane was the least resistant, exhibiting failure at lower exposure stress levels than typical for Al 2219-T6. The remaining pole and membrane regions showed intermediate resistance.
- The LT orientation appeared to be significantly more resistant to SCC than the ST orientation. Residual strength after exposure was significantly higher for LT specimens than ST specimens.

F-7. The 90-day alternate immersion exposure appears to be too long for the spin formed Al 2219-T62 material since failures can occur by corrosion mechanisms (general and pitting corrosion) different than those for SCC, which can interfere with the SCC evaluation.

12.2 Observations

The following observations were identified:

O-1. The rationale for the variations in tensile properties with location in the aft bulkhead was not fully characterized. The microstructure at the through-thickness location tested (t/2) was more uniform throughout the aft bulkhead than at other locations.

O-2. Limited data was available in handbooks or open literature publications for Al 2219-T6 material for comparison with the aft bulkhead properties, consequently it was difficult to assess the aft bulkhead in the context of other commercial Al 2219-T6 products.

- Tensile data were unavailable in handbooks or open literature publications for the ST and ST45 orientations, consequently these properties could only be assessed in comparison with established values for the L and LT orientations.
- Fracture toughness data was only available in handbooks and open literature publications for Al 2219-T6 and -T8 plate. No fracture toughness data was publicly available for 2219 spin formed products.
- The SCC data for the aft bulkhead provides insight about the SCC resistance of the spin formed 2219-T62 material, but is insufficient to establish a threshold level.

O-3. Fracture toughness data suggests excellent damage tolerance in the 2219-T6 spin formed material; however, surface crack tension and da/dN testing is necessary to more fully characterize damage tolerance.

O-4. Questions arose regarding SCC test procedures, particularly the basis for exposure stress levels and test durations, which may impact direct comparison of the aft bulkhead SCC results with the very limited handbook and open literature data.

O-5. The SCC tests performed provided an initial indication of the SCC susceptibility of the spin formed 2219-T62 material; however, environmentally assisted fracture toughness (KEAC) and fatigue $(da/dN)_{SCC}$)) in the S-T orientation in a 3.5% NaCl environment is required to understand the impact of the SCC susceptibility on fracture and fatigue.

O-6. The laboratory 30-day alternate immersion accelerated test condition provides adequate screening methodology for SCC; however, longer test durations of 90 days did lead to severe general corrosion and pitting. For determining actual serviceability of the material, other stress corrosion tests should be performed in the intended service environment.

12.3 NESC Recommendations

The following NESC recommendations were identified and directed towards the MPCV Program and the NESC:

R-1. The microstructural variability of the Orion first article spin formed aft bulkhead should be determined and mechanical property testing designed to sample regions of maximum and minimum grain size in order to evaluate the effect of variable microstructures, if observed. (***F-1, F-2, O-1***)

R-2. Additional testing should be performed on first article and initial serial production aft bulkhead components to generate data to populate the material property database for Al 2219-T6 spin formed products. (***O-2***)

- Tensile testing should be continued until sufficient data is generated to demonstrate consistency in material properties and build confidence that the spin forming process is reproducible.
- Fracture testing should generate data to more substantially populate the K_{JIc} fracture toughness database.
- Stress corrosion cracking testing should be continued until sufficient data is generated to establish the SCC threshold stress level.

R-3. Perform surface crack tension fracture toughness and fatigue crack growth rate (da/dN) testing in order to fully characterize damage tolerance. ***(O-3)***

R-4. Exercise caution in using published handbook and table ratings for the SCC resistance of Al 2219-T6. Handbook and open literature publications should be reviewed in order to substantiate that the SCC test procedures and data generated are directly comparable to the MSFC-STD-3029 standard used in the SCC evaluation of the Al 2219-T62 aft bulkhead **(*O-4*)**

R-5. Perform environmentally assisted fracture toughness (KEAC) and fatigue ($(da/dN)_{SCC}$) tests in the S-T orientation in a 3.5% NaCl environment in order to understand the impact of the SCC susceptibility of the material on fracture toughness and fatigue. (***O-5***)

R-6. Perform seacoast exposure SCC testing to characterize the corrosion performance of the aft bulkhead in the natural service environment. (***O-6***)

13.0 Alternate Viewpoint

There were no alternate viewpoints identified during the course of this assessment by the NESC team or the NRB quorum.

14.0 Other Deliverables

No unique hardware, software, or data packages, outside those contained in this report, were disseminated to other parties outside this assessment.

15.0 Lessons Learned

No applicable lessons learned were identified for entry into the NASA Lessons Learned Information System (LLIS) as a result of this assessment.

16.0 Recommendations for NASA Standards and Specifications

No recommendations for NASA standards and specifications were identified as a result of this assessment.

17.0 Definition of Terms

Corrective Actions	Changes to design processes, work instructions, workmanship practices, training, inspections, tests, procedures, specifications, drawings, tools, equipment, facilities, resources, or material that result in preventing, minimizing, or limiting the potential for recurrence of a problem.
Finding	A relevant factual conclusion and/or issue that is within the assessment scope and that the team has rigorously based on data from their independent analyses, tests, inspections, and/or reviews of technical documentation.
Lessons Learned	Knowledge, understanding, or conclusive insight gained by experience that may benefit other current or future NASA programs and projects. The experience may be positive, as in a successful test or mission, or negative, as in a mishap or failure.
Observation	A noteworthy fact, issue, and/or risk, which may not be directly within the assessment scope, but could generate a separate issue or concern if not addressed. Alternatively, an observation can be a positive acknowledgement of a Center/Program/Project/Organization’s operational structure, tools, and/or support provided.
Problem	The subject of the independent technical assessment.
Proximate Cause	The event(s) that occurred, including any condition(s) that existed immediately before the undesired outcome, directly resulted in its

	occurrence and, if eliminated or modified, would have prevented the undesired outcome.
Recommendation	A proposed measurable stakeholder action directly supported by specific Finding(s) and/or Observation(s) that will correct or mitigate an identified issue or risk.
Root Cause	One of multiple factors (events, conditions, or organizational factors) that contributed to or created the proximate cause and subsequent undesired outcome and, if eliminated or modified, would have prevented the undesired outcome. Typically, multiple root causes contribute to an undesired outcome.
Supporting Narrative	A paragraph, or section, in an NESC final report that provides the detailed explanation of a succinctly worded finding or observation. For example, the logical deduction that led to a finding or observation; descriptions of assumptions, exceptions, clarifications, and boundary conditions. Avoid squeezing all of this information into a finding or observation

18.0 Acronyms List

AM	Additive Manufacturing
AMA	Analytical Mechanics Associates
AMS	Aerospace Material Specifications
APVBH	Aft Pressure Vessel Bulkhead
ASTM	American Society for Testing and Materials
BH	Bulkhead
C(T)	Compact Tension
CL	Centerline
CM	Crew Module
CPST	Cryogenic Propellant Storage and Transfer
COD	Crack-Mouth Opening Displacement
E	Modulus
EBSD	Electron Backscatter Diffraction
ESCG	Engineering and Science Contract Group
FPPW	Friction Pull Plug Welding
FPVBH	Forward Pressure Vessel Bulkhead
FSW	Friction Stir Weld
FSWSFD	Friction Stir Welded Spin Formed Dome
FTU	Design Ultimate Tensile Strength, Tension
FTY	Design Yield Strength, Tension
IML	Inner Mold Line
in	Inch
ipm	Inches Per Minute
JIC	J integral

JSC	Johnson Space Center
K	Crack Tip Stress Intensity, ksi√in
K_{IC}	Critical Crack Tip Stress Intensity
K_{IC}	Plane Strain Fracture Toughness
kips	1,000 pounds
K_{JIC}	Plane Strain Fracture Toughness
KSC	Kennedy Space Center
ksi	Kilopound per square inch, 10^3
L	Length
L	Longitudinal (direction parallel to plate rolling direction)
LALab	Light Alloy Laboratory
LaRC	Langley Research Center
LM	Lockheed Martin
LT	Long Transverse (direction perpendicular to rolling direction)
M&P	Materials and Processes
MAF	Michoud Assembly Facility
MUA	Materials Usage Agreement
MMPDS	Metallic Material Properties Development and Standardization
MPCV	Multi-Purpose Crew Vehicle
MSFC	Marshall Space Flight Center
Msi	Megapound per square inch, 10^6
NaCl	Sodium Chloride
NASA	National Aeronautics and Space Administration
NESC	NASA Engineering and Safety Center
NRB	NESC Review Board
OML	Outer Mold Line
psi	Pounds Per Square Inch
R-curve	Resistance Curve
S/N	Serial Number
SCC	Stress Corrosion Cracking
SHT	Solution Heat Treatment
SiC	Silicon Carbide
SLS	Space Launch System
SR-FSW	Self-Reacting Friction Stir Weld
SSC	Stennis Space Center
ST	Short Transverse (direction perpendicular to rolling direction)
ST45	45 Degree Through-Thickness (direction perpendicular to rolling direction)
t	Thickness
WCM	Welded Crew Module
YS	Yield Strength

19.0 References

1. M. S. Domack, E. K. Hoffman, I. S. Raju, R. S. Piascik. *Spin Forming Aluminum Alloy Crew Module (CM) Metallic Forward Pressure Vessel Bulkhead (FPVBH) – Phase I.* February 2014. NASA/TM-2014-218163; NESC-RP-12-00776.
2. Runge, Manfred. *Spinning and Flow Forming.* [trans.] David H. Pollitt. s.l.: verlag modern industrie AG, 1993. Original title: Drücken and Drückwalzen.
3. AMS-QQ-A-250/30. *Aerospace Material Specification: Aluminum Alloy 2219, Plate and Sheet.* Warrendale, PA: SAE International, 2010. AMS-QQ-A-250/30.
4. Cullen, R. M. *Spin Formed Aluminum 2219 Aft Bulkhead Pathfinder Component.* North Billerica, MA: Spincraft Engineering Technologies Group, January 15, 2014. Contract NNL13AF652P.
5. AMS 2770H. *Aerospace Materials Specification: Heat Treatment of Wrought Aluminum Alloy Parts.* Warrendale, PA: SAE International, 2006. AMS 2770H.
6. AMS 2658. *Aerospace Material Specificatin: Hardness and Conductivity Inspection of Wrought Aluminum Alloy Parts.* Warrendale, PA: SAE International, 2003. AMS 2658.
7. *ASTM E8 - Standard Test Methods for Tension Testing of Metallic Materials.* West Conshohocken, PA: ASTM International, 2011. E8.
8. *ASTM E1820 - Standard Test Method for Measurement of Fracture Toughness.* West Conshohocken, PA: American Society for Testing and Materials, 2013. E1820.
9. *ASTM G49 - Standard Practice for Preparation and Use of Direct Tension Stress-Corrosion Test Specimens.* West Conshohocken, PA: ASTM International, 2011. G49.
10. *ASTM G44 -Standard Practice for Exposure of Metals and Alloys by Alternate Immersion in Neutral 3.5 % Sodium Chloride Solution.* West Conshohocken, PA: ASTM International, 2013. G44.
11. *ASTM B117: Standard Practice for Operating Salt Spray (Fog) Apparatus1*. West Conshohocken, PA: ASTM International, 2011.
12. *MSFC-STD-3029, Rev. A: Guidelines for the Selection of Metallic Materials for Stress Corrosion Cracking Resistance in Sodium Chloride Environments.* Huntsville, AL: NASA MSFC, 2005. MSFC-3029A.
13. *ASTM G47 - Standard Test Method for Determining Susceptibility to Stress-Corrosion Cracking of 2XXX and 7XXX Aluminum Alloy Products.* West Conshohocken, PA: ASTM International, 2011. G47.
14. F. J. Humphreys, M. Hatherly. *Recrystallization and Related Annealing Phenomena, 2nd Edition.* New York, NY: Elsevier Ltd., 2004. pp. 314-325.
15. J. E. Hatch, ed. *Aluminum - Properties and Physical Metallurgy.* Metals Park, OH: American Society for Metals, 1984. pp. 134-199.
16. *Atlas of Microstructures of Industrial Alloys, Metals Handbook.* Metals Park, OH: American Society for Metals, 1972. p. 284.
17. *Metallic Materials Properties Development and Standardization (MMPDS) Handbook.* Columbus, OH: Battelle Memorial Institute, April 2013. MMPDS-08.
18. *Aluminum Standards and Data 2013.* s.l.: The Aluminum Association, Inc., November 2013.

19. Cullen, R.M. *Single Piece Orion Forward Bulkhead Demonstrator, Summary Report.* North Billerica, MA: Spincraft, April 2012. ITAR Restricted - Export Control; Lockheed Martin Purchase Order 4100270793.
20. *Orion Bulkhead Test Data.* s.l.: Westmoreland Mechanical Test Laboratory, June 14, 2012. Addendum to Single Piece Orion Forward Bulkhead Demonstrator, Summary Report.
21. McGill, P., Talton, M. *Materials and Processes Laboratory Flash Report, MPFR-14-019: CPST Spun Dome Material Characterization, July, 2014.* Huntsville, AL: NASA Marshall Space Flight Center, July 2014. MPFR-14-09.
22. Cullen, R. M. *Senior Manufacturing Engineer, Spincraft.* North Billerica, MA: s.n., May 18, 2014. Private communication.
23. *Aluminum Alloy Forgings and Rolled or Forged Rings 6.3Cu - 0.30Mn - 0.18Zr - 0.10V - 0.06Ti (2219-T6).* Aerospace Material Specification. Warrendale, PA: SAE International, July 2012. AMS 4143E.
24. Anderson, T. L. *Fracture Mechanics, 3rd Edition.* s.l.: CRC Press, Taylor and Francis Group, 2005.
25. McGill, P. *2219 Aluminum Fracture Characterization as a Function of Temper.* Huntsville, AL: NASA Marshall Space Flight Center, August, 2014. Materials and Processes Laboratory Flash Report. MPFR-14-024.
26. *Fatigue and Fracture, ASM Handbook.* Metals Park, OH: ASM International, 1996. p. 776. Vol. 19.
27. *ASTM E647 - Standard Test Method for Measurement of Fatigue Crack Growth Rates.* West Conshohocken, PA: ASTM International, 2013. E647.
28. *ASTM E2899 - Standard Test Method for Measurement of Initiation Toughness in Surface Cracks Under Tension and Bending.* West Conshohocken, PA: ASTM International, 2013. E2899.
29. *NASA-STD-5019, Fracture Control Requirements for Spaceflight Hardware.* Washington, DC: National Aeronautics and Space Administration, January 2008. NASA-STD-5019.
30. *API 579-1/ASME FFS-1 - Fitness-For-Service.* Washington, DC: American Petroleum Institute/American Society of Mechanical Engineers, June 5, 2007. API 579 2nd edition; February 2009 Errata. 579.
31. Mayer, L. W. *Alcoa Green Letter 176 - Alcoa Aluminum Alloy 2219.* New Kensington, PA: Aluminum Company of America, Applications Engineering Division, June 1957. 176.
32. Spuhler, E. H. and Brown, C. L. *Alcoa Green Letter 188 - Avoiding Stress-Corrosion Cracking in High Strength Aluminum Alloy Structures.* New Kensington, PA: Aluminum Company of America, August 1, 1962.
33. *ASTM G64 - Standard Classification of Resistance to Stress-Corrosion Cracking of Heat-Treatable Aluminum Alloys.* West Conshohocken, PA: ASTM International, 2013. G64.
34. Sprowls, D. O., Lifka, B. W., Vandenburgh, D. G., R.L. Horst, R. L., Shumaker, M. B.,. *NASA-CR-88110. Investigation of the Stress-Corrosion Cracking of High-Strength Aluminum Alloys.* New Kensington, PA: Aluminum Company of America, Alcoa Research Laboratories, Final Report for the period May 6, 1963 – October 6, 1966. Contract Number NAS 8-5340.

35. Stewart, T. J. SCC Test Methods Regarding Aluminum Alloy 2219. *Letter from T.J. Stewart to F. Oaks. Memo 3-4820-194.* Meeting at Alcoa Research Laboratories, New Kensington, PA: s.n., June 20, 1963.
36. Sprowls, D. O., Lifka, B. W., King, W., Shumaker, M. B. *Investigation of the Stress-Corrosion Cracking of High-Strength Aluminum Alloys.* New Kensington, PA.: Aluminum Company of America, Fifth Quarterly Report May 1 – July 31, 1964. NASA-CR-155461.
37. Speidel, M. O. *A Chapter Prepared for ARPA Handbook Stress Corrosion Cracking of Aluminum Alloys.* Ohio State University. 1976. 1976-00-00. Advanced Research Projects Agency (ARPA).
38. *MSFC Memorandum EH24 (94-107); Stress Corrosion Cracking Evaluation of Aluminum Lithium Alloy 2195.* Huntsville, AL: NASA, October 31, 1994.
39. *NASA MSFC Memorandum EH24 (95-97) Stress Corrosion Evaluation of Aluminum Alloy 2219-T87, 10.2-cm (4-in) Thick Plate.* Huntsville, AL: s.n., October 1995.
40. *Influence of quench and heating rates on the ageing response of an Al–Zn–Mg–(Zr) alloy.* A. Deschamps, Y. Bre´chet. 1998, Materials Science and Engineering, Vol. A251, pp. 200-207.
41. *American National Standard Alloy and Temper Designation Systems for Aluminum.* Arlington, VA: The Aluminum Association, Inc., 2013. ANSI H35.1/H35.
42. M. S. Domack, E. K. Hoffman, I. S. Raju, R. S. Piascik. *Spin Forming Aluminum Crew Module (CM) Metallic Aft Pressure Vessel Bulkhead (APVBH) – Phase II.* November 2014. NASA/TP–2015-218674, NESC-RP-1300884.
43. M. S. Domack, E. K. Hoffman. *Supplemental Report - Spin Forming Aluminum Crew Module (CM) Metallic Aft Pressure Vessel Bulkhead (APVBH)* – NASA-TM-2015-218797.

20.0 Appendix

20.1 Appendix A: Temper Designations (41)

F	As fabricated (no mechanical property limits specified).
O	Annealed - products achieving the required annealed properties after hot forming processes may be designated as O temper.
T4	Solution heat treated and naturally aged to a substantially stable condition.
T6	Solution heat treated and then artificially aged by the material producer.
T62	Solution heat treated and then artificially aged. Applies to test material heat treated from annealed or F temper or to products heat treated from any temper by the user.
T8	Solution heat treated, cold worked and then artificially aged.
T851	Solution heat treated, stress relieved by controlled stretching (permanent set 1.5% to 3% for plate, 1% to 5% for hand or ring forging and rolled ring) and then artificially aged.
T87	Solution heat treated, cold worked by a thickness reduction of approximately 7% and then artificially aged.

20.2 Appendix B: Material Certification

A material certification report was provided by Alcoa for the plate used in fabrication of the pathfinder aft bulkhead and is shown in Figure 20.2-1.

CERTIFIED INSPECTION REPORT

Alcoa Inc. DAVENPORT WORKS 4879 State Street Bettendorf, ..52722

We hereby certify that the material covered by this certificate has been inspected with, and has been found to meet the applicable requirements described therein, including any specifications forming a part of the description and that samples representative of the material met the composition limits and had the mechanical properties shown on the face of this sheet.

This test report shall not be reproduced except in full, without the written approval of the Quality Department. No alteration, addition or other change is authorized to be made to this certificate. The recording of false, fictitious, or otherwise fraudulent statements or entries on this certificate by any recipient may be punished as a felony under applicable law.

Per:

Rob Woodall, Director of Manufacturing Davenport Works

Terrance Thom, Quality Assurance Manager

Ship From:

1629397 Ship Date	0 B.L. No.	Invoice No.	Alcoa No. Item	
2013-10-08	8828477	00000	1000527171-1	DP-27171-1

P.O. No./Govt Contract No.	Customer Alcoa Item
31064 Ln#: 1	STANDEX-SPINCRAFT G041130911R01

Page 1 of 2

Ship To: STANDEX INTERNATIONAL CORP
SPINCRAFT DIV
500 IRON HORSE PARK
NORTH BILLERICA, MA 01862

Item Description
2.3 IN TK (+.015 -.100) X 141.0 IN W (+.500 - 0.000) X 141.0 IN LN (+.5 -0.0) (N) A/T 2219-F RECTANGULAR MILL FINISH, USI 3MM DEAD ZONE, SAWED 2219-F PLATE. AMS-QQ-A-250/30 IS 2010 AMS-STD-2154 REV A AS9103 D6-82479 REV F ((MARKED)) NOT INTERLEAVED MAX GROSS SKID WGT: 10000 LB QUAN TOL +/- 10 % USI CL A 3 MM CQR 0240249 REV 01 CUST REQ 13-10-04 *** W/E 13-09-28 ***

Num	Package Ticket	Lot	Weight	Quantity	UOM	Inspector Clock Numbers
1	561380	446391	4849	1	PC	37331

Notes for CQR: 0240249.1
PRODUCT PRODUCED TO THE REQUIREMENTS OF MIL-STD-2154 ALSO MEET THE REQUIREMENTS OF AMS-STD-2154 REV A. PRODUCT PRODU CED TO THE REQUIREMENTS OF AMS-STD-2154 REV A ALSO MEET TH E REQUIREMENTS OF MIL-STD-2154.
THIS MATERIAL HAS BEEN ULTRASONICALLY INSPECTED FULLY IMME RSION - TYPE I.
PRODUCT PRODUCED AND MARKED TO THE REQUIREMENTS OF AMS-QQ- A-250/30 ALSO MEETS THE REQUIREMENTS OF QQ-A-250/30A, AMEN DMENT 1. PRODUCT PRODUCED AND MARKED TO THE REQUIREMENTS O F QQ-A-250/30A, AMENDMENT 1, ALSO MEETS THE REQUIREMENTS O F AMS-QQ-A-250/30.

CQR: 0240249.1 -Specification Limits

Tmpr	Dir		UTS KSI	TYS KSI	EL4D PCT
T62	Long Transv.	Max			
		Min	54	36	6

Chemical Composition		SI	FE	CU	MN	MG	V	ZN	TI	ZR	Other Each	Other Total	Aluminum
	Max	0.20	0.30	6.8	0.40	0.02	0.15	0.10	0.10	0.25	0.05	0.15	
Alloy 2219	Min			5.8	0.20		0.05		0.02	0.10			REMAIN

S/N 31177-1

CERTIFIED INSPECTION REPORT

Alcoa Inc. DAVENPORT WORKS 4879 State Street Bettendorf, ..52722

We hereby certify that the material covered by this certificate has been inspected with, and has been found to meet the applicable requirements described therein, including any specifications forming a part of the description and that samples representative of the material met the composition limits and had the mechanical properties shown on the face of this sheet.

This test report shall not be reproduced except in full, without the written approval of the Quality Department. No alteration, addition or other change is authorized to be made to this certificate. The recording of false, fictitious, or otherwise fraudulent statements or entries on this certificate by any recipient may be punished as a felony under applicable law.

Per:

Rob Woodall, Director of Manufacturing Davenport Works

Terrance Thom, Quality Assurance Manager

Ship From:

1629397 Ship Date	0 B.L. No.	Invoice No.	Alcoa No. Item	
2013-10-08	8828477	00000	1000527171-1	DP-27171-1

P.O. No./Govt Contract No.	Customer Alcoa Item
31064 Ln#: 1	STANDEX-SPINCRAFT G041130911R01

Page 2 of 2

CQR: 0240249.1 -Specification Limits (cont.)
Lot: 446391 - Mechanical, Physical, Metallography, Quantometer Results

Tmpr	Dir	No-> Test	UTS KSI	TYS KSI	EL4D PCT
T62	Long Transv.	2	60.9	42.3	11.4
			61.6	42.4	10.7

Cast Number	Chemical - OES	SI	FE	CU	MN	MG	V	ZN	TI	ZR
H9134063	Actuals	0.06	0.14	6.3	0.25	0.01	0.09	0.02	0.04	0.13

This material was melted in the United States or a Qualifying Country [REF DFARS 225.872.1(a)]; it was manufactured in the United States

Figure 20.2-1. Material certification report for the Al 2219-F plate.

20.3 Appendix C: Fracture Toughness Data

A complete data report for each fracture toughness specimen is provided.

Mechanical Test Facilities

EM10

Fracture Toughness J_{Ic} Task Results

Version 4.3

MSFC Work Order	2014-0061	Control Mode	Stroke	Nominal Temperature (°F)	73
Work Order Task	5	Test Frame	TS-5	Nominal Pressure (psig)	0
Testing Organization	MTF	Drawing Number	S-294/ S-295	Material	AL 2219-T62
Customer Work Order	N/A	Pre-Load (LBS)	25		
Test Standard	ASTM E1820-9				

Results

EM10 Specimen ID	Other Specimen ID	Coupon #	Orientation	Jq (in*lbs/in^2)	Kjq (ksi(in)^2)	Jq Validity as J_{Ic} (See test results for specifics)
140061359	CP-406-191	M1	L-T	105.6	35.08	Jq is fully valid J_{Ic}.
140061361	CP-406-193	M1	L-T	114.80	36.58	Jq is fully valid J_{Ic}.
140061364	CP-406-196	M1	T-L	91.50	32.65	Jq is not fully valid Jlc.
140061366	CP-406-198	M1	T-L	90.60	32.49	Jq is not fully valid Jlc.
140061369	CP-406-201	M1	S-T	62.60	27.01	Jq is fully valid J_{Ic}.
140061371	CP-406-203	M1	S-T	62.20	26.92	Jq is fully valid J_{Ic}.
140061374	CP-406-206	M2	L-T	115.10	36.61	Jq is fully valid J_{Ic}.
140061376	CP-406-208	M2	L-T	112.80	36.25	Jq is fully valid J_{Ic}.
140061379	CP-406-211	M2	T-L	86.20	31.69	Jq is not fully valid Jlc.
140061381	CP-406-213	M2	T-L	91.00	32.56	Jq is fully valid J_{Ic}.
140061384	CP-406-216	M2	S-T	89.90	32.36	Jq is fully valid J_{Ic}.
140061386	CP-406-218	M2	S-T	56.00	25.55	Jq is fully valid J_{Ic}.
140061389	CP-406-221	M3	L-T	117.20	36.95	Jq is fully valid J_{Ic}.
140061391	CP-406-223	M3	L-T	125.70	38.27	Jq is fully valid J_{Ic}.
140061394	CP-406-226	M3	T-L	84.90	31.45	Jq is fully valid J_{Ic}.
140061396	CP-406-228	M3	T-L	93.10	32.93	Jq is fully valid J_{Ic}.
140061399	CP-406-231	M3	S-T	66.00	27.73	Jq is fully valid J_{Ic}.
140061401	CP-406-233	M3	S-T	90.70	32.51	Jq is fully valid J_{Ic}.
140061404	CP-406-236	M4	L-T	102.50	34.55	Jq is fully valid J_{Ic}.
140061406	CP-406-238	M4	L-T	99.10	33.97	Jq is fully valid J_{Ic}.
140061409	CP-406-241	M4	T-L	86.00	31.65	Jq is fully valid J_{Ic}.
140061411	CP-406-243	M4	T-L	93.40	32.99	Jq is not fully valid Jlc.
140061414	CP-406-246	M4	S-T	78.00	30.14	Jq is fully valid J_{Ic}.
140061416	CP-406-248	M4	S-T	50.90	24.35	Jq is fully valid J_{Ic}.
140061419	CP-406-251	M5	L-T	108.40	35.53	Jq is fully valid J_{Ic}.
140061421	CP-406-253	M5	L-T	107.30	35.35	Jq is fully valid J_{Ic}.
140061424	CP-406-256	M5	T-L	86.30	31.71	Jq is fully valid J_{Ic}.
140061426	CP-406-258	M5	T-L	85.60	31.57	Jq is fully valid J_{Ic}.
140061429	CP-406-261	M5	S-T	67.80	28.10	Jq is fully valid J_{Ic}.
140061431	CP-406-263	M5	S-T	77.40	30.03	Jq is fully valid J_{Ic}.
140061434	CP-406-266	M6	L-T	118.70	37.18	Jq is fully valid J_{Ic}.
140061436	CP-406-268	M6	L-T	114.00	36.44	Jq is fully valid J_{Ic}.
140061439	CP-406-271	M6	T-L	86.50	31.74	Jq is fully valid J_{Ic}.
140061441	CP-406-273	M6	T-L	85.00	31.47	Jq is fully valid J_{Ic}.
140061444	CP-406-276	M6	S-T	59.10	26.23	Jq is fully valid J_{Ic}.
140061446	CP-406-278	M6	S-T	57.40	25.85	Jq is not fully valid Jlc.

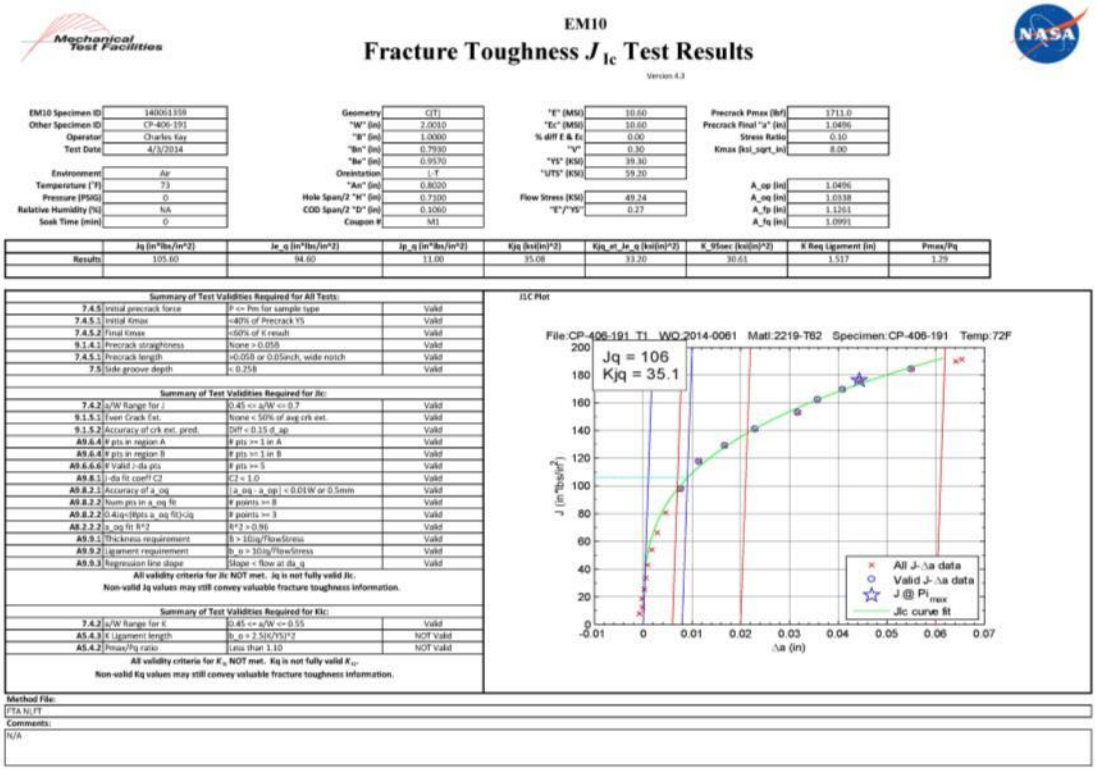

Mechanical Test Facilities

EM10

Fracture Toughness J_{Ic} Test Results

Version 4.3

EM10 Specimen ID	140061359
Other Specimen ID	CP-406-191
Operator	Charles Kay
Test Date	4/3/2014
Environment	Air
Temperature (°F)	73
Pressure (PSIG)	0
Relative Humidity (%)	NA
Soak Time (min)	0

Geometry	C(T)
"W" (in)	2.0010
"B" (in)	1.0000
"Bn" (in)	0.7930
"Be" (in)	0.9570
Oreintation	L-T
"An" (in)	0.8020
Hole Span/2 "H" (in)	0.7100
COD Span/2 "D" (in)	0.1060
Coupon #	M1

"E" (MSI)	10.60
"Ec" (MSI)	10.60
% diff E & Ec	0.00
"V"	0.30
"YS" (KSI)	39.30
"UTS" (KSI)	59.20
Flow Stress (KSI)	49.24
"E"/"YS"	0.27

Precrack Pmax (lbf)	1711.0
Precrack Final "a" (in)	1.0496
Stress Ratio	0.10
Kmax (ksi_sqrt_in)	8.00
A_op (in)	1.0496
A_oq (in)	1.0338
A_fp (in)	1.1261
A_fq (in)	1.0991

	Jq (in*lbs/in^2)	Je_q (in*lbs/in^2)	Jp_q (in*lbs/in^2)	Kjq (ksi(in)^2)	Kjq_at_Je_q (ksi(in)^2)	K_95sec (ksi(in)^2)	K Req Ligament (in)	Pmax/Pq
Results	105.60	94.60	11.00	35.08	33.20	30.61	1.517	1.29

Summary of Test Validities Required for All Tests:			
7.4.5	Initial precrack force	P <= Pm for sample type	Valid
7.4.5.1	Initial Kmax	<40% of Precrack YS	Valid
7.4.5.2	Final Kmax	<60% of K result	Valid
9.1.4.1	Precrack straightness	None > 0.05B	Valid
7.4.5.1	Precrack length	>0.05B or 0.05inch, wide notch	Valid
7.5	Side groove depth	< 0.25B	Valid
Summary of Test Validities Required for Jic:			
7.4.2	a/W Range for J	0.45 <= a/W <= 0.7	Valid
9.1.5.1	Even Crack Ext.	None < 50% of avg crk ext.	Valid
9.1.5.2	Accuracy of crk ext. pred.	Diff < 0.15 d_ap	Valid
A9.6.4	# pts in region A	# pts >= 1 in A	Valid
A9.6.4	# pts in region B	# pts >= 1 in B	Valid
A9.6.6.6	# Valid J-da pts	# pts >= 5	Valid
A9.8.1	J-da fit coeff C2	C2 < 1.0	Valid
A9.8.2.1	Accuracy of a_oq	|a_oq - a_op| < 0.01W or 0.5mm	Valid
A9.8.2.2	Num pts in a_oq fit	# points >= 8	Valid
A9.8.2.2	0.4Jq<(#pts a_oq fit)<Jq	# points >= 3	Valid
A8.2.2.2	a_oq fit R^2	R^2 > 0.96	Valid
A9.9.1	Thickness requirement	B > 10Jq/FlowStress	Valid
A9.9.2	Ligament requirement	b_o > 10Jq/FlowStress	Valid
A9.9.3	Regression line slope	Slope < flow at da_q	Valid
All validity criteria for Jic NOT met. Jq is not fully valid Jic.			
Non-valid Jq values may still convey valuable fracture toughness information.			
Summary of Test Validities Required for Kic:			
7.4.2	a/W Range for K	0.45 <= a/W <= 0.55	Valid
A5.4.3	K Ligament length	b_o > 2.5(K/YS)^2	NOT Valid
A5.4.2	Pmax/Pq ratio	Less than 1.10	NOT Valid
All validity criteria for K_{Ic} NOT met. Kq is not fully valid K_{Ic}.			
Non-valid Kq values may still convey valuable fracture toughness information.			

J1C Plot

File:CP-406-191_T1 WO:2014-0061 Matl:2219-T62 Specimen:CP-406-191 Temp:72F

Jq = 106
Kjq = 35.1

J (in*lbs/in^2)

Δa (in)

All J-Δa data
Valid J-Δa data
J @ Pi_max
Jlc curve fit

Method File:
FTA NLFT

Comments:
N/A

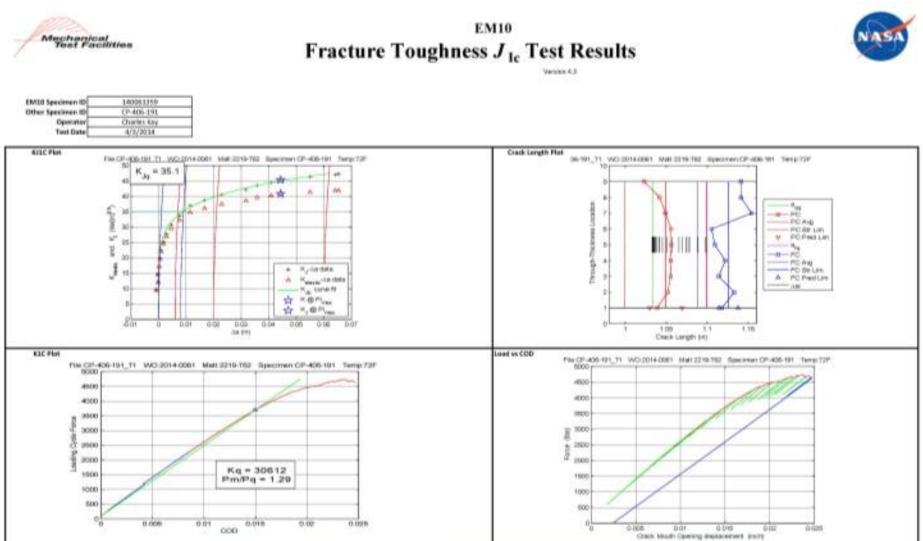

Mechanical Test Facilities

EM10

Fracture Toughness J_{Ic} Test Results

Version 4.3

EM10 Specimen ID	140061361	Geometry	C(T)	"E" (MSI)	10.60	Precrack Pmax (lbf)	1465.0
Other Specimen ID	CP-406-193	"W" (in)	2.0000	"Ec" (MSI)	10.60	Precrack Final "a" (in)	1.0466
Operator	Charles Kay	"B" (in)	1.0000	% diff E & Ec	0.00	Stress Ratio	0.10
Test Date	4/6/2014	"Bn" (in)	0.7990	"V"	0.30	Kmax (ksi_sqrt_in)	8.00
		"Be" (in)	0.9600	"YS" (KSI)	39.30		
Environment	Air	Oreintation	L-T	"UTS" (KSI)	59.20		
Temperature (°F)	73	"An" (in)	0.7990			A_op (in)	1.0466
Pressure (PSIG)	0	Hole Span/2 "H" (in)	0.7100	Flow Stress (KSI)	49.24	A_oq (in)	1.0272
Relative Humidity (%)	NA	COD Span/2 "D" (in)	0.1050	"E"/"YS"	0.27	A_fp (in)	1.1234
Soak Time (min)	0	Coupon #	M1			A_fq (in)	1.1061

	Jq (in*lbs/in^2)	Je_q (in*lbs/in^2)	Jp_q (in*lbs/in^2)	Kjq (ksi(in)^2)	Kjq_at_Je_q (ksi(in)^2)	K_95sec (ksi(in)^2)	K Req Ligament (in)	Pmax/Pq
Results	114.80	100.20	14.60	36.58	34.17	29.36	1.395	1.33

Summary of Test Validities Required for All Tests:			
7.4.5	Initial precrack force	P <= Pm for sample type	Valid
7.4.5.1	Initial Kmax	<40% of Precrack YS	Valid
7.4.5.2	Final Kmax	<60% of K result	Valid
9.1.4.1	Precrack straightness	None > 0.05B	Valid
7.4.5.1	Precrack length	>0.05B or 0.05inch, wide notch	Valid
7.5	Side groove depth	< 0.25B	Valid
Summary of Test Validities Required for Jic:			
7.4.2	a/W Range for J	0.45 <= a/W <= 0.7	Valid
9.1.5.1	Even Crack Ext.	None < 50% of avg crk ext.	Valid
9.1.5.2	Accuracy of crk ext. pred.	Diff < 0.15 d_ap	Valid
A9.6.4	# pts in region A	# pts >= 1 in A	Valid
A9.6.4	# pts in region B	# pts >= 1 in B	Valid
A9.6.6.6	# Valid J-da pts	# pts >= 5	Valid
A9.8.1	J-da fit coeff C2	C2 < 1.0	Valid
A9.8.2.1	Accuracy of a_oq	|a_oq - a_op| < 0.01W or 0.5mm	Valid
A9.8.2.2	Num pts in a_oq fit	# points >= 8	Valid
A9.8.2.2	0.4Jq<(#pts a_oq fit)<Jq	# points >= 3	Valid
A8.2.2.2	a_oq fit R^2	R^2 > 0.96	Valid
A9.9.1	Thickness requirement	B > 10Jq/FlowStress	Valid
A9.9.2	Ligament requirement	b_o > 10Jq/FlowStress	Valid
A9.9.3	Regression line slope	Slope < flow at da_q	Valid
All validity criteria for Jic NOT met. Jq is not fully valid Jic. Non-valid Jq values may still convey valuable fracture toughness information.			
Summary of Test Validities Required for Kic:			
7.4.2	a/W Range for K	0.45 <= a/W <= 0.55	Valid
A5.4.3	K Ligament length	b_o > 2.5(K/YS)^2	NOT Valid
A5.4.2	Pmax/Pq ratio	Less than 1.10	NOT Valid
All validity criteria for K_{Ic} NOT met. Kq is not fully valid K_{Ic}. Non-valid Kq values may still convey valuable fracture toughness information.			

J1C Plot

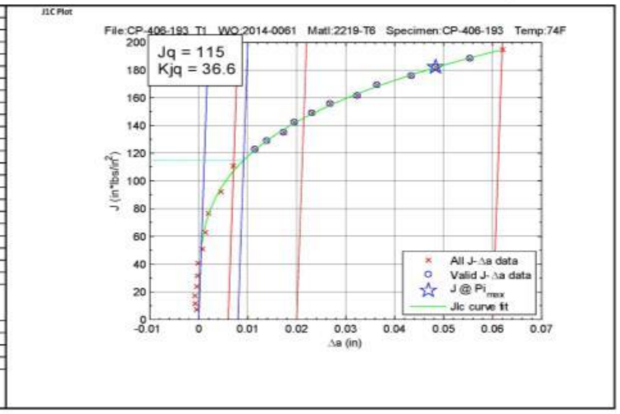

Method File:
FTA NLFT
Comments:
N/A

Mechanical Test Facilities

EM10

Fracture Toughness J_{Ic} Test Results

Version 4.3

EM10 Specimen ID	140061361
Other Specimen ID	CP-406-193
Operator	Charles Kay
Test Date	4/6/2014

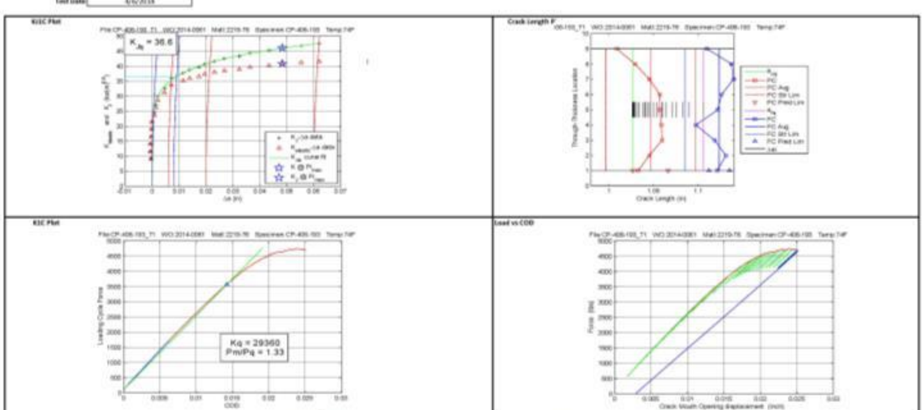

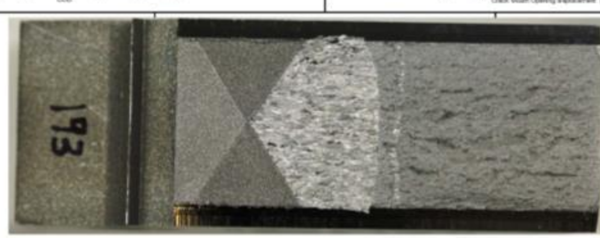

Mechanical Test Facilities

EM10
Fracture Toughness J_{Ic} Test Results

Version 4.3

EM10 Specimen ID	140061364
Other Specimen ID	CP-406-196
Operator	Charles Kay
Test Date	4/9/2014
Environment	Air
Temperature (°F)	73
Pressure (PSIG)	0
Relative Humidity (%)	NA
Soak Time (min)	0

Geometry	C(T)
"W" (in)	2.0010
"B" (in)	1.0010
"Bn" (in)	0.7950
"Be" (in)	0.9590
Oreintation	T-L
"An" (in)	0.7990
Hole Span/2 "H" (in)	0.7100
COD Span/2 "D" (in)	0.1050
Coupon #	M1

"E" (MSI)	10.60
"Ec" (MSI)	11.08
% diff E & Ec	4.50
"V"	0.30
"YS" (KSI)	38.70
"UTS" (KSI)	58.60
Flow Stress (KSI)	48.63
"E"/"YS"	0.27

Precrack Pmax (lbf)	1508.0
Precrack Final "a" (in)	1.0321
Stress Ratio	0.10
Kmax (ksi_sqrt_in)	8.00
A_op (in)	1.0321
A_oq (in)	1.0328
A_fp (in)	1.1352
A_fq (in)	1.1191

	Jq (in*lbs/in^2)	Je_q (in*lbs/in^2)	Jp_q (in*lbs/in^2)	Kjq (ksi(in)^2)	Kjq_at_Je_q (ksi(in)^2)	K_95sec (ksi(in)^2)	K Req Ligament (in)	Pmax/Pq
Results	91.50	83.00	8.50	32.65	31.10	28.09	1.317	1.17

Summary of Test Validities Required for All Tests:			
7.4.5	Initial precrack force	P <= Pm for sample type	Valid
7.4.5.1	Initial Kmax	<40% of Precrack YS	Valid
7.4.5.2	Final Kmax	<60% of K result	Valid
9.1.4.1	Precrack straightness	None > 0.05B	Valid
7.4.5.1	Precrack length	>0.05B or 0.05inch, wide notch	Valid
7.5	Side groove depth	< 0.25B	Valid
Summary of Test Validities Required for Jic:			
7.4.2	a/W Range for J	0.45 <= a/W <= 0.7	Valid
9.1.5.1	Even Crack Ext.	None < 50% of avg crk ext.	Valid
9.1.5.2	Accuracy of crk ext. pred.	Diff < 0.15 d_ap	NOT Valid
A9.6.4	# pts in region A	# pts >= 1 in A	Valid
A9.6.4	# pts in region B	# pts >= 1 in B	Valid
A9.6.6.6	# Valid J-da pts	# pts >= 5	Valid
A9.8.1	J-da fit coeff C2	C2 < 1.0	Valid
A9.8.2.1	Accuracy of a_oq	|a_oq - a_op| < 0.01W or 0.5mm	Valid
A9.8.2.2	Num pts in a_oq fit	# points >= 8	Valid
A9.8.2.2	0.4Jq<(#pts a_oq fit)<Jq	# points >= 3	Valid
A8.2.2.2	a_oq fit R^2	R^2 > 0.96	Valid
A9.9.1	Thickness requirement	B > 10Jq/FlowStress	Valid
A9.9.2	Ligament requirement	b_o > 10Jq/FlowStress	Valid
A9.9.3	Regression line slope	Slope < flow at da_q	Valid
All validity criteria for Jic NOT met. Jq is not fully valid Jic. Non-valid Jq values may still convey valuable fracture toughness information.			
Summary of Test Validities Required for Kic:			
7.4.2	a/W Range for K	0.45 <= a/W <= 0.55	Valid
A5.4.3	K Ligament length	b_o > 2.5(K/YS)^2	NOT Valid
A5.4.2	Pmax/Pq ratio	Less than 1.10	NOT Valid
All validity criteria for K_{Ic} NOT met. Kq is not fully valid K_{Ic}. Non-valid Kq values may still convey valuable fracture toughness information.			

J1C Plot

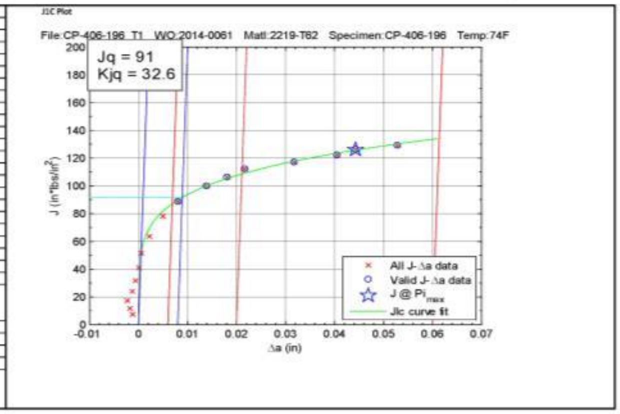

Method File:
FTA NLFT

Comments:
N/A

Mechanical Test Facilities

EM10
Fracture Toughness J_{Ic} Test Results

Version 4.3

EM10 Specimen ID	140061364
Other Specimen ID	CP-406-196
Operator	Charles Kay
Test Date	4/9/2014

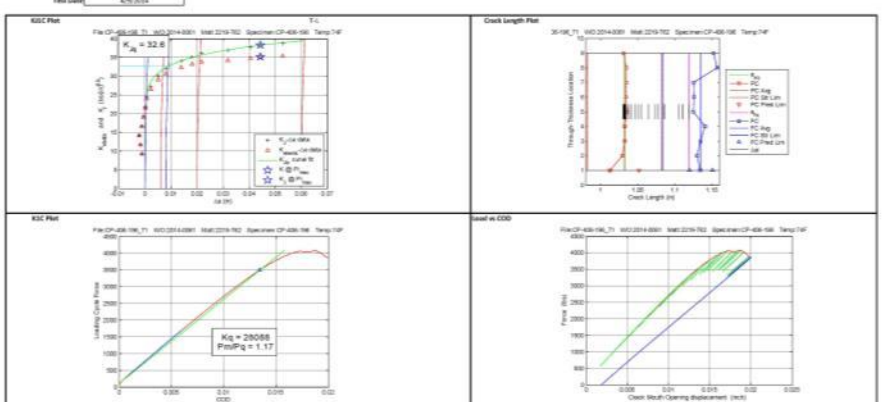

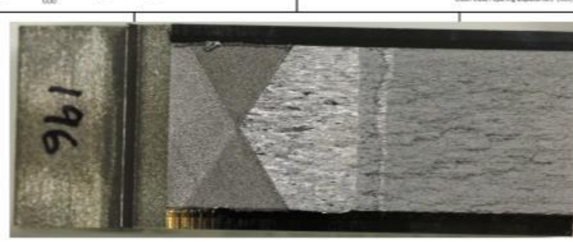

Mechanical Test Facilities

EM10

Fracture Toughness J_{Ic} Test Results

Version 4.3

EM10 Specimen ID	140061366	Geometry	C(T)	"E" (MSI)	10.60	Precrack Pmax (lbf)	1501.0
Other Specimen ID	CP-406-198	"W" (in)	2.0000	"Ec" (MSI)	11.08	Precrack Final "a" (in)	1.0301
Operator	Charles Kay	"B" (in)	0.9990	% diff E & Ec	4.60	Stress Ratio	0.10
Test Date	4/9/2014	"Bn" (in)	0.7970	"V"	0.30	Kmax (ksi_sqrt_in)	8.00
		"Be" (in)	0.9580	"YS" (KSI)	38.70		
Environment	Air	Oreintation	T-L	"UTS" (KSI)	58.60		
Temperature (°F)	73	"An" (in)	0.8000			A_op (in)	1.0301
Pressure (PSIG)	0	Hole Span/2 "H" (in)	0.7100	Flow Stress (KSI)	48.63	A_oq (in)	1.0299
Relative Humidity (%)	NA	COD Span/2 "D" (in)	0.1050	"E"/"YS"	0.27	A_fp (in)	1.1345
Soak Time (min)	0	Coupon #	M1			A_fq (in)	1.1169

	Jq (in*lbs/in^2)	Je_q (in*lbs/in^2)	Jp_q (in*lbs/in^2)	Kjq (ksi(in)^2)	Kjq_at_Je_q (ksi(in)^2)	K_95sec (ksi(in)^2)	K Req Ligament (in)	Pmax/Pq
Results	90.60	83.00	7.60	32.49	31.10	28.31	1.338	1.22

Summary of Test Validities Required for All Tests:			
7.4.5	Initial precrack force	P <= Pm for sample type	Valid
7.4.5.1	Initial Kmax	<40% of Precrack YS	Valid
7.4.5.2	Final Kmax	<60% of K result	Valid
9.1.4.1	Precrack straightness	None > 0.05B	Valid
7.4.5.1	Precrack length	>0.05B or 0.05inch, wide notch	Valid
7.5	Side groove depth	< 0.25B	Valid
Summary of Test Validities Required for Jic:			
7.4.2	a/W Range for J	0.45 <= a/W <= 0.7	Valid
9.1.5.1	Even Crack Ext.	None < 50% of avg crk ext.	Valid
9.1.5.2	Accuracy of crk ext. pred.	Diff < 0.15 d_ap	NOT Valid
A9.6.4	# pts in region A	# pts >= 1 in A	Valid
A9.6.4	# pts in region B	# pts >= 1 in B	Valid
A9.6.6.6	# Valid J-da pts	# pts >= 5	Valid
A9.8.1	J-da fit coeff C2	C2 < 1.0	Valid
A9.8.2.1	Accuracy of a_oq	|a_oq - a_op| < 0.01W or 0.5mm	Valid
A9.8.2.2	Num pts in a_oq fit	# points >= 8	Valid
A9.8.2.2	0.4Jq<(#pts a_oq fit)<Jq	# points >= 3	Valid
A8.2.2.2	a_oq fit R^2	R^2 > 0.96	Valid
A9.9.1	Thickness requirement	B > 10Jq/FlowStress	Valid
A9.9.2	Ligament requirement	b_o > 10Jq/FlowStress	Valid
A9.9.3	Regression line slope	Slope < flow at da_q	Valid
All validity criteria for Jic NOT met. Jq is not fully valid Jic. Non-valid Jq values may still convey valuable fracture toughness information.			
Summary of Test Validities Required for Kic:			
7.4.2	a/W Range for K	0.45 <= a/W <= 0.55	Valid
A5.4.3	K Ligament length	b_o > 2.5(K/YS)^2	NOT Valid
A5.4.2	Pmax/Pq ratio	Less than 1.10	NOT Valid
All validity criteria for K_{Ic} NOT met. Kq is not fully valid K_{Ic}. Non-valid Kq values may still convey valuable fracture toughness information.			

J1C Plot

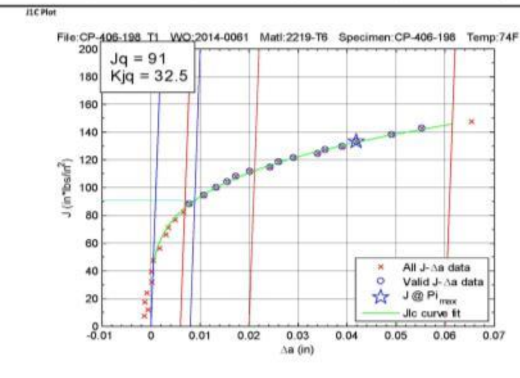

Method File:
FTA NLFT

Comments:
N/A

Mechanical Test Facilities

EM10

Fracture Toughness J_{Ic} Test Results

Version 4.3

EM10 Specimen ID	140061366
Other Specimen ID	CP-406-198
Operator	Charles Kay
Test Date	4/9/2014

KJ1C Plot

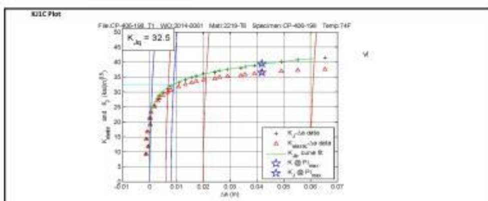

Crack Length Plot

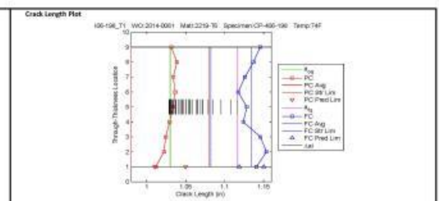

K1C Plot

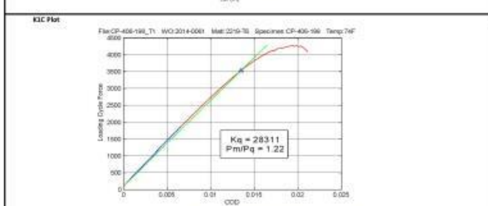

Load vs COD

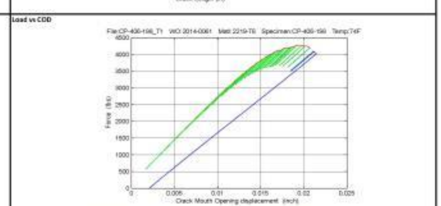

Mechanical Test Facilities

EM10

Fracture Toughness J_{Ic} Test Results

Version 4.3

EM10 Specimen ID	140061369	Geometry	C(T)	"E" (MSI)	10.60	Precrack Pmax (lbf)	525.0
Other Specimen ID	CP-406-201	"W" (in)	1.0000	"Ec" (MSI)	10.60	Precrack Final "a" (in)	0.5334
Operator	Charles Kay	"B" (in)	0.4930	% diff E & Ec	0.00	Stress Ratio	0.10
Test Date	4/11/2014	"Bn" (in)	0.4060	"V"	0.30	Kmax (ksi_sqrt_in)	8.00
		"Be" (in)	0.4780	"YS" (KSI)	37.50		
Environment	Air	Oreintation	S-T	"UTS" (KSI)	60.20		
Temperature (°F)	73	"An" (in)	0.4020			A_op (in)	0.5334
Pressure (PSIG)	0	Hole Span/2 "H" (in)	0.3550	Flow Stress (KSI)	48.87	A_oq (in)	0.5262
Relative Humidity (%)	NA	COD Span/2 "D" (in)	0.0990	"E"/"YS"	0.28	A_fp (in)	0.6062
Soak Time (min)	0	Coupon #	M1			A_fq (in)	0.5951

	Jq (in*lbs/in^2)	Je_q (in*lbs/in^2)	Jp_q (in*lbs/in^2)	Kjq (ksi(in)^2)	Kjq_at_Je_q (ksi(in)^2)	K_95sec (ksi(in)^2)	K Req Ligament (in)	Pmax/Pq
Results	62.60	53.80	8.90	27.01	25.03	21.87	0.850	1.21

Summary of Test Validities Required for All Tests:			
7.4.5	Initial precrack force	P <= Pm for sample type	Valid
7.4.5.1	Initial Kmax	<40% of Precrack YS	Valid
7.4.5.2	Final Kmax	<60% of K result	Valid
9.1.4.1	Precrack straightness	None > 0.05B	Valid
7.4.5.1	Precrack length	>0.05B or 0.05inch, wide notch	Valid
7.5	Side groove depth	< 0.25B	Valid
Summary of Test Validities Required for Jic:			
7.4.2	a/W Range for J	0.45 <= a/W <= 0.7	Valid
9.1.5.1	Even Crack Ext.	None < 50% of avg crk ext.	Valid
9.1.5.2	Accuracy of crk ext. pred.	Diff < 0.15 d_ap	
A9.6.4	# pts in region A	# pts >= 1 in A	Valid
A9.6.4	# pts in region B	# pts >= 1 in B	Valid
A9.6.6.6	# Valid J-da pts	# pts >= 5	Valid
A9.8.1	J-da fit coeff C2	C2 < 1.0	Valid
A9.8.2.1	Accuracy of a_oq	|a_oq - a_op| < 0.01W or 0.5mm	Valid
A9.8.2.2	Num pts in a_oq fit	# points >= 8	Valid
A9.8.2.2	0.4Jq<(#pts a_oq fit)<Jq	# points >= 3	Valid
A8.2.2.2	a_oq fit R^2	R^2 > 0.96	Valid
A9.9.1	Thickness requirement	B > 10Jq/FlowStress	Valid
A9.9.2	Ligament requirement	b_o > 10Jq/FlowStress	Valid
A9.9.3	Regression line slope	Slope < flow at da_q	Valid
All validity criteria for Jic NOT met. Jq is not fully valid Jic. Non-valid Jq values may still convey valuable fracture toughness information.			
Summary of Test Validities Required for Kic:			
7.4.2	a/W Range for K	0.45 <= a/W <= 0.55	Valid
A5.4.3	K Ligament length	b_o > 2.5(K/YS)^2	NOT Valid
A5.4.2	Pmax/Pq ratio	Less than 1.10	NOT Valid
All validity criteria for K_{Ic} NOT met. Kq is not fully valid K_{Ic}. Non-valid Kq values may still convey valuable fracture toughness information.			

J1C Plot

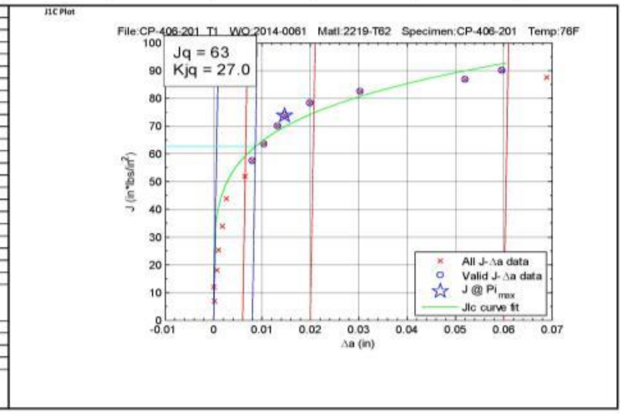

Method File:

FTA NLFT

Comments:

N/A

Mechanical Test Facilities

EM10

Fracture Toughness J_{Ic} Test Results

Version 4.3

EM10 Specimen ID	140061169
Other Specimen ID	CP-406-201
Operator	Charles Kay
Test Date	4/11/2014

KJIC Plot

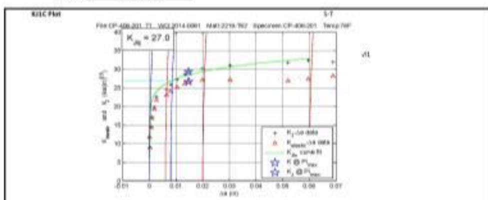

Crack Length Plot

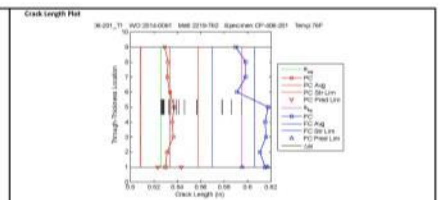

K1C Plot

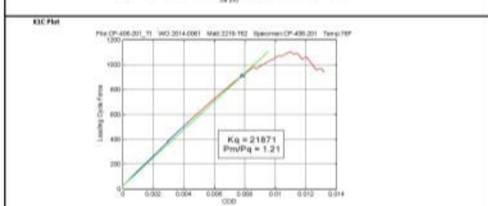

Load vs COD

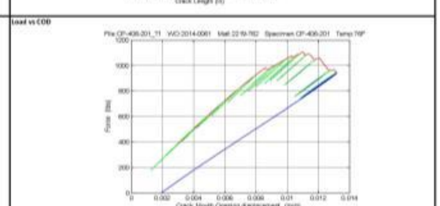

Mechanical Test Facilities

EM10

Fracture Toughness J_{Ic} Test Results

Version 4.3

EM10 Specimen ID	140061371	Geometry	C(T)	"E" (MSI)	10.60	Precrack Pmax (lbf)	525.0
Other Specimen ID	CP-406-203	"W" (in)	1.0000	"Ec" (MSI)	11.19	Precrack Final "a" (in)	0.5370
Operator	Charles Kay	"B" (in)	0.5010	% diff E & Ec	5.60	Stress Ratio	0.10
Test Date	4/11/2014	"Bn" (in)	0.3970	"V"	0.30	Kmax (ksi_sqrt_in)	8.00
		"Be" (in)	0.4780	"YS" (KSI)	37.50		
Environment	Air	Oreintation	S-T	"UTS" (KSI)	60.20		
Temperature (°F)	73	"An" (in)	0.4010			A_op (in)	0.5370
Pressure (PSIG)	0	Hole Span/2 "H" (in)	0.3550	Flow Stress (KSI)	78.87	A_oq (in)	0.5369
Relative Humidity (%)	NA	COD Span/2 "D" (in)	0.0990	"E"/"YS"	0.28	A_fp (in)	0.6196
Soak Time (min)	0	Coupon #	M1			A_fq (in)	0.6144

	Jq (in*lbs/in^2)	Je_q (in*lbs/in^2)	Jp_q (in*lbs/in^2)	Kjq (ksi(in)^2)	Kjq_at_Je_q (ksi(in)^2)	K_95sec (ksi(in)^2)	K Req Ligament (in)	Pmax/Pq
Results	62.20	55.00	7.20	26.92	25.32	21.11	0.792	1.41

Summary of Test Validities Required for All Tests:			
7.4.5	Initial precrack force	P <= Pm for sample type	Valid
7.4.5.1	Initial Kmax	<40% of Precrack YS	Valid
7.4.5.2	Final Kmax	<60% of K result	Valid
9.1.4.1	Precrack straightness	None > 0.05B	Valid
7.4.5.1	Precrack length	>0.05B or 0.05inch, wide notch	Valid
7.5	Side groove depth	< 0.25B	Valid

Summary of Test Validities Required for Jic:			
7.4.2	a/W Range for J	0.45 <= a/W <= 0.7	Valid
9.1.5.1	Even Crack Ext.	None < 50% of avg crk ext.	Valid
9.1.5.2	Accuracy of crk ext. pred.	Diff < 0.15 d_ap	Valid
A9.6.4	# pts in region A	# pts >= 1 in A	Valid
A9.6.4	# pts in region B	# pts >= 1 in B	Valid
A9.6.6.6	# Valid J-da pts	# pts >= 5	Valid
A9.8.1	J-da fit coeff C2	C2 < 1.0	Valid
A9.8.2.1	Accuracy of a_oq	|a_oq - a_op| < 0.01W or 0.5mm	Valid
A9.8.2.2	Num pts in a_oq fit	# points >= 8	Valid
A9.8.2.2	0.4Jq<(#pts a_oq fit)<Jq	# points >= 3	Valid
A8.2.2.2	a_oq fit R^2	R^2 > 0.96	Valid
A9.9.1	Thickness requirement	B > 10Jq/FlowStress	Valid
A9.9.2	Ligament requirement	b_o > 10Jq/FlowStress	Valid
A9.9.3	Regression line slope	Slope < flow at da_q	Valid

All validity criteria for Jic NOT met. Jq is not fully valid Jic.
Non-valid Jq values may still convey valuable fracture toughness information.

Summary of Test Validities Required for Kic:			
7.4.2	a/W Range for K	0.45 <= a/W <= 0.55	Valid
A5.4.3	K Ligament length	b_o > 2.5(K/YS)^2	NOT Valid
A5.4.2	Pmax/Pq ratio	Less than 1.10	NOT Valid

All validity criteria for K_{Ic} NOT met. Kq is not fully valid K_{Ic}.
Non-valid Kq values may still convey valuable fracture toughness information.

J1C Plot

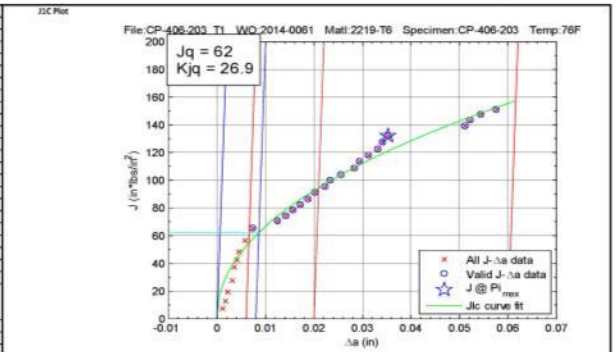

Method File:
FTA NLFT
Comments:
N/A

Mechanical Test Facilities

EM10

Fracture Toughness J_{Ic} Test Results

Version 4.3

EM10 Specimen ID	140061371
Other Specimen ID	CP-406-203
Operator	Charles Kay
Test Date	4/11/2014

KJ1C Plot

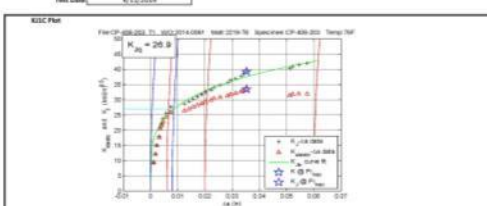

Crack Length Plot

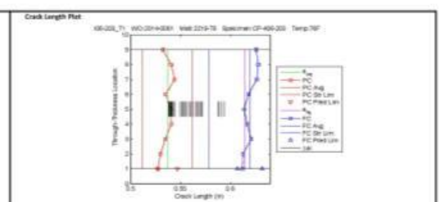

K1C Plot

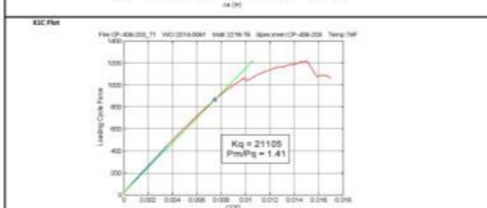

Load vs COD

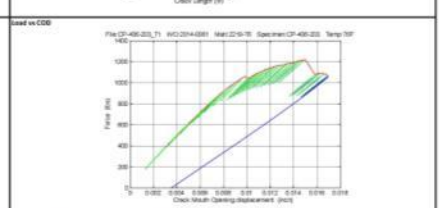

Mechanical Test Facilities

EM10

Fracture Toughness J_{Ic} Test Results

Version 4.3

EM10 Specimen ID	140061374	Geometry	C(T)	"E" (MSI)	10.60	Precrack Pmax (lbf)	1508.0
Other Specimen ID	CP-406-206	"W" (in)	1.9990	"Ec" (MSI)	11.10	Precrack Final "a" (in)	1.0426
Operator	Charles Kay	"B" (in)	1.0000	% diff E & Ec	4.70	Stress Ratio	0.10
Test Date	4/9/2014	"Bn" (in)	0.7980	"V"	0.30	Kmax (ksi_sqrt_in)	8.00
		"Be" (in)	0.9590	"YS" (KSI)	38.00		
Environment	Air	Oreintation	L-T	"UTS" (KSI)	57.00		
Temperature (°F)	73	"An" (in)	0.7990			A_op (in)	1.0426
Pressure (PSIG)	0	Hole Span/2 "H" (in)	0.7100	Flow Stress (KSI)	47.53	A_oq (in)	1.0425
Relative Humidity (%)	NA	COD Span/2 "D" (in)	0.1050	"E"/"YS"	0.28	A_fp (in)	1.1231
Soak Time (min)	0	Coupon #	M2			A_fq (in)	1.1156

	Jq (in*lbs/in^2)	Je_q (in*lbs/in^2)	Jp_q (in*lbs/in^2)	Kjq (ksi(in)^2)	Kjq_at_Je_q (ksi(in)^2)	K_95sec (ksi(in)^2)	K Req Ligament (in)	Pmax/Pq
Results	115.10	102.70	12.40	36.61	34.59	29.49	1.505	1.28

Summary of Test Validities Required for All Tests:			
7.4.5	Initial precrack force	P <= Pm for sample type	Valid
7.4.5.1	Initial Kmax	<40% of Precrack YS	Valid
7.4.5.2	Final Kmax	<60% of K result	Valid
9.1.4.1	Precrack straightness	None > 0.05B	Valid
7.4.5.1	Precrack length	>0.05B or 0.05inch, wide notch	Valid
7.5	Side groove depth	< 0.25B	Valid
Summary of Test Validities Required for Jic:			
7.4.2	a/W Range for J	0.45 <= a/W <= 0.7	Valid
9.1.5.1	Even Crack Ext.	None < 50% of avg crk ext.	Valid
9.1.5.2	Accuracy of crk ext. pred.	Diff < 0.15 d_ap	Valid
A9.6.4	# pts in region A	# pts >= 1 in A	Valid
A9.6.4	# pts in region B	# pts >= 1 in B	Valid
A9.6.6.6	# Valid J-da pts	# pts >= 5	Valid
A9.8.1	J-da fit coeff C2	C2 < 1.0	Valid
A9.8.2.1	Accuracy of a_oq	|a_oq - a_op| < 0.01W or 0.5mm	Valid
A9.8.2.2	Num pts in a_oq fit	# points >= 8	Valid
A9.8.2.2	0.4Jq<(#pts a_oq fit)<Jq	# points >= 3	Valid
A8.2.2.2	a_oq fit R^2	R^2 > 0.96	Valid
A9.9.1	Thickness requirement	B > 10Jq/FlowStress	Valid
A9.9.2	Ligament requirement	b_o > 10Jq/FlowStress	Valid
A9.9.3	Regression line slope	Slope < flow at da_q	Valid
All validity criteria for Jic NOT met. Jq is not fully valid Jic. Non-valid Jq values may still convey valuable fracture toughness information.			
Summary of Test Validities Required for Kic:			
7.4.2	a/W Range for K	0.45 <= a/W <= 0.55	Valid
A5.4.3	K Ligament length	b_o > 2.5(K/YS)^2	NOT Valid
A5.4.2	Pmax/Pq ratio	Less than 1.10	NOT Valid
All validity criteria for K_{Ic} NOT met. Kq is not fully valid K_{Ic}. Non-valid Kq values may still convey valuable fracture toughness information.			

J1C Plot

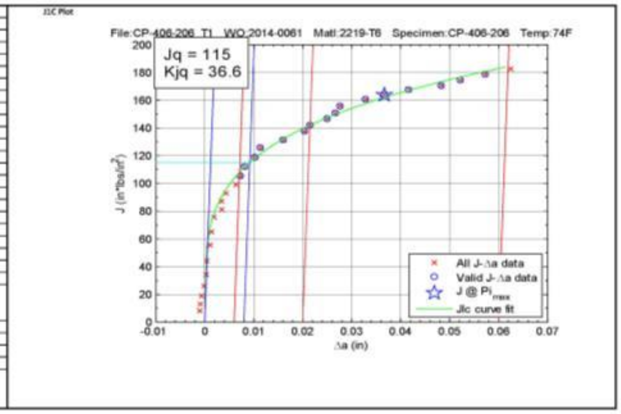

Method File:

FTA NLFT

Comments:

N/A

Mechanical Test Facilities

EM10

Fracture Toughness J_{Ic} Test Results

Version 4.3

EM10 Specimen ID	140061374
Other Specimen ID	CP-406-206
Operator	Charles Kay
Test Date	4/9/2014

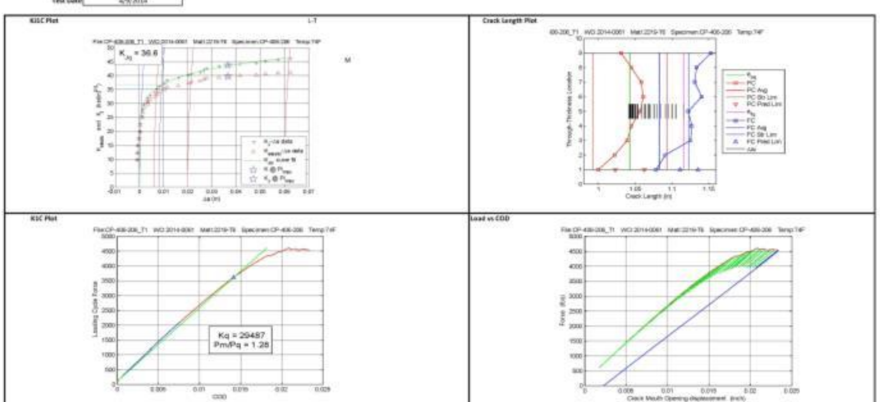

Mechanical Test Facilities

EM10

Fracture Toughness J_{Ic} Test Results

Version 4.3

EM10 Specimen ID	140061376	Geometry	C(T)	"E" (MSI)	10.60	Precrack Pmax (lbf)	1500.0
Other Specimen ID	CP-406-208	"W" (in)	2.0000	"Ec" (MSI)	10.60	Precrack Final "a" (in)	1.0134
Operator	Charles Kay	"B" (in)	0.9980	% diff E & Ec	0.00	Stress Ratio	0.10
Test Date	4/9/2014	"Bn" (in)	0.7960	"V"	0.30	Kmax (ksi_sqrt_in)	8.00
		"Be" (in)	0.9570	"YS" (KSI)	38.00		
Environment	Air	Oreintation	L-T	"UTS" (KSI)	57.00		
Temperature (°F)	73	"An" (in)	0.8000			A_op (in)	1.0134
Pressure (PSIG)	0	Hole Span/2 "H" (in)	0.7100	Flow Stress (KSI)	47.53	A_oq (in)	0.9937
Relative Humidity (%)	NA	COD Span/2 "D" (in)	0.1050	"E"/"YS"	0.28	A_fp (in)	1.0827
Soak Time (min)	0	Coupon #	M2			A_fq (in)	1.0538

	Jq (in*lbs/in^2)	Je_q (in*lbs/in^2)	Jp_q (in*lbs/in^2)	Kjq (ksi(in)^2)	Kjq_at_Je_q (ksi(in)^2)	K_95sec (ksi(in)^2)	K Req Ligament (in)	Pmax/Pq
Results	112.80	99.30	13.50	36.25	34.01	30.46	1.607	1.28

Summary of Test Validities Required for All Tests:			
7.4.5	Initial precrack force	P <= Pm for sample type	Valid
7.4.5.1	Initial Kmax	<40% of Precrack YS	Valid
7.4.5.2	Final Kmax	<60% of K result	Valid
9.1.4.1	Precrack straightness	None > 0.05B	Valid
7.4.5.1	Precrack length	>0.05B or 0.05inch, wide notch	Valid
7.5	Side groove depth	< 0.25B	Valid
Summary of Test Validities Required for Jic:			
7.4.2	a/W Range for J	0.45 <= a/W <= 0.7	Valid
9.1.5.1	Even Crack Ext.	None < 50% of avg crk ext.	Valid
9.1.5.2	Accuracy of crk ext. pred.	Diff < 0.15 d_ap	Valid
A9.6.4	# pts in region A	# pts >= 1 in A	Valid
A9.6.4	# pts in region B	# pts >= 1 in B	Valid
A9.6.6.6	# Valid J-da pts	# pts >= 5	Valid
A9.8.1	J-da fit coeff C2	C2 < 1.0	Valid
A9.8.2.1	Accuracy of a_oq	|a_oq - a_op| < 0.01W or 0.5mm	Valid
A9.8.2.2	Num pts in a_oq fit	# points >= 8	Valid
A9.8.2.2	0.4Jq<(#pts a_oq fit)<Jq	# points >= 3	Valid
A8.2.2.2	a_oq fit R^2	R^2 > 0.96	Valid
A9.9.1	Thickness requirement	B > 10Jq/FlowStress	Valid
A9.9.2	Ligament requirement	b_o > 10Jq/FlowStress	Valid
A9.9.3	Regression line slope	Slope < flow at da_q	Valid
All validity criteria for Jic NOT met. Jq is not fully valid Jic. Non-valid Jq values may still convey valuable fracture toughness information.			
Summary of Test Validities Required for Kic:			
7.4.2	a/W Range for K	0.45 <= a/W <= 0.55	Valid
A5.4.3	K Ligament length	b_o > 2.5(K/YS)^2	NOT Valid
A5.4.2	Pmax/Pq ratio	Less than 1.10	NOT Valid
All validity criteria for K_{Ic} NOT met. Kq is not fully valid K_{Ic}. Non-valid Kq values may still convey valuable fracture toughness information.			

J1C Plot

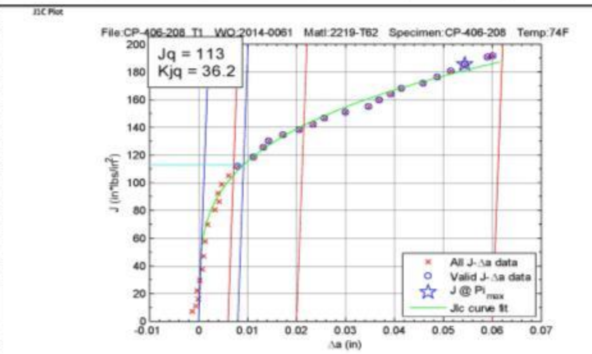

Method File:
FTA NLFT

Comments:
N/A

Mechanical Test Facilities

EM10

Fracture Toughness J_{Ic} Test Results

Version 4.3

EM10 Specimen ID	140061376
Other Specimen ID	CP-406-208
Operator	Charles Kay
Test Date	4/9/2014

KJIC Plot

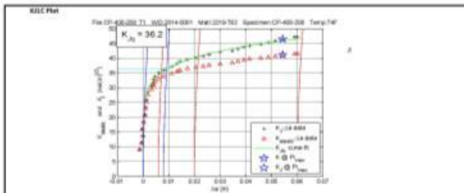

Crack Length Plot

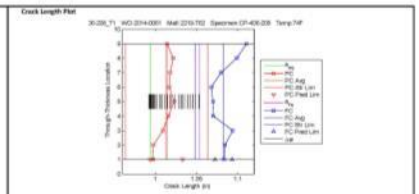

KIC Plot

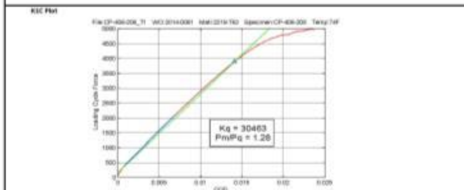

Load vs COD

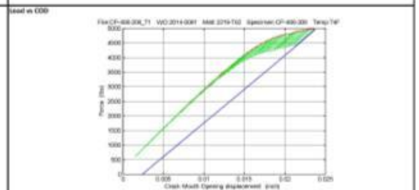

Mechanical Test Facilities

EM10

Fracture Toughness J_{Ic} Test Results

Version 4.3

EM10 Specimen ID	140061379
Other Specimen ID	CP-406-211
Operator	Charles Kay
Test Date	4/9/2014
Environment	Air
Temperature (°F)	73
Pressure (PSIG)	0
Relative Humidity (%)	NA
Soak Time (min)	0

Geometry	C(T)
"W" (in)	2.0000
"B" (in)	0.9980
"Bn" (in)	0.7980
"Be" (in)	0.9580
Oreintation	T-L
"An" (in)	0.7990
Hole Span/2 "H" (in)	0.7100
COD Span/2 "D" (in)	0.1050
Coupon #	M2

"E" (MSI)	10.60
"Ec" (MSI)	11.13
% diff E & Ec	5.00
"V"	0.30
"YS" (KSI)	37.80
"UTS" (KSI)	57.30
Flow Stress (KSI)	47.40
"E"/"YS"	0.28

Precrack Pmax (lbf)	1510.0
Precrack Final "a" (in)	1.0416
Stress Ratio	0.10
Kmax (ksi_sqrt_in)	8.00
A_op (in)	1.0416
A_oq (in)	1.0460
A_fp (in)	1.1247
A_fq (in)	1.1131

	Jq (in*lbs/in^2)	Je_q (in*lbs/in^2)	Jp_q (in*lbs/in^2)	Kjq (ksi(in)^2)	Kjq_at_Je_q (ksi(in)^2)	K_95sec (ksi(in)^2)	K Req Ligament (in)	Pmax/Pq
Results	86.20	78.60	7.60	31.69	30.26	27.61	1.334	1.14

Summary of Test Validities Required for All Tests:			
7.4.5	Initial precrack force	P <= Pm for sample type	Valid
7.4.5.1	Initial Kmax	<40% of Precrack YS	Valid
7.4.5.2	Final Kmax	<60% of K result	Valid
9.1.4.1	Precrack straightness	None > 0.05B	Valid
7.4.5.1	Precrack length	>0.05B or 0.05inch, wide notch	Valid
7.5	Side groove depth	< 0.25B	Valid
Summary of Test Validities Required for Jic:			
7.4.2	a/W Range for J	0.45 <= a/W <= 0.7	Valid
9.1.5.1	Even Crack Ext.	None < 50% of avg crk ext.	Valid
9.1.5.2	Accuracy of crk ext. pred.	Diff < 0.15 d_ap	NOT Valid
A9.6.4	# pts in region A	# pts >= 1 in A	Valid
A9.6.4	# pts in region B	# pts >= 1 in B	Valid
A9.6.6.6	# Valid J-da pts	# pts >= 5	Valid
A9.8.1	J-da fit coeff C2	C2 < 1.0	Valid
A9.8.2.1	Accuracy of a_oq	|a_oq - a_op| < 0.01W or 0.5mm	Valid
A9.8.2.2	Num pts in a_oq fit	# points >= 8	Valid
A9.8.2.2	0.4Jq<(#pts a_oq fit)<Jq	# points >= 3	Valid
A8.2.2.2	a_oq fit R^2	R^2 > 0.96	Valid
A9.9.1	Thickness requirement	B > 10Jq/FlowStress	Valid
A9.9.2	Ligament requirement	b_o > 10Jq/FlowStress	Valid
A9.9.3	Regression line slope	Slope < flow at da_q	Valid
All validity criteria for Jic NOT met. Jq is not fully valid Jic. Non-valid Jq values may still convey valuable fracture toughness information.			
Summary of Test Validities Required for KIc:			
7.4.2	a/W Range for K	0.45 <= a/W <= 0.55	Valid
A5.4.3	K Ligament length	b_o > 2.5(K/YS)^2	NOT Valid
A5.4.2	Pmax/Pq ratio	Less than 1.10	NOT Valid
All validity criteria for K_{Ic} NOT met. Kq is not fully valid K_{Ic}. Non-valid Kq values may still convey valuable fracture toughness information.			

J1C Plot

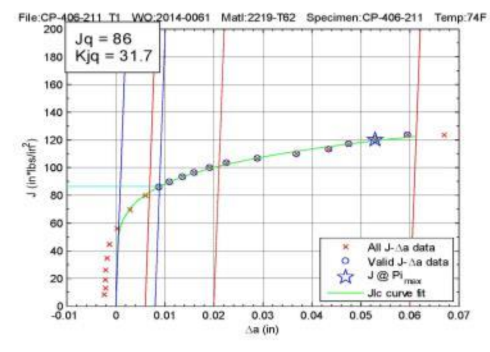

Method File:
FTA NLFT
Comments:
N/A

Mechanical Test Facilities

EM10

Fracture Toughness J_{Ic} Test Results

Version 4.3

EM10 Specimen ID	140061379
Other Specimen ID	CP-406-211
Operator	Charles Kay
Test Date	4/9/2014

KJIC Plot

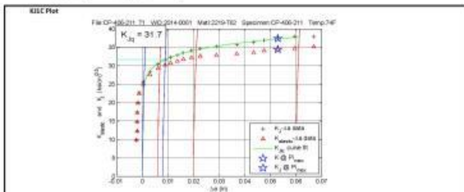

Crack Length Plot

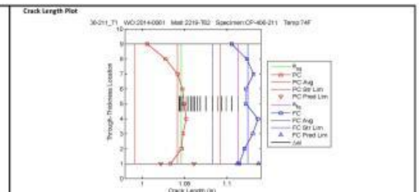

KIC Plot

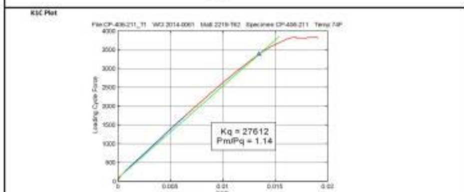

Load vs COD

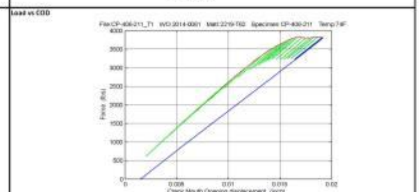

Mechanical Test Facilities

EM10

Fracture Toughness J_{Ic} Test Results

Version 4.3

EM10 Specimen ID	140061381	Geometry	C(T)	"E" (MSI)	10.60	Precrack Pmax (lbf)	1513.0
Other Specimen ID	CP-406-213	"W" (in)	2.0010	"Ec" (MSI)	10.60	Precrack Final "a" (in)	1.0331
Operator	Charles Kay	"B" (in)	0.9980	% diff E & Ec	0.00	Stress Ratio	0.10
Test Date	4/9/2014	"Bn" (in)	0.7980	"V"	0.30	Kmax (ksi_sqrt_in)	8.00
		"Be" (in)	0.9580	"YS" (KSI)	37.80		
Environment	Air	Oreintation	T-L	"UTS" (KSI)	57.30		
Temperature (°F)	73	"An" (in)	0.8010			A_op (in)	1.0331
Pressure (PSIG)	0	Hole Span/2 "H" (in)	0.7100	Flow Stress (KSI)	47.56	A_oq (in)	1.0150
Relative Humidity (%)	NA	COD Span/2 "D" (in)	0.1050	"E"/"YS"	0.28	A_fp (in)	1.1152
Soak Time (min)	0	Coupon #	M2			A_fq (in)	1.0875

	Jq (in*lbs/in^2)	Je_q (in*lbs/in^2)	Jp_q (in*lbs/in^2)	Kjq (ksi(in)^2)	Kjq_at_Je_q (ksi(in)^2)	K_95sec (ksi(in)^2)	K Req Ligament (in)	Pmax/Pq
Results	91.00	81.60	9.40	32.56	30.83	27.81	1.353	1.19

Summary of Test Validities Required for All Tests:			
7.4.5	Initial precrack force	P <= Pm for sample type	Valid
7.4.5.1	Initial Kmax	<40% of Precrack YS	Valid
7.4.5.2	Final Kmax	<60% of K result	Valid
9.1.4.1	Precrack straightness	None > 0.05B	Valid
7.4.5.1	Precrack length	>0.05B or 0.05inch, wide notch	Valid
7.5	Side groove depth	< 0.25B	Valid
Summary of Test Validities Required for Jic:			
7.4.2	a/W Range for J	0.45 <= a/W <= 0.7	Valid
9.1.5.1	Even Crack Ext.	None < 50% of avg crk ext.	Valid
9.1.5.2	Accuracy of crk ext. pred.	Diff < 0.15 d_ap	Valid
A9.6.4	# pts in region A	# pts >= 1 in A	Valid
A9.6.4	# pts in region B	# pts >= 1 in B	Valid
A9.6.6.6	# Valid J-da pts	# pts >= 5	Valid
A9.8.1	J-da fit coeff C2	C2 < 1.0	Valid
A9.8.2.1	Accuracy of a_oq	|a_oq - a_op| < 0.01W or 0.5mm	Valid
A9.8.2.2	Num pts in a_oq fit	# points >= 8	Valid
A9.8.2.2	0.4Jq<(#pts a_oq fit)<Jq	# points >= 3	Valid
A8.2.2.2	a_oq fit R^2	R^2 > 0.96	Valid
A9.9.1	Thickness requirement	B > 10Jq/FlowStress	Valid
A9.9.2	Ligament requirement	b_o > 10Jq/FlowStress	Valid
A9.9.3	Regression line slope	Slope < flow at da_q	Valid
All validity criteria for Jic NOT met. Jq is not fully valid Jic.			
Non-valid Jq values may still convey valuable fracture toughness information.			
Summary of Test Validities Required for KIc:			
7.4.2	a/W Range for K	0.45 <= a/W <= 0.55	Valid
A5.4.3	K Ligament length	b_o > 2.5(K/YS)^2	NOT Valid
A5.4.2	Pmax/Pq ratio	Less than 1.10	NOT Valid
All validity criteria for K_{Ic} NOT met. Kq is not fully valid K_{Ic}.			
Non-valid Kq values may still convey valuable fracture toughness information.			

J1C Plot

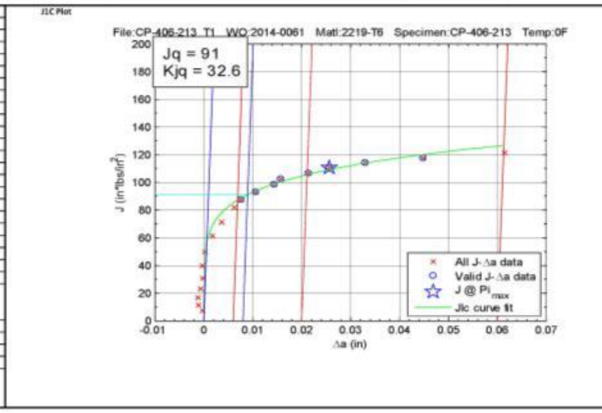

Method File:
FTA NLFT

Comments:
N/A

Mechanical Test Facilities

EM10

Fracture Toughness J_{Ic} Test Results

Version 4.3

EM10 Specimen ID	140061381
Other Specimen ID	CP-406-213
Operator	Charles Kay
Test Date	4/9/2014

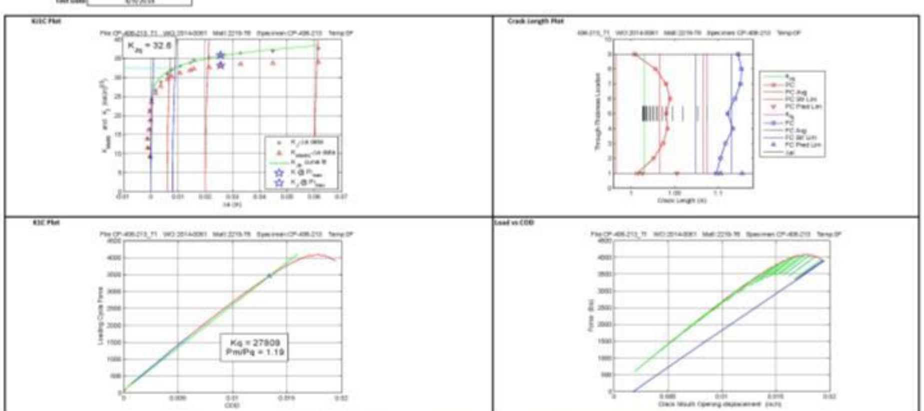

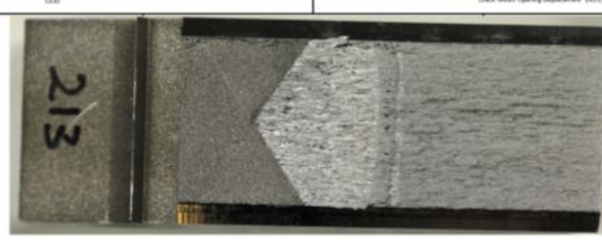

Mechanical Test Facilities

EM10

Fracture Toughness J_{Ic} Test Results

Version 4.3

EM10 Specimen ID	140061384	Geometry	C(T)	"E" (MSI)	10.60	Precrack Pmax (lbf)	409.0
Other Specimen ID	CP-406-216	"W" (in)	1.0000	"Ec" (MSI)	10.60	Precrack Final "a" (in)	0.5197
Operator	Charles Kay	"B" (in)	0.5020	% diff E & Ec	0.00	Stress Ratio	0.10
Test Date	4/3/2014	"Bn" (in)	0.4000	"V"	0.30	Kmax (ksi_sqrt_in)	8.00
		"Be" (in)	0.4810	"YS" (KSI)	41.40		
Environment	Air	Orientation	S-T	"UTS" (KSI)	59.80		
Temperature (°F)	70	"An" (in)	0.4020			A_op (in)	0.5197
Pressure (PSIG)	0	Hole Span/2 "H" (in)	0.3550	Flow Stress (KSI)	50.58	A_oq (in)	0.5184
Relative Humidity (%)	NA	COD Span/2 "D" (in)	0.1000	"E"/"YS"	256.00	A_fp (in)	0.5911
Soak Time (min)	0	Coupon #	M2			A_fq (in)	0.5843

	Jq (in*lbs/in^2)	Je_q (in*lbs/in^2)	Jp_q (in*lbs/in^2)	Kjq (ksi(in)^2)	Kjq_at_Je_q (ksi(in)^2)	K_95sec (ksi(in)^2)	K Req Ligament (in)	Pmax/Pq
Results	89.90	73.80	16.10	32.36	29.32	21.50	0.674	1.38

Summary of Test Validities Required for All Tests:			
7.4.5	Initial precrack force	P <= Pm for sample type	Valid
7.4.5.1	Initial Kmax	<40% of Precrack YS	Valid
7.4.5.2	Final Kmax	<60% of K result	Valid
9.1.4.1	Precrack straightness	None > 0.05B	Valid
7.4.5.1	Precrack length	>0.05B or 0.05inch, wide notch	Valid
7.5	Side groove depth	< 0.25B	Valid
Summary of Test Validities Required for Jlc:			
7.4.2	a/W Range for J	0.45 <= a/W <= 0.7	Valid
9.1.5.1	Even Crack Ext.	None < 50% of avg crk ext.	Valid
9.1.5.2	Accuracy of crk ext. pred.	Diff < 0.15 d_ap	Valid
A9.6.4	# pts in region A	# pts >= 1 in A	Valid
A9.6.4	# pts in region B	# pts >= 1 in B	Valid
A9.6.6.6	# Valid J-da pts	# pts >= 5	Valid
A9.8.1	J-da fit coeff C2	C2 < 1.0	Valid
A9.8.2.1	Accuracy of a_oq	|a_oq - a_op| < 0.01W or 0.5mm	Valid
A9.8.2.2	Num pts in a_oq fit	# points >= 8	Valid
A9.8.2.2	0.4Jq<(#pts a_oq fit)<Jq	# points >= 3	Valid
A8.2.2.2	a_oq fit R^2	R^2 > 0.96	Valid
A9.9.1	Thickness requirement	B > 10Jq/FlowStress	Valid
A9.9.2	Ligament requirement	b_o > 10Jq/FlowStress	Valid
A9.9.3	Regression line slope	Slope < flow at da_q	Valid
All validity criteria for Jlc NOT met. Jq is not fully valid Jlc. Non-valid Jq values may still convey valuable fracture toughness information.			
Summary of Test Validities Required for Klc:			
7.4.2	a/W Range for K	0.45 <= a/W <= 0.55	Valid
A5.4.3	K Ligament length	b_o > 2.5(K/YS)^2	NOT Valid
A5.4.2	Pmax/Pq ratio	Less than 1.10	NOT Valid
All validity criteria for K_{Ic} NOT met. Kq is not fully valid K_{Ic}. Non-valid Kq values may still convey valuable fracture toughness information.			

J1C Plot

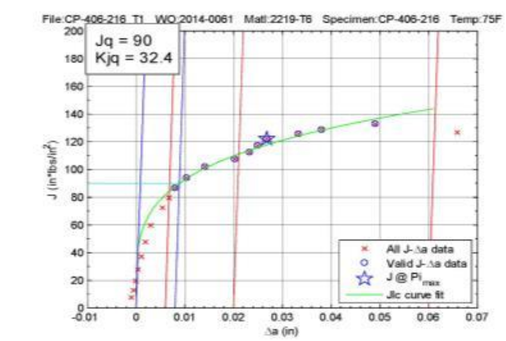

Method File:
FTA NLFT

Comments:
N/A

Mechanical Test Facilities

EM10

Fracture Toughness J_{Ic} Test Results

Version 4.3

EM10 Specimen ID	140061384
Other Specimen ID	CP-406-216
Operator	Charles Kay
Test Date	4/3/2014

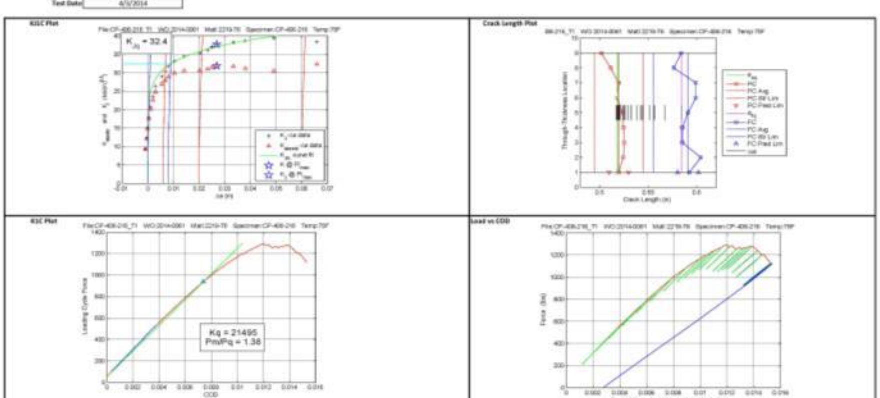

Mechanical Test Facilities

EM10

Fracture Toughness J_{Ic} Test Results

Version 4.3

EM10 Specimen ID	140061386	Geometry	C(T)	"E" (MSI)	1.06E+01	Precrack Pmax (lbf)	260.0
Other Specimen ID	CP-406-218	"W" (in)	1.0000	"Ec" (MSI)	1.06E+01	Precrack Final "a" (in)	0.6575
Operator	Charles Kay	"B" (in)	0.5020	% diff E & Ec	0	Stress Ratio	0.10
Test Date	4/11/2014	"Bn" (in)	0.3960	"V"	0.3	Kmax (ksi_sqrt_in)	8.00
		"Be" (in)	0.4800	"YS" (KSI)	41.4		
Environment	Air	Oreintation	S-T	"UTS" (KSI)	59.8		
Temperature (°F)	76	"An" (in)	0.6190			A_op (in)	0.6575
Pressure (PSIG)	0	Hole Span/2 "H" (in)	0.3550	Flow Stress (KSI)		A_oq (in)	0.6529
Relative Humidity (%)	NA	COD Span/2 "D" (in)	0.0980	"E"/"YS"		A_fp (in)	0.7241
Soak Time (min)	0	Coupon #	M2			A_fq (in)	0.7205

	Jq (in*lbs/in^2)	Je_q (in*lbs/in^2)	Jp_q (in*lbs/in^2)	Kjq (ksi(in)^2)	Kjq_at_Je_q (ksi(in)^2)	K_95sec (ksi(in)^2)	K Req Ligament (in)	Pmax/Pq
Results	56	44.3	11.7	25.545	22.709	18.376	0.492	1.3

Summary of Test Validities Required for All Tests:			
7.4.5	Initial precrack force	P <= Pm for sample type	Valid
7.4.5.1	Initial Kmax	<40% of Precrack YS	Valid
7.4.5.2	Final Kmax	<60% of K result	Valid
9.1.4.1	Precrack straightness	None > 0.05B	Valid
7.4.5.1	Precrack length	>0.05B or 0.05inch, wide notch	Valid
7.5	Side groove depth	< 0.25B	Valid
Summary of Test Validities Required for Jlc:			
7.4.2	a/W Range for J	0.45 <= a/W <= 0.7	Valid
9.1.5.1	Even Crack Ext.	None < 50% of avg crk ext.	Valid
9.1.5.2	Accuracy of crk ext. pred.	Diff < 0.15 d_ap	Valid
A9.6.4	# pts in region A	# pts >= 1 in A	Valid
A9.6.4	# pts in region B	# pts >= 1 in B	Valid
A9.6.6.6	# Valid J-da pts	# pts >= 5	Valid
A9.8.1	J-da fit coeff C2	C2 < 1.0	Valid
A9.8.2.1	Accuracy of a_oq	|a_oq - a_op| < 0.01W or 0.5mm	Valid
A9.8.2.2	Num pts in a_oq fit	# points >= 8	Valid
A9.8.2.2	0.4Jq<(#pts a_oq fit)<Jq	# points >= 3	Valid
A8.2.2.2	a_oq fit R^2	R^2 > 0.96	Valid
A9.9.1	Thickness requirement	B > 10Jq/FlowStress	Valid
A9.9.2	Ligament requirement	b_o > 10Jq/FlowStress	Valid
A9.9.3	Regression line slope	Slope < flow at da_q	Valid
All validity criteria for Jlc NOT met. Jq is not fully valid Jlc. Non-valid Jq values may still convey valuable fracture toughness information.			
Summary of Test Validities Required for Klc:			
7.4.2	a/W Range for K	0.45 <= a/W <= 0.55	NOT Valid
A5.4.3	K Ligament length	b_o > 2.5(K/YS)^2	NOT Valid
A5.4.2	Pmax/Pq ratio	Less than 1.10	NOT Valid
All validity criteria for K_{Ic} NOT met. Kq is not fully valid K_{Ic}. Non-valid Kq values may still convey valuable fracture toughness information.			

JIC Plot

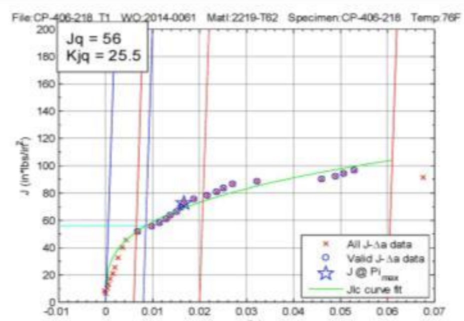

Method File:
FTA NLFT

Comments:
N/A

Mechanical Test Facilities

EM10

Fracture Toughness J_{Ic} Test Results

Version 4.3

EM10 Specimen ID	140061386
Other Specimen ID	CP-406-218
Operator	Charles Kay
Test Date	4/11/2014

K1C Plot

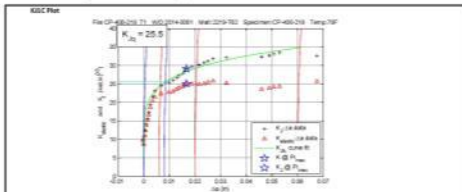

Crack Length Plot

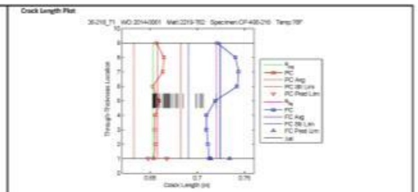

KIC Plot

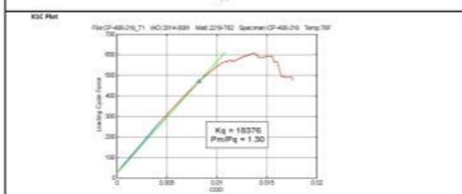

Load vs COD

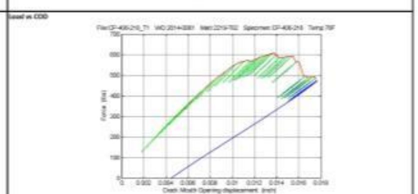

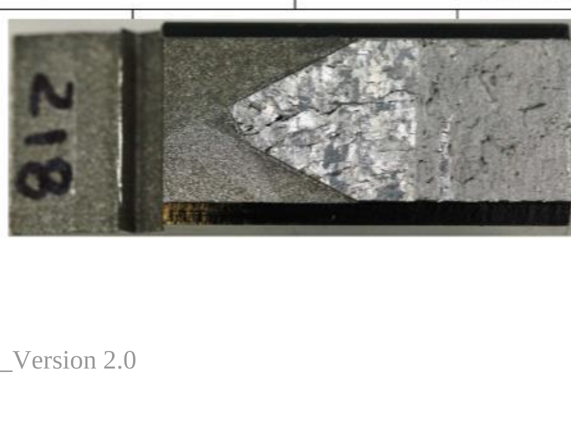

Mechanical Test Facilities

EM10

Fracture Toughness J_{Ic} Test Results

Version 4.3

EM10 Specimen ID	140061389	Geometry	C(T)	"E" (MSI)	10.60	Precrack Pmax (lbf)	1523.0
Other Specimen ID	CP-406-221	"W" (in)	2.0000	"Ec" (MSI)	10.60	Precrack Final "a" (in)	1.0256
Operator	Charles Kay	"B" (in)	0.9980	% diff E & Ec	0.00	Stress Ratio	0.10
Test Date	4/9/2014	"Bn" (in)	0.7960	"V"	0.30	Kmax (ksi_sqrt_in)	8.00
		"Be" (in)	0.9570	"YS" (KSI)	37.30		
Environment	Air	Oreintation	L-T	"UTS" (KSI)	55.20		
Temperature (°F)	73	"An" (in)	0.7990			A_op (in)	1.0256
Pressure (PSIG)	0	Hole Span/2 "H" (in)	0.7100	Flow Stress (KSI)	46.26	A_oq (in)	1.0083
Relative Humidity (%)	NA	COD Span/2 "D" (in)	0.1040	"E"/"YS"	0.28	A_fp (in)	1.1092
Soak Time (min)	0	Coupon #	M3			A_fq (in)	1.0824

	Jq (in*lbs/in^2)	Je_q (in*lbs/in^2)	Jp_q (in*lbs/in^2)	Kjq (ksi(in)^2)	Kjq_at_Je_q (ksi(in)^2)	K_95sec (ksi(in)^2)	K Req Ligament (in)	Pmax/Pq
Results	117.20	102.70	14.50	36.95	34.59	29.79	1.594	1.26

Summary of Test Validities Required for All Tests:			
7.4.5	Initial precrack force	P <= Pm for sample type	Valid
7.4.5.1	Initial Kmax	<40% of Precrack YS	Valid
7.4.5.2	Final Kmax	<60% of K result	Valid
9.1.4.1	Precrack straightness	None > 0.05B	Valid
7.4.5.1	Precrack length	>0.05B or 0.05inch, wide notch	Valid
7.5	Side groove depth	< 0.25B	Valid
Summary of Test Validities Required for Jic:			
7.4.2	a/W Range for J	0.45 <= a/W <= 0.7	Valid
9.1.5.1	Even Crack Ext.	None < 50% of avg crk ext.	Valid
9.1.5.2	Accuracy of crk ext. pred.	Diff < 0.15 d_ap	Valid
A9.6.4	# pts in region A	# pts >= 1 in A	Valid
A9.6.4	# pts in region B	# pts >= 1 in B	Valid
A9.6.6.6	# Valid J-da pts	# pts >= 5	Valid
A9.8.1	J-da fit coeff C2	C2 < 1.0	Valid
A9.8.2.1	Accuracy of a_oq	|a_oq - a_op| < 0.01W or 0.5mm	Valid
A9.8.2.2	Num pts in a_oq fit	# points >= 8	Valid
A9.8.2.2	0.4Jq<(#pts a_oq fit)<Jq	# points >= 3	Valid
A8.2.2.2	a_oq fit R^2	R^2 > 0.96	Valid
A9.9.1	Thickness requirement	B > 10Jq/FlowStress	Valid
A9.9.2	Ligament requirement	b_o > 10Jq/FlowStress	Valid
A9.9.3	Regression line slope	Slope < flow at da_q	Valid
All validity criteria for Jic NOT met. Jq is not fully valid Jic. Non-valid Jq values may still convey valuable fracture toughness information.			
Summary of Test Validities Required for Kic:			
7.4.2	a/W Range for K	0.45 <= a/W <= 0.55	Valid
A5.4.3	K Ligament length	b_o > 2.5(K/YS)^2	NOT Valid
A5.4.2	Pmax/Pq ratio	Less than 1.10	NOT Valid
All validity criteria for K_{Ic} NOT met. Kq is not fully valid K_{Ic}. Non-valid Kq values may still convey valuable fracture toughness information.			

J1C Plot

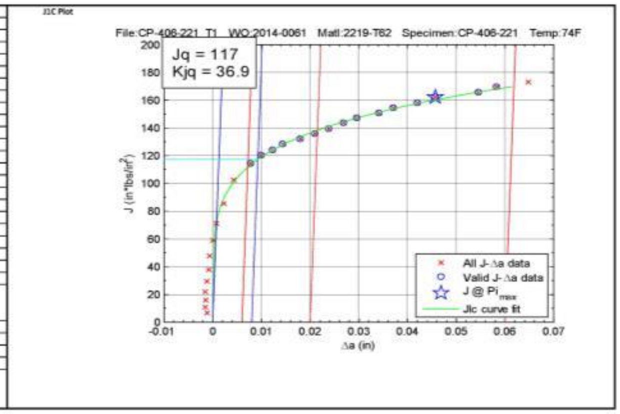

Method File:

FTA NLFT

Comments:

N/A

Mechanical Test Facilities

EM10

Fracture Toughness J_{Ic} Test Results

Version 4.3

EM10 Specimen ID	140061389
Other Specimen ID	CP-406-221
Operator	Charles Kay
Test Date	4/9/2014

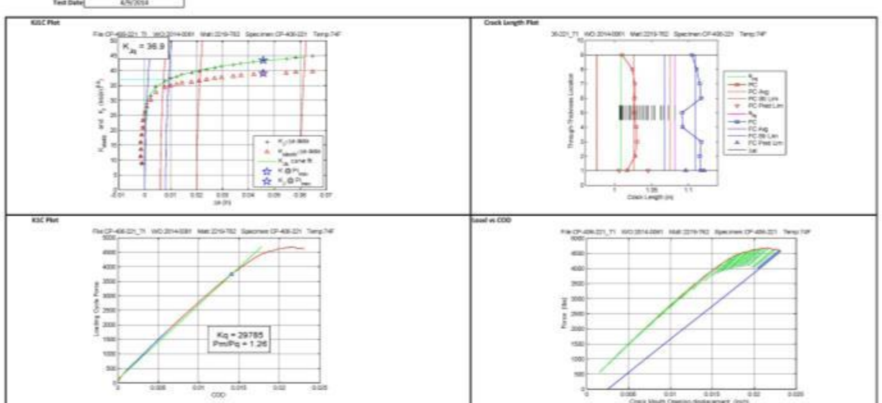

Mechanical Test Facilities

EM10

Fracture Toughness J_{Ic} Test Results

Version 4.3

EM10 Specimen ID	140061391	Geometry	C(T)	"E" (MSI)	10600000.00	Precrack Pmax (lbf)	1518.0
Other Specimen ID	CP-406-223	"W" (in)	2.0000	"Ec" (MSI)	10600000.00	Precrack Final "a" (in)	1.0391
Operator	Charles Kay	"B" (in)	1.0000	% diff E & Ec	0.00	Stress Ratio	0.10
Test Date	4/10/2014	"Bn" (in)	0.7990	"V"	0.30	Kmax (ksi_sqrt_in)	8.00
		"Be" (in)	0.9600	"YS" (KSI)	37300.00		
Environment	Air	Oreintation	L-T	"UTS" (KSI)	55200.00		
Temperature (°F)	73	"An" (in)	0.7990			A_op (in)	1.0391
Pressure (PSIG)	0	Hole Span/2 "H" (in)	0.7100	Flow Stress (KSI)	46.26	A_oq (in)	1.0239
Relative Humidity (%)	NA	COD Span/2 "D" (in)	0.1050	"E"/"YS"	0.28	A_fp (in)	1.1235
Soak Time (min)	0	Coupon #	M3			A_fq (in)	1.1022

	Jq (in*lbs/in^2)	Je_q (in*lbs/in^2)	Jp_q (in*lbs/in^2)	Kjq (ksi(in)^2)	Kjq_at_Je_q (ksi(in)^2)	K_95sec (ksi(in)^2)	K Req Ligament (in)	Pmax/Pq
Results	125.70	109.30	16.40	38.27	35.68	32.51	1.899	1.19

Summary of Test Validities Required for All Tests:			
7.4.5	Initial precrack force	P <= Pm for sample type	Valid
7.4.5.1	Initial Kmax	<40% of Precrack YS	Valid
7.4.5.2	Final Kmax	<60% of K result	Valid
9.1.4.1	Precrack straightness	None > 0.05B	Valid
7.4.5.1	Precrack length	>0.05B or 0.05inch, wide notch	Valid
7.5	Side groove depth	< 0.25B	Valid
Summary of Test Validities Required for Jic:			
7.4.2	a/W Range for J	0.45 <= a/W <= 0.7	Valid
9.1.5.1	Even Crack Ext.	None < 50% of avg crk ext.	Valid
9.1.5.2	Accuracy of crk ext. pred.	Diff < 0.15 d_ap	Valid
A9.6.4	# pts in region A	# pts >= 1 in A	Valid
A9.6.4	# pts in region B	# pts >= 1 in B	Valid
A9.6.6.6	# Valid J-da pts	# pts >= 5	Valid
A9.8.1	J-da fit coeff C2	C2 < 1.0	Valid
A9.8.2.1	Accuracy of a_oq	|a_oq - a_op| < 0.01W or 0.5mm	Valid
A9.8.2.2	Num pts in a_oq fit	# points >= 8	Valid
A9.8.2.2	0.4Jq<(#pts a_oq fit)<Jq	# points >= 3	Valid
A8.2.2.2	a_oq fit R^2	R^2 > 0.96	Valid
A9.9.1	Thickness requirement	B > 10Jq/FlowStress	Valid
A9.9.2	Ligament requirement	b_o > 10Jq/FlowStress	Valid
A9.9.3	Regression line slope	Slope < flow at da_q	Valid
All validity criteria for Jic NOT met. Jq is not fully valid Jic.			
Non-valid Jq values may still convey valuable fracture toughness information.			
Summary of Test Validities Required for Kic:			
7.4.2	a/W Range for K	0.45 <= a/W <= 0.55	Valid
A5.4.3	K Ligament length	b_o > 2.5(K/YS)^2	NOT Valid
A5.4.2	Pmax/Pq ratio	Less than 1.10	NOT Valid
All validity criteria for K_{Ic} NOT met. Kq is not fully valid K_{Ic}.			
Non-valid Kq values may still convey valuable fracture toughness information.			

J1C Plot

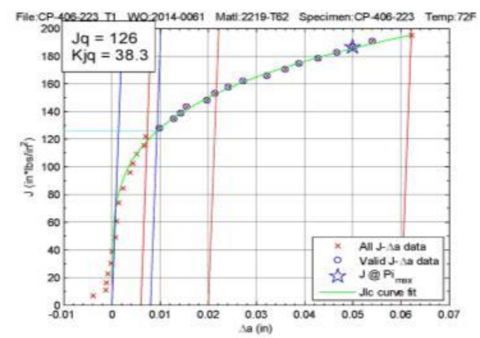

Method File:
FTA NLFT

Comments:
N/A

Mechanical Test Facilities

EM10

Fracture Toughness J_{Ic} Test Results

Version 4.3

EM10 Specimen ID	140061391
Other Specimen ID	CP-406-223
Operator	Charles Kay
Test Date	4/10/2014

KIIC Plot

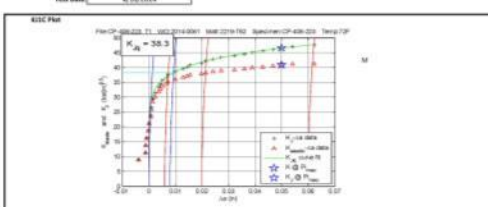

Crack Length Plot

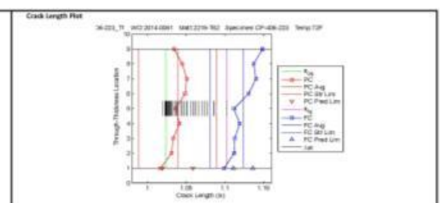

KIC Plot

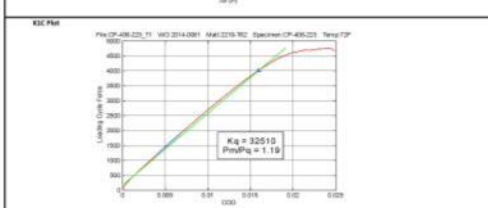

Load vs COD

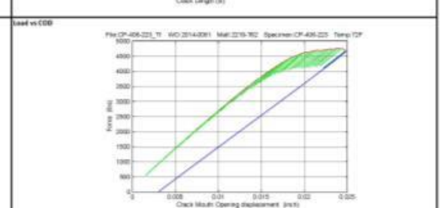

Mechanical Test Facilities

EM10

Fracture Toughness J_{Ic} Test Results

Version 4.3

EM10 Specimen ID	140061394
Other Specimen ID	CP-406-226
Operator	Charles Kay
Test Date	4/10/2014
Environment	Air
Temperature (°F)	73
Pressure (PSIG)	0
Relative Humidity (%)	NA
Soak Time (min)	0

Geometry	C(T)
"W" (in)	1.9980
"B" (in)	0.9980
"Bn" (in)	0.8010
"Be" (in)	0.9590
Oreintation	T-L
"An" (in)	0.7990
Hole Span/2 "H" (in)	0.7100
COD Span/2 "D" (in)	0.1050
Coupon #	M3

"E" (MSI)	10.60
"Ec" (MSI)	10.72
% diff E & Ec	1.10
"V"	0.30
"YS" (KSI)	37.10
"UTS" (KSI)	55.10
Flow Stress (KSI)	46.10
"E"/"YS"	0.29

Precrack Pmax (lbf)	1526.0
Precrack Final "a" (in)	1.0555
Stress Ratio	0.10
Kmax (ksi_sqrt_in)	8.00
A_op (in)	1.0555
A_oq (in)	1.0390
A_fp (in)	1.1424
A_fq (in)	1.1129

	Jq (in*lbs/in^2)	Je_q (in*lbs/in^2)	Jp_q (in*lbs/in^2)	Kjq (ksi(in)^2)	Kjq_at_Je_q (ksi(in)^2)	K_95sec (ksi(in)^2)	K Req Ligament (in)	Pmax/Pq
Results	84.90	76.70	8.20	31.45	29.88	28.04	1.429	1.12

Summary of Test Validities Required for All Tests:			
7.4.5	Initial precrack force	P <= Pm for sample type	Valid
7.4.5.1	Initial Kmax	<40% of Precrack YS	Valid
7.4.5.2	Final Kmax	<60% of K result	Valid
9.1.4.1	Precrack straightness	None > 0.05B	Valid
7.4.5.1	Precrack length	>0.05B or 0.05inch, wide notch	Valid
7.5	Side groove depth	< 0.25B	Valid
Summary of Test Validities Required for Jic:			
7.4.2	a/W Range for J	0.45 <= a/W <= 0.7	Valid
9.1.5.1	Even Crack Ext.	None < 50% of avg crk ext.	Valid
9.1.5.2	Accuracy of crk ext. pred.	Diff < 0.15 d_ap	Valid
A9.6.4	# pts in region A	# pts >= 1 in A	Valid
A9.6.4	# pts in region B	# pts >= 1 in B	Valid
A9.6.6.6	# Valid J-da pts	# pts >= 5	Valid
A9.8.1	J-da fit coeff C2	C2 < 1.0	Valid
A9.8.2.1	Accuracy of a_oq	|a_oq - a_op| < 0.01W or 0.5mm	Valid
A9.8.2.2	Num pts in a_oq fit	# points >= 8	Valid
A9.8.2.2	0.4Jq<(#pts a_oq fit)<Jq	# points >= 3	Valid
A8.2.2.2	a_oq fit R^2	R^2 > 0.96	Valid
A9.9.1	Thickness requirement	B > 10Jq/FlowStress	Valid
A9.9.2	Ligament requirement	b_o > 10Jq/FlowStress	Valid
A9.9.3	Regression line slope	Slope < flow at da_q	Valid
All validity criteria for Jic NOT met. Jq is not fully valid Jic. Non-valid Jq values may still convey valuable fracture toughness information.			
Summary of Test Validities Required for KIc:			
7.4.2	a/W Range for K	0.45 <= a/W <= 0.55	Valid
A5.4.3	K Ligament length	b_o > 2.5(K/YS)^2	NOT Valid
A5.4.2	Pmax/Pq ratio	Less than 1.10	NOT Valid
All validity criteria for K_{Ic} NOT met. Kq is not fully valid K_{Ic}. Non-valid Kq values may still convey valuable fracture toughness information.			

J1C Plot

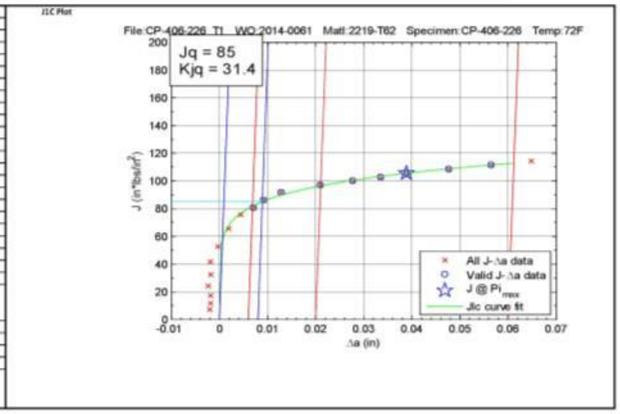

Method File:
FTA NLFT

Comments:
N/A

Mechanical Test Facilities

EM10

Fracture Toughness J_{Ic} Test Results

Version 4.3

EM10 Specimen ID	140061394
Other Specimen ID	CP-406-226
Operator	Charles Kay
Test Date	4/10/2014

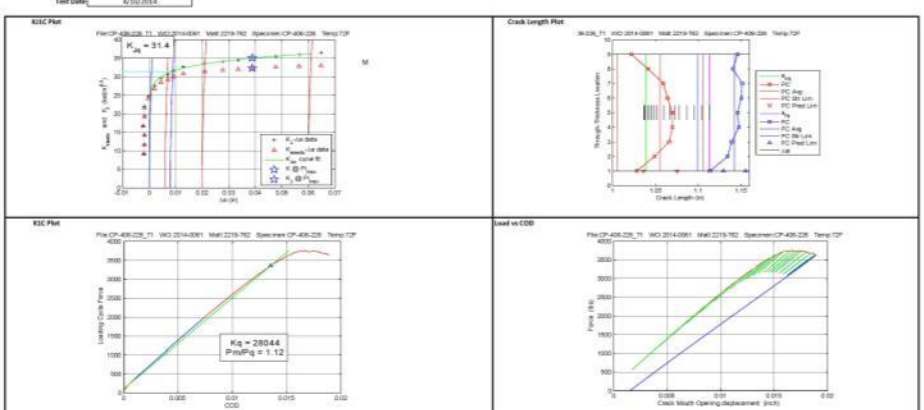

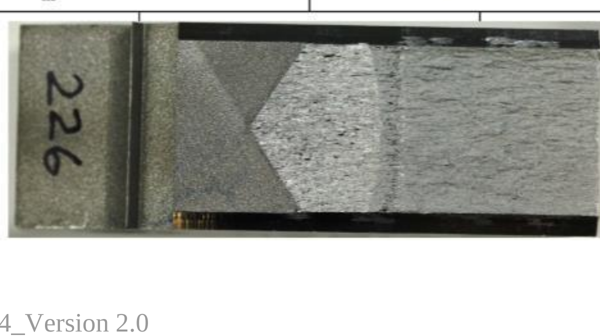

Mechanical Test Facilities

EM10

Fracture Toughness J_{Ic} Test Results

Version 4.3

EM10 Specimen ID	140061396	Geometry	C(T)	"E" (MSI)	10.60	Precrack Pmax (lbf)	1530.0
Other Specimen ID	CP-406-228	"W" (in)	2.0000	"Ec" (MSI)	10.62	Precrack Final "a" (in)	1.0526
Operator	Charles Kay	"B" (in)	0.9990	% diff E & Ec	0.20	Stress Ratio	0.10
Test Date	4/10/2014	"Bn" (in)	0.7990	"V"	0.30	Kmax (ksi_sqrt_in)	8.00
		"Be" (in)	0.9590	"YS" (KSI)	37.10		
Environment	Air	Oreintation	T-L	"UTS" (KSI)	55.10		
Temperature (°F)	73	"An" (in)	0.7990			A_op (in)	1.0526
Pressure (PSIG)	0	Hole Span/2 "H" (in)	0.7100	Flow Stress (KSI)	46.10	A_oq (in)	1.0359
Relative Humidity (%)	NA	COD Span/2 "D" (in)	0.1050	"E"/"YS"	0.29	A_fp (in)	1.1417
Soak Time (min)	0	Coupon #	M3			A_fq (in)	1.1128

	Jq (in*lbs/in^2)	Je_q (in*lbs/in^2)	Jp_q (in*lbs/in^2)	Kjq (ksi(in)^2)	Kjq_at_Je_q (ksi(in)^2)	K_95sec (ksi(in)^2)	K Req Ligament (in)	Pmax/Pq
Results	93.10	82.70	10.40	32.93	31.03	28.37	1.462	1.15

Summary of Test Validities Required for All Tests:			
7.4.5	Initial precrack force	P <= Pm for sample type	Valid
7.4.5.1	Initial Kmax	<40% of Precrack YS	Valid
7.4.5.2	Final Kmax	<60% of K result	Valid
9.1.4.1	Precrack straightness	None > 0.05B	Valid
7.4.5.1	Precrack length	>0.05B or 0.05inch, wide notch	Valid
7.5	Side groove depth	< 0.25B	Valid
Summary of Test Validities Required for Jic:			
7.4.2	a/W Range for J	0.45 <= a/W <= 0.7	Valid
9.1.5.1	Even Crack Ext.	None < 50% of avg crk ext.	Valid
9.1.5.2	Accuracy of crk ext. pred.	Diff < 0.15 d_ap	Valid
A9.6.4	# pts in region A	# pts >= 1 in A	Valid
A9.6.4	# pts in region B	# pts >= 1 in B	Valid
A9.6.6.6	# Valid J-da pts	# pts >= 5	Valid
A9.8.1	J-da fit coeff C2	C2 < 1.0	Valid
A9.8.2.1	Accuracy of a_oq	|a_oq - a_op| < 0.01W or 0.5mm	Valid
A9.8.2.2	Num pts in a_oq fit	# points >= 8	Valid
A9.8.2.2	0.4Jq<(#pts a_oq fit)<Jq	# points >= 3	Valid
A8.2.2.2	a_oq fit R^2	R^2 > 0.96	Valid
A9.9.1	Thickness requirement	B > 10Jq/FlowStress	Valid
A9.9.2	Ligament requirement	b_o > 10Jq/FlowStress	Valid
A9.9.3	Regression line slope	Slope < flow at da_q	Valid
All validity criteria for Jic NOT met. Jq is not fully valid Jic. Non-valid Jq values may still convey valuable fracture toughness information.			
Summary of Test Validities Required for Kic:			
7.4.2	a/W Range for K	0.45 <= a/W <= 0.55	Valid
A5.4.3	K Ligament length	b_o > 2.5(K/YS)^2	NOT Valid
A5.4.2	Pmax/Pq ratio	Less than 1.10	NOT Valid
All validity criteria for K_{Ic} NOT met. Kq is not fully valid K_{Ic}. Non-valid Kq values may still convey valuable fracture toughness information.			

J1C Plot

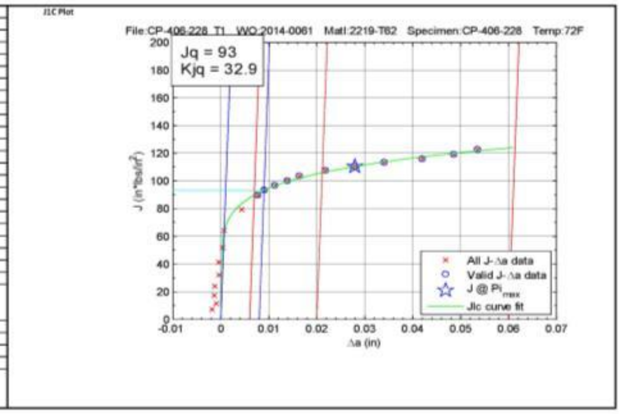

Method File:

FTA NLFT

Comments:

N/A

Mechanical Test Facilities

EM10

Fracture Toughness J_{Ic} Test Results

Version 4.3

EM10 Specimen ID	140061396
Other Specimen ID	CP-406-228
Operator	Charles Kay
Test Date	4/10/2014

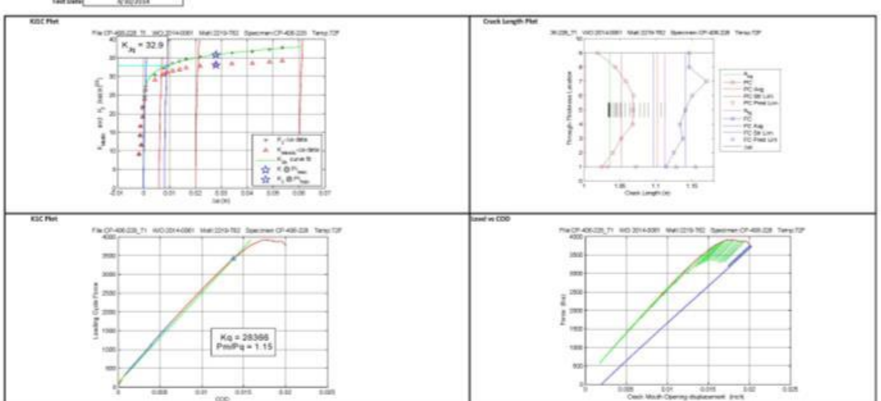

Mechanical Test Facilities

EM10

Fracture Toughness J_{Ic} Test Results

Version 4.3

EM10 Specimen ID	140061399
Other Specimen ID	CP-406-231
Operator	Charles Kay
Test Date	4/11/2014
Environment	Air
Temperature (°F)	73
Pressure (PSIG)	0
Relative Humidity (%)	NA
Soak Time (min)	0

Geometry	C(T)
"W" (in)	1.0000
"B" (in)	0.5010
"Bn" (in)	0.3950
"Be" (in)	0.4790
Oreintation	S-T
"An" (in)	0.4010
Hole Span/2 "H" (in)	0.3550
COD Span/2 "D" (in)	0.0990
Coupon #	M3

"E" (MSI)	10.60
"Ec" (MSI)	10.60
% diff E & Ec	0.00
"V"	0.30
"YS" (KSI)	37.30
"UTS" (KSI)	57.10
Flow Stress (KSI)	47.19
"E"/"YS"	0.28

Precrack Pmax (lbf)	534.0
Precrack Final "a" (in)	0.5294
Stress Ratio	0.10
Kmax (ksi_sqrt_in)	8.00
A_op (in)	0.5294
A_oq (in)	0.5263
A_fp (in)	0.6078
A_fq (in)	0.5946

	Jq (in*lbs/in^2)	Je_q (in*lbs/in^2)	Jp_q (in*lbs/in^2)	Kjq (ksi(in)^2)	Kjq_at_Je_q (ksi(in)^2)	K_95sec (ksi(in)^2)	K Req Ligament (in)	Pmax/Pq
Results	66.00	58.10	8.00	27.73	26.01	22.35	0.897	1.20

Summary of Test Validities Required for All Tests:			
7.4.5	Initial precrack force	P <= Pm for sample type	Valid
7.4.5.1	Initial Kmax	<40% of Precrack YS	Valid
7.4.5.2	Final Kmax	<60% of K result	Valid
9.1.4.1	Precrack straightness	None > 0.05B	Valid
7.4.5.1	Precrack length	>0.05B or 0.05inch, wide notch	Valid
7.5	Side groove depth	< 0.25B	Valid
Summary of Test Validities Required for JIc:			
7.4.2	a/W Range for J	0.45 <= a/W <= 0.7	Valid
9.1.5.1	Even Crack Ext.	None < 50% of avg crk ext.	Valid
9.1.5.2	Accuracy of crk ext. pred.	Diff < 0.15 d_ap	Valid
A9.6.4	# pts in region A	# pts >= 1 in A	Valid
A9.6.4	# pts in region B	# pts >= 1 in B	Valid
A9.6.6.6	# Valid J-da pts	# pts >= 5	Valid
A9.8.1	J-da fit coeff C2	C2 < 1.0	Valid
A9.8.2.1	Accuracy of a_oq	|a_oq - a_op| < 0.01W or 0.5mm	Valid
A9.8.2.2	Num pts in a_oq fit	# points >= 8	Valid
A9.8.2.2	0.4Jq<(#pts a_oq fit)<Jq	# points >= 3	Valid
A8.2.2.2	a_oq fit R^2	R^2 > 0.96	Valid
A9.9.1	Thickness requirement	B > 10Jq/FlowStress	Valid
A9.9.2	Ligament requirement	b_o > 10Jq/FlowStress	Valid
A9.9.3	Regression line slope	Slope < flow at da_q	Valid
All validity criteria for JIc NOT met. Jq is not fully valid JIc. Non-valid Jq values may still convey valuable fracture toughness information.			
Summary of Test Validities Required for KIc:			
7.4.2	a/W Range for K	0.45 <= a/W <= 0.55	Valid
A5.4.3	K Ligament length	b_o > 2.5(K/YS)^2	NOT Valid
A5.4.2	Pmax/Pq ratio	Less than 1.10	NOT Valid
All validity criteria for K_{Ic} NOT met. Kq is not fully valid K_{Ic}. Non-valid Kq values may still convey valuable fracture toughness information.			

JIC Plot

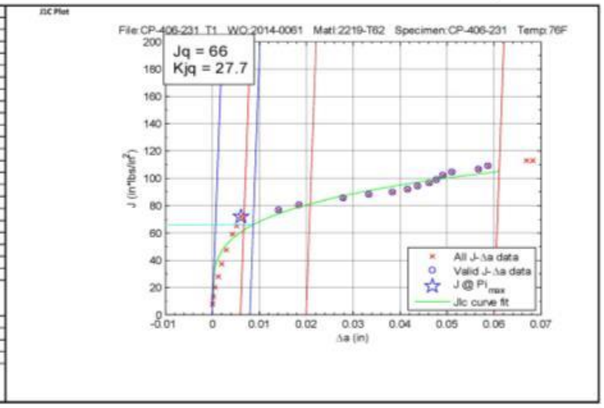

Method File:
FTA NL/T

Comments:
N/A

Mechanical Test Facilities

EM10

Fracture Toughness J_{Ic} Test Results

Version 4.3

EM10 Specimen ID	140061399
Other Specimen ID	CP-406-231
Operator	Charles Kay
Test Date	4/11/2014

KJIC Plot

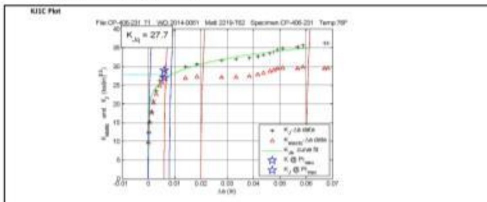

Crack Length Plot

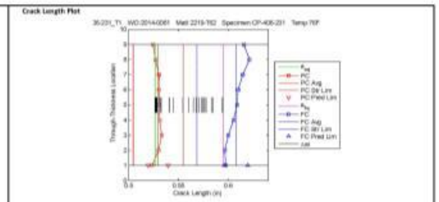

KIC Plot

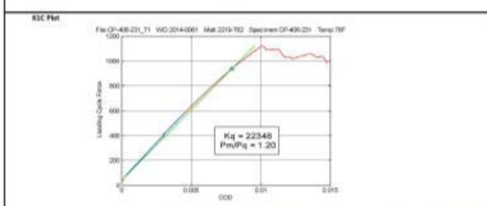

Load vs COD

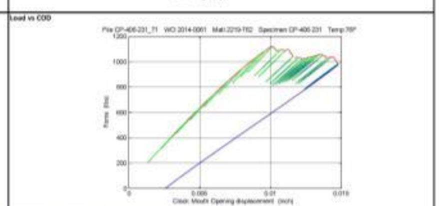

Mechanical Test Facilities

EM10

Fracture Toughness J_{Ic} Test Results

Version 4.3

EM10 Specimen ID	140061401	Geometry	C(T)	"E" (MSI)	10.60	Precrack Pmax (lbf)	525.0
Other Specimen ID	CP-406-233	"W" (in)	1.0000	"Ec" (MSI)	10.60	Precrack Final "a" (in)	0.5518
Operator	Charles Kay	"B" (in)	0.5020	% diff E & Ec	0.00	Stress Ratio	0.10
Test Date	4/11/2014	"Bn" (in)	0.3980	"V"	0.30	Kmax (ksi_sqrt_in)	8.00
		"Be" (in)	0.4800	"YS" (KSI)	37.30		
Environment	Air	Oreintation	S-T	"UTS" (KSI)	57.10		
Temperature (°F)	73	"An" (in)	0.4050			A_op (in)	0.5518
Pressure (PSIG)	0	Hole Span/2 "H" (in)	0.3550	Flow Stress (KSI)	47.19	A_oq (in)	0.5444
Relative Humidity (%)	NA	COD Span/2 "D" (in)	0.1000	"E"/"YS"	0.28	A_fp (in)	0.6175
Soak Time (min)	0	Coupon #	M3			A_fq (in)	0.6107

	Jq (in*lbs/in^2)	Je_q (in*lbs/in^2)	Jp_q (in*lbs/in^2)	Kjq (ksi(in)^2)	Kjq_at_Je_q (ksi(in)^2)	K_95sec (ksi(in)^2)	K Req Ligament (in)	Pmax/Pq
Results	90.70	72.40	18.30	32.51	29.04	21.32	0.817	1.43

Summary of Test Validities Required for All Tests:			
7.4.5	Initial precrack force	P <= Pm for sample type	Valid
7.4.5.1	Initial Kmax	<40% of Precrack YS	Valid
7.4.5.2	Final Kmax	<60% of K result	Valid
9.1.4.1	Precrack straightness	None > 0.05B	Valid
7.4.5.1	Precrack length	>0.05B or 0.05inch, wide notch	Valid
7.5	Side groove depth	< 0.25B	Valid
Summary of Test Validities Required for Jic:			
7.4.2	a/W Range for J	0.45 <= a/W <= 0.7	Valid
9.1.5.1	Even Crack Ext.	None < 50% of avg crk ext.	Valid
9.1.5.2	Accuracy of crk ext. pred.	Diff < 0.15 d_ap	Valid
A9.6.4	# pts in region A	# pts >= 1 in A	Valid
A9.6.4	# pts in region B	# pts >= 1 in B	Valid
A9.6.6.6	# Valid J-da pts	# pts >= 5	Valid
A9.8.1	J-da fit coeff C2	C2 < 1.0	Valid
A9.8.2.1	Accuracy of a_oq	|a_oq - a_op| < 0.01W or 0.5mm	Valid
A9.8.2.2	Num pts in a_oq fit	# points >= 8	Valid
A9.8.2.2	0.4Jq<(#pts a_oq fit)<Jq	# points >= 3	Valid
A8.2.2.2	a_oq fit R^2	R^2 > 0.96	Valid
A9.9.1	Thickness requirement	B > 10Jq/FlowStress	Valid
A9.9.2	Ligament requirement	b_o > 10Jq/FlowStress	Valid
A9.9.3	Regression line slope	Slope < flow at da_q	Valid
All validity criteria for Jic NOT met. Jq is not fully valid Jic. Non-valid Jq values may still convey valuable fracture toughness information.			
Summary of Test Validities Required for Kic:			
7.4.2	a/W Range for K	0.45 <= a/W <= 0.55	Valid
A5.4.3	K Ligament length	b_o > 2.5(K/YS)^2	NOT Valid
A5.4.2	Pmax/Pq ratio	Less than 1.10	NOT Valid
All validity criteria for K_{Ic} NOT met. Kq is not fully valid K_{Ic}. Non-valid Kq values may still convey valuable fracture toughness information.			

J1C Plot

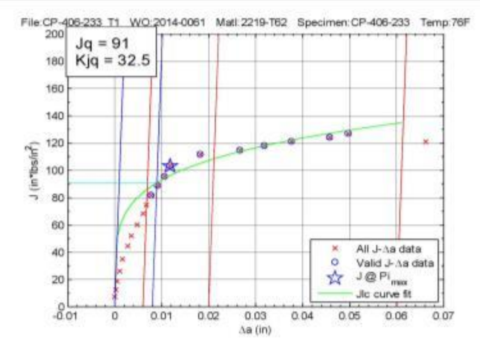

Method File:
FTA NLFT

Comments:
N/A

Mechanical Test Facilities

EM10

Fracture Toughness J_{Ic} Test Results

Version 4.3

EM10 Specimen ID	140061401
Other Specimen ID	CP-406-233
Operator	Charles Kay
Test Date	4/11/2014

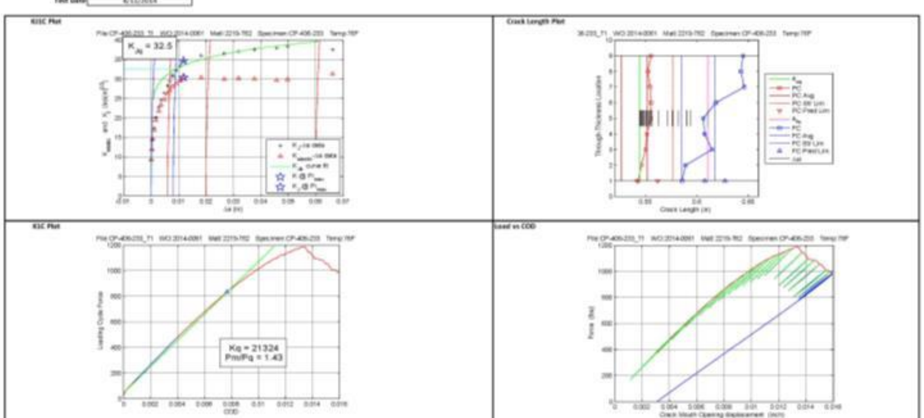

Mechanical Test Facilities

EM10

Fracture Toughness J_{Ic} Test Results

Version 4.3

EM10 Specimen ID	140061404	Geometry	C(T)	"E" (MSI)	10.60	Precrack Pmax (lbf)	1500.0
Other Specimen ID	CP-406-236	"W" (in)	2.0000	"Ec" (MSI)	10.60	Precrack Final "a" (in)	1.0226
Operator	Charles Kay	"B" (in)	0.9990	% diff E & Ec	0.00	Stress Ratio	0.10
Test Date	4/10/2014	"Bn" (in)	0.7980	"V"	0.30	Kmax (ksi_sqrt_in)	8.00
		"Be" (in)	0.9580	"YS" (KSI)	39.30		
Environment	Air	Oreintation	L-T	"UTS" (KSI)	59.10		
Temperature (°F)	73	"An" (in)	0.8000			A_op (in)	1.0226
Pressure (PSIG)	0	Hole Span/2 "H" (in)	0.7100	Flow Stress (KSI)	49.20	A_oq (in)	1.0042
Relative Humidity (%)	NA	COD Span/2 "D" (in)	0.1050	"E"/"YS"	0.27	A_fp (in)	1.1053
Soak Time (min)	0	Coupon #	M4			A_fq (in)	1.0791

	Jq (in*lbs/in^2)	Je_q (in*lbs/in^2)	Jp_q (in*lbs/in^2)	Kjq (ksi(in)^2)	Kjq_at_Je_q (ksi(in)^2)	K_95sec (ksi(in)^2)	K Req Ligament (in)	Pmax/Pq
Results	102.50	92.40	10.10	34.55	32.81	29.25	1.385	1.33

Summary of Test Validities Required for All Tests:			
7.4.5	Initial precrack force	P <= Pm for sample type	Valid
7.4.5.1	Initial Kmax	<40% of Precrack YS	Valid
7.4.5.2	Final Kmax	<60% of K result	Valid
9.1.4.1	Precrack straightness	None > 0.05B	Valid
7.4.5.1	Precrack length	>0.05B or 0.05inch, wide notch	Valid
7.5	Side groove depth	< 0.25B	Valid
Summary of Test Validities Required for Jlc:			
7.4.2	a/W Range for J	0.45 <= a/W <= 0.7	Valid
9.1.5.1	Even Crack Ext.	None < 50% of avg crk ext.	Valid
9.1.5.2	Accuracy of crk ext. pred.	Diff < 0.15 d_ap	Valid
A9.6.4	# pts in region A	# pts >= 1 in A	Valid
A9.6.4	# pts in region B	# pts >= 1 in B	Valid
A9.6.6.6	# Valid J-da pts	# pts >= 5	Valid
A9.8.1	J-da fit coeff C2	C2 < 1.0	Valid
A9.8.2.1	Accuracy of a_oq	|a_oq - a_op| < 0.01W or 0.5mm	Valid
A9.8.2.2	Num pts in a_oq fit	# points >= 8	Valid
A9.8.2.2	0.4Jq<(#pts a_oq fit)<Jq	# points >= 3	Valid
A8.2.2.2	a_oq fit R^2	R^2 > 0.96	Valid
A9.9.1	Thickness requirement	B > 10Jq/FlowStress	Valid
A9.9.2	Ligament requirement	b_o > 10Jq/FlowStress	Valid
A9.9.3	Regression line slope	Slope < flow at da_q	Valid
All validity criteria for Jlc NOT met. Jq is not fully valid Jlc. Non-valid Jq values may still convey valuable fracture toughness information.			
Summary of Test Validities Required for Klc:			
7.4.2	a/W Range for K	0.45 <= a/W <= 0.55	Valid
A5.4.3	K Ligament length	b_o > 2.5(K/YS)^2	NOT Valid
A5.4.2	Pmax/Pq ratio	Less than 1.10	NOT Valid
All validity criteria for K_{Ic} NOT met. Kq is not fully valid K_{Ic}. Non-valid Kq values may still convey valuable fracture toughness information.			

J1C Plot

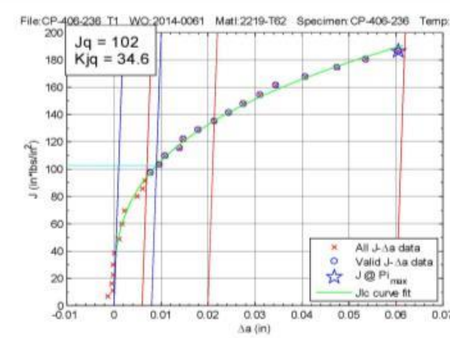

Method File:
FTA NLFT
Comments:
N/A

Mechanical Test Facilities

EM10

Fracture Toughness J_{Ic} Test Results

Version 4.3

EM10 Specimen ID	140061404
Other Specimen ID	CP-406-236
Operator	Charles Kay
Test Date	4/10/2014

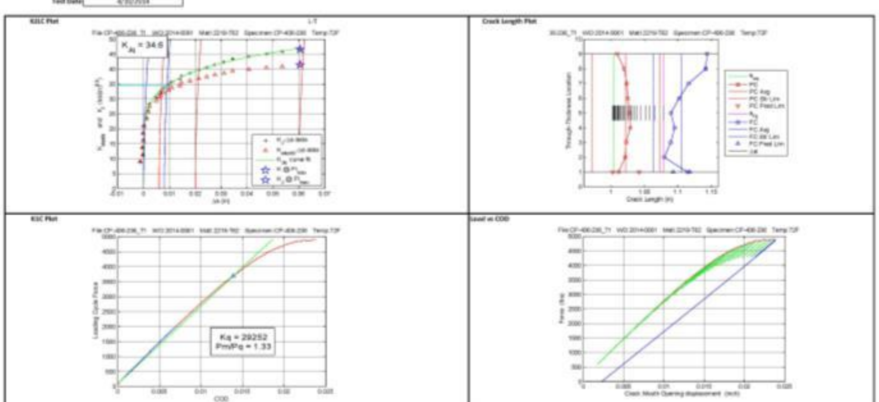

Mechanical Test Facilities

EM10

Fracture Toughness J_{Ic} Test Results

Version 4.3

EM10 Specimen ID	140061406	Geometry	C(T)	"E" (MSI)	10.60	Precrack Pmax (lbf)	1520.0
Other Specimen ID	CP-406-238	"W" (in)	2.0000	"Ec" (MSI)	10.60	Precrack Final "a" (in)	1.0327
Operator	Charles Kay	"B" (in)	1.0020	% diff E & Ec	0.00	Stress Ratio	0.10
Test Date	4/10/2014	"Bn" (in)	0.7980	"V"	0.30	Kmax (ksi_sqrt_in)	8.00
		"Be" (in)	0.9610	"YS" (KSI)	39.30		
Environment	Air	Oreintation	L-T	"UTS" (KSI)	59.10		
Temperature (°F)	72	"An" (in)	0.8000			A_op (in)	1.0327
Pressure (PSIG)	0	Hole Span/2 "H" (in)	0.7110	Flow Stress (KSI)	49.20	A_oq (in)	1.0137
Relative Humidity (%)	NA	COD Span/2 "D" (in)	0.1050	"E"/"YS"	0.27	A_fp (in)	1.1109
Soak Time (min)	0	Coupon #	M4			A_fq (in)	1.0998

	Jq (in*lbs/in^2)	Je_q (in*lbs/in^2)	Jp_q (in*lbs/in^2)	Kjq (ksi(in)^2)	Kjq_at_Je_q (ksi(in)^2)	K_95sec (ksi(in)^2)	K Req Ligament (in)	Pmax/Pq
Results	99.10	89.10	10.00	33.97	32.21	32.56	1.716	1.24

Summary of Test Validities Required for All Tests:			
7.4.5	Initial precrack force	P <= Pm for sample type	Valid
7.4.5.1	Initial Kmax	<40% of Precrack YS	Valid
7.4.5.2	Final Kmax	<60% of K result	Valid
9.1.4.1	Precrack straightness	None > 0.05B	Valid
7.4.5.1	Precrack length	>0.05B or 0.05inch, wide notch	Valid
7.5	Side groove depth	< 0.25B	Valid
Summary of Test Validities Required for Jic:			
7.4.2	a/W Range for J	0.45 <= a/W <= 0.7	Valid
9.1.5.1	Even Crack Ext.	None < 50% of avg crk ext.	Valid
9.1.5.2	Accuracy of crk ext. pred.	Diff < 0.15 d_ap	Valid
A9.6.4	# pts in region A	# pts >= 1 in A	Valid
A9.6.4	# pts in region B	# pts >= 1 in B	Valid
A9.6.6.6	# Valid J-da pts	# pts >= 5	Valid
A9.8.1	J-da fit coeff C2	C2 < 1.0	Valid
A9.8.2.1	Accuracy of a_oq	|a_oq - a_op| < 0.01W or 0.5mm	Valid
A9.8.2.2	Num pts in a_oq fit	# points >= 8	Valid
A9.8.2.2	0.4Jq<(#pts a_oq fit)<Jq	# points >= 3	Valid
A8.2.2.2	a_oq fit R^2	R^2 > 0.96	Valid
A9.9.1	Thickness requirement	B > 10Jq/FlowStress	Valid
A9.9.2	Ligament requirement	b_o > 10Jq/FlowStress	Valid
A9.9.3	Regression line slope	Slope < flow at da_q	Valid
All validity criteria for Jic NOT met. Jq is not fully valid Jic. Non-valid Jq values may still convey valuable fracture toughness information.			
Summary of Test Validities Required for Kic:			
7.4.2	a/W Range for K	0.45 <= a/W <= 0.55	Valid
A5.4.3	K Ligament length	b_o > 2.5(K/YS)^2	NOT Valid
A5.4.2	Pmax/Pq ratio	Less than 1.10	NOT Valid
All validity criteria for K_{Ic} NOT met. Kq is not fully valid K_{Ic}. Non-valid Kq values may still convey valuable fracture toughness information.			

J1C Plot

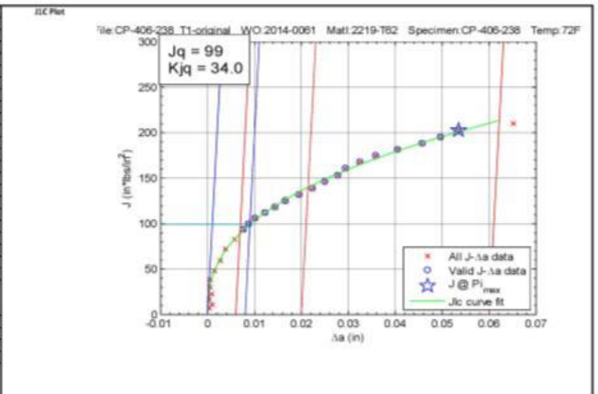

Method File:
FTA NLFT

Comments:
N/A

Mechanical Test Facilities

EM10

Fracture Toughness J_{Ic} Test Results

Version 4.3

EM10 Specimen ID	140061406
Other Specimen ID	CP-406-238
Operator	Charles Kay
Test Date	4/10/2014

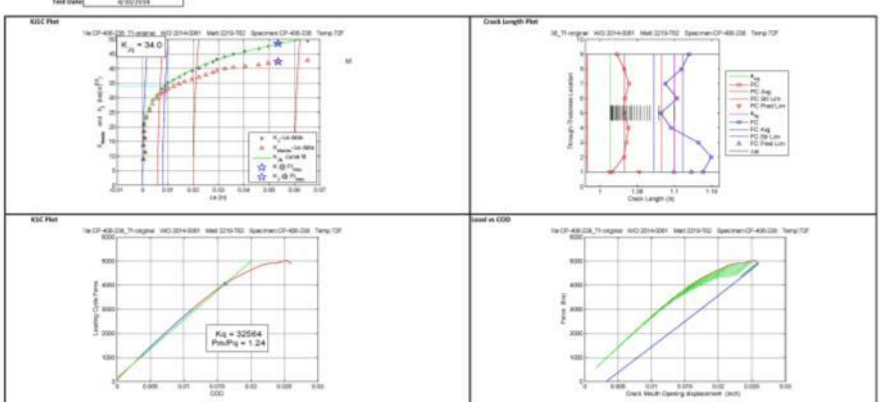

Mechanical Test Facilities

EM10

Fracture Toughness J_{Ic} Test Results

Version 4.3

EM10 Specimen ID	140061409	Geometry	C(T)	"E" (MSI)	10.60	Precrack Pmax (lbf)	1508.0
Other Specimen ID	CP-406-241	"W" (in)	2.0000	"Ec" (MSI)	10.60	Precrack Final "a" (in)	1.0399
Operator	Charles Kay	"B" (in)	0.9990	% diff E & Ec	0.00	Stress Ratio	0.10
Test Date	4/10/2014	"Bn" (in)	0.7960	"V"	0.30	Kmax (ksi_sqrt_in)	8.00
		"Be" (in)	0.9570	"YS" (KSI)	39.10		
Environment	Air	Oreintation	T-L	"UTS" (KSI)	59.00		
Temperature (°F)	73	"An" (in)	0.8000			A_op (in)	1.0399
Pressure (PSIG)	0	Hole Span/2 "H" (in)	0.7100	Flow Stress (KSI)	49.06	A_oq (in)	1.0237
Relative Humidity (%)	NA	COD Span/2 "D" (in)	0.1050	"E"/"YS"	0.27	A_fp (in)	1.1228
Soak Time (min)	0	Coupon #	M4			A_fq (in)	1.0982

	Jq (in*lbs/in^2)	Je_q (in*lbs/in^2)	Jp_q (in*lbs/in^2)	Kjq (ksi(in)^2)	Kjq_at_Je_q (ksi(in)^2)	K_95sec (ksi(in)^2)	K Req Ligament (in)	Pmax/Pq
Results	86.00	78.50	7.50	31.65	30.24	28.41	1.320	1.17

Summary of Test Validities Required for All Tests:			
7.4.5	Initial precrack force	P <= Pm for sample type	Valid
7.4.5.1	Initial Kmax	<40% of Precrack YS	Valid
7.4.5.2	Final Kmax	<60% of K result	Valid
9.1.4.1	Precrack straightness	None > 0.05B	Valid
7.4.5.1	Precrack length	>0.05B or 0.05inch, wide notch	Valid
7.5	Side groove depth	< 0.25B	Valid
Summary of Test Validities Required for Jlc:			
7.4.2	a/W Range for J	0.45 <= a/W <= 0.7	Valid
9.1.5.1	Even Crack Ext.	None < 50% of avg crk ext.	Valid
9.1.5.2	Accuracy of crk ext. pred.	Diff < 0.15 d_ap	Valid
A9.6.4	# pts in region A	# pts >= 1 in A	Valid
A9.6.4	# pts in region B	# pts >= 1 in B	Valid
A9.6.6.6	# Valid J-da pts	# pts >= 5	Valid
A9.8.1	J-da fit coeff C2	C2 < 1.0	Valid
A9.8.2.1	Accuracy of a_oq	|a_oq - a_op| < 0.01W or 0.5mm	Valid
A9.8.2.2	Num pts in a_oq fit	# points >= 8	Valid
A9.8.2.2	0.4Jq<(#pts a_oq fit)<Jq	# points >= 3	Valid
A8.2.2.2	a_oq fit R^2	R^2 > 0.96	Valid
A9.9.1	Thickness requirement	B > 10Jq/FlowStress	Valid
A9.9.2	Ligament requirement	b_o > 10Jq/FlowStress	Valid
A9.9.3	Regression line slope	Slope < flow at da_q	Valid
All validity criteria for Jlc NOT met. Jq is not fully valid Jlc.			
Non-valid Jq values may still convey valuable fracture toughness information.			
Summary of Test Validities Required for Klc:			
7.4.2	a/W Range for K	0.45 <= a/W <= 0.55	Valid
A5.4.3	K Ligament length	b_o > 2.5(K/YS)^2	NOT Valid
A5.4.2	Pmax/Pq ratio	Less than 1.10	NOT Valid
All validity criteria for K_{Ic} NOT met. Kq is not fully valid K_{Ic}.			
Non-valid Kq values may still convey valuable fracture toughness information.			

J1C Plot

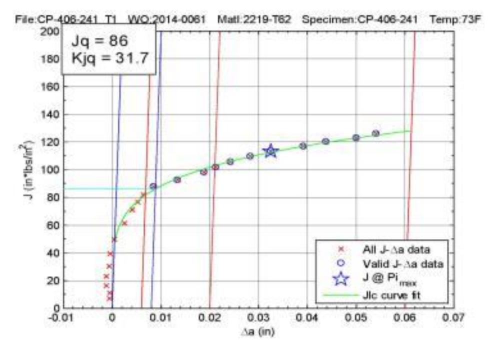

Method File:

FTA NLFT

Comments:

N/A

Mechanical Test Facilities

EM10

Fracture Toughness J_{Ic} Test Results

Version 4.3

EM10 Specimen ID	140061409
Other Specimen ID	CP-406-241
Operator	Charles Kay
Test Date	4/10/2014

KJ1C Plot

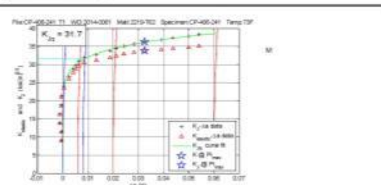

Crack Length Plot

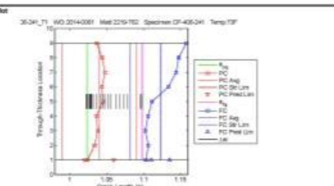

KSC Plot

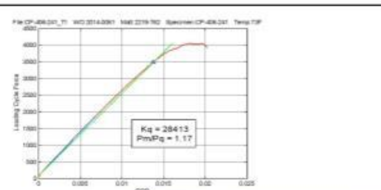

Load vs COD

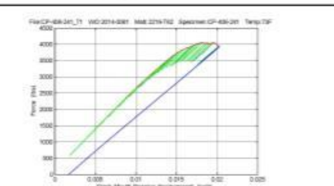

Mechanical Test Facilities

EM10

Fracture Toughness J_{Ic} Test Results

Version 4.3

EM10 Specimen ID	140061411	Geometry	C(T)	"E" (MSI)	10.60	Precrack Pmax (lbf)	1919.0
Other Specimen ID	CP-406-243	"W" (in)	2.0000	"Ec" (MSI)	10.60	Precrack Final "a" (in)	1.0304
Operator	Charles Kay	"B" (in)	1.0000	% diff E & Ec	0.00	Stress Ratio	0.10
Test Date	4/10/2014	"Bn" (in)	0.7990	"V"	0.30	Kmax (ksi_sqrt_in)	8.00
		"Be" (in)	0.9600	"YS" (KSI)	39.10		
Environment	Air	Oreintation	T-L	"UTS" (KSI)	59.00		
Temperature (°F)	73	"An" (in)	0.7990			A_op (in)	1.0304
Pressure (PSIG)	0	Hole Span/2 "H" (in)	0.7100	Flow Stress (KSI)	49.06	A_oq (in)	1.0148
Relative Humidity (%)	NA	COD Span/2 "D" (in)	0.1030	"E"/"YS"	0.27	A_fp (in)	1.1348
Soak Time (min)	0	Coupon #	M4			A_fq (in)	1.0818

	Jq (in*lbs/in^2)	Je_q (in*lbs/in^2)	Jp_q (in*lbs/in^2)	Kjq (ksi(in)^2)	Kjq_at_Je_q (ksi(in)^2)	K_95sec (ksi(in)^2)	K Req Ligament (in)	Pmax/Pq
Results	93.40	84.10	9.30	32.99	31.30	28.66	1.343	1.19

Summary of Test Validities Required for All Tests:			
7.4.5	Initial precrack force	P <= Pm for sample type	Valid
7.4.5.1	Initial Kmax	<40% of Precrack YS	Valid
7.4.5.2	Final Kmax	<60% of K result	Valid
9.1.4.1	Precrack straightness	None > 0.05B	Valid
7.4.5.1	Precrack length	>0.05B or 0.05inch, wide notch	Valid
7.5	Side groove depth	< 0.25B	Valid
Summary of Test Validities Required for Jic:			
7.4.2	a/W Range for J	0.45 <= a/W <= 0.7	Valid
9.1.5.1	Even Crack Ext.	None < 50% of avg crk ext.	Valid
9.1.5.2	Accuracy of crk ext. pred.	Diff < 0.15 d_ap	NOT Valid
A9.6.4	# pts in region A	# pts >= 1 in A	Valid
A9.6.4	# pts in region B	# pts >= 1 in B	Valid
A9.6.6.6	# Valid J-da pts	# pts >= 5	Valid
A9.8.1	J-da fit coeff C2	C2 < 1.0	Valid
A9.8.2.1	Accuracy of a_oq	|a_oq - a_op| < 0.01W or 0.5mm	Valid
A9.8.2.2	Num pts in a_oq fit	# points >= 8	Valid
A9.8.2.2	0.4Jq<(#pts a_oq fit)<Jq	# points >= 3	Valid
A8.2.2.2	a_oq fit R^2	R^2 > 0.96	Valid
A9.9.1	Thickness requirement	B > 10Jq/FlowStress	Valid
A9.9.2	Ligament requirement	b_o > 10Jq/FlowStress	Valid
A9.9.3	Regression line slope	Slope < flow at da_q	Valid
All validity criteria for Jic NOT met. Jq is not fully valid Jic. Non-valid Jq values may still convey valuable fracture toughness information.			
Summary of Test Validities Required for Kic:			
7.4.2	a/W Range for K	0.45 <= a/W <= 0.55	Valid
A5.4.3	K Ligament length	b_o > 2.5(K/YS)^2	NOT Valid
A5.4.2	Pmax/Pq ratio	Less than 1.10	NOT Valid
All validity criteria for K_{Ic} NOT met. Kq is not fully valid K_{Ic}. Non-valid Kq values may still convey valuable fracture toughness information.			

J1C Plot

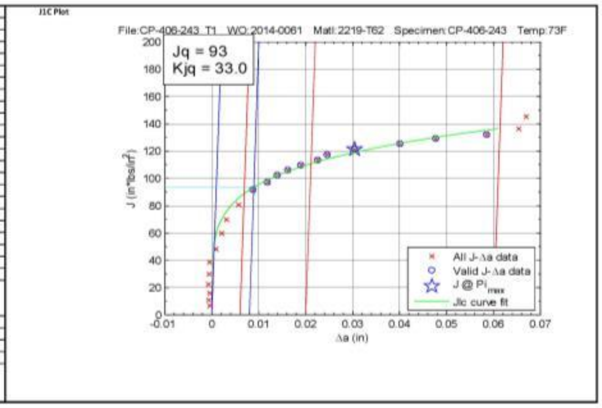

Method File:

FTA NLFT

Comments:

N/A

Mechanical Test Facilities

EM10

Fracture Toughness J_{Ic} Test Results

Version 4.3

EM10 Specimen ID	140061411
Other Specimen ID	CP-406-243
Operator	Charles Kay
Test Date	4/10/2014

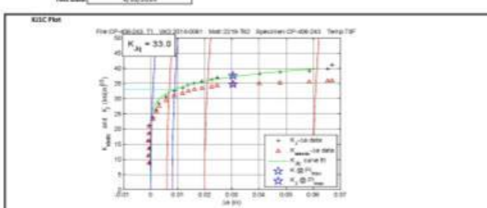

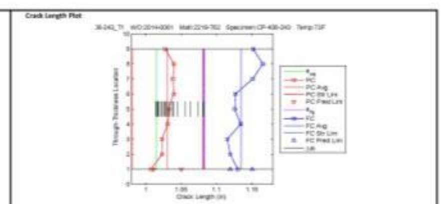

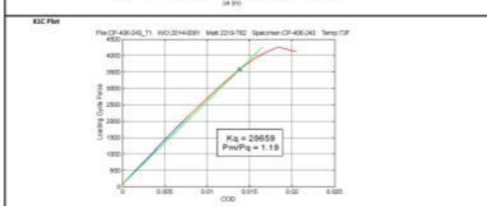

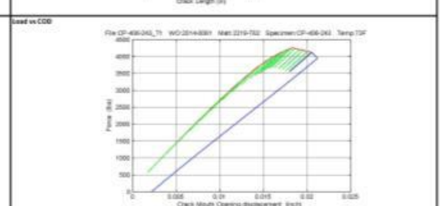

Mechanical Test Facilities

EM10

Fracture Toughness J_{Ic} Test Results

Version 4.3

EM10 Specimen ID	140061414
Other Specimen ID	CP-406-246
Operator	Charles Kay
Test Date	4/11/2014
Environment	Air
Temperature (°F)	73
Pressure (PSIG)	0
Relative Humidity (%)	NA
Soak Time (min)	0

Geometry	C(T)
"W" (in)	1.0000
"B" (in)	0.5020
"Bn" (in)	0.3980
"Be" (in)	0.4800
Oreintation	S-T
"An" (in)	0.4040
Hole Span/2 "H" (in)	0.3550
COD Span/2 "D" (in)	0.0990
Coupon #	M4

"E" (MSI)	10.60
"Ec" (MSI)	10.60
% diff E & Ec	0.00
"V"	0.30
"YS" (KSI)	39.20
"UTS" (KSI)	60.10
Flow Stress (KSI)	49.63
"E"/"YS"	0.27

Precrack Pmax (lbf)	665.0
Precrack Final "a" (in)	0.5257
Stress Ratio	0.10
Kmax (ksi_sqrt_in)	10.00
A_op (in)	0.5257
A_oq (in)	0.5226
A_fp (in)	0.6169
A_fq (in)	0.6026

	Jq (in*lbs/in^2)	Je_q (in*lbs/in^2)	Jp_q (in*lbs/in^2)	Kjq (ksi(in)^2)	Kjq_at_Je_q (ksi(in)^2)	K_95sec (ksi(in)^2)	K Req Ligament (in)	Pmax/Pq
Results	78.00	66.20	11.80	30.14	27.76	22.80	0.846	1.24

Summary of Test Validities Required for All Tests:			
7.4.5	Initial precrack force	P <= Pm for sample type	Valid
7.4.5.1	Initial Kmax	<40% of Precrack YS	Valid
7.4.5.2	Final Kmax	<60% of K result	Valid
9.1.4.1	Precrack straightness	None > 0.05B	Valid
7.4.5.1	Precrack length	>0.05B or 0.05inch, wide notch	Valid
7.5	Side groove depth	< 0.25B	Valid
Summary of Test Validities Required for Jlc:			
7.4.2	a/W Range for J	0.45 <= a/W <= 0.7	Valid
9.1.5.1	Even Crack Ext.	None < 50% of avg crk ext.	Valid
9.1.5.2	Accuracy of crk ext. pred.	Diff < 0.15 d_ap	Valid
A9.6.4	# pts in region A	# pts >= 1 in A	Valid
A9.6.4	# pts in region B	# pts >= 1 in B	Valid
A9.6.6.6	# Valid J-da pts	# pts >= 5	Valid
A9.8.1	J-da fit coeff C2	C2 < 1.0	Valid
A9.8.2.1	Accuracy of a_oq	|a_oq - a_op| < 0.01W or 0.5mm	Valid
A9.8.2.2	Num pts in a_oq fit	# points >= 8	Valid
A9.8.2.2	0.4Jq<(#pts a_oq fit)<Jq	# points >= 3	Valid
A8.2.2.2	a_oq fit R^2	R^2 > 0.96	Valid
A9.9.1	Thickness requirement	B > 10Jq/FlowStress	Valid
A9.9.2	Ligament requirement	b_o > 10Jq/FlowStress	Valid
A9.9.3	Regression line slope	Slope < flow at da_q	Valid
All validity criteria for Jlc NOT met. Jq is not fully valid Jlc. Non-valid Jq values may still convey valuable fracture toughness information.			
Summary of Test Validities Required for Klc:			
7.4.2	a/W Range for K	0.45 <= a/W <= 0.55	Valid
A5.4.3	K Ligament length	b_o > 2.5(K/YS)^2	NOT Valid
A5.4.2	Pmax/Pq ratio	Less than 1.10	NOT Valid
All validity criteria for K_{Ic} NOT met. Kq is not fully valid K_{Ic}. Non-valid Kq values may still convey valuable fracture toughness information.			

J1C Plot

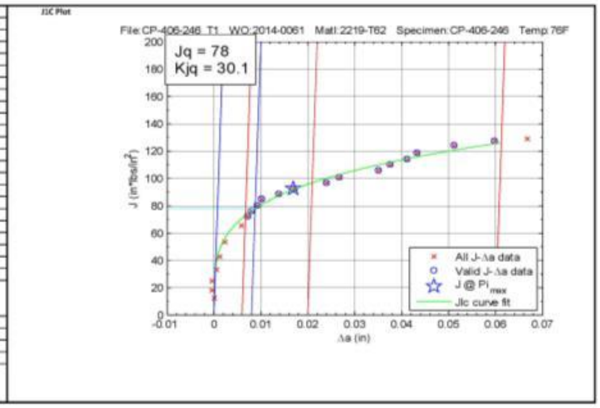

Method File:

FTA NLFT

Comments:

N/A

Mechanical Test Facilities

EM10

Fracture Toughness J_{Ic} Test Results

Version 4.3

EM10 Specimen ID	140061414
Other Specimen ID	CP-406-246
Operator	Charles Kay
Test Date	4/11/2014

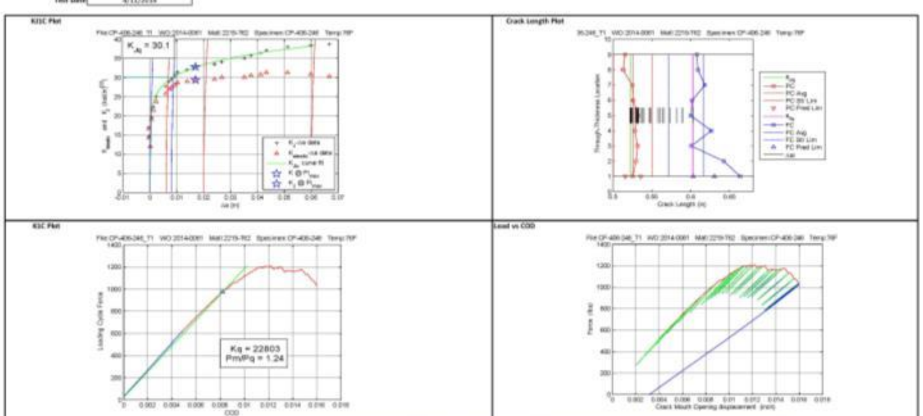

Mechanical Test Facilities

EM10

Fracture Toughness J_{Ic} Test Results

Version 4.3

EM10 Specimen ID	140061416	Geometry	C(T)	"E" (MSI)	10.60	Precrack Pmax (lbf)	528.0
Other Specimen ID	CP-406-248	"W" (in)	1.0000	"Ec" (MSI)	10.60	Precrack Final "a" (in)	0.5303
Operator	Charles Kay	"B" (in)	0.5020	% diff E & Ec	0.00	Stress Ratio	0.10
Test Date	4/11/2014	"Bn" (in)	0.3970	"V"	0.30	Kmax (ksi_sqrt_in)	8.00
		"Be" (in)	0.4800	"YS" (KSI)	39.20		
Environment	Air	Oreintation	S-T	"UTS" (KSI)	60.10		
Temperature (°F)	73	"An" (in)	0.4010			A_op (in)	0.5303
Pressure (PSIG)	0	Hole Span/2 "H" (in)	0.3550	Flow Stress (KSI)	49.63	A_oq (in)	0.5255
Relative Humidity (%)	NA	COD Span/2 "D" (in)	0.0990	"E"/"YS"	0.27	A_fp (in)	0.6109
Soak Time (min)	0	Coupon #	M4			A_fq (in)	0.6087

	Jq (in*lbs/in^2)	Je_q (in*lbs/in^2)	Jp_q (in*lbs/in^2)	Kjq (ksi(in)^2)	Kjq_at_Je_q (ksi(in)^2)	K_95sec (ksi(in)^2)	K Req Ligament (in)	Pmax/Pq
Results	50.90	44.20	6.70	24.35	22.68	20.72	0.699	1.26

Summary of Test Validities Required for All Tests:			
7.4.5	Initial precrack force	P <= Pm for sample type	Valid
7.4.5.1	Initial Kmax	<40% of Precrack YS	Valid
7.4.5.2	Final Kmax	<60% of K result	Valid
9.1.4.1	Precrack straightness	None > 0.05B	Valid
7.4.5.1	Precrack length	>0.05B or 0.05inch, wide notch	Valid
7.5	Side groove depth	< 0.25B	Valid
Summary of Test Validities Required for Jic:			
7.4.2	a/W Range for J	0.45 <= a/W <= 0.7	Valid
9.1.5.1	Even Crack Ext.	None < 50% of avg crk ext.	Valid
9.1.5.2	Accuracy of crk ext. pred.	Diff < 0.15 d_ap	Valid
A9.6.4	# pts in region A	# pts >= 1 in A	Valid
A9.6.4	# pts in region B	# pts >= 1 in B	Valid
A9.6.6.6	# Valid J-da pts	# pts >= 5	Valid
A9.8.1	J-da fit coeff C2	C2 < 1.0	Valid
A9.8.2.1	Accuracy of a_oq	|a_oq - a_op| < 0.01W or 0.5mm	Valid
A9.8.2.2	Num pts in a_oq fit	# points >= 8	Valid
A9.8.2.2	0.4Jq<(#pts a_oq fit)<Jq	# points >= 3	Valid
A8.2.2.2	a_oq fit R^2	R^2 > 0.96	Valid
A9.9.1	Thickness requirement	B > 10Jq/FlowStress	Valid
A9.9.2	Ligament requirement	b_o > 10Jq/FlowStress	Valid
A9.9.3	Regression line slope	Slope < flow at da_q	Valid
All validity criteria for Jic NOT met. Jq is not fully valid Jic. Non-valid Jq values may still convey valuable fracture toughness information.			
Summary of Test Validities Required for Kic:			
7.4.2	a/W Range for K	0.45 <= a/W <= 0.55	Valid
A5.4.3	K Ligament length	b_o > 2.5(K/YS)^2	NOT Valid
A5.4.2	Pmax/Pq ratio	Less than 1.10	NOT Valid
All validity criteria for K_{Ic} NOT met. Kq is not fully valid K_{Ic}. Non-valid Kq values may still convey valuable fracture toughness information.			

J1C Plot

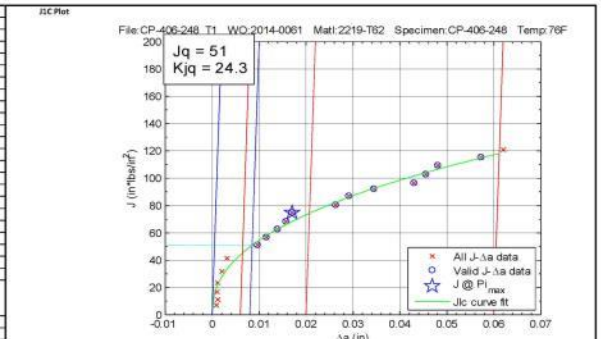

Method File:

FTA NLFT

Comments:

N/A

Mechanical Test Facilities

EM10

Fracture Toughness J_{Ic} Test Results

Version 4.3

EM10 Specimen ID	140061416
Other Specimen ID	CP-406-248
Operator	Charles Kay
Test Date	4/11/2014

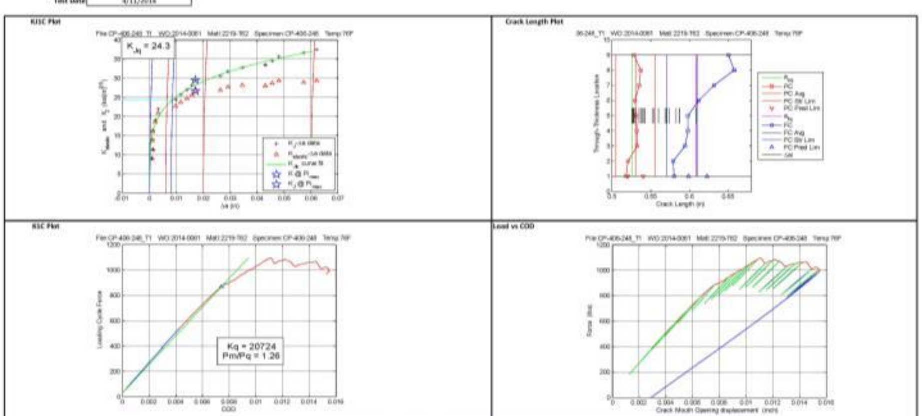

Mechanical Test Facilities

EM10

Fracture Toughness J_{Ic} Test Results

Version 4.3

EM10 Specimen ID	140061419
Other Specimen ID	CP-406-251
Operator	Charles Kay
Test Date	4/10/2014
Environment	Air
Temperature (°F)	73
Pressure (PSIG)	0
Relative Humidity (%)	NA
Soak Time (min)	0

Geometry	C(T)
"W" (in)	2.0000
"B" (in)	0.9990
"Bn" (in)	0.7940
"Be" (in)	0.9570
Orientation	L-T
"An" (in)	0.7980
Hole Span/2 "H" (in)	0.7100
COD Span/2 "D" (in)	0.1040
Coupon #	M5

"E" (MSI)	10.60
"Ec" (MSI)	10.60
% diff E & Ec	0.00
"V"	0.30
"YS" (KSI)	38.00
"UTS" (KSI)	57.80
Flow Stress (KSI)	47.94
"E"/"YS"	0.28

Precrack Pmax (lbf)	1527.0
Precrack Final "a" (in)	1.0378
Stress Ratio	0.10
Kmax (ksi_sqrt_in)	8.00
A_op (in)	1.0378
A_oq (in)	1.0183
A_fp (in)	1.1209
A_fq (in)	1.0978

	Jq (in*lbs/in^2)	Je_q (in*lbs/in^2)	Jp_q (in*lbs/in^2)	Kjq (ksi(in)^2)	Kjq_at_Je_q (ksi(in)^2)	K_95sec (ksi(in)^2)	K Req Ligament (in)	Pmax/Pq
Results	108.40	96.30	12.10	35.53	33.50	29.48	1.504	1.29

Summary of Test Validities Required for All Tests:			
7.4.5	Initial precrack force	P <= Pm for sample type	Valid
7.4.5.1	Initial Kmax	<40% of Precrack YS	Valid
7.4.5.2	Final Kmax	<60% of K result	Valid
9.1.4.1	Precrack straightness	None > 0.05B	Valid
7.4.5.1	Precrack length	>0.05B or 0.05inch, wide notch	Valid
7.5	Side groove depth	< 0.25B	Valid
Summary of Test Validities Required for Jic:			
7.4.2	a/W Range for J	0.45 <= a/W <= 0.7	Valid
9.1.5.1	Even Crack Ext.	None < 50% of avg crk ext.	Valid
9.1.5.2	Accuracy of crk ext. pred.	Diff < 0.15 d_ap	Valid
A9.6.4	# pts in region A	# pts >= 1 in A	Valid
A9.6.4	# pts in region B	# pts >= 1 in B	Valid
A9.6.6.6	# Valid J-da pts	# pts >= 5	Valid
A9.8.1	J-da fit coeff C2	C2 < 1.0	Valid
A9.8.2.1	Accuracy of a_oq	|a_oq - a_op| < 0.01W or 0.5mm	Valid
A9.8.2.2	Num pts in a_oq fit	# points >= 8	Valid
A9.8.2.2	0.4Jq<(#pts a_oq fit)<Jq	# points >= 3	Valid
A8.2.2.2	a_oq fit R^2	R^2 > 0.96	Valid
A9.9.1	Thickness requirement	B > 10Jq/FlowStress	Valid
A9.9.2	Ligament requirement	b_o > 10Jq/FlowStress	Valid
A9.9.3	Regression line slope	Slope < flow at da_q	Valid
All validity criteria for Jic NOT met. Jq is not fully valid Jic. Non-valid Jq values may still convey valuable fracture toughness information.			
Summary of Test Validities Required for Kic:			
7.4.2	a/W Range for K	0.45 <= a/W <= 0.55	Valid
A5.4.3	K Ligament length	b_o > 2.5(K/YS)^2	NOT Valid
A5.4.2	Pmax/Pq ratio	Less than 1.10	NOT Valid
All validity criteria for K_{Ic} NOT met. Kq is not fully valid K_{Ic}. Non-valid Kq values may still convey valuable fracture toughness information.			

J1C Plot

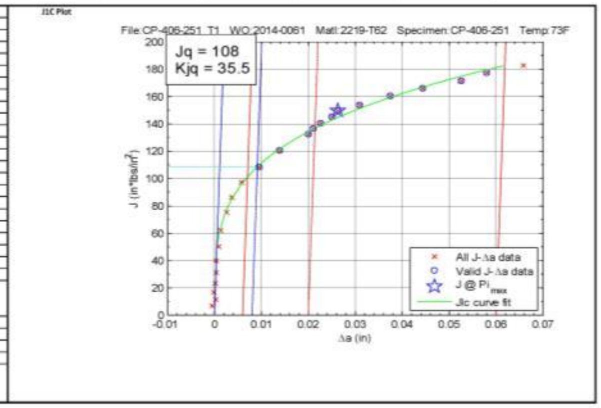

Method File:
FTA NLFT

Comments:
N/A

Mechanical Test Facilities

EM10

Fracture Toughness J_{Ic} Test Results

Version 4.3

EM10 Specimen ID	140061419
Other Specimen ID	CP-406-251
Operator	Charles Kay
Test Date	4/10/2014

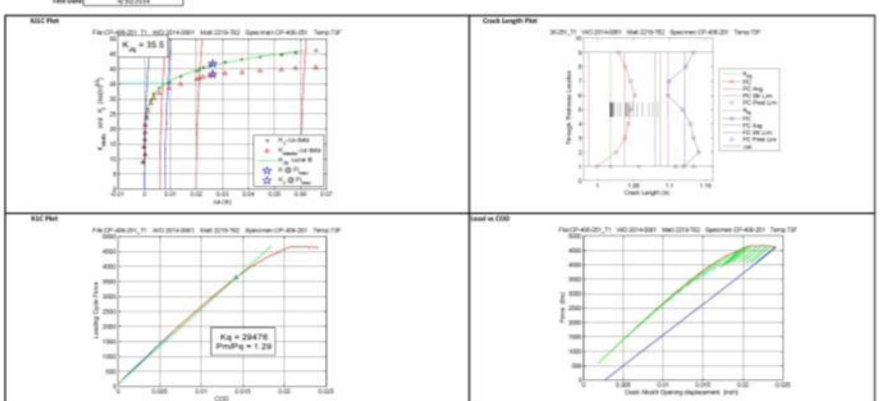

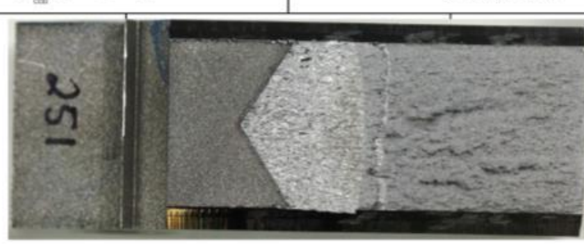

Mechanical Test Facilities

EM10

Fracture Toughness J_{Ic} Test Results

Version 4.3

EM10 Specimen ID	140061421	Geometry	C(T)	"E" (MSI)	10.60	Precrack Pmax (lbf)	1534.0
Other Specimen ID	CP-406-253	"W" (in)	2.0000	"Ec" (MSI)	10.60	Precrack Final "a" (in)	1.0485
Operator	Charles Kay	"B" (in)	1.0000	% diff E & Ec	0.00	Stress Ratio	0.10
Test Date	4/10/2014	"Bn" (in)	0.7970	"V"	0.30	Kmax (ksi_sqrt_in)	8.00
		"Be" (in)	0.9590	"YS" (KSI)	38.00		
Environment	Air	Oreintation	L-T	"UTS" (KSI)	57.80		
Temperature (°F)	73	"An" (in)	0.7990			A_op (in)	1.0485
Pressure (PSIG)	0	Hole Span/2 "H" (in)	0.7100	Flow Stress (KSI)	47.94	A_oq (in)	1.0297
Relative Humidity (%)	NA	COD Span/2 "D" (in)	0.1050	"E"/"YS"	0.28	A_fp (in)	1.1305
Soak Time (min)	0	Coupon #	M5			A_fq (in)	1.1138

	Jq (in*lbs/in^2)	Je_q (in*lbs/in^2)	Jp_q (in*lbs/in^2)	Kjq (ksi(in)^2)	Kjq_at_Je_q (ksi(in)^2)	K_95sec (ksi(in)^2)	K Req Ligament (in)	Pmax/Pq
Results	107.30	95.40	11.90	35.35	33.34	29.74	1.531	1.31

Summary of Test Validities Required for All Tests:			
7.4.5	Initial precrack force	P <= Pm for sample type	Valid
7.4.5.1	Initial Kmax	<40% of Precrack YS	Valid
7.4.5.2	Final Kmax	<60% of K result	Valid
9.1.4.1	Precrack straightness	None > 0.05B	Valid
7.4.5.1	Precrack length	>0.05B or 0.05inch, wide notch	Valid
7.5	Side groove depth	< 0.25B	Valid
Summary of Test Validities Required for Jic:			
7.4.2	a/W Range for J	0.45 <= a/W <= 0.7	Valid
9.1.5.1	Even Crack Ext.	None < 50% of avg crk ext.	Valid
9.1.5.2	Accuracy of crk ext. pred.	Diff < 0.15 d_ap	Valid
A9.6.4	# pts in region A	# pts >= 1 in A	Valid
A9.6.4	# pts in region B	# pts >= 1 in B	Valid
A9.6.6.6	# Valid J-da pts	# pts >= 5	Valid
A9.8.1	J-da fit coeff C2	C2 < 1.0	Valid
A9.8.2.1	Accuracy of a_oq	|a_oq - a_op| < 0.01W or 0.5mm	Valid
A9.8.2.2	Num pts in a_oq fit	# points >= 8	Valid
A9.8.2.2	0.4Jq<(#pts a_oq fit)<Jq	# points >= 3	Valid
A8.2.2.2	a_oq fit R^2	R^2 > 0.96	Valid
A9.9.1	Thickness requirement	B > 10Jq/FlowStress	Valid
A9.9.2	Ligament requirement	b_o > 10Jq/FlowStress	Valid
A9.9.3	Regression line slope	Slope < flow at da_q	Valid
All validity criteria for Jic NOT met. Jq is not fully valid Jic. Non-valid Jq values may still convey valuable fracture toughness information.			
Summary of Test Validities Required for KIc:			
7.4.2	a/W Range for K	0.45 <= a/W <= 0.55	Valid
A5.4.3	K Ligament length	b_o > 2.5(K/YS)^2	NOT Valid
A5.4.2	Pmax/Pq ratio	Less than 1.10	NOT Valid
All validity criteria for K_{Ic} NOT met. Kq is not fully valid K_{Ic}. Non-valid Kq values may still convey valuable fracture toughness information.			

J1C Plot

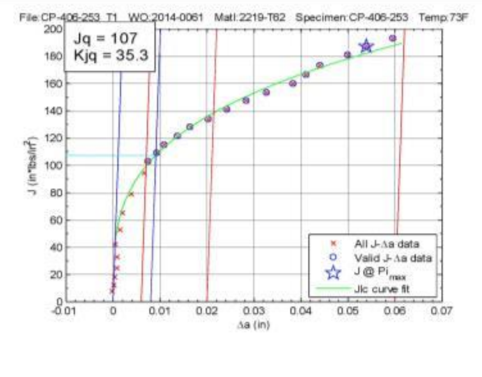

Method File:
FTA NLFT

Comments:
N/A

Mechanical Test Facilities

EM10

Fracture Toughness J_{Ic} Test Results

Version 4.3

EM10 Specimen ID	140061421
Other Specimen ID	CP-406-253
Operator	Charles Kay
Test Date	4/10/2014

KJ1C Plot

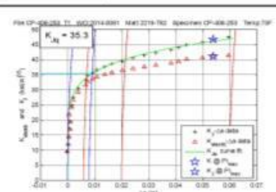

Crack Length Plot

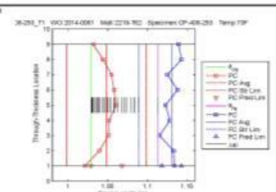

K1C Plot

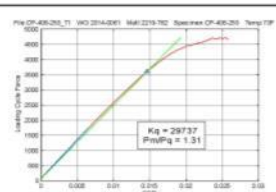

Load vs COD

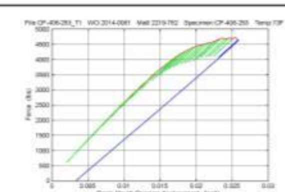

Mechanical Test Facilities

EM10

Fracture Toughness J_{Ic} Test Results

Version 4.3

EM10 Specimen ID	140061424	Geometry	C(T)	"E" (MSI)	10.60	Precrack Pmax (lbf)	1524.0
Other Specimen ID	CP-406-256	"W" (in)	1.9990	"Ec" (MSI)	10.60	Precrack Final "a" (in)	1.0555
Operator	Charles Kay	"B" (in)	0.9990	% diff E & Ec	0.00	Stress Ratio	0.10
Test Date	4/1/2014	"Bn" (in)	0.7960	"V"	0.30	Kmax (ksi_sqrt_in)	8.00
		"Be" (in)	0.9580	"YS" (KSI)	37.40		
Environment	Air	Oreintation	T-L	"UTS" (KSI)	56.60		
Temperature (°F)	73	"An" (in)	0.7990			A_op (in)	1.0555
Pressure (PSIG)	0	Hole Span/2 "H" (in)	0.7100	Flow Stress (KSI)	47.00	A_oq (in)	1.0373
Relative Humidity (%)	NA	COD Span/2 "D" (in)	0.1050	"E"/"YS"	0.28	A_fp (in)	1.1339
Soak Time (min)	0	Coupon #	M5			A_fq (in)	1.1107

	Jq (in*lbs/in^2)	Je_q (in*lbs/in^2)	Jp_q (in*lbs/in^2)	Kjq (ksi(in)^2)	Kjq_at_Je_q (ksi(in)^2)	K_95sec (ksi(in)^2)	K Req Ligament (in)	Pmax/Pq
Results	86.30	77.30	9.00	31.71	30.01	27.88	1.389	1.15

Summary of Test Validities Required for All Tests:			
7.4.5	Initial precrack force	P <= Pm for sample type	Valid
7.4.5.1	Initial Kmax	<40% of Precrack YS	Valid
7.4.5.2	Final Kmax	<60% of K result	Valid
9.1.4.1	Precrack straightness	None > 0.05B	Valid
7.4.5.1	Precrack length	>0.05B or 0.05inch, wide notch	Valid
7.5	Side groove depth	< 0.25B	Valid
Summary of Test Validities Required for Jlc:			
7.4.2	a/W Range for J	0.45 <= a/W <= 0.7	Valid
9.1.5.1	Even Crack Ext.	None < 50% of avg crk ext.	Valid
9.1.5.2	Accuracy of crk ext. pred.	Diff < 0.15 d_ap	Valid
A9.6.4	# pts in region A	# pts >= 1 in A	Valid
A9.6.4	# pts in region B	# pts >= 1 in B	Valid
A9.6.6.6	# Valid J-da pts	# pts >= 5	Valid
A9.8.1	J-da fit coeff C2	C2 < 1.0	Valid
A9.8.2.1	Accuracy of a_oq	|a_oq - a_op| < 0.01W or 0.5mm	Valid
A9.8.2.2	Num pts in a_oq fit	# points >= 8	Valid
A9.8.2.2	0.4Jq<(#pts a_oq fit)<Jq	# points >= 3	Valid
A8.2.2.2	a_oq fit R^2	R^2 > 0.96	Valid
A9.9.1	Thickness requirement	B > 10Jq/FlowStress	Valid
A9.9.2	Ligament requirement	b_o > 10Jq/FlowStress	Valid
A9.9.3	Regression line slope	Slope < flow at da_q	Valid
All validity criteria for Jlc NOT met. Jq is not fully valid Jlc. Non-valid Jq values may still convey valuable fracture toughness information.			
Summary of Test Validities Required for Klc:			
7.4.2	a/W Range for K	0.45 <= a/W <= 0.55	Valid
A5.4.3	K Ligament length	b_o > 2.5(K/YS)^2	NOT Valid
A5.4.2	Pmax/Pq ratio	Less than 1.10	NOT Valid
All validity criteria for K_{Ic} NOT met. Kq is not fully valid K_{Ic}. Non-valid Kq values may still convey valuable fracture toughness information.			

J1C Plot

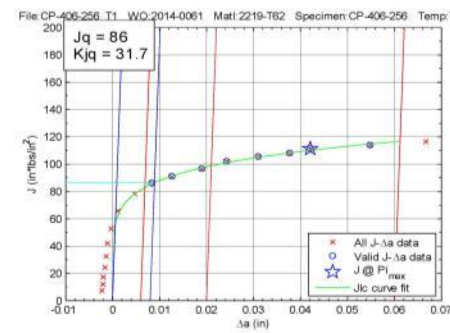

Method File:

FTA NLFT

Comments:

N/A

Mechanical Test Facilities

EM10

Fracture Toughness J_{Ic} Test Results

Version 4.3

EM10 Specimen ID	140061424
Other Specimen ID	CP-406-256
Operator	Charles Kay
Test Date	4/1/2014

KJIC Plot

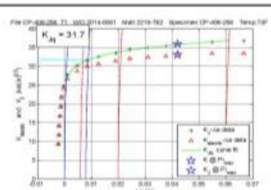

Crack Length Plot

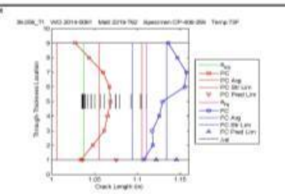

KIC Plot

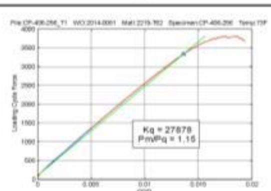

Load vs COD

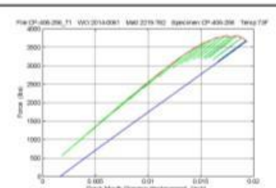

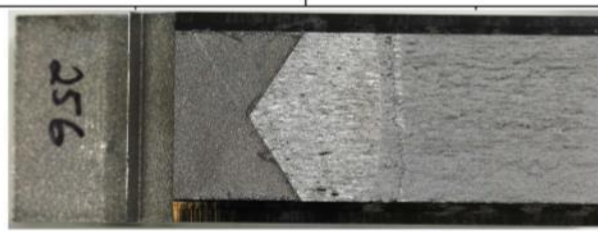

Mechanical Test Facilities

EM10

Fracture Toughness J_{Ic} Test Results

Version 4.3

EM10 Specimen ID	140061426	Geometry	C(T)	"E" (MSI)	10.60	Precrack Pmax (lbf)	1537.0
Other Specimen ID	CP-406-258	"W" (in)	2.0000	"Ec" (MSI)	10.60	Precrack Final "a" (in)	1.0666
Operator	Charles Kay	"B" (in)	1.0000	% diff E & Ec	0.00	Stress Ratio	0.10
Test Date	4/10/2014	"Bn" (in)	0.7980	"V"	0.30	Kmax (ksi_sqrt_in)	8.00
		"Be" (in)	0.9590	"YS" (KSI)	37.40		
Environment	Air	Oreintation	T-L	"UTS" (KSI)	56.60		
Temperature (°F)	73	"An" (in)	0.8000			A_op (in)	1.0666
Pressure (PSIG)	0	Hole Span/2 "H" (in)	0.7100	Flow Stress (KSI)	47.00	A_oq (in)	1.0513
Relative Humidity (%)	NA	COD Span/2 "D" (in)	0.1040	"E"/"YS"	0.28	A_fp (in)	1.1619
Soak Time (min)	0	Coupon #	MS			A_fq (in)	1.1349

	Jq (in*lbs/in^2)	Je_q (in*lbs/in^2)	Jp_q (in*lbs/in^2)	Kjq (ksi(in)^2)	Kjq_at_Je_q (ksi(in)^2)	K_95sec (ksi(in)^2)	K Req Ligament (in)	Pmax/Pq
Results	85.60	77.40	8.20	31.57	30.02	27.91	1.392	1.15

Summary of Test Validities Required for All Tests:			
7.4.5	Initial precrack force	P <= Pm for sample type	Valid
7.4.5.1	Initial Kmax	<40% of Precrack YS	Valid
7.4.5.2	Final Kmax	<60% of K result	Valid
9.1.4.1	Precrack straightness	None > 0.05B	Valid
7.4.5.1	Precrack length	>0.05B or 0.05inch, wide notch	Valid
7.5	Side groove depth	< 0.25B	Valid
Summary of Test Validities Required for Jic:			
7.4.2	a/W Range for J	0.45 <= a/W <= 0.7	Valid
9.1.5.1	Even Crack Ext.	None < 50% of avg crk ext.	Valid
9.1.5.2	Accuracy of crk ext. pred.	Diff < 0.15 d_ap	Valid
A9.6.4	# pts in region A	# pts >= 1 in A	Valid
A9.6.4	# pts in region B	# pts >= 1 in B	Valid
A9.6.6.6	# Valid J-da pts	# pts >= 5	Valid
A9.8.1	J-da fit coeff C2	C2 < 1.0	Valid
A9.8.2.1	Accuracy of a_oq	|a_oq - a_op| < 0.01W or 0.5mm	Valid
A9.8.2.2	Num pts in a_oq fit	# points >= 8	Valid
A9.8.2.2	0.4Jq<(#pts a_oq fit)<Jq	# points >= 3	Valid
A8.2.2.2	a_oq fit R^2	R^2 > 0.96	Valid
A9.9.1	Thickness requirement	B > 10Jq/FlowStress	Valid
A9.9.2	Ligament requirement	b_o > 10Jq/FlowStress	Valid
A9.9.3	Regression line slope	Slope < flow at da_q	Valid
All validity criteria for Jic NOT met. Jq is not fully valid Jic. Non-valid Jq values may still convey valuable fracture toughness information.			
Summary of Test Validities Required for Kic:			
7.4.2	a/W Range for K	0.45 <= a/W <= 0.55	Valid
A5.4.3	K Ligament length	b_o > 2.5(K/YS)^2	NOT Valid
A5.4.2	Pmax/Pq ratio	Less than 1.10	NOT Valid
All validity criteria for K_{Ic} NOT met. Kq is not fully valid K_{Ic}. Non-valid Kq values may still convey valuable fracture toughness information.			

J1C Plot

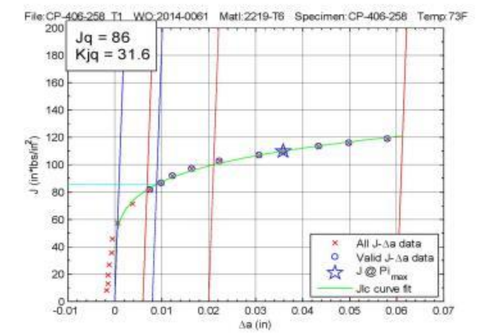

Method File:
FTA NLFT

Comments:
N/A

Mechanical Test Facilities

EM10

Fracture Toughness J_{Ic} Test Results

Version 4.3

EM10 Specimen ID	140061426
Other Specimen ID	CP-406-258
Operator	Charles Kay
Test Date	4/10/2014

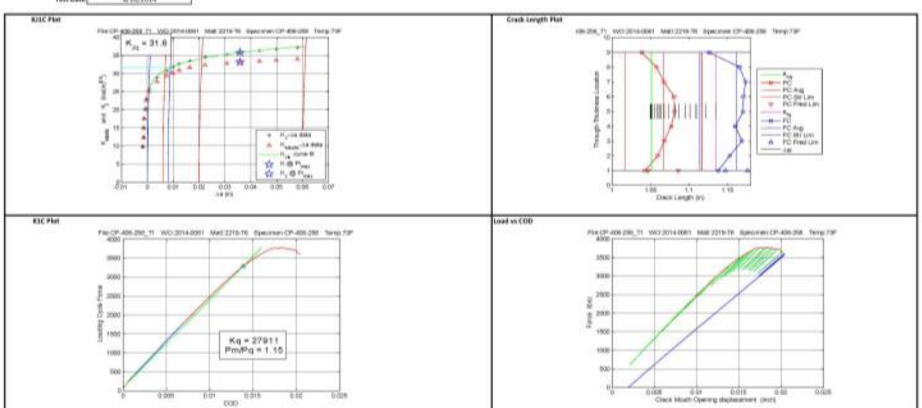

EM10

Fracture Toughness J_{Ic} Test Results

Version 4.3

EM10 Specimen ID	140061429	Geometry	C(T)	"E" (MSI)	10.60	Precrack Pmax (lbf)	524.0
Other Specimen ID	CP-406-261	"W" (in)	1.0000	"Ec" (MSI)	10.60	Precrack Final "a" (in)	0.5000
Operator	Charles Kay	"B" (in)	0.5010	% diff E & Ec	0.00	Stress Ratio	0.10
Test Date	4/12/2014	"Bn" (in)	0.3960	"V"	0.30	Kmax (ksi_sqrt_in)	8.00
		"Be" (in)	0.4790	"YS" (KSI)	38.70		
Environment	Air	Oreintation	S-T	"UTS" (KSI)	59.80		
Temperature (°F)	75	"An" (in)	0.4020			A_op (in)	0.5000
Pressure (PSIG)	0	Hole Span/2 "H" (in)	0.3550	Flow Stress (KSI)	49.25	A_oq (in)	0.4958
Relative Humidity (%)	NA	COD Span/2 "D" (in)	0.0980	"E"/"YS"	0.27	A_fp (in)	0.5873
Soak Time (min)	0	Coupon #	M5			A_fq (in)	0.5777

	Jq (in*lbs/in^2)	Je_q (in*lbs/in^2)	Jp_q (in*lbs/in^2)	Kjq (ksi(in)^2)	Kjq_at_Je_q (ksi(in)^2)	K_95sec (ksi(in)^2)	K Req Ligament (in)	Pmax/Pq
Results	67.80	57.70	10.00	28.10	25.93	20.89	0.729	1.37

Summary of Test Validities Required for All Tests:			
7.4.5	Initial precrack force	P <= Pm for sample type	Valid
7.4.5.1	Initial Kmax	<40% of Precrack YS	Valid
7.4.5.2	Final Kmax	<60% of K result	Valid
9.1.4.1	Precrack straightness	None > 0.05B	Valid
7.4.5.1	Precrack length	>0.05B or 0.05inch, wide notch	Valid
7.5	Side groove depth	< 0.25B	Valid

Summary of Test Validities Required for Jic:			
7.4.2	a/W Range for J	0.45 <= a/W <= 0.7	Valid
9.1.5.1	Even Crack Ext.	None < 50% of avg crk ext.	Valid
9.1.5.2	Accuracy of crk ext. pred.	Diff < 0.15 d_ap	Valid
A9.6.4	# pts in region A	# pts >= 1 in A	Valid
A9.6.4	# pts in region B	# pts >= 1 in B	Valid
A9.6.6.6	# Valid J-da pts	# pts >= 5	Valid
A9.8.1	J-da fit coeff C2	C2 < 1.0	Valid
A9.8.2.1	Accuracy of a_oq	|a_oq - a_op| < 0.01W or 0.5mm	Valid
A9.8.2.2	Num pts in a_oq fit	# points >= 8	Valid
A9.8.2.2	0.4Jq<(#pts a_oq fit)<Jq	# points >= 3	Valid
A8.2.2.2	a_oq fit R^2	R^2 > 0.96	Valid
A9.9.1	Thickness requirement	B > 10Jq/FlowStress	Valid
A9.9.2	Ligament requirement	b_o > 10Jq/FlowStress	Valid
A9.9.3	Regression line slope	Slope < flow at da_q	Valid

All validity criteria for Jic NOT met. Jq is not fully valid Jic.
Non-valid Jq values may still convey valuable fracture toughness information.

Summary of Test Validities Required for Kic:			
7.4.2	a/W Range for K	0.45 <= a/W <= 0.55	Valid
A5.4.3	K Ligament length	b_o > 2.5(K/YS)^2	NOT Valid
A5.4.2	Pmax/Pq ratio	Less than 1.10	NOT Valid

All validity criteria for K_{Ic} NOT met. Kq is not fully valid K_{Ic}.
Non-valid Kq values may still convey valuable fracture toughness information.

J1C Plot

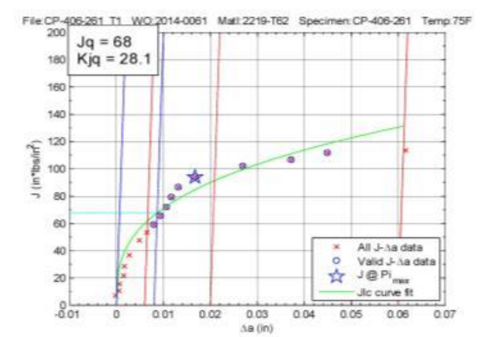

Method File:
FTA NLFT

Comments:
N/A

EM10

Fracture Toughness J_{Ic} Test Results

Version 4.3

EM10 Specimen ID	140061429
Other Specimen ID	CP-406-261
Operator	Charles Kay
Test Date	4/12/2014

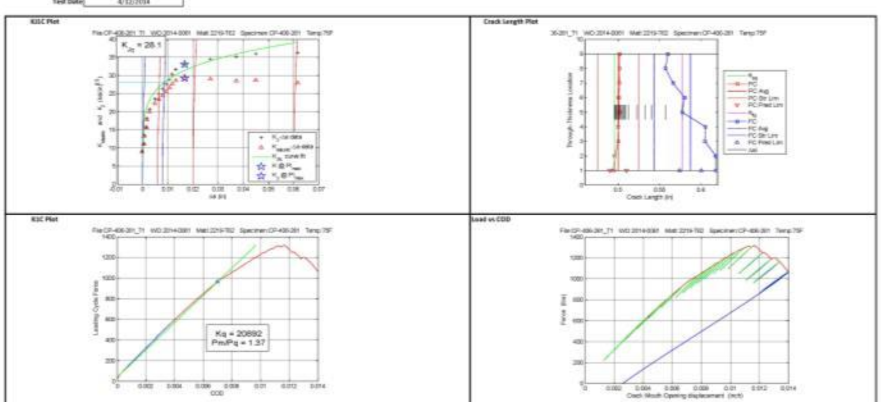

Mechanical Test Facilities

EM10

Fracture Toughness J_{Ic} Test Results

Version 4.3

EM10 Specimen ID	140061431	Geometry	C(T)	"E" (MSI)	10.60	Precrack Pmax (lbf)	529.0
Other Specimen ID	CP-406-263	"W" (in)	1.0000	"Ec" (MSI)	10.60	Precrack Final "a" (in)	0.5109
Operator	Charles Kay	"B" (in)	0.5010	% diff E & Ec	0.00	Stress Ratio	0.10
Test Date	4/12/2014	"Bn" (in)	0.3960	"V"	0.30	Kmax (ksi_sqrt_in)	8.00
		"Be" (in)	0.4790	"YS" (KSI)	38.70		
Environment	Air	Oreintation	S-T	"UTS" (KSI)	59.80		
Temperature (°F)	75	"An" (in)	0.4030			A_op (in)	0.5109
Pressure (PSIG)	0	Hole Span/2 "H" (in)	0.3550	Flow Stress (KSI)	49.25	A_oq (in)	0.5100
Relative Humidity (%)	NA	COD Span/2 "D" (in)	0.0990	"E"/"YS"	0.27	A_fp (in)	0.5823
Soak Time (min)	0	Coupon #	M5			A_fq (in)	0.5796

	Jq (in*lbs/in^2)	Je_q (in*lbs/in^2)	Jp_q (in*lbs/in^2)	Kjq (ksi(in)^2)	Kjq_at_Je_q (ksi(in)^2)	K_95sec (ksi(in)^2)	K Req Ligament (in)	Pmax/Pq
Results	77.40	65.40	12.00	30.03	27.61	21.86	0.797	1.27

Summary of Test Validities Required for All Tests:			
7.4.5	Initial precrack force	P <= Pm for sample type	Valid
7.4.5.1	Initial Kmax	<40% of Precrack YS	Valid
7.4.5.2	Final Kmax	<60% of K result	Valid
9.1.4.1	Precrack straightness	None > 0.05B	Valid
7.4.5.1	Precrack length	>0.05B or 0.05inch, wide notch	Valid
7.5	Side groove depth	< 0.25B	Valid
Summary of Test Validities Required for Jlc:			
7.4.2	a/W Range for J	0.45 <= a/W <= 0.7	Valid
9.1.5.1	Even Crack Ext.	None < 50% of avg crk ext.	Valid
9.1.5.2	Accuracy of crk ext. pred.	Diff < 0.15 d_ap	Valid
A9.6.4	# pts in region A	# pts >= 1 in A	Valid
A9.6.4	# pts in region B	# pts >= 1 in B	Valid
A9.6.6.6	# Valid J-da pts	# pts >= 5	Valid
A9.8.1	J-da fit coeff C2	C2 < 1.0	Valid
A9.8.2.1	Accuracy of a_oq	|a_oq - a_op| < 0.01W or 0.5mm	Valid
A9.8.2.2	Num pts in a_oq fit	# points >= 8	Valid
A9.8.2.2	0.4Jq<(#pts a_oq fit)<Jq	# points >= 3	Valid
A8.2.2.2	a_oq fit R^2	R^2 > 0.96	Valid
A9.9.1	Thickness requirement	B > 10Jq/FlowStress	Valid
A9.9.2	Ligament requirement	b_o > 10Jq/FlowStress	Valid
A9.9.3	Regression line slope	Slope < flow at da_q	Valid
All validity criteria for Jlc NOT met. Jq is not fully valid Jlc. Non-valid Jq values may still convey valuable fracture toughness information.			
Summary of Test Validities Required for Klc:			
7.4.2	a/W Range for K	0.45 <= a/W <= 0.55	Valid
A5.4.3	K Ligament length	b_o > 2.5(K/YS)^2	NOT Valid
A5.4.2	Pmax/Pq ratio	Less than 1.10	NOT Valid
All validity criteria for K_{Ic} NOT met. Kq is not fully valid K_{Ic}. Non-valid Kq values may still convey valuable fracture toughness information.			

J1C Plot

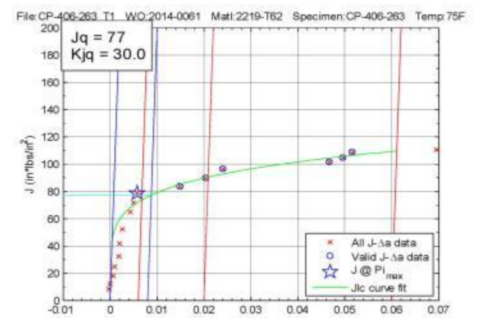

Method File:

FTA NUT

Comments:

N/A

Mechanical Test Facilities

EM10

Fracture Toughness J_{Ic} Test Results

Version 4.3

EM10 Specimen ID	140061431
Other Specimen ID	CP-406-263
Operator	Charles Kay
Test Date	4/12/2014

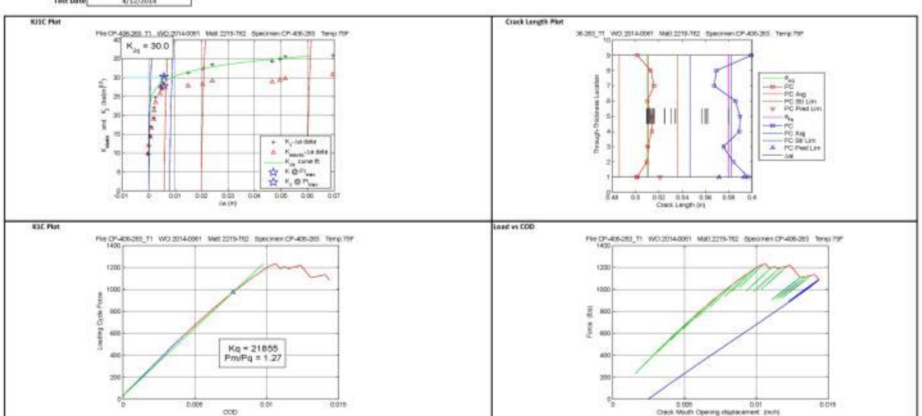

Mechanical Test Facilities

EM10

Fracture Toughness J_{Ic} Test Results

Version 4.3

EM10 Specimen ID	140061434	Geometry	C(T)	"E" (MSI)	10.60	Precrack Pmax (lbf)	1520.0
Other Specimen ID	CP-406-266	"W" (in)	2.0000	"Ec" (MSI)	10.60	Precrack Final "a" (in)	1.0545
Operator	Charles Kay	"B" (in)	1.0000	% diff E & Ec	0.00	Stress Ratio	0.10
Test Date	4/10/2014	"Bn" (in)	0.7960	"V"	0.30	Kmax (ksi_sqrt_in)	8.00
		"Be" (in)	0.9590	"YS" (KSI)	38.30		
Environment	Air	Oreintation	L-T	"UTS" (KSI)	57.80		
Temperature (°F)	73	"An" (in)	0.8000			A_op (in)	1.0545
Pressure (PSIG)	0	Hole Span/2 "H" (in)	0.7100	Flow Stress (KSI)	48.04	A_oq (in)	1.0359
Relative Humidity (%)	NA	COD Span/2 "D" (in)	0.1060	"E"/"YS"	0.28	A_fp (in)	1.1379
Soak Time (min)	0	Coupon #	M6			A_fq (in)	1.1095

	Jq (in*lbs/in^2)	Je_q (in*lbs/in^2)	Jp_q (in*lbs/in^2)	Kjq (ksi(in)^2)	Kjq_at_Je_q (ksi(in)^2)	K_95sec (ksi(in)^2)	K Req Ligament (in)	Pmax/Pq
Results	118.70	103.50	15.20	37.18	34.72	28.95	1.428	1.36

Summary of Test Validities Required for All Tests:			
7.4.5	Initial precrack force	P <= Pm for sample type	Valid
7.4.5.1	Initial Kmax	<40% of Precrack YS	Valid
7.4.5.2	Final Kmax	<60% of K result	Valid
9.1.4.1	Precrack straightness	None > 0.05B	Valid
7.4.5.1	Precrack length	>0.05B or 0.05inch, wide notch	Valid
7.5	Side groove depth	< 0.25B	Valid
Summary of Test Validities Required for Jlc:			
7.4.2	a/W Range for J	0.45 <= a/W <= 0.7	Valid
9.1.5.1	Even Crack Ext.	None < 50% of avg crk ext.	Valid
9.1.5.2	Accuracy of crk ext. pred.	Diff < 0.15 d_ap	Valid
A9.6.4	# pts in region A	# pts >= 1 in A	Valid
A9.6.4	# pts in region B	# pts >= 1 in B	Valid
A9.6.6.6	# Valid J-da pts	# pts >= 5	Valid
A9.8.1	J-da fit coeff C2	C2 < 1.0	Valid
A9.8.2.1	Accuracy of a_oq	|a_oq - a_op| < 0.01W or 0.5mm	Valid
A9.8.2.2	Num pts in a_oq fit	# points >= 8	Valid
A9.8.2.2	0.4Jq<(#pts a_oq fit)<Jq	# points >= 3	Valid
A8.2.2.2	a_oq fit R^2	R^2 > 0.96	Valid
A9.9.1	Thickness requirement	B > 10Jq/FlowStress	Valid
A9.9.2	Ligament requirement	b_o > 10Jq/FlowStress	Valid
A9.9.3	Regression line slope	Slope < flow at da_q	Valid
All validity criteria for Jlc NOT met. Jq is not fully valid Jlc. Non-valid Jq values may still convey valuable fracture toughness information.			
Summary of Test Validities Required for Klc:			
7.4.2	a/W Range for K	0.45 <= a/W <= 0.55	Valid
A5.4.3	K Ligament length	b_o > 2.5(K/YS)^2	NOT Valid
A5.4.2	Pmax/Pq ratio	Less than 1.10	NOT Valid
All validity criteria for K_{Ic} NOT met. Kq is not fully valid K_{Ic}. Non-valid Kq values may still convey valuable fracture toughness information.			

J1C Plot

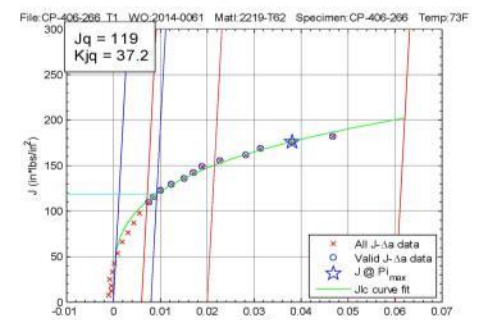

Method File:
FTA NLFT

Comments:
N/A

Mechanical Test Facilities

EM10

Fracture Toughness J_{Ic} Test Results

Version 4.3

EM10 Specimen ID	140061434
Other Specimen ID	CP-406-266
Operator	Charles Kay
Test Date	4/10/2014

KJIC Plot

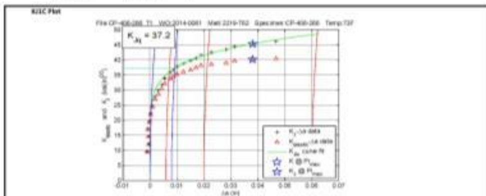

Crack Length Plot

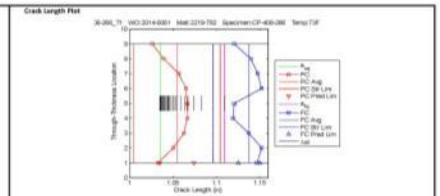

KIC Plot

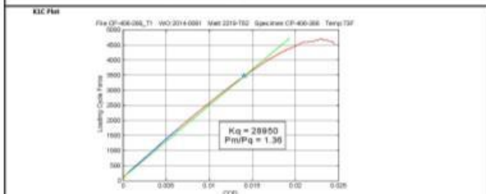

Load vs COD

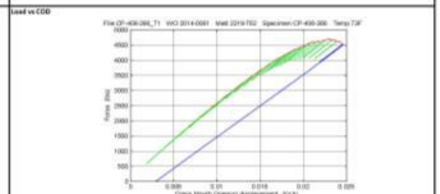

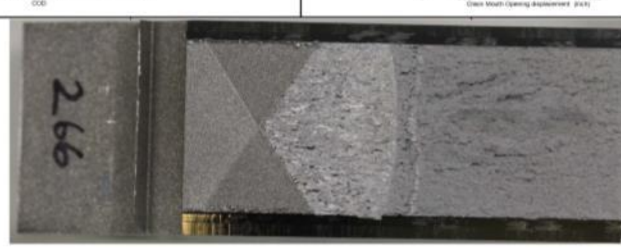

Mechanical Test Facilities

EM10

Fracture Toughness J_{Ic} Test Results

Version 4.3

EM10 Specimen ID	140061436	Geometry	C(T)	"E" (MSI)	10.60	Precrack Pmax (lbf)	1511.0
Other Specimen ID	CP-406-268	"W" (in)	2.0000	"Ec" (MSI)	10.60	Precrack Final "a" (in)	1.0603
Operator	Charles Kay	"B" (in)	1.0030	% diff E & Ec	0.00	Stress Ratio	0.10
Test Date	4/10/2014	"Bn" (in)	0.7950	"V"	0.30	Kmax (ksi_sqrt_in)	8.00
		"Be" (in)	0.9610	"YS" (KSI)	38.30		
Environment	Air	Oreintation	L-T	"UTS" (KSI)	57.80		
Temperature (°F)	73	"An" (in)	0.7980			A_op (in)	1.0603
Pressure (PSIG)	0	Hole Span/2 "H" (in)	0.7100	Flow Stress (KSI)	48.04	A_oq (in)	1.0432
Relative Humidity (%)	NA	COD Span/2 "D" (in)	0.1050	"E"/"YS"	0.28	A_fp (in)	1.1366
Soak Time (min)	0	Coupon #	M6			A_fq (in)	1.1133

	Jq (in*lbs/in^2)	Je_q (in*lbs/in^2)	Jp_q (in*lbs/in^2)	Kjq (ksi(in)^2)	Kjq_at_Je_q (ksi(in)^2)	K_95sec (ksi(in)^2)	K Req Ligament (in)	Pmax/Pq
Results	114.00	100.00	14.00	36.44	34.13	29.20	1.453	1.28

Summary of Test Validities Required for All Tests:			
7.4.5	Initial precrack force	P <= Pm for sample type	Valid
7.4.5.1	Initial Kmax	<40% of Precrack YS	Valid
7.4.5.2	Final Kmax	<60% of K result	Valid
9.1.4.1	Precrack straightness	None > 0.05B	Valid
7.4.5.1	Precrack length	>0.05B or 0.05inch, wide notch	Valid
7.5	Side groove depth	< 0.25B	Valid
Summary of Test Validities Required for Jic:			
7.4.2	a/W Range for J	0.45 <= a/W <= 0.7	Valid
9.1.5.1	Even Crack Ext.	None < 50% of avg crk ext.	Valid
9.1.5.2	Accuracy of crk ext. pred.	Diff < 0.15 d_ap	Valid
A9.6.4	# pts in region A	# pts >= 1 in A	Valid
A9.6.4	# pts in region B	# pts >= 1 in B	Valid
A9.6.6.6	# Valid J-da pts	# pts >= 5	Valid
A9.8.1	J-da fit coeff C2	C2 < 1.0	Valid
A9.8.2.1	Accuracy of a_oq	|a_oq - a_op| < 0.01W or 0.5mm	Valid
A9.8.2.2	Num pts in a_oq fit	# points >= 8	Valid
A9.8.2.2	0.4Jq<(#pts a_oq fit)<Jq	# points >= 3	Valid
A8.2.2.2	a_oq fit R^2	R^2 > 0.96	Valid
A9.9.1	Thickness requirement	B > 10Jq/FlowStress	Valid
A9.9.2	Ligament requirement	b_o > 10Jq/FlowStress	Valid
A9.9.3	Regression line slope	Slope < flow at da_q	Valid
All validity criteria for Jic NOT met. Jq is not fully valid Jic. **Non-valid Jq values may still convey valuable fracture toughness information.**			
Summary of Test Validities Required for KIc:			
7.4.2	a/W Range for K	0.45 <= a/W <= 0.55	Valid
A5.4.3	K Ligament length	b_o > 2.5(K/YS)^2	NOT Valid
A5.4.2	Pmax/Pq ratio	Less than 1.10	NOT Valid
All validity criteria for K_{Ic} NOT met. Kq is not fully valid K_{Ic}. **Non-valid Kq values may still convey valuable fracture toughness information.**			

J1C Plot

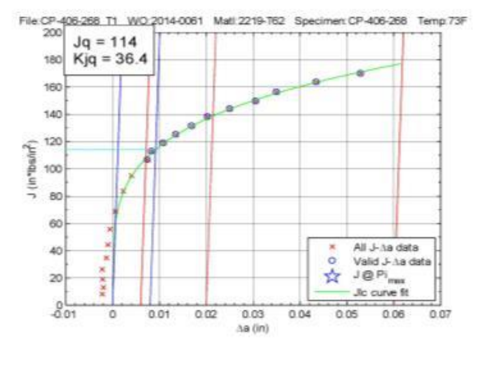

Method File:

FTA NLFT

Comments:

N/A

Mechanical Test Facilities

EM10

Fracture Toughness J_{Ic} Test Results

Version 4.3

EM10 Specimen ID	140061436
Other Specimen ID	CP-406-268
Operator	Charles Kay
Test Date	4/10/2014

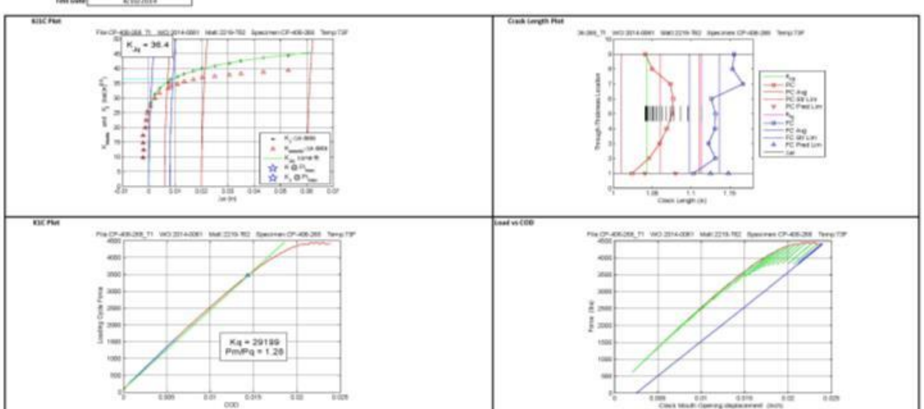

Mechanical Test Facilities

EM10

Fracture Toughness J_{Ic} Test Results

Version 4.3

EM10 Specimen ID	140061439
Other Specimen ID	CP-406-271
Operator	Charles Kay
Test Date	4/10/2014
Environment	Air
Temperature (°F)	73
Pressure (PSIG)	0
Relative Humidity (%)	NA
Soak Time (min)	0

Geometry	C(T)
"W" (in)	1.9990
"B" (in)	1.0020
"Bn" (in)	0.7990
"Be" (in)	0.9610
Oreintation	T-L
"An" (in)	0.7980
Hole Span/2 "H" (in)	0.7100
COD Span/2 "D" (in)	0.1050
Coupon #	M6

"E" (MSI)	10.60
"Ec" (MSI)	10.60
% diff E & Ec	0.00
"V"	0.30
"YS" (KSI)	37.60
"UTS" (KSI)	56.70
Flow Stress (KSI)	47.16
"E"/"YS"	0.28

Precrack Pmax (lbf)	1505.0
Precrack Final "a" (in)	1.0597
Stress Ratio	0.10
Kmax (ksi_sqrt_in)	8.00
A_op (in)	1.0597
A_oq (in)	1.0408
A_fp (in)	1.1341
A_fq (in)	1.1087

	Jq (in*lbs/in^2)	Je_q (in*lbs/in^2)	Jp_q (in*lbs/in^2)	Kjq (ksi(in)^2)	Kjq_at_Je_q (ksi(in)^2)	K_95sec (ksi(in)^2)	K Req Ligament (in)	Pmax/Pq
Results	86.50	78.20	8.30	31.74	30.17	28.34	1.420	1.14

Summary of Test Validities Required for All Tests:			
7.4.5	Initial precrack force	P <= Pm for sample type	Valid
7.4.5.1	Initial Kmax	<40% of Precrack YS	Valid
7.4.5.2	Final Kmax	<60% of K result	Valid
9.1.4.1	Precrack straightness	None > 0.05B	Valid
7.4.5.1	Precrack length	>0.05B or 0.05inch, wide notch	Valid
7.5	Side groove depth	< 0.25B	Valid
Summary of Test Validities Required for Jic:			
7.4.2	a/W Range for J	0.45 <= a/W <= 0.7	Valid
9.1.5.1	Even Crack Ext.	None < 50% of avg crk ext.	Valid
9.1.5.2	Accuracy of crk ext. pred.	Diff < 0.15 d_ap	Valid
A9.6.4	# pts in region A	# pts >= 1 in A	Valid
A9.6.4	# pts in region B	# pts >= 1 in B	Valid
A9.6.6.6	# Valid J-da pts	# pts >= 5	Valid
A9.8.1	J-da fit coeff C2	C2 < 1.0	Valid
A9.8.2.1	Accuracy of a_oq	|a_oq - a_op| < 0.01W or 0.5mm	Valid
A9.8.2.2	Num pts in a_oq fit	# points >= 8	Valid
A9.8.2.2	0.4Jq<(#pts a_oq fit)<Jq	# points >= 3	Valid
A8.2.2.2	a_oq fit R^2	R^2 > 0.96	Valid
A9.9.1	Thickness requirement	B > 10Jq/FlowStress	Valid
A9.9.2	Ligament requirement	b_o > 10Jq/FlowStress	Valid
A9.9.3	Regression line slope	Slope < flow at da_q	Valid
All validity criteria for Jic NOT met. Jq is not fully valid Jic. Non-valid Jq values may still convey valuable fracture toughness information.			
Summary of Test Validities Required for Kic:			
7.4.2	a/W Range for K	0.45 <= a/W <= 0.55	Valid
A5.4.3	K Ligament length	b_o > 2.5(K/YS)^2	NOT Valid
A5.4.2	Pmax/Pq ratio	Less than 1.10	NOT Valid
All validity criteria for K_{Ic} NOT met. Kq is not fully valid K_{Ic}. Non-valid Kq values may still convey valuable fracture toughness information.			

J1C Plot

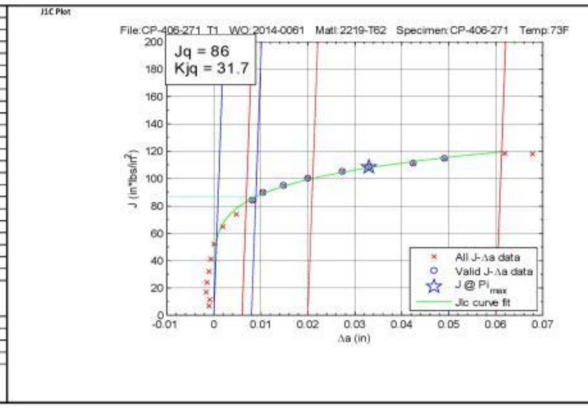

Method File:
FTA NLFT

Comments:
N/A

Mechanical Test Facilities

EM10

Fracture Toughness J_{Ic} Test Results

Version 4.3

EM10 Specimen ID	140061439
Other Specimen ID	CP-406-271
Operator	Charles Kay
Test Date	4/10/2014

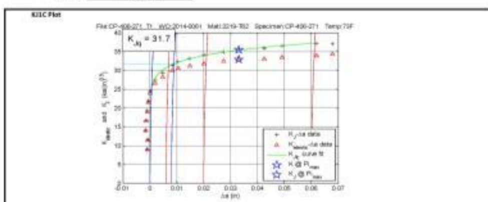

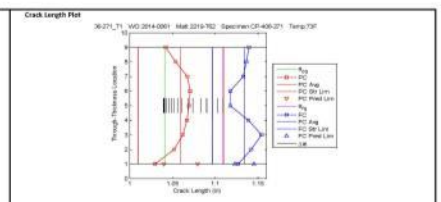

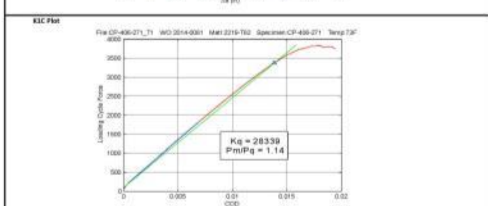

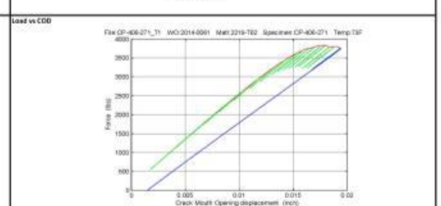

Mechanical Test Facilities

EM10

Fracture Toughness J_{Ic} Test Results

Version 4.3

EM10 Specimen ID	140061441
Other Specimen ID	CP-406-273
Operator	Charles Kay
Test Date	
Environment	Air
Temperature (°F)	73
Pressure (PSIG)	0
Relative Humidity (%)	NA
Soak Time (min)	0

Geometry	C(T)
"W" (in)	1.9990
"B" (in)	1.0000
"Bn" (in)	0.7980
"Be" (in)	0.9590
Oreintation	T-L
"An" (in)	0.7910
Hole Span/2 "H" (in)	0.7100
COD Span/2 "D" (in)	0.1060
Coupon #	M6

"E" (MSI)	10.60
"Ec" (MSI)	10.60
% diff E & Ec	0.00
"V"	0.30
"YS" (KSI)	37.60
"UTS" (KSI)	56.70
Flow Stress (KSI)	47.16
"E"/"YS"	0.28

Precrack Pmax (lbf)	1515.0
Precrack Final "a" (in)	1.0810
Stress Ratio	0.10
Kmax (ksi_sqrt_in)	8.00
A_op (in)	1.0810
A_oq (in)	1.0650
A_fp (in)	1.1591
A_fq (in)	1.1362

	Jq (in*lbs/in^2)	Je_q (in*lbs/in^2)	Jp_q (in*lbs/in^2)	Kjq (ksi(in)^2)	Kjq_at_Je_q (ksi(in)^2)	K_95sec (ksi(in)^2)	K Req Ligament (in)	Pmax/Pq
Results	85.00	76.10	9.00	31.47	29.76	27.60	1.347	1.17

Summary of Test Validities Required for All Tests:			
7.4.5	Initial precrack force	P <= Pm for sample type	Valid
7.4.5.1	Initial Kmax	<40% of Precrack YS	Valid
7.4.5.2	Final Kmax	<60% of K result	Valid
9.1.4.1	Precrack straightness	None > 0.05B	Valid
7.4.5.1	Precrack length	>0.05B or 0.05inch, wide notch	Valid
7.5	Side groove depth	< 0.25B	Valid
Summary of Test Validities Required for Jlc:			
7.4.2	a/W Range for J	0.45 <= a/W <= 0.7	Valid
9.1.5.1	Even Crack Ext.	None < 50% of avg crk ext.	Valid
9.1.5.2	Accuracy of crk ext. pred.	Diff < 0.15 d_ap	Valid
A9.6.4	# pts in region A	# pts >= 1 in A	Valid
A9.6.4	# pts in region B	# pts >= 1 in B	Valid
A9.6.6.6	# Valid J-da pts	# pts >= 5	Valid
A9.8.1	J-da fit coeff C2	C2 < 1.0	Valid
A9.8.2.1	Accuracy of a_oq	|a_oq - a_op| < 0.01W or 0.5mm	Valid
A9.8.2.2	Num pts in a_oq fit	# points >= 8	Valid
A9.8.2.2	0.4Jq<(#pts a_oq fit)<Jq	# points >= 3	Valid
A8.2.2.2	a_oq fit R^2	R^2 > 0.96	Valid
A9.9.1	Thickness requirement	B > 10Jq/FlowStress	Valid
A9.9.2	Ligament requirement	b_o > 10Jq/FlowStress	Valid
A9.9.3	Regression line slope	Slope < flow at da_q	Valid
All validity criteria for Jlc NOT met. Jq is not fully valid Jlc. Non-valid Jq values may still convey valuable fracture toughness information.			
Summary of Test Validities Required for Klc:			
7.4.2	a/W Range for K	0.45 <= a/W <= 0.55	Valid
A5.4.3	K Ligament length	b_o > 2.5(K/YS)^2	NOT Valid
A5.4.2	Pmax/Pq ratio	Less than 1.10	NOT Valid
All validity criteria for K_{Ic} NOT met. Kq is not fully valid K_{Ic}. Non-valid Kq values may still convey valuable fracture toughness information.			

J1C Plot

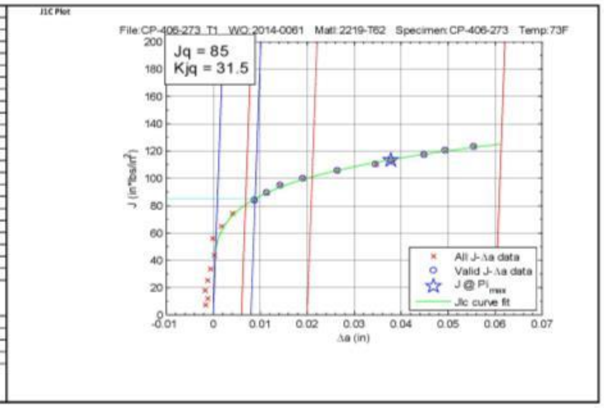

Method File:

FTA NLFT

Comments:

N/A

Mechanical Test Facilities

EM10

Fracture Toughness J_{Ic} Test Results

Version 4.3

EM10 Specimen ID	140061441
Other Specimen ID	CP-406-273
Operator	Charles Kay
Test Date	0

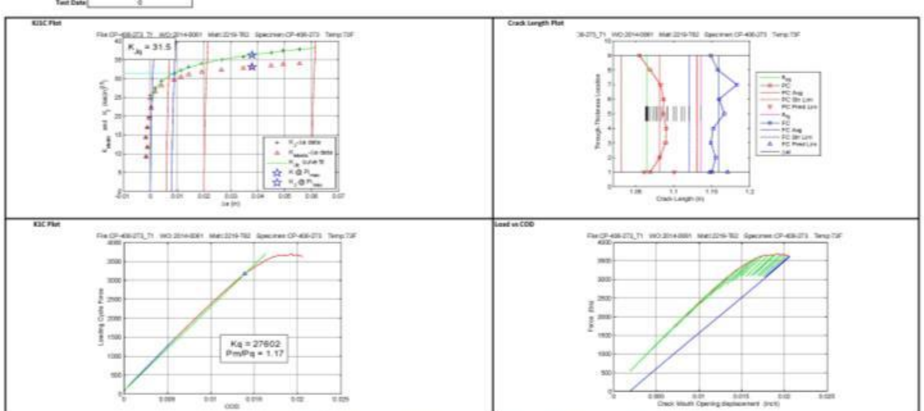

Mechanical Test Facilities

EM10

Fracture Toughness J_{Ic} Test Results

Version 4.3

EM10 Specimen ID	140061444	Geometry	C(T)	"E" (MSI)	10.60	Precrack Pmax (lbf)	525.0
Other Specimen ID	CP-406-276	"W" (in)	1.0000	"Ec" (MSI)	10.60	Precrack Final "a" (in)	0.5275
Operator	Charles Kay	"B" (in)	0.5010	% diff E & Ec	0.00	Stress Ratio	0.10
Test Date	4/12/2014	"Bn" (in)	0.3990	"V"	0.30	Kmax (ksi_sqrt_in)	8.00
		"Be" (in)	0.4800	"YS" (KSI)	40.30		
Environment	Air	Oreintation	S-T	"UTS" (KSI)	58.50		
Temperature (°F)	73	"An" (in)	0.4010			A_op (in)	0.5275
Pressure (PSIG)	0	Hole Span/2 "H" (in)	0.3550	Flow Stress (KSI)	49.42	A_oq (in)	0.5234
Relative Humidity (%)	NA	COD Span/2 "D" (in)	0.0990	"E"/"YS"	0.26	A_fp (in)	0.6568
Soak Time (min)	0	Coupon #	M6			A_fq (in)	0.6452

	Jq (in*lbs/in^2)	Je_q (in*lbs/in^2)	Jp_q (in*lbs/in^2)	Kjq (ksi(in)^2)	Kjq_at_Je_q (ksi(in)^2)	K_95sec (ksi(in)^2)	K Req Ligament (in)	Pmax/Pq
Results	59.10	51.60	7.50	26.23	24.51	20.00	0.616	1.32

Summary of Test Validities Required for All Tests:			
7.4.5	Initial precrack force	P <= Pm for sample type	Valid
7.4.5.1	Initial Kmax	<40% of Precrack YS	Valid
7.4.5.2	Final Kmax	<60% of K result	Valid
9.1.4.1	Precrack straightness	None > 0.05B	Valid
7.4.5.1	Precrack length	>0.05B or 0.05inch, wide notch	Valid
7.5	Side groove depth	< 0.25B	Valid

Summary of Test Validities Required for Jic:			
7.4.2	a/W Range for J	0.45 <= a/W <= 0.7	Valid
9.1.5.1	Even Crack Ext.	None < 50% of avg crk ext.	Valid
9.1.5.2	Accuracy of crk ext. pred.	Diff < 0.15 d_ap	Valid
A9.6.4	# pts in region A	# pts >= 1 in A	Valid
A9.6.4	# pts in region B	# pts >= 1 in B	Valid
A9.6.6.6	# Valid J-da pts	# pts >= 5	Valid
A9.8.1	J-da fit coeff C2	C2 < 1.0	Valid
A9.8.2.1	Accuracy of a_oq	|a_oq - a_op| < 0.01W or 0.5mm	Valid
A9.8.2.2	Num pts in a_oq fit	# points >= 8	Valid
A9.8.2.2	0.4Jq<(#pts a_oq fit)<Jq	# points >= 3	Valid
A8.2.2.2	a_oq fit R^2	R^2 > 0.96	Valid
A9.9.1	Thickness requirement	B > 10Jq/FlowStress	Valid
A9.9.2	Ligament requirement	b_o > 10Jq/FlowStress	Valid
A9.9.3	Regression line slope	Slope < flow at da_q	Valid

All validity criteria for Jic NOT met. Jq is not fully valid Jic.

Non-valid Jq values may still convey valuable fracture toughness information.

Summary of Test Validities Required for Kic:			
7.4.2	a/W Range for K	0.45 <= a/W <= 0.55	Valid
A5.4.3	K Ligament length	b_o > 2.5(K/YS)^2	NOT Valid
A5.4.2	Pmax/Pq ratio	Less than 1.10	NOT Valid

All validity criteria for K_{Ic} NOT met. Kq is not fully valid K_{Ic}.

Non-valid Kq values may still convey valuable fracture toughness information.

J1C Plot

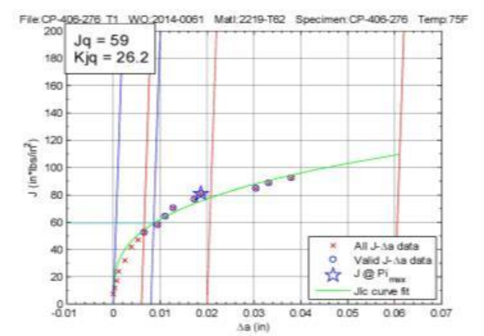

Method File:

FTA NLFT

Comments:

N/A

Mechanical Test Facilities

EM10

Fracture Toughness J_{Ic} Test Results

Version 4.3

EM10 Specimen ID	140061444
Other Specimen ID	CP-406-276
Operator	Charles Kay
Test Date	4/12/2014

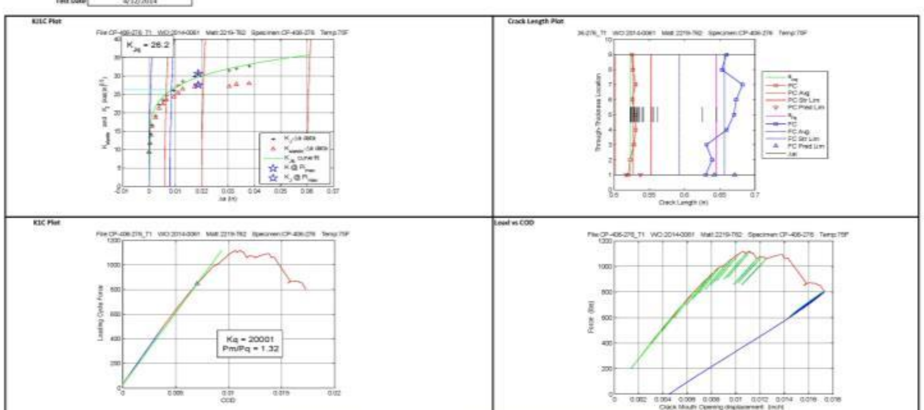

Mechanical Test Facilities

EM10

Fracture Toughness J_{Ic} Test Results

Version 4.3

EM10 Specimen ID	140061446	Geometry	C(T)	"E" (MSI)	10.60	Precrack Pmax (lbf)	542.0
Other Specimen ID	CP-406-278	"W" (in)	0.9990		10.60	Precrack Final "a" (in)	0.5312
Operator	Charles Kay	"B" (in)	0.5010		0.00	Stress Ratio	0.10
Test Date	4/12/2014	"Bn" (in)	0.3970		0.30	Kmax (ksi_sqrt_in)	8.00
		"Be" (in)	0.4790		40.30		
Environment	Air	Oreintation	S-T	"UTS" (KSI)	58.50		
Temperature (°F)	73	"An" (in)	0.4030			A_op (in)	0.5312
Pressure (PSIG)	0	Hole Span/2 "H" (in)	0.3550	Flow Stress (KSI)	49.42	A_oq (in)	0.5312
Relative Humidity (%)	NA	COD Span/2 "D" (in)	0.0980	"E"/"YS"	0.26	A_fp (in)	0.6170
Soak Time (min)	0	Coupon #	M6			A_fq (in)	0.6037

	Jq (in*lbs/in^2)	Je_q (in*lbs/in^2)	Jp_q (in*lbs/in^2)	Kjq (ksi(in)^2)	Kjq_at_Je_q (ksi(in)^2)	K_95sec (ksi(in)^2)	K Req Ligament (in)	Pmax/Pq
Results	57.40	49.90	7.50	25.85	24.10	20.99	0.678	1.18

Summary of Test Validities Required for All Tests:			
7.4.5	Initial precrack force	P <= Pm for sample type	Valid
7.4.5.1	Initial Kmax	<40% of Precrack YS	Valid
7.4.5.2	Final Kmax	<60% of K result	Valid
9.1.4.1	Precrack straightness	None > 0.05B	Valid
7.4.5.1	Precrack length	>0.05B or 0.05inch, wide notch	Valid
7.5	Side groove depth	< 0.25B	Valid

Summary of Test Validities Required for Jic:			
7.4.2	a/W Range for J	0.45 <= a/W <= 0.7	Valid
9.1.5.1	Even Crack Ext.	None < 50% of avg crk ext.	Valid
9.1.5.2	Accuracy of crk ext. pred.	Diff < 0.15 d_ap	NOT Valid
A9.6.4	# pts in region A	# pts >= 1 in A	Valid
A9.6.4	# pts in region B	# pts >= 1 in B	Valid
A9.6.6.6	# Valid J-da pts	# pts >= 5	Valid
A9.8.1	J-da fit coeff C2	C2 < 1.0	Valid
A9.8.2.1	Accuracy of a_oq	|a_oq - a_op| < 0.01W or 0.5mm	Valid
A9.8.2.2	Num pts in a_oq fit	# points >= 8	Valid
A9.8.2.2	0.4Jq<(#pts a_oq fit)<Jq	# points >= 3	Valid
A8.2.2.2	a_oq fit R^2	R^2 > 0.96	Valid
A9.9.1	Thickness requirement	B > 10Jq/FlowStress	Valid
A9.9.2	Ligament requirement	b_o > 10Jq/FlowStress	Valid
A9.9.3	Regression line slope	Slope < flow at da_q	Valid

All validity criteria for Jic NOT met. Jq is not fully valid Jic.
Non-valid Jq values may still convey valuable fracture toughness information.

Summary of Test Validities Required for Kic:			
7.4.2	a/W Range for K	0.45 <= a/W <= 0.55	
A5.4.3	K Ligament length	b_o > 2.5(K/YS)^2	NOT Valid
A5.4.2	Pmax/Pq ratio	less than 1.10	NOT Valid

All validity criteria for K_{Ic} NOT met. Kq is not fully valid K_{Ic}.
Non-valid Kq values may still convey valuable fracture toughness information.

J1C Plot

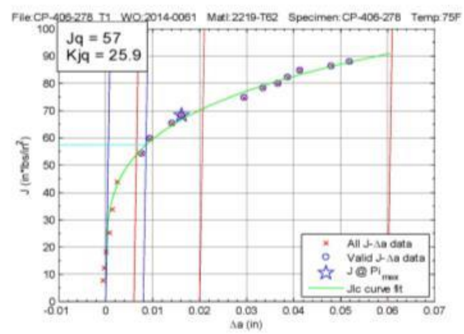

Method File:
FTA NLFT

Comments:
N/A

Mechanical Test Facilities

EM10

Fracture Toughness J_{Ic} Test Results

Version 4.3

EM10 Specimen ID	140061446
Other Specimen ID	CP-406-278
Operator	Charles Kay
Test Date	4/12/2014

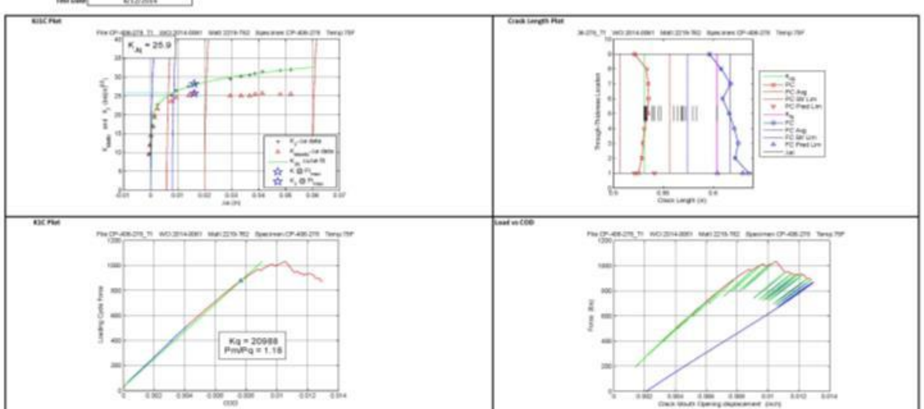

REPORT DOCUMENTATION PAGE	*Form Approved OMB No. 0704-0188*

1. REPORT DATE *(DD-MM-YYYY)*	**2. REPORT TYPE**	**3. DATES COVERED** *(From - To)*
01- 01 - 2015	Technical Publication	July 2013 - November 2014

4. TITLE AND SUBTITLE	**5a. CONTRACT NUMBER**
Spin Forming Aluminum Crew Module (CM) Metallic Aft Pressure Vessel Bulkhead (APVBH) - Phase II	
	5b. GRANT NUMBER
	5c. PROGRAM ELEMENT NUMBER
6. AUTHOR(S)	**5d. PROJECT NUMBER**
Hoffman, Eric K.; Domack, Marcia S.; Torres, Pablo D.; McGill, Preston B.; Tayon, Wesley A.; Bennett, Jay E.; Murphy, Joseph T.	**5e. TASK NUMBER**
	5f. WORK UNIT NUMBER 869021.05.07.09.43

7. PERFORMING ORGANIZATION NAME(S) AND ADDRESS(ES)	**8. PERFORMING ORGANIZATION REPORT NUMBER**
NASA Langley Research Center Hampton, VA 23681-2199	L-20645 NESC-RP-13-00884
9. SPONSORING/MONITORING AGENCY NAME(S) AND ADDRESS(ES)	**10. SPONSOR/MONITOR'S ACRONYM(S)**
National Aeronautics and Space Administration Washington, DC 20546-0001	NASA
	11. SPONSOR/MONITOR'S REPORT NUMBER(S)
	NASA/TP-2015-218674

12. DISTRIBUTION/AVAILABILITY STATEMENT
Unclassified - Unlimited
Subject Category 16 Space Transportation and Safety
Availability: NASA CASI (443) 757-5802

13. SUPPLEMENTARY NOTES

14. ABSTRACT

The principal focus of this project was to assist the Multi-Purpose Crew Vehicle (MPCV) program in developing a spin forming fabrication process for manufacture of the Orion crew module (CM) aft pressure vessel bulkhead. The spin forming process would result in a single piece aluminum (Al) alloy 2219 aft bulkhead resulting in the elimination of the current multiple piece welded construction, simplify CM fabrication, and lead to an enhanced design. This report will focus on the aft bulkhead portion of this study only. Phase I (NASA TM-2014-218163, (1)) of this assessment explored spin forming the single-piece CM forward pressure vessel bulkhead.

15. SUBJECT TERMS
Spin Forming; Crew Module; Aft Pressure Vessel Bulkhead; NASA Engineering and Safety Center; Multi-Purpose Crew Vehicle

16. SECURITY CLASSIFICATION OF:			**17. LIMITATION OF ABSTRACT**	**18. NUMBER OF PAGES**	**19a. NAME OF RESPONSIBLE PERSON**
a. REPORT	**b. ABSTRACT**	**c. THIS PAGE**			STI Help Desk (email: help@sti.nasa.gov)
					19b. TELEPHONE NUMBER ***(Include area code)***
U	U	U	UU	228	(443) 757-5802